EPFL

Reliability analysis and partial safety format calibration considering the characteristics of the resistance of reinforced concrete structures

Qianhui YU

■ École
polytechnique
fédérale
de Lausanne

2023

献给奶奶孙玉华

献给在天上的姥姥钟亚琴，姥爷赵子云，爷爷于景武

To my grandma Sun Yuhua

To my grandma Zhong Yaqin, grandpa Zhao Ziyun and grandpa Yu Jingwu in heaven

Foreword

The idea of verifying reinforced concrete structures at Ultimate Limit State using partial safety factors has been proposed almost 100 years ago and partial factors have been defined in standards since the 60s of last century. These factors have been usually calibrated to achieve the same safety level as according to previous standards which were based on the verification with allowable stresses. Since several decades, it is possible to calibrate them on the basis of reliability analyses in a rational manner, but some open questions still remain.

The thesis of Qianhui Yu deals with these open questions related to the calibration of partial factors, namely the pertinence of this approach in case of multiple failure modes (as for instance flexure, shear and bond failures where both concrete crushing and steel yielding can be involved), the approach to be followed in case of mechanical strain based models (examples of the shear and the punching resistance according to the Critical Shear Crack Theory) and the model uncertainties in the calculation of internal forces in case of very brittle behaviour (example of textile reinforcement consisting of carbon or glass fibres).

The topics of this research were also inspired by the works related to the draft of the second generation of the European code for concrete structures and the related discussions in two committees at international level (CEN/TC250/CSC2/WG1/TG6 and fib TG 3.1 Reliability and safety evaluation: full-probabilistic and semi-probabilistic methods for existing structures). As a result of these discussions, some results of this research have been implemented in the latest draft of this code and in the new fib Model Code 2020. For these reasons also, the outcome of this research has a significant practical relevance.

Lausanne, May 2023

Prof. Aurelio Muttoni

Acknowledgement

I am really grateful to have the opportunity to work with Prof. Muttoni in the Structural Concrete Laboratory (IBETON) of EPFL during the past five years. The rigorous, creative and enthusiastic work attitude of Prof. Muttoni inspired me. The systematic work on structural concrete performed in IBETON will always influence my vision of research.

I would like to acknowledge the members of the jury, Prof. Alain Nussbaumer from EPFL, Prof. Paolo Castaldo from Politecnico di Torino, Prof. David Ruggiero from EPFL and Prof. Alfred Strauss from University of Natural Resources and Life Sciences, for the careful evaluation of the manuscript and the valuable comments and questions in the oral exam. Their remarks helped me improve the quality of the thesis.

This thesis includes scientific articles written in co-authorship with the director of this thesis, as well as with Prof. Miguel Fernández Ruiz, Dr. Patrick Valeri and Dr. João Simões. To all of them I would like to express my gratitude for their contributions. Especially I would like to thank Prof. Fernández Ruiz and Dr. Simões for their guidance in writing styles.

This thesis included experimental campaign carried out in the laboratory. I would like to thank the generous help from all the technicians: Armin, François, Gérald, Gilles, Sylvain and Serge. Thanks for helping me with the lab work and for practicing French with me with a lot of patience.I would also like to thank Dr. Olivier Burdet for the discussions and patient help with all the technical and computational issues. Special thanks to Yvonne for always being there to answer all the questions regarding administrative issues as well as practically every aspect of daily life. Thanks to Jessica for the help with administrative tasks.

During past five years I am also very grateful to have the chance to meet a lot of good friends in IBETON. I would like to express my gratitude to my officemates Fred and Marie-Rose. All the discussions and daily chats will always be part of my cherished memory. Special thanks to Fred for inspiring me with his enthusiasm in structural design as well as his organized working style. I would like to thank Filip, Raffa, Patrick, João, Francesco Moccia, Darko and Francesco Cavagnis for the warmest welcome and for helping me settle in when I first arrived in Switzerland. Special thanks to Max and Korinna for always being supportive in every aspect of work and life, which I really appreciated a lot. In the end, I would like to thank 'the gang', Marko, Xhemsi and Bea, Diego and Maite, Enrique, and Xianlin, for the constant company, which makes Lausanne a real home for me.

I would also like to thank some other friends. Special thanks to Liu Dong, Cao Linlin, Zhang Yueyun and Shui Sailan for always being there with me through thick and thin. I would also like to thank Liu Lulu, Zhan Jian, Wang Congzhe, Wang Qianqing and Zhang Shenghang for all the insightful discussions, as well as the relaxing moments we spent together through this long journey.

Abstract

Every engineering calculation is an approximation of reality, with inevitable uncertainties involved. This fact implies that a reliability verification accounting for the uncertainties is a necessary step in the design and assessment of structures. Nowadays, probability-based partial safety factor format is widely adopted in the structural reliability verification in design codes. The safety format calibration is a continuing updating process with the advancements of knowledge in structural engineering.

For reinforced concrete structures, open questions for the safety format calibration emerge with the increasing application of advanced nonlinear structural resistance analysis approaches (e.g. strain-based approaches and numerical methods like the NonLinear Finite Element Analysis) as well as the application of new materials. Aiming at meeting these new challenges, several topics within the partial safety factor format framework are investigated.

In the first part of this work, the simplifications and assumptions in the classical partial safety factor format for the resistance of reinforced concrete structures are examined. Their suitability for the implicit nonlinear analysis models is investigated focusing on the influence of multiple failure modes. Reliability analysis case studies at different scales (cross-sectional resistance or load-bearing capacity of structural elements and of simple structural systems) show that the partial safety factors applied to material strength variables leads to a satisfactory level of reliability, independent of the development of different failure modes induced by material uncertainties.

In the second part of this work, the characteristic of the model uncertainties of strain-based approaches is investigated using the punching shear resistance model based on the Critical Shear Crack Theory (CSCT) as an example. It is shown that the model uncertainty of global resistance solution of strain-based approach can be viewed as the resultant of the model uncertainties of the sub-models. In addition, the model uncertainty of the global resistance solution can be lower than those of the sub-models, depending on their sensitivity relationship. Based on these observations, different types of partial safety formats for strain-based approaches are compared. The relationship between the safety factors of the punching shear provisions in the second generation of Eurocode 2 for the design of new structures and the assessment of existing critical ones is established.

The last part of this work deals with the partial safety factor format calibration problem for structures with brittle response. As an example, the partial safety format for the flexural resistance of Textile Reinforced Concrete (TRC) is calibrated focusing on the model uncertainties of action effect for brittle systems.

Based on these works, it is concluded that a suitable probabilistic modelling of the basic uncertainties is fundamental for the effective calibration of the partial safety format and it should be based on a good understanding of the relevant load bearing mechanisms. On its basis, a

detailed safety format composed of calibrated partial safety factors for the dominating uncertainties is an effective reliability verification approach for both classical analytical design equations and advanced nonlinear analysis methods.

Résumé

Tout calcul en ingénierie est une approximation de la réalité et comporte des incertitudes inévitables. Ce constat implique qu'il est nécessaire d'effectuer une vérification de la fiabilité prenant en compte ces incertitudes lors du dimensionnement et de la vérification des structures. Actuellement, le format de sécurité probabiliste comprenant les coefficients partiels de sécurité, est largement utilisé dans les normes de dimensionnement lors de la vérification de la fiabilité des structures. La calibration de ce format de sécurité est un processus en constante évolution et progresse en fonction des avancées dans le domaine de l'ingénierie structurale.

En ce qui concerne les structures en béton armé, l'utilisation croissante d'analyses non-linéaire avancées pour le calcul de la résistance telles que les analyses basées sur les déformations et les méthodes numériques comme l'analyse non-linéaire par éléments finis, ainsi que l'utilisation de nouveaux matériaux, suscitent des questions quant à l'adéquation du format des coefficients partiels de sécurité. Face à ces nouveaux défis, plusieurs sujets sont étudiés dans le cadre du format des coefficients partiels de sécurité.

Dans la première partie de ce travail, les simplifications et les hypothèses du format classique des coefficients partiels de sécurité pour la résistance des structures en béton armé sont examinées. Leur adéquation aux modèles d'analyse non-linéaire implicite est étudiée en mettant l'accent sur l'impact des modes de ruptures multiples. Plusieurs cas d'étude portent sur l'analyse de fiabilité des structures à différentes échelles (résistance en section ou capacité portante d'éléments structurels et de systèmes structurels simples). Ils démontrent que l'application des coefficients partiels de sécurité aux variables de résistance des matériaux permettent d'obtenir un niveau de fiabilité satisfaisant, indépendamment du développement des différents modes de rupture induits par les incertitudes liées aux matériaux.

Dans la deuxième partie de ce travail, les caractéristiques des incertitudes du modèle des approches basées sur les déformations sont examinées en utilisant comme exemple le modèle de résistance au poinçonnement basé sur la théorie de la fissure critique (CSCT). Il est démontré que l'incertitude du modèle de la résistance globale dans l'analyse basée sur les déformations peut être considérée comme la résultat des incertitudes du modèle des sous-modèles. De plus, il est également démontré que l'incertitude du modèle de la résistance globale peut être inférieure à celle des sous-modèles, en fonction de la sensibilité les liants. Sur la base de ces observations, différents types de formats partiels de sécurité pour les analyses basées sur les déformations sont comparés. La relation entre les facteurs de sécurité liés à la vérification du poinçonnement dans la deuxième génération de l'Eurocode 2 pour le dimensionnement de nouvelles structures et la vérification des structures critiques existantes est établie.

La dernière partie de ce travail aborde le problème de la calibration du format des coefficients partiels de sécurité pour les structures présentant une réponse fragile. A titre d'exemple, le format partiel de sécurité pour la résistance à la flexion du béton textile (BT) est calibré en se concentrant sur l'incertitude du modèle des efforts internes pour les systèmes fragiles.

Sur la base de ces travaux, il est conclu qu'une modélisation probabiliste appropriée des incertitudes de base est essentielle pour une calibration efficace du format partiel de sécurité. Cette modélisation doit reposer sur une bonne compréhension du comportement mécanique de la transmission des charges. En se basant sur cette approche, l'utilisation d'un format de sécurité détaillé composé de facteurs de sécurité partiels calibrés pour les incertitudes prédominantes s'avère être une approche de vérification de la fiabilité efficace pour les équations de dimensionnement analytiques classiques ainsi que les méthodes d'analyse non-linéaire avancées, telles que les approches basées sur les déformations et l'analyse non-linéaire par éléments finis..

Mots-clefs : structures en béton armé, analyse de fiabilité, format des coefficients partiels de sécurité, analyse de sensibilité des exposants, analyse non linéaire, modes de rupture multiples, analyse basée sur les déformations, quantification de l'incertitude du modèle, inférence bayésienne, systèmes fragiles, béton textile.

摘要

工程计算是对现实世界的一种近似，不可避免地会引入不确定性。因此，在结构设计和评估中，有必要考虑不确定性开展可靠度校核。目前基于概率论的分项系数被广泛应用于结构设计规范的结构可靠度校核条文中。伴随着工程知识技术的发展，安全系数也需要相应地标定和更新。

对于钢筋混凝土结构，随着非线性结构抗力分析方法（例如基于应变的抗力分析和非线性有限元分析等数值方法）的广泛使用和新材料的应用，安全系数系统标定面临着一些新的挑战。本项研究在分项安全系数的框架体系内研究了以下几个问题：

本论文的第一部分，针对隐式的非线性结构分析模型中多重失效模式的影响，首先研究了经典钢筋混凝土结构抗力分项系数标定过程中所采用的简化和假设的适用性。基于不同尺度结构承载力（截面、构件和体系）的可靠度案例分析表明，应用于材料强度变量的分项系数可以实现有效的可靠度校核，并且不受材料不确定性引发的多重失效模式的影响。

本论文的第二部分，以基于"临界斜裂缝理论（CSCT）"的冲切抗剪模型为例，研究了基于应变的抗力分析方法的模型不确定性特点。结果表明，对此类模型，抗力解的总模型不确定性可被视为子模型不确定性的结果；而总模型的不确定性可能小于子模型的不确定性；他们之间的关系取决于总模型与子模型之间的敏感性关系。针对这一特点，提出了两种适用于基于应变的抗力模型的分项系数体系。此外，本研究还阐明了第二代欧洲混凝土结构设计规范中针对新结构设计和既有结构评估的冲切抗剪模型分项安全系数之间的关系。

本论文的最后一部分研究了脆性结构的安全系数标定问题。以织物增强混凝土结构（TRC）抗弯分析的分项安全系数为例，研究了脆性结构体系的内力分析模型的不确定性特点及其对此类结构的可靠度与安全系数的影响。

本文研究表明，对基本不确定性（材料，几何尺寸和模型不确定性）合理概率建模是有效标定分项系数基础，而基本不确定性的概率建模则需要基于对结构承载机制的全面认知。在此基础上，无论对于经典的显式设计公式还是更为复杂的非线性结构抗力分析方法而言，由施加于主导的不确定性上的分项系数组成的分项安全系数体系都是一项有效的结构可靠度验核手段。

关键词: 钢筋混凝土结构, 可靠度分析, 分项安全系数体系, 指数敏感性分析, 非线性分析, 多重失效模式, 基于应变的结构抗力分析, 模型不确定性量化, 贝叶斯推断, 脆性结构体系, 织物增强混凝土.

x

Contents

Chapter 2 Considerations on the partial safety factor format for reinforced concrete structures accounting for multiple failure modes $\qquad$ 11

Chapter 3 Model uncertainties and partial safety factors of strain-based approaches for structural concrete: example of punching shear   51

Chapter 4   A consistent safety format and design approach for brittle systems and application to Textile Reinforced Concrete structures   95

Chapter 1

Introduction

1.1　Structural reliability and partial safety factor format

It is pointed out in [CEB80a] that until the 19th century, all constructions were performed based on empirical design and safety depended on the experience and intuition of the builders. In the 19th century, with the invention of metallic structures and the "Strength of Materials", the concept of safety limit appeared in the form of allowable stress which were then considered by a "safety coefficient" applied to the material strength. The modern probability-based structural safety concept can be traced back to the 1920s. In the book "The Safety of Structures" (in German: Die Sicherheit der Bauwerke [May26]), Max Mayer proposed to calculate the safety factors for the loads, geometrical quantities and material strengths consistently with their mean values and standard deviations respectively and accounting for the concept of error propagation.

Significant progress of the probabilistic-based structural safety theory and its application to codified design was made from the 1940s to the 1990s. Works on the relevant concepts (the interpretation of the probability of structural failure, categorization of uncertainties, limit states, action models, load combination models etc.)[CEB80a, CEB80b, CEB88, Ell78, Ell80, ISO86] and the reliability analysis approaches based on the First Order Reliability Method [Fre56, Cor69, Ros72, Has74] led to the formulation of the detailed probability-based partial safety factor format in modern design codes.

The typical partial safety factor format used in structural design codes is briefly introduced in the following.

The basic form of the structural reliability problem is the classical "R and E" problem [CEN02, Sch17], where E refers to the action effect and R refers to the corresponding structural resistance. Considering R and E as random variables, the probability of failure P_f and the corresponding reliability index β for a given limit state are defined as:

$$P_f = \mathrm{P}(R - E \leq 0) \tag{1}$$

$$\beta = -\Phi^{-1}(P_f) \tag{2}$$

Where $P(\cdot)$ is the probability function and $\Phi^{-1}(\cdot)$ is the reversed cumulative distribution function of the standard normal distribution.

The structural safety verification is performed by checking that the reliability index of the relevant limit state is not lower than the target reliability index: $\beta \geq \beta_t$. The target reliability index β_t is defined based on the acceptable risk of failure of society, the economic criteria as well as the accumulated experience of the engineering profession form past practice [Dit96, Ell94]. For example, for the ultimate limit state of structures with medium consequence class with a 50 years reference period, a target reliability index of $\beta_t = 3.8$ is required in EN 1990 [CEN02] and *fib* Model Code 2010 [FIB13].

In design codes, the verification of structure reliability is further simplified by the so-called semi-probabilistic approach [CEN02], in which the verification of $\beta \geq \beta_t$ is transferred into the verification that the design resistance R_d is no lower than the design action effect E_d:

$$E_d \leq R_d \tag{3}$$

Within the FORM framework [Has74], the design values (R_d and E_d) should be based on the values of the basic variables at the FORM design point. The basic principle of the FORM is to calculate probability of failure (and the corresponding reliability index) by performing a first order Taylor expansion of the limit state function at the FORM design point, which is the point on the limit state surface ($R - E = 0$) closest to the mean value point in the standard normalised space (where the basic variables are transformed into standard normal distribution random variables). The FORM is based on the fact that the Joint Probability Density Function (JPDF) in the standardized normal space is axisymmetric and its value is rapidly decreasing with the increasing distance from the mean value point. A qualitative illustration of the location of the FORM design point is plotted in Figure 1.1 assuming that both R and E are normally distributed random variables.

With the help of the FORM sensitivity factors α_E and α_R (refer to Figure 1.1) [Has74], the reliability verification can be further separated to the action effect side and the resistance side:

$$P(E \geq E_d) = \Phi(\alpha_E \beta) \tag{4}$$

$$P(R \leq R_d) = \Phi(-\alpha_R \beta) \tag{5}$$
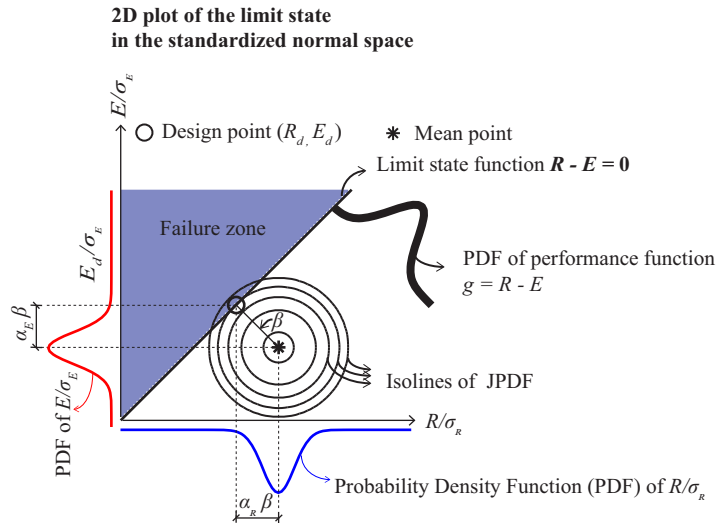
Figure 1.1:   Illustration of the reliability index and the FORM design point for the limit state function $R - E = 0$ assuming independent normal distributions of R and E (figure adapted from EN 1990:2002 [CEN02])

The limit state function plotted in Figure.1.1 can be seen as the simplest form of the structural reliability problem. In design practice, both the resistance and the action effect involve multiple sources of basic uncertainties and the limit state function can have complex shape in high dimension space. A general summary of the basic uncertainties involved in the structural design problem is shown in Figure 1.2.
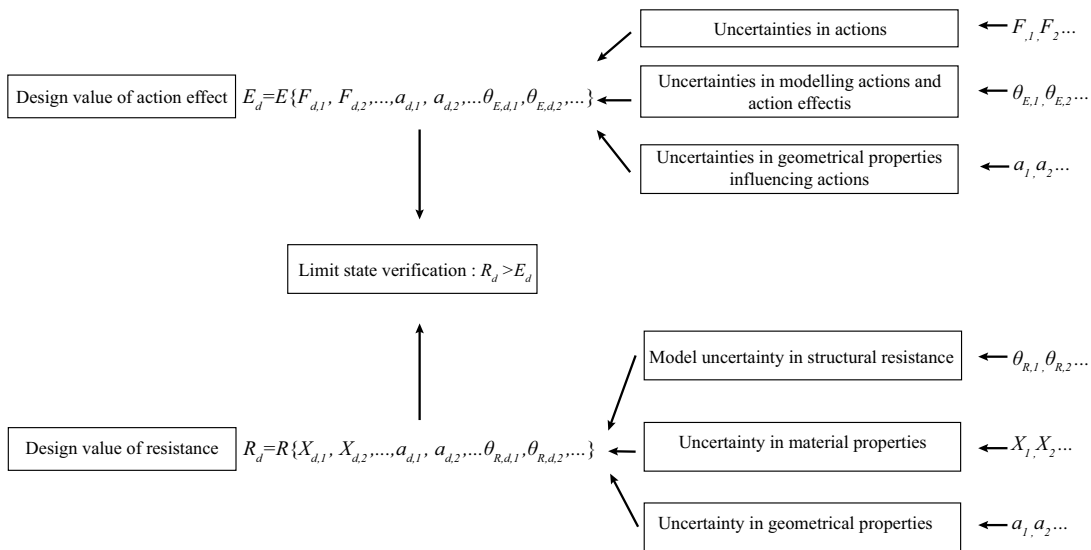
Figure 1.2:   Summary of the basic uncertainties involved in structural design

Accounting for different sources of basic uncertainties (Figure 1.2) and using the FORM concept, the design action effect and design resistance can be assumed to be calculated with the

design values of the basic random variables (refer to Figure 1.2 for notations of basic uncertainty variables):

$$E_d = E\{F_{d1}, F_{d2}, ..., a_{d1}, a_{d2}, ... \theta_{E,d1}, \theta_{E,d2}, ...\} \tag{6}$$

$$R_d = R\{X_{d1}, X_{d2}, ..., a_{d1}, a_{d2}, ... \theta_{R,d1}, \theta_{R,d2}, ...\} \tag{7}$$

The design values of the basic variables can be calculated with the suitably calibrated partial safety factors for the basic variables. Theoretically, an individual partial safety factor can be calibrated for each basic random variable accounting for the shape of the limit state function of each specific case to achieve the exactly target reliability level. This approach is however not applicable to daily engineering practice. Instead, usually some assumptions are made in order to simplify the safety format calibration for codified design.

The first common assumption is to adopt standardized FORM sensitivity factors for the action effect and the resistance side respectively. For example, in EN 1990:2002 [CEN02]) , it is suggested that the values of $\alpha_E = -0.7$ and $\alpha_R = 0.8$ can be adopted provided that the ratio between the standard deviations of the action effect and the resistance is within the limit between 0.16 and 7.6 [CEN02, Kön81]. This assumption makes it possible to calibrate the partial safety factors on the action side and the resistance side separately and also to calibrate the partial safety factors for actions regardless of the type of construction material, which significantly simplifies the safety format in practice.

Another important simplification is that typically some partial safety factors for different basic variables are lumped together to reduce the total number of the partial safety factors in the design format. For example, for the design resistance, it is suggested in EN 1990:2002 [CEN02] that the partial safety factors for the geometrical, material and model uncertainties (denoted as Δa, γ_m and $\gamma_{R,d}$ respectively) may be applied individually in the design resistance equation (see Figure 1.3) or they can be lumped into the partial safety factors applied to material strength variables directly (denoted as γ_M, see Figure 1.4).
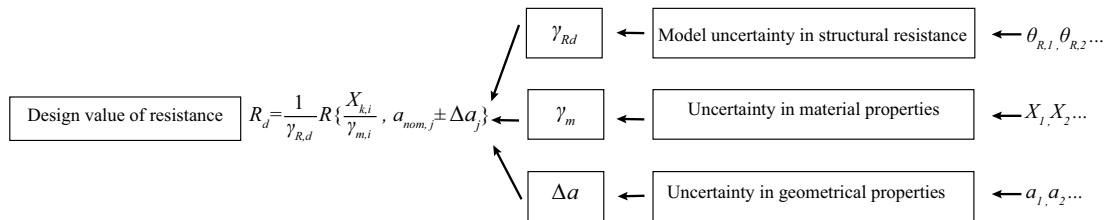
Figure 1.3: Format for the design resistance of structures composing of partial safety factors accounting for geometrical, material and model uncertainties individually
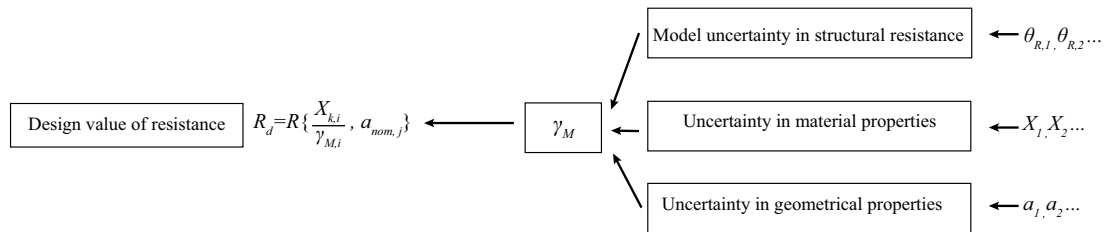
Figure 1.4:   Safety format for the design resistance of structures composing of partial safety factors applied to material strength variables (accounting for geometrical, material and model uncertainties integrally)

The partial safety factor format (with possible simplification of lumping several partial safety factors together) should be optimized in order to make the representative structures achieve a reliability index as close as possible to the target level. The choice of the safety format needs to account for the dominating uncertainties (which depends on the variability of basic uncertainties and the sensitivity of the structural resistance to them) and also the convenience of use for engineering practice.

In this thesis, the scope is limited to the safety format calibration problem of the resistance side of reinforced concrete structures. In the following section, the new challenges in this field are briefly introduced.

1.2   Reliability analysis and safety format calibration for the resistance of reinforced concrete structures: open questions

For reinforced concrete structures, despite the wide application of the partial safety factor format in codified design, open questions emerge with the increasing application of advanced nonlinear structural resistance analysis approaches (e.g. strain-based design approaches and numerical methods like the NonLinear Finite Element Analysis) as well as the application of new materials.

The first fundamental question is the influence of multiple failure modes on the reliability of design resistance of reinforced concrete structures. In suitably designed reinforced concrete structures, the concrete and steel reinforcement are supposed to sustain the compression and tension forces respectively in order to make full use of the advantages of both materials. From this perspective, reinforced concrete structures have multiple failure modes by design (dominated by concrete compression failure and steel yielding failure respectively). Based on this consideration, a widely used partial safety factor format for the resistance of reinforced concrete structures is composed of two partial safety factors, γ_C and γ_S, applied to the material strength variables for concrete and steel reinforcement respectively (this type of partial safety format is applied in [CEN04, FIB13, TÉC14, GB10] and other design standards inspired

on CEB-FIP Model Code 90 [CEB93] and previous versions [CEB64]). This pair of partial safety factors are usually considered suitable when the design resistance of structures is evaluated by analytical design equations. However, when nonlinear analysis methods are used and potentially multiple action effects and the corresponding failure modes are verified simultaneously, the effectiveness and the applicability of these partial safety factors needs to be further investigated [All13, Cer08, Sch11].

Another crucial question is the model uncertainty quantification of nonlinear structural resistance models [Cas18, Cer18, Eng17, Hau11, Kad15, Sch11]. With the increasing complexity of the structure resistance models, the complexity of the model uncertainty is also increased. A typical example can be found in the strain-based punching shear resistance model of the Critical Shear Crack Theory [Mut08], which is composed of two sub-models: the failure criterion model and the load-rotation relationship. The punching shear resistance is calculated by solving the equation set of these two sub-models. In this case, the model uncertainty can be represented and quantified at the sub-model level or at the global resistance solution level. Proper quantification of the model uncertainties and interpretation of the relationship between the model uncertainties of the global resistance solution and those of the sub-models is a fundamental question for the safety format calibration of such models.

Last but not least, the partial safety format needs to be re-evaluated when the structural response is different from that of ordinary concrete structures. This is typically the case when new types of reinforcement materials are applied. For example, when reinforcement with brittle behaviour is used (e.g. Textile Reinforced Concrete with carbon or glass fabric [Val17]), the simplifications and assumptions in the partial safety format of reinforced concrete structures needs to be re-evaluated regarding the change of the internal force redistribution capacity. For the design of ordinary concrete structures, when sufficient redistribution capacity can be assumed (e.g. for the flexural resistance of suitably reinforced beams), the model uncertainty in the calculation of the action effect in structural members has a relatively low influence on the structural reliability. However, since the redistribution capacity of the structure is limited when brittle reinforcement material is used, the action effect model uncertainty can have more significant influence and needs to be properly accounted for in its safety format calibration.

1.3   Objective of the thesis

Following the context described above, the general objective of this work is to re-evaluate the partial safety factor format framework for the design resistance of reinforced concrete structures considering the challenges related to nonlinear structural resistance analysis approaches (e.g. the strain-based approach for punching shear resistance [Mut08] and the NonLinear Finite Element

Analysis) as well as the application of new materials (e.g. Textile Reinforced Concrete [Val17])). More specifically, the objectives are the following:

- To develop a suitable sensitivity analysis tool for the resistance of reinforced concrete structures that is convenient to use for the task of safety format calibration

- To understand the similarities and differences between the explicit (e.g. classical design equations) and implicit nonlinear structural resistance analysis models (e.g. strain-based approaches and Nonlinear Finite Element Analysis in general) for concrete structures from the perspective of reliability analysis

- To understand how the multiple failure modes involved in the implicit structural resistance models of reinforced concrete structures influence the reliability of the design resistance and to verify the applicability of the partial safety factor format in such cases

- To investigate the relationship between the model uncertainties of the global resistance solution and the sub-models of the strain-based approaches for reinforced concrete structures based on relevant experimental data and to develop a suitable model uncertainty quantification approach for similar nonlinear analysis approaches

- To investigate the suitable partial safety format for the strain-based punching shear resistance model based on the Critical Shear Crack Theory

- To quantify the potentially increased action effect model uncertainty of reinforced concrete structures with brittle behaviour and to calibrate the partial safety factors for the flexural resistance design of Textile Reinforce Concrete structures on its basis

1.4   Structure of the thesis

This work is a compilation of three scientific articles. In addition to the Introduction, the four chapters included in the thesis are described below:

- Chapter 2 presents an article published in the scientific journal *Engineering Structures* [Yu22]. This chapter presents a systematic investigate of the influence of the multiple failure modes induced by material uncertainties on the reliability of design resistance of reinforced concrete structures when the classical partial safety factor format (composed of two safety factors applied to material strength variables) is applied. Cases with increasing complexities in terms of the interaction between failure modes are investigated in order to clarify the consistency and applicability of the partial safety factors to such cases. In addition, the suitability of the simplification of lumping the safety element for geometrical and model uncertainties into the partial safety factors for the material strength variables is discussed on the basis of the exponent sensitivity analysis of typical cases.

- Chapter 3 presents an article that is submitted to the scientific journal Engineering Structures [Yu23]. In this work, the model uncertainties of strain-based approaches for structural concrete are investigated using the punching shear resistance model of the Critical Shear Crack Theory (CSCT) as an example. The relationship between the model uncertainties of the sub-models and the global resistance solution in the strain-based approach is investigated through evaluation of the statistics of the model uncertainty data gathered based on relevant experimental test results. Furthermore, the model uncertainties of the different Levels-of-Approximation (LoAs) of the punching shear resistance are also quantified and compared. On the basis of the model uncertainty quantification result, different safety formats for the design models of strain-based approaches are compared, focusing particularly on the provisions for the punching shear design according to the new generation of Eurocode 2.

- Chapter 4 presents an article published in the scientific journal Engineering Structures [Yu21]. In this work, the consistent design and safety format calibration of brittle reinforced concrete structure systems is investigated. The model uncertainty of the action effect in brittle systems of textile reinforced concrete structures is investigated based on test data and the result is applied to the calibration of the partial safety factors for the textile reinforced concrete structures subjected to flexural failure mode.

- Chapter 5 summarizes the main conclusions of the thesis and discusses topics for future research.

- Appendix A presents an example of the partial safety format calibration of the mechanical-based anchorage strength model of shear reinforcement in beams and slabs applying the methodology developed in this work.

It should be noted that Chapter 2 to 4 include their own introduction, literature review, conclusions, annexes and notations as the present thesis is a compilation of journal articles (paper-based thesis). The full bibliography is provided at the end of the thesis.

1.5   Scientific contribution of the thesis

The main contributions of this thesis can be summarized as following:

- A simple and intuitive local sensitivity analysis method (the exponent sensitivity analysis) is proposed to provide sensitivity information of the resistance models of reinforced concrete structures that can be conveniently used in the approximated reliability analysis with the FORM.
- The exponent sensitivity analysis results of typical resistance models of reinforced concrete structures (e.g. the cross-sectional bending resistance, the in-plane shear

resistance of reinforced concrete panel, the coupled bending and shear resistance of reinforced concrete girder) are presented.

- On the basis of the exponent sensitivity analysis result, the influence of the occurrence of multiple failure modes induced by material uncertainties on the reliability of the design resistance of reinforced concrete structures is clarified.
- The methodology for the suitable representation and quantification of the model uncertainties of strain-based approaches for reinforced concrete structures is presented and applied to the punching shear resistance model of the Critical Shear Crack Theory (CSCT).
- The relationship between the model uncertainty of the global resistance solution and those of the sub-models of strain-based approaches is established based on the exponent sensitivity analysis.
- The suitable safety format for different Levels-of-Approximation (LoAs) of the punching shear resistance models of the CSCT are provided.
- The methodology for quantification of the action effect model uncertainty of structural systems based on test data of structural elements is developed. The action effect model uncertainties of brittle reinforced concrete structural systems of Textile Reinforced Concrete (TRC) beams are quantified using the proposed approach.
- Partial safety factor format for the flexural resistance design of TRC structures is calibrated accounting for the brittle behaviour as well as the influence of the potentially low thickness of TRC structural elements compared with traditional reinforced concrete structures.

1.6 Limitations of the thesis

This work is limited to the resistance side of reinforced concrete structures. The uncertainties and the safety factor calibration of the actions are not investigated. In addition, this work is limited to the Ultimate Limit State (ULS) verification of structures.

No data is collected regarding the material strengths and the geometrical uncertainties in ordinary reinforced concrete structures. This work is performed based on established probabilistic models of these uncertainties from literature.

The influence of the spatial variation and correlation of the basic geometrical, material and model uncertainties on the reliability of concrete structures is not investigated in this work.

1.7 List of publications

The research was conducted at the Stuctural Concrete Laboratory (IBETON) of the Swiss Institute of Technology of Lausanne (Ecole polytechnique Fédérale de Lausanne, EPFL) resulting in the following publications:

- **Yu Q, Fernández Ruiz M., Muttoni A.,** *Considerations on the partial safety factor format for reinforced concrete structures accounting for multiple failure modes*, Engineering Structures, Vol. 264, 114442, 2022.
  DOI: https://doi.org/10.1016/j.engstruct.2022.114442

- **Yu Q., Valeri P., Fernández Ruiz M., Muttoni A.,** *A consistent safety format and design approach for brittle systems and application to textile reinforced concrete structures*, Engineering Structures, Vol. 249, 113306, 2021.
  DOI: https://doi.org/10.1016/j.engstruct.2021.113306

- **Yu Q., Simões J. T., Fernández Ruiz M., Muttoni A.,** *Model uncertainties and partial safety factors of strain-based approaches for structural concrete: example of punching shear*, Engineering Structures. [submitted, March 2023].

- **Moccia F., Yu Q., Fernández Ruiz M., Muttoni A.,** *Concrete compressive strength: From material characterization to a structural value*, Structural Concrete, Vol. 22, E634-E654, 2021.
  DOI: https://doi.org/10.1002/suco.202000211

- **Monney F., Yu Q., Fernández Ruiz M., Muttoni A**., *Anchorage of shear reinforcement in beams and slabs*, Engineering Structures, Vol. 265, 114340, 2022.
  DOI: https://doi.org/10.1016/j.engstruct.2022.114340

Chapter 2

Considerations on the partial safety factor format for reinforced concrete structures accounting for multiple failure modes

This chapter is the post-print version of the article mentioned below, published in Engineering Structures Journal. The authors of the article are Qianhui Yu (PhD Candidate), Prof. Miguel Fernández Ruiz and Prof. Aurelio Muttoni (thesis director). The reference is the following:

Yu Q., Fernández Ruiz M., Muttoni A., *Considerations on the partial safety factor format for reinforced concrete structures accounting for multiple failure modes*, Engineering Structures, Vol. 264, 114442, 2022. (DOI: https://doi.org/10.1016/j.engstruct.2022.114442)

The work presented in this publication was performed by Qianhui Yu collaborating with Prof. Miguel Fernández Ruiz and under the supervision of Prof. Aurelio Muttoni, who provided constant and valuable feedback, proofreading and revisions of the manuscript.

The main contributions of Qianhui Yu to this article and chapter are the followings:

- Comprehensive literature review regarding the application of partial safety factor format and global safety factor format for the codified design of reinforced concrete structures.

- Proposition of a simple and intuitive sensitivity analysis approach (exponent sensitivity analysis) to quantitatively represent different failure modes.

- Reliability analysis of typical resistance models of reinforced concrete structures at difference scales (cross-sectional resistance or load-bearing capacity of structural element and simple structural systems).

- Interpretation of the reliability analysis result for typical resistance models with a detailed analysis of the shape of the corresponding limit state functions and the exponent sensitivity analysis.

- Clarification of the influence of multiple failure modes induced by material uncertainties on the achieved reliability of design resistance for reinforced concrete structures with the partial safety factor format.

- Interpretation of the influence of tail approximation in the reliability analysis of the resistance of reinforced concrete structures.

- Proposition of a simple and practical test procedure for the validity of the non-decreasing assumption of the structural resistance model and the corresponding applicability of the partial safety factor format.

- Elaboration of the figures and tables included in the article.

- Writing of the manuscript of the article.

Abstract

The increasing usage of nonlinear analyses for the design of reinforced concrete structures and the necessity of codes of practice to provide a consistent safety format for them is one of the challenges that new generations of codes of practice are facing. Suitable safety formats shall thus account for the peculiarities of nonlinear analysis, such as the possibility of having multiple potential failure modes. In this work, the applicability of the classical Partial Safety Factor Format (PSFF) for the resistance of reinforced concrete structures (composed of two safety factors: γ_C for concrete compressive strength and γ_S for reinforcement yield strength) is investigated accounting for the possibility of multiple failure modes in nonlinear analysis. In addition, the similarities between nonlinear analysis and typical simple cases in the design of structural concrete are shown. Reliability analysis is performed for the design resistance of concrete structures according to PSFF under different design situations (cross-sectional resistance or load-bearing capacity of structural elements and of simple structural systems). The results show that the PSFF applied to material strength variables leads to a satisfactory level of reliability, independently of the development of different failure modes induced by material uncertainties in nonlinear analysis. In addition, it is also observed that the simplification of integrating geometrical and model uncertainties into the partial safety factors for material strength variables can potentially underestimate their influence on the structural reliability in some cases. The case studies shows that occurrence of multiple failure modes can result into significantly different distribution characteristics between the tail and most probable region of the resistance of concrete structures. Attention should also be paid to a proper tail approximation of the probability distribution of the resistance when calibrating safety formats for concrete structures.

Keywords: reliability verification, partial safety factor format, structural concrete resistance, multiple failure modes, nonlinear finite element analysis

2.1 Introduction

Every engineering calculation is an approximation of reality, with unavoidable epistemic and aleatoric uncertainties. This fact implies that a reliability verification is a necessary step within a design or verification procedure, as provisioned in codes of practice under various formats. Within this context, the Partial Safety Factor Format (PSFF) is one of the most widely adopted approaches to ensure reliable designs, due to its robustness, simplicity and generality [Dit96].

The PSFF results from the application of the semi-probabilistic approach, in which the reliability verification is simplified to verify if a structure fulfils a given set of inequalities using design values of the basic variables [CEN02]. The reliability requirement is accounted for in the design values of the basic variables by means of partial safety factors calibrated on the basis of

reliability analysis. A major advantage of PSFF is that it can be formulation-invariant [Dit96]. Different forms of PSFF are used in modern design codes for structures, which result from the different choices in the assumptions and simplifications adopted in the calibration procedures. One widely used simplification in the PSFF is to calibrate the partial factors on the resistance and action side separately by adopting standardized First Order Reliability Method (FORM) sensitivity factors [CEN04, FIB13, Kön81]. This treatment largely reduces the complexity of the safety format calibration and also makes it possible to use a fixed set of partial factors on the action side, independently of the material used for construction. It also allows to define the partial safety factors for materials independently of the governing loading situation. For the evaluation of the resistance of structures, with particular application to structural concrete, there are two major approaches to implement the PSFF [Ell80]:

- Providing partial safety factors for calculating the design values of material strength variables. This PSFF is adopted in many design codes, such as Eurocode 2 for concrete construction (EN1992-1-1:2004) [CEN04], Model Code 2010 [FIB13] , the Brazilian standard NBR 6118:2014 [TÉC14] , the Chinese standard GB50010-2010 [GB10] and other design standards inspired on the CEB-FIP Model Code 90 [CEB93] and previous versions [CEB64] .

- Providing tailored partial safety factors for calculating the design value of a structural member's resistance for different action effects (such as axial force, bending or shear). This approach is for instance implemented in American standards (such as ACI 318-19 [ACI19] and AASHTO LRFD [AAS20]), the Canadian standard CSA A23.3 [CSA14] and the Australian standard AS3600-2018 [Sta18].

The PSFF implemented on material strength variables will be the focus of this work, consistently with the provisions of Eurocode 2 for concrete construction (EN 1992-1-1:2004 [CEN04]). In this approach, the partial safety factors of concrete and reinforcement strength are calibrated separately, accounting for different values of material, geometrical and model uncertainties. The partial safety factor of concrete (γ_C) is typically calibrated using probabilistic modelling of basic geometrical and model uncertainties of compression members, where the reinforcement uncertainties are neglected. Conversely, the partial safety factor of reinforcing steel (γ_S) is typically calibrated based on data of bending of a cross section with moderate reinforcement ratio, which is the most common case where γ_S applies [Eur08]. As it can be noted, no interactions between the two materials are explicitly accounted for in the safety format calibration [Eur08]. Such an approach is very simple to use and to understand by designers, but has received criticism particularly concerning nonlinear analysis [All13, Cas19, Cer08, Sch12]. Whether this classical combination of safety factors of γ_C and γ_S for reinforced concrete structures is still suitable to be extended to nonlinear analysis method has been discussed extensively in the development process of the 2nd generation of Eurocode for concrete structure [CEN23]. The main concerns with this respect deal with the potential development of

different failures modes, particularly when Nonlinear Finite Element Analysis (NLFEA) is performed[All13, Cas19, Sch12] to assess structural resistance.

In nonlinear analyses, usually, there is no closed-form solution for the resistance as a function of the basic design variables and the shape of the limit state function may vary from case to case [Bel15, Syk18, Yu20]. Furthermore, when NLFEA is used, different types of action effects and failure modes are implicitly verified at the same time, leading to a complex limit state function. The safety format calibration procedure for this type of problem is thus not straightforward.

Research efforts have been devoted in the past to the study of safety formats for NLFEA of concrete structures at ultimate limit state [All13, Ben12, Cas19, Cer08, Pim14, Sch11, Sch12]. An alternative to PSFF to account for reliability in design are approaches based on the Global Safety Factor Format (GSFF). For reinforced concrete structures and nonlinear analysis, developments have been proposed by Ben Ftima et al. [Ben12], Cervenka et al. [Cer08], Schlune et al. [Sch12] and Allaix et al. [All13]. In these approaches, the resistance random variable is approximated with a given type of probabilistic distribution (usually lognormal) and by statistics of resistance data of sampling points around the mean values of the basic variables. An obvious drawback of these methods is that the sampling points used for the distribution parameter estimation of the resistance variable are potentially far away from the limit state function and the tail distribution of the resistance variable. This can lead to poor fit of the probabilistic distribution of the resistance variable in the tail region [Pim14], which is a the most relevant region concerning structural reliability [Rac77, Sch17]. In addition, the goodness-of-fit in the tail region is difficult to investigate on the basis of standard tests [Dit94, Der09]. Besides the above-mentioned methods, other approaches to the safety format problem for NLFEA have also been developed. For instance, Castaldo et al. [Cas19] have proposed a method based on testing whether multiple failure modes exist (by checking if sets of sampling points have the same failure modes). In such case, it is proposed in [Cas19] to consider an additional safety factor accounting for the influence of multiple failure modes.

In this work, the applicability of PSFF to cases involving multiple failure modes is investigated. The manuscript presents in a detailed manner the simplifications and assumptions used in PSFF to consider multiple failure modes. These concepts are eventually applied to a number of case studies focusing on nonlinear analyses for structural concrete design. The cases are selected to have increasing complexity in terms of the interaction between failure modes, in an effort to clarify the consistency and applicability of the PSFF to such cases. Since the issue of multiple failure modes is usually considered as a consequence of the combination of different material strengths [Cas19], this work will focus first on material uncertainties. Subsequently, the question of proper consideration of geometrical and model uncertainties will be addressed.

2.2 Partial safety factor format for structural concrete design

2.2.1 Assumptions and simplifications of the PSFF formulation

In the reliability verification of reinforced concrete structures, the limit state functions for the resistance to different action effects have different forms. Ideally, to achieve a uniform reliability level, the partial safety factors for material strengths need to be calibrated for each individual case according to the pertinent limit state function. A direct application of such approach, considering different partial safety factors for different structural verifications, may however be inconvenient for practice. As a consequence, some simplifications are usually assumed when deriving partial safety factors for the design and the verification of reinforced concrete structures.

In Eurocode 2 [CEN04], the calibration of partial safety factor γ_M for material strengths is based on the principles of the First Order Reliability Method (FORM) [CEN02, Has74]. Background to the application of this approach in Eurocode 2 [CEN04] is provided in its commentary [Eur08], where the following equation is introduced to calculate the partial safety factors for concrete and reinforcement:

$$\gamma_M = \frac{f_k}{f_d} = \exp(\alpha_R \beta_t V_R - 1.64 V_f) = \exp(3.04 V_R - 1.64 V_f) \tag{1}$$

$$V_R = \sqrt{V_{mod}^2 + V_{geom}^2 + V_f^2} \tag{2}$$

Where γ_M is the partial safety factor for material strength; f_k and f_d are the characteristic and the design value of material strength, respectively; α_R is the standardized FORM sensitivity factor for resistance (typically $\alpha_R = 0.8$ [CEN02, Kön81]; β_t is the target reliability ($\beta_t = 3.8$ for the ultimate limit state of structural elements with moderate consequence class with 50 years reference period [CEN02]; V_R is the Coefficient of Variation (CoV) of the resistance random variable; V_{mod}, V_{geom} and V_f are the CoV of model, geometrical and material uncertainties, respectively. The value of -1.64 in Eq.(1) refers to the 5% fractile of a standard normal distribution, resulting from the fact that the partial factor is used to calculate the design value of the material strength on the basis of the 5% fractile characteristic value. It should be noted that the formulation of Eq. (1) assumes both the resistance and the material strength follow lognormal distributions.

It can be observed from Eqs. (1) and (2) that since the standardized FORM sensitivity factor (α_R = 0.8 [CEN02, Kön81]) for resistance is adopted, the target reliability index for the design resistance is set as $\alpha_R \beta_t$. Correspondingly, the failure probability for the design resistance (denoted as $P_{f,R}$) can be defined as the probability of the resistance being lower than the design

value ($P_{f,R} = P(R - R_d \leq 0)$) and its corresponding target value is set as $P_{f,tag,R} = \Phi(-\alpha_R \beta_t)$. It should be noted that $P_{f,R}$ is different from the failure probability of the structure (denoted as P_f), since P_f refers to the probability of the resistance being lower than the action effect ($P_f = P(R - E \leq 0)$). The target failure probability for the structure is $P_{f,tag} = \Phi(-\beta_t)$. It can be noted the value of $P_{f,tag,R}$ is higher than $P_{f,tag}$. In this work, the scope is limited to the resistance side (the limit state of $R - R_d = 0$ and the corresponding reliability index of $\alpha_R \beta_t$). It should be noted that parameters on the action side (e.g. the ratio of design variable load to the total design load [Pac21]) can have a significant influence on the applicability and adequacy of the standardized sensitivity factor α_R. This aspect will not be explicitly addressed in this work, which focusses on the multiple failure modes problem on the resistance side and its reliability implications.

Eqs. (1) and (2) also show that for each material, the random variables representing model and geometrical uncertainties are lumped with the material uncertainty into one random variable. This is a simplification of the resistance function whose suitability will be discussed in Section 2.9 of this work. In addition, the partial safety factors for concrete and steel reinforcement are calibrated separately. This treatment can be seen as another simplification of the limit state function, implying that two limit state functions are verified independently: one governed by concrete compressive strength only and another governed by steel yield strength only. These two limit states will be referred to as Boundary Limit States (BLSs). Applying PSFF ensures that the probability of failure for each BLS ($P_{f,R,i}$) respects the target probability of failure for resistance ($P_{f,tag,R}$):

$$P_{f,R,i} = P(F_i) = P(f_i \leq f_{id}) = \Phi(-\alpha_R \beta_t) = P_{f,tag,R} \qquad i = 1, 2 \qquad (3)$$

where $P_{f,R,i}$ is the probability of failure for boundary limit state i, $P(\cdot)$ is the cumulative probability function, F_i is the failure domain of boundary limit state of material i, f_i is the random variable of strength of material i, f_{id} is the design value of material i, $\Phi(\cdot)$ is the Cumulative Distribution Function (CDF) of standardized normal distribution, $P_{f,tag,R}$ is the target probability of failure for resistance, and $i = 1, 2$ refers to steel reinforcement and concrete, respectively.

When considering the material uncertainty only (the issue of model and geometrical uncertainties will be discussed later in Section 2.10), the shape of the two BLSs can be plotted in the standard normal space as shown in Figure 2.1, where X_{f_y} and X_{f_c} represent the yield strength of the reinforcement and the concrete compressive strength random variable transformed into the standard normal space (where both variables are transformed into standard normal distributed random variables). In the case that both material strengths are assumed to follow lognormal distribution, the transformation function are as follows:

$$X_{f_y} = \frac{\ln(f_y) - \mu_{\ln f_y}}{\sigma_{\ln f_y}} \qquad (4)$$

$$X_{f_c} = \frac{\ln(f_c) - \mu_{\ln f_c}}{\sigma_{\ln f_c}} \tag{5}$$

Where X_{f_y} and X_{f_c} are the material strength random variables transformed to the standard normal space, f_y is the reinforcement yield strength, f_c is the concrete compressive strength, $\mu_{\ln f_y}$ and $\mu_{\ln f_c}$ are the mean values of the logarithmic material strength random variables and $\sigma_{\ln f_y}$ and $\sigma_{\ln f_c}$ are the corresponding standard deviations.
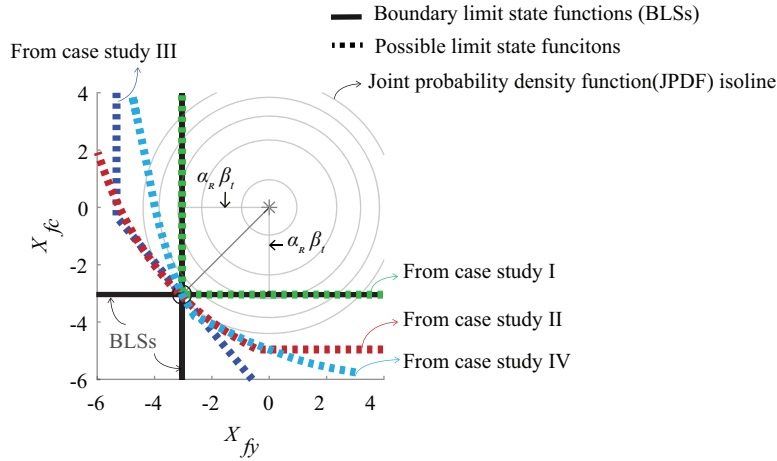
Figure 2.1:   Illustration of relation between actual limit state from case study I, II and IV in Section 2.4-2.7 and BLSs (X_{fy} and X_{fc} are the material strength random variables transformed to the standard normal space).

The actual limit state functions can be quite different from the BLSs (example of the shapes of actual limit state functions from case study I, II and IV in Section 2.4-2.7 are also plotted in Figure 2.1 for comparison). To make a connection between the actual limit state and BLSs, a reasonable assumption is made on the resistance function. The assumption is as follows: If some of the material strengths increase and the rest remains unchanged, the resistance of the structure will not decrease; if all the material strengths increase, the resistance will also increase (as for the assumption according to limit analysis [Pra51]). This assumption will be referred to as the *non-decreasing assumption* in the following. The suitability of this assumption will be discussed later. Based on the non-decreasing assumption of the resistance function, the sum of the two BLSs forms an envelope for the actual limit state, as is illustrated in Figure 2.1. An upper bound of the actual probability of failure can then be easily derived:

$$P_{f,R} = P(F) \leq P(F_1 \cup F_2) = P(F_1) + P(F_2) - P(F_1 \cap F_2) < 2 \cdot P_{f,tag,R} \tag{6}$$

Where F is the actual failure domain.

For a structural resistance subjected to two independent material strength random variables, applying PSFF, the upper bound for the actual probability of failure corresponds to twice the target value, $2P_{f,tag,R,}$ which seems to be within the acceptable range for reliability verification

using semi-probabilistic methods [Kön81], since the reliability index would decrease from 3.04 ($= \alpha_R \cdot \beta_t = 0.8 \cdot 3.8$, corresponding to a $P_{f,R} = 1.2 \cdot 10^{-3}$) to 2.82 ($P_{f,R} = 2 \cdot 1.2 \cdot 10^{-3}$) in the worst case.

From another perspective, the treatment of calibrating the partial safety factors for concrete and steel reinforcement strength separately can also be interpreted as both concrete and steel reinforcement strength are assumed to be dominating and both of their FORM sensitivity factors [Mad86] assumed equal to one:

$$\alpha_{f_{c,a}} = 1 \tag{7}$$

$$\alpha_{f_{y,a}} = 1 \tag{8}$$

Where $\alpha_{f_{c,a}}$ and $\alpha_{f_{y,a}}$ are the FORM sensitivity factors of concrete strength and of steel reinforcement yield strength, respectively (in addition to the standardized FORM sensitivity factor for resistance (α_R)). It should be emphasized that $\alpha_{f_{c,a}}$ and $\alpha_{f_{y,a}}$ are the FORM sensitivity factors corresponding to the limit state of $R - R_d = 0$ with the target reliability index of $\alpha_R \beta_t$.

From the FORM perspective, this seems a conservative assumption since the sum of squares of $\alpha_{f_{c,a}}$ and $\alpha_{f_{y,a}}$ are higher than one. The suitability of this assumption will however be examined by studying the shape of the actual limit state functions in some representative cases of concrete structures (see case studies presented in Sections 2.4-2.7).

From Figure 2.1, it can also be observed that by applying the PSFF, the distance from the closest point (the FORM design point) on the BLSs to the origin point in the standard normal space is limited to $\alpha_R \beta_t$. Since the actual limit state function is bounded by the BLSs (on the basis of the non-decreasing assumption), the distance from the FORM design point on the actual limit state function to the origin point should also not be smaller than $\alpha_R \beta_t$. In other words, PSFF ensures that the probability of failure estimated with FORM respects the target value.

It should be noted that in the previous derivation, only two basic variables, f_c and f_y, are considered for the material uncertainties. When other material parameters are dominating (for instance, the concrete tensile strength or the elastic moduli), additional considerations need to be taken into account.

The previous analysis shows that for a non-decreasing structural resistance, PSFF should yield a satisfactory reliability level with respect to material uncertainties. However, for cases where the non-decreasing assumption of the resistance function is invalid (as those governed by crack localization), the reliability verification is more complex, requiring to identify such cases by means of a simplified method as later discussed in Section 2.9.

The previous considerations show that the applicability of PSFF depends on the shape of the limit state function, which is governed by the mechanical response of the member. In Sections 2.4-2.7, the reliability analysis of some typical cases of reinforced concrete structural elements is investigated in detail. The actual limit state functions of these cases are compared with the

BLSs assumed by PSFF. The reliability analysis is performed for these cases to verify the result of the previous theoretical analysis. Before going into detail on the reliability analysis of concrete structures, a simple and intuitive sensitivity analysis method is introduced as a tool to quantitatively identify different failure modes and also to help interpreting the results of reliability analyses.

2.3   Exponent sensitivity analysis

Sensitivity analysis can describe how the variability of the model response is affected by the variability of each input variable or their combinations [Mar21]. It is a widely used tool for model interpretation and simplification [Ioo15]. In this section, a simple local sensitivity analysis method is developed for the resistance of reinforced concrete structures, in an effort to understand and to distinguish different failure modes. The partial derivatives of the logarithmic resistance to the logarithmic basic variables is used as the sensitivity factor and the finite-difference approximation method [Sal00] is used to calculate them. This local sensitivity factor is referred to as the "*exponent sensitivity factor*" (or only "*exponent*") in the rest of the work. The detailed procedure for derivation of the exponent sensitivity factor will be introduced and the motivations for using it will be explained more in detail in the following.

Consider the resistance R as a function of basic parameters $(f_1, f_2, ..., f_p)$:

$$R = R(f_1, f_2, ..., f_p) \tag{9}$$

Components of the basic parameter vector $(f_1, f_2, ..., f_p)$ can be any model parameter, including material strengths, material elastic moduli and geometrical parameters. The exponent sensitivity factors are defined based on the power multiplicative form approximation of the resistance function:

$$R \approx R_0 \cdot \prod_{j=1}^{p} \left(\frac{f_j}{f_{j,0}} \right)^{n_{f_j}} \tag{10}$$

Where R_0 is the resistance at a reference point $(f_{1,0}, f_{2,0}, ..., f_{p,0})$ and n_{f_j} is the exponent sensitivity factor for parameter f_j.

The approximation in Eq. (10) is equivalent to perform first order Taylor expansion of the logarithm of the resistance function in the logarithmic space of the model parameters. The exponent sensitivity factor n_{f_j} for each parameter f_i can be easily derived by calculating the direct differentiation of $\ln(R)$ over $\ln(f_j)$ numerically at the reference point:

$$n_{fj} = \frac{\partial(\ln(R))}{\partial(\ln(f_j))} \approx \frac{\ln(R(f_{1,0},...,f_{j,0} \bullet e^{\Delta},...,f_{p,0})) - \ln(R(f_{1,0},...,f_{j,0},...,f_{p,0}))}{\Delta} \tag{11}$$

Where Δ is a sufficiently small increment of parameter $\ln(f_j)$.

There are several considerations for using the exponent sensitivity factors in the reliability analysis of concrete structures:

According to dimensional analysis, the sum of all exponents of material strength variables and the elastic modulus variables should be equal to 1 (refer to Appendix 2.A for cases where the sum of exponents can be less than 1). The same consideration applies also to the geometrical variables (the sum of the exponents of the geometrical variables is equal to 2 for forces and equal to 3 for moments). This property can help making comparisons of the exponent sensitivity factors of material strength variables (and geometrical variables) between different failure modes.

When only material uncertainties are accounted for and they are modelled with lognormal distributions, the FORM sensitivity factors can be calculated directly from the exponent sensitivity factors and the CoV of the basic variables at the FORM design point by Eq.(12) and (13). In the following case studies, the exponent sensitivity factors of material strength variables are calculated at the PSFF design point (f_{yd}, f_{cd}). Although the position to calculate the exponent sensitivity factors are not strictly the FORM design point, the exponents can still give useful information for the reliability analysis. It should be noted that the intention of the proposed exponent sensitivity factors is not to replace the FORM sensitivity factors, but to provide additional sensitivity information that has direct link to the mechanical behaviour of concrete structures.

The exponent sensitivity factors provide valuable information about the mechanical behaviour of concrete structures, which are independent from the probabilistic models of the basic variables as well as from other assumptions and simplifications in the safety format calibration procedure. For a given resistance model, the exponent sensitivity factors for the full applicable range of the model are especially useful since they can be used for the safety format calibration accounting for different probabilistic models of the basic variables in different design situations.

$$\alpha_{f_{c,a}} = \frac{n_{fc}V_{fc}}{\sqrt{n_{fc}^2 V_{fc}^2 + n_{fy}^2 V_{fy}^2}} \tag{12}$$

$$\alpha_{f_{y,a}} = \frac{n_{fy}V_{fy}}{\sqrt{n_{fc}^2 V_{fc}^2 + n_{fy}^2 V_{fy}^2}} \tag{13}$$

Based on the above-mentioned considerations, the exponent sensitivity analysis is used for understanding and distinguishing different failure modes of concrete structures (i.e. which material or materials govern the resistance). In the following sections, the reliability analysis of

some typical concrete structure resistance cases will be studied and the exponent sensitivity analysis will also be performed to help interpret the results of reliability analysis.

2.4 Case study I: System with uncoupled concrete and steel failure

2.4.1. Definition of the case study

In this section, a simple case is analysed illustrating a situation where the upper bound of the probability of failure ($2P_{f,tag,R}$ for cases with two material basic variables) is reached. The case considers a structure composed of three elements: a steel tie and a column bearing a rigid beam subjected to a concentrated load Q (see Figure 2.2, self-weight neglected). The resistance of the structure is represented by a resistance variable R which is equal to the concentrated load Q.

(a) Column and tie structure   (b) Concrete constitutive law   (c) Steel constitutive law
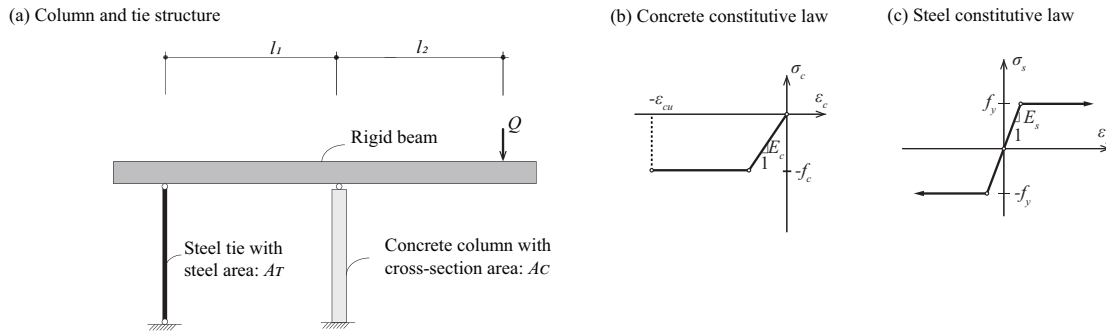
Figure 2.2:   (a) Column and tie system (unit of dimensions: mm); (b) concrete constitutive law; and (c) steel constitutive law.

In this structure, the beam is assumed to be a non-critical element, with failures only occurring in the column or in the tie. In the column, the 2nd order effects are assumed to be negligible and the contributions of both longitudinal and confinement reinforcements are neglected. Since the system is statically determinate, the resistance function of the system can be directly derived, as:

$$R = R(f_y, f_c) = \min(f_y \cdot A_T \frac{l_1}{l_2}, f_c \cdot A_C \frac{l_1}{l_1 + l_2}) \tag{14}$$

Where $R(\cdot)$ is the resistance function, f_y is the yield strength of steel, f_c is the compressive concrete strength , A_T is the area of the steel tie and A_C is the cross-section area of the concrete column (refer to Figure 2.2). In the following, the cross section area of the concrete column A_C is assumed to be constant while the area of the steel tie A_T is varied.

As previously explained, the reliability analysis presented in this section considers only material strength parameters as random variables in the resistance function. A lognormal distribution is

assumed for both materials strengths with the CoVs as follows: V_{fc} = 0.15 for concrete and V_{fy} = 0.04 for steel. It should be noted that the mean values of the material variables are not specified so the following conclusions are independent of them.

For each case, when applying PSFF, the design resistance and the corresponding limit state function for the resistance can be formulated as:

$$G_R = R - R_d = R(f_y, f_c) - R(f_{yd}, f_{cd}) = R(f_y, f_c) - R(\frac{f_{yk}}{\gamma_s}, \frac{f_{ck}}{\gamma_c}) = 0 \tag{15}$$

Where G_R is the limit state function for the design resistance; R_d is the design resistance with PSFF, f_{yk} and f_{yd} are the characteristic and design values of steel yield strength, respectively; f_{ck} and f_{cd} are the characteristic and design values for concrete compressive strength, respectively; γ_s is the partial factor for steel yield strength considering material uncertainty only and γ_c is the partial factor for concrete compressive strength considering material uncertainty only (the terminology of according to EN 1990:2002 [CEN02] is adopted here, where lowercase indices refer to partial safety factors accounting for material uncertainties only, whereas uppercase indices refer to the partial safety factors accounting for the geometrical and model uncertainties also).

For the values of the partial factors, considering only the material uncertainties, Eq.(1) can be reformulated as Eq. (16) and (17):

$$\gamma_c = \exp(\alpha_R \beta_t V_{f_c} - 1.64 V_{f_c}) \tag{16}$$

$$\gamma_s = \exp(\alpha_R \beta_t V_{fy} - 1.64 V_{fy}) \tag{17}$$

In the following, the reliability analysis for the limit state defined in Eq.(15) for each case will be performed with Monte Carlo simulation.

For the purpose of performing reliability analysis, the crude Monte Carlo simulation [Mel18] with Latin Hypercube Sampling (LHS) method [Mck00, Ols03] is used to analyse the distribution of resistance R. Based on the resulting distribution from Monte Carlo analysis, the actual achieved probability of failure $P_{f,R}$ and reliability index β_{MC} by PSFF can be determined. One million sample points are used in each Monte Carlo simulation to reduce the statistical uncertainty in the estimated probability of failure [Sho68].

Besides the reliability index β_{MC} directly derived from empirical distribution of the Monte Carlo simulation data, another reliability index β_{LN} is also calculated by directly approximating the distribution of resistance variable R with a lognormal distribution. The distribution parameters are approximated with the mean and CoV of the corresponding Monte Carlo simulation data. It should be pointed out that β_{LN} has the drawback of potentially neglecting tail approximation of the resistance distribution. The motivation for calculating the index β_{LN} is to verify the approach when a lognormal distribution is used to approximate the distribution of R, which has been

adopted in several researches about GSFF [All13, Cas19, Cer08, Sch12]. By comparing β_{LN} and β_{MC}, one can examine the error generated by neglecting the tail approximation and determine if the approximation performed in calculating β_{LN} is suitable.

2.4.2. Reliability analysis result

Monte Carlo simulations are performed for all cases and the actual achieved reliability index β_{MC} and the lognormal distribution approximated reliability index β_{LN} are given in Figure 2.3. It should be noted in Figure 2.3, the results are plotted with the normalized steel tie cross section area variable $A_{T,\omega}$, which is defined by the expression $A_{T,\omega} = \dfrac{A_T}{A_C} \cdot \dfrac{f_{yd}}{f_{cd}} \cdot (1 + l_1 / l_2)$. Comparing with Eq.(14), it can be observed that $A_{T,\omega}$ is equal to one when the steel tie and the concrete column fails at the same time at the PSFF design point (f_{yd}, f_{cd}). The limit state function for the case of $A_{T,\omega} = 1$ is plotted in Figure 2.4. This case corresponds to the lowest achieved reliability level ($\beta_{MC,\min,I} = 2.82$) of this case study. From the limit state function plot of Figure 2.4, it can be directly observed that the two BLSs are both activated in this case and the achieved $P_{f,d}$ is approximately twice the target value as previously discussed in Section 2.2. However, from the β_{MC} plot in Figure 2.3, it can be observed that as long as one of the elements is designed with certain strength margin, the resulting $P_{f,R}$ will be less than $2P_{f,tag.R}$ and the corresponding reliability index will be closer to the target level.
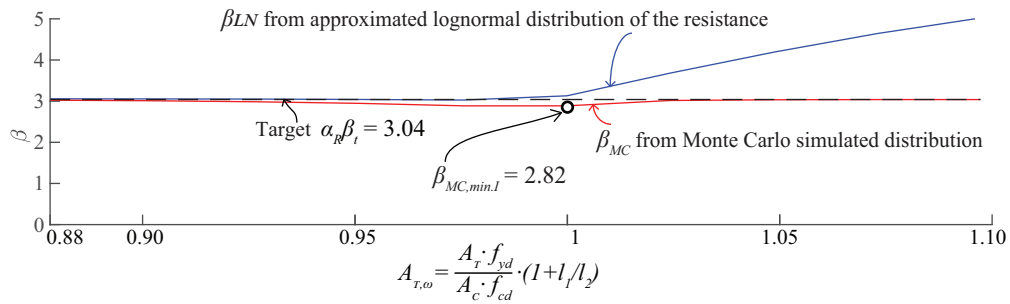
Figure 2.3:   Reliability index achieved by PSFF for cases with different cross-section area for the reinforcement tie

24
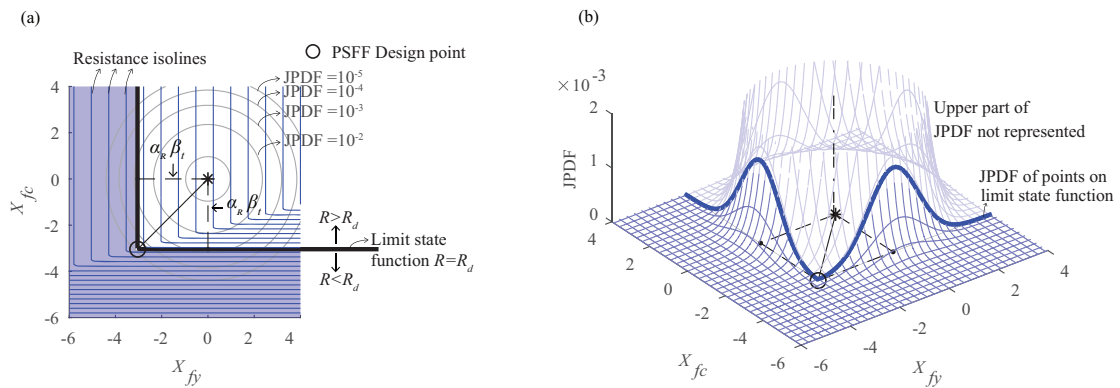
Figure 2.4: Resistance function isolines, limit state function and Joint Probability Density Function (JPDF) plot for $A_{T,\omega} = 1$ case: (a) 2D view and (b) 3D view.

2.5 Case study II: bending resistance of A cross-section (coupled failure modes)

In this section, a bending resistance case study is presented to further clarify the performance of PSFF for a limit state potentially dominated by two failure modes. The reliability analysis is developed for the bending resistance of a rectangular beam cross section (Figure 2.5a). The bending resistance is evaluated by considering a bi-linear response of concrete with strain limitation and neglected tensile strength, an elastic-perfectly plastic response of steel (Figure 2.5b-c) and assuming that sections remain plane after deformation (Euler-Bernoulli hypothesis).
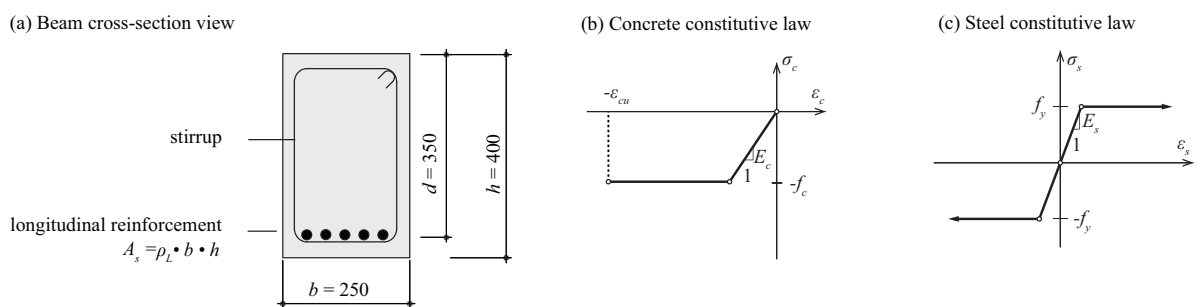
Figure 2.5: (a) Cross-section (unit of dimensions: mm); (b) concrete constitutive law; and (c) steel constitutive law.

25

2.5.1   Definition of case study series and reliability analysis results

A lognormal distribution is assumed for both materials strengths with the mean values and the CoVs as follows: $f_{cm} = 38$ MPa ; $V_{fc} = 0.15$ for concrete and $f_{ym} = 540$ MPa; $V_{fy} = 0.04$ for steel (resulting $f_{cd} = 24.1$ MPa and $f_{yd} = 478.2$ MPa according to Eq.(16) and (17). It should be noted that the elastic moduli of both materials are accounted for as deterministic values, with $E_c = 30000$ MPa and $E_s = 200000$ MPa.

The width b and effective depth d of the cross section are assumed constant whereas the longitudinal reinforcement ratio ρ_L is varied (deterministically) between 0.16% and 4% in order to generate cases governed by different failure modes.

Similar to the previous case study series, the achieved reliability index for the limit state of $R - R_d = 0$ (the same formulation as in Eq.(15)) is investigated. The results of Monte Carlo analysis are presented in Figure 2.6(a). It can be noted that, within the range of simulation, the achieved reliability index is either close to or higher than the target reliability index ($\beta_{MC,\min,II} = 2.98$). This shows that PSFF yields an acceptable reliability level. By comparing also β_{LN} with β_{MC}, it is observed that, in some cases, β_{LN} is significantly higher than β_{MC}, which shows that there is a significant difference between the approximated lognormal distribution (used in calculating β_{LN}) and the actual distribution of the resistance variable. For the case where β_{LN} is higher than β_{MC}, the CoV of the whole sampling data is lower than that of the tail region of the distribution. This result shows that calibrating the partial factor by a direct approximation of the resistance function with a lognormal distribution using the CoV of the whole sampling data can lead to unsafe result. This issue will be discussed in more detail Section 2.5.4.
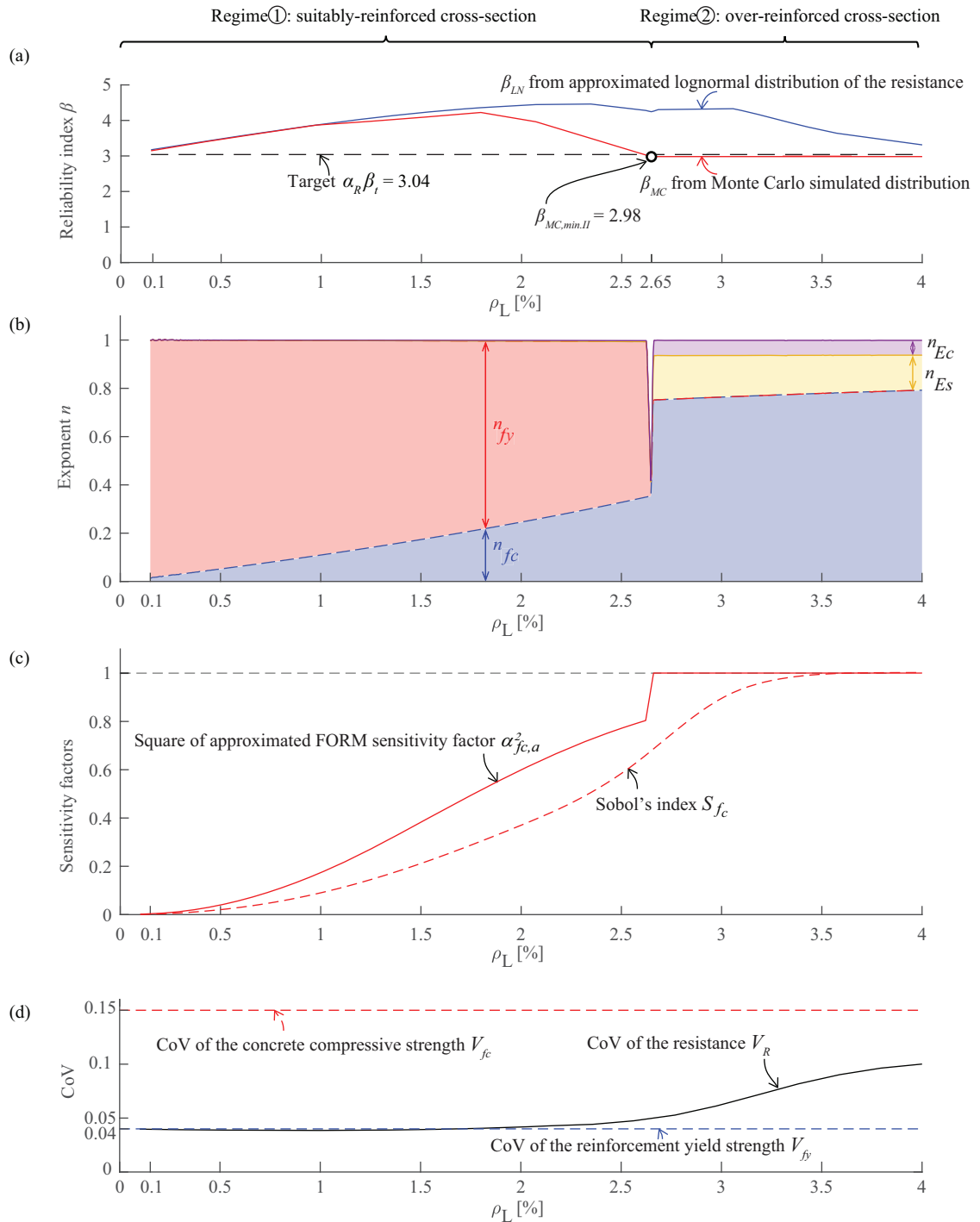
Figure 2.6: (a) Reliability index achieved by PSFF for different flexural reinforcement ratio ρ_L; (b) exponent sensitivity factor n of concrete compressive strength f_c, steel yield strength f_y, concrete elastic modulus E_c and steel elastic modulus E_s; (c) comparison between square of approximated FORM sensitivity factor $\alpha^2_{fc,a}$ and Sobol's total index S_{fc} and (d) CoV of the resistance variable based on Monte Carlo analysis

2.5.2   Exponent sensitivity analysis and failure regimes study

To help understanding the simulation results, the exponent sensitivity factor for f_c, f_y, E_s, and E_c, are calculated at the PSFF design point for each case. The results are plotted in Figure 2.6b.

Although E_s, and E_c are considered as deterministic parameters in this study, their exponent sensitivity factors are presented here to help understanding the different mechanical behaviour of different failure modes. It can be observed that there is a discontinuous point on each exponent curve at the reinforcement ratio $\rho_L = 2.65\%$ (corresponding to a mechanical reinforcement ratio $\omega_L = \rho_L \cdot \dfrac{f_{yd}}{f_{cd}} = 0.53$). This shows that there is an abrupt change in the regime of the resistance function at this point. From a mechanical point of view, the failure mode changes at this point. At the PSFF design point, when $\rho_L < 2.65\%$, both n_{fy} and n_{fc} are non-zero and their sum is equal to one, implying a suitably-reinforced behaviour governed by both material strengths (Regime ①). When $\rho_L > 2.65\%$, n_{fy} is reduced to zero, which implies that over-reinforced bending behaviour is governed only by concrete strength (Regime ②, where the elastic moduli have also an influence on the resistance, but their uncertainty is neglected here). Comparing the β_{MC} curve in Figure 2.6a with the exponent curves in Figure 2.6b, it can be observed that when the PSFF design point is governed by Regime ①, the achieved reliability β_{MC} is usually higher than the target value. This means that the PSFF gives a conservative estimate of the design resistance. When the PSFF design point is however governed by Regime ②, the achieved reliability β_{MC} is close to the target value.

For comparison reason, the FORM sensitivity factor for concrete strength estimated based on exponent sensitivity factors (calculated with Eq. (12)) is compared with the classical global sensitivity measurement total Sobol's index [Sob90] in Figure 2.6c. It can be observed that while Sobol's index provides valuable information about the global sensitivity of the performance function, it does not reflect the shift of regime of the reliability analysis result. The latter occurs due to the local change of shape of the limit state function. For the purpose of identifying multiple failure modes and their influence on the reliability, the FORM sensitivity factor (estimated based on the exponent sensitivity analysis) provides thus a more straightforward information. The FORM sensitivity factor plot reflects the shift of regime in the achieved reliability index β_{MC}. In addition, the relation between the occurrence of the maximum value of β_{MC} and the FORM sensitivity factor will be explained with more detail in the following.

It is also interesting to observe from Figure 2.6d that in the over-reinforced regime (Regime ②), the CoV of the resistance variable (V_R) is lower than the CoV of f_c even though in this regime the resistance is dominated by concrete strength only. The result can be explained by an approximation of the CoV of the resistance with the help of the exponent sensitivity factors. In this range, since $n_{fy} = 0$, the CoV of the resistance can be roughly approximated as

$V_R \approx \sqrt{n_{fc}^2 V_{fc}^2 + n_{fy}^2 V_{fy}^2} = n_{fc} V_{fc}$. Since n_{fc} is lower than 1 (due to the influence of n_{Ec} and n_{Es}), it naturally leads to the result of $V_R < V_{fc}$.

2.5.3 Analysis of selected cases

To help understanding the two types of performance of PSFF, two representative cases are presented in the following, corresponding to flexural reinforcement ratios ρ_L equal to 1.8% and 2.65%, whose results are plotted in the standard normal space in Figure 2.7 and Figure 2.8, respectively. It can be observed that the limit state functions are both composed of two parts for the two investigated cases. The first part has an inclined slope, which corresponds to Regime ① (suitably-reinforced bending governed by both material strengths) while the second part is perpendicular to the X_{fc} axis, which corresponds to Regime ② (over-reinforced bending governed by concrete strength only). The most important conclusions are presented below:

- In the case ρ_L=1.8% shown in Figure 2.7, the PSFF design point $(X_{fyd}, X_{fcd}) = (-\alpha_R \beta_t, -\alpha_R \beta_t)$ is coincident with the FORM design point, which leads to the result that both $\alpha_{fc,a}$ and $\alpha_{fy,a}$ are equal to $\dfrac{\sqrt{2}}{2}$. In this case, the maximum reliability level is achieved, which is the $\sqrt{2}\alpha_R \beta_t$.

- In the case ρ_L=2.65% shown in Figure 2.8, the PSFF design point corresponds to the intersection point between the two regimes on the limit state function. For this case, the achieved reliability index is close to the target one. This is justified because (i) the horizontal branch of the limit sate function (Regime ②) is coincident with the BLS dominated by concrete strength; (ii) the FORM design point locates on the horizontal branch and the distance between the origin point (0, 0) and the FORM design point is exactly $\alpha_R \beta_t$; and (iii) the probability mass within the Regime ① failure domain is much smaller than the corresponding for Regime ② (see volume below the joint probability density function (JPDF) in Figure 2.8b).
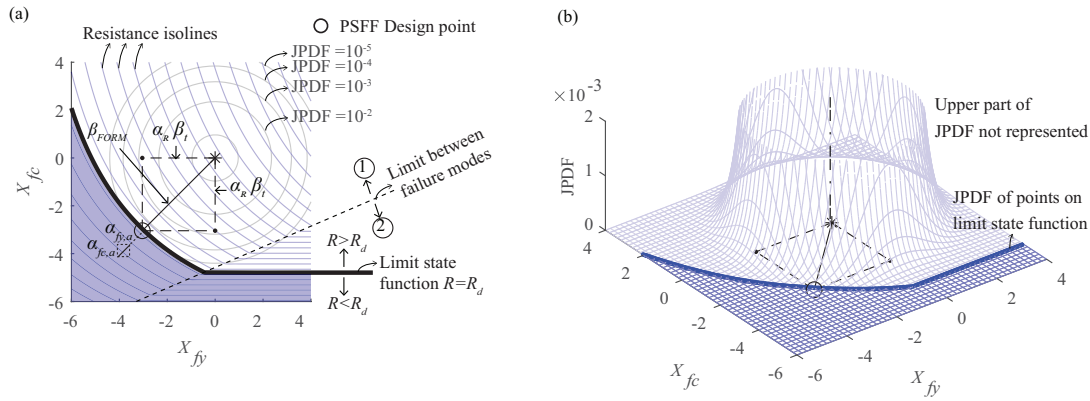
Figure 2.7: Resistance function isolines, limit state function and JPDF plot for $\rho_L=1.8\%$ ($\omega_L=0.36$) case: (a) 2D view and (b) 3D view
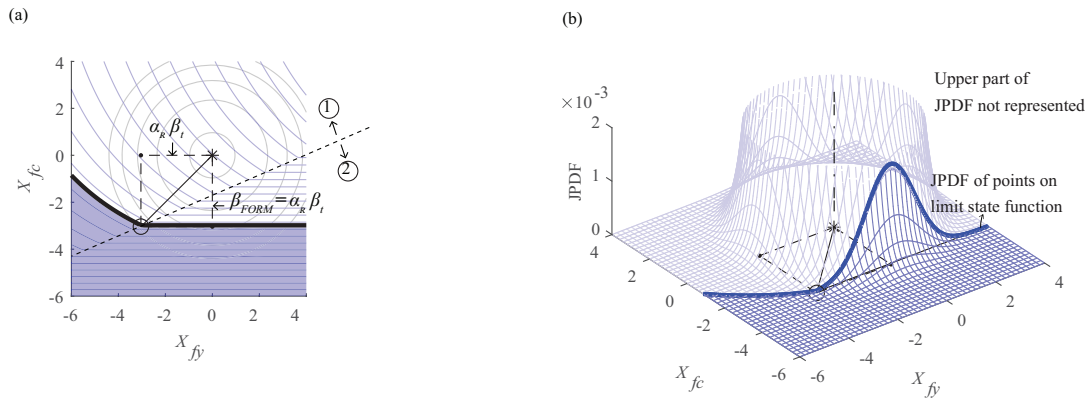
Figure 2.8: Resistance function isolines, limit state function and JPDF plot for $\rho_L=2.65\%$ ($\omega_L=0.53$) case: (a) 2D view and (b) 3D view

2.5.4 Discussion on proper tail approximation

In the GSFF from literature, a lognormal distribution is often used to approximate the distribution of the resistance variable and the distribution parameters (mean value and CoV) are usually estimated with a few sampling points near the origin point in the standard normal space of basic variables. To evaluate the efficiency of such approximation, the assumed lognormal distribution is compared with the actual distribution from the Monte Carlo simulation. The Monte Carlo simulation data for the $\rho_L=2.65\%$ case is investigated in detail.

The Probability Density Function (PDF) plots of both the approximated lognormal distribution and the simulated empirical distribution are shown in Figure 2.9a. The quantile-quantile plot (Q-Q plot) of $\ln(R/R_m)$ (where R_m is the mean value of the simulated data) is also presented in Figure 2.9b. The comparison shows that there is a significant difference between these two distributions in the tail region.

This difference is to a large extent motivated by the fact that there are two potential governing regimes (① and ②), which can be neatly observed in the Q-Q plot in Figure 2.9b (the governing failure mode changes from Regime ② to Regime ① as R increases). This fact is also shown in Figure 2.9c, showing that the closest point on the resistance isoline to the origin point in the standard normal space locates in Regime ② for low values of R while it locates in Regime ① for higher values of R.

This result shows the necessity for a proper tail approximation. The approximated lognormal distribution used in GSFF neglects the actual distribution in the tail region and leads to unsafe estimates of the reliability level for this case. This is shown in Figure 2.9b, where the $-\alpha_R\beta_t$ quantile value of the actual distribution is lower than that of the approximated lognormal distribution. Interestingly, it can be noted that since the PSFF directly evaluates the design resistance with a point on the limit state function, it shall yield a relatively good tail approximation result. This confirms the pertinence of the PSFF approach with this respect. Specific methods to achieve proper tail approximation in the safety format calibration of reinforced concrete structures have also been proposed by other researchers (for instance in Foster et al. [Fos16]).
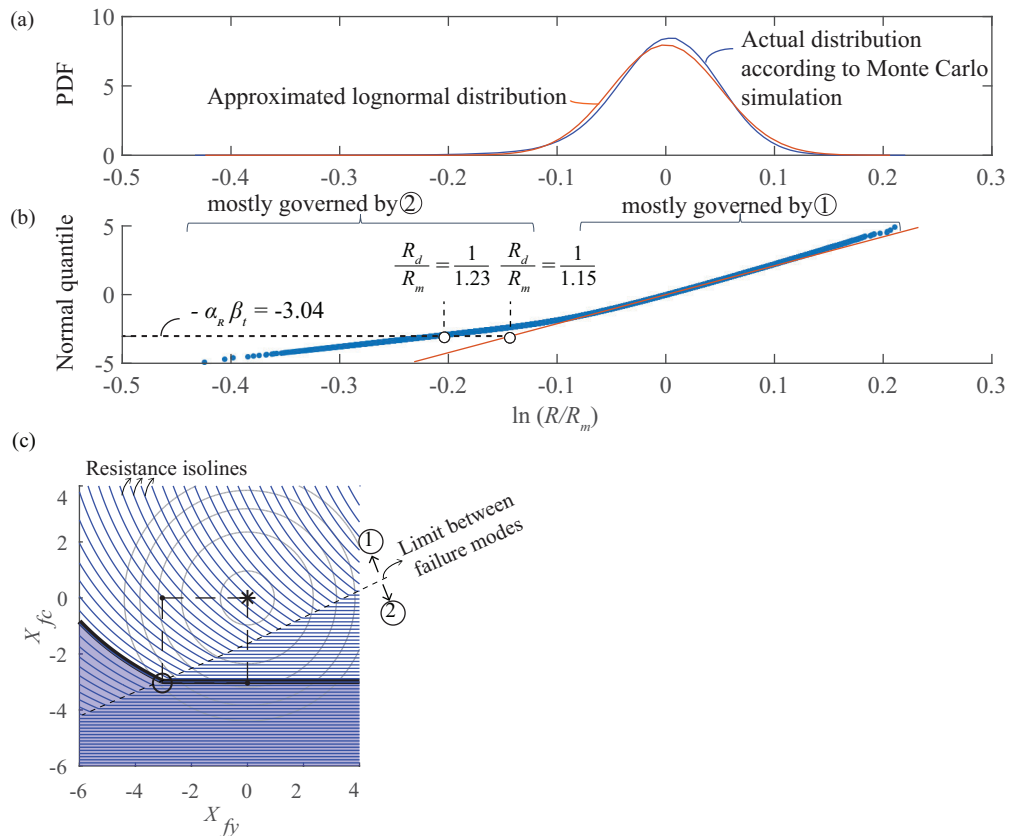
Figure 2.9: Distribution plot of $\ln(R/R_m)$: (a) Probability density function (PDF) plot and (b) Q-Q plot of approximated lognormal distribution and the actual distribution and (c) resistance isoline plot of ρ_L=2.65% case.

2.6 Case study III: shear resistance of reinforced concrete panels

In this section, to investigate different shapes of limit state functions, a case study on the shear resistance of reinforced concrete panels is presented (see Figure 2.10(a)). Compared to the bending resistance, the shear resistance involves damage of the concrete compressive strength due to cracking (compression softening [Vec86]). It is thus useful to have a clear view on the shape of the limit state function for this type of mechanical model.

2.6.1 Definition of case study series and reliability analysis results

The reliability analysis is performed for a reinforced concrete panel subjected to pure shear with plane stress behaviour. The shear resistance is evaluated with Elastic-Plastic Stress Field method (EPSF [Fer07]) where the reinforcement in the panel is considered as smeared and is modelled by a uniaxial response with an elastic-perfectly plastic law (refer to Appendix 2.A and Figure 2.15 for details). The material model for concrete corresponds to a coupled damage elasto-plastic model where the plastic behaviour follows a Mohr-Coulumb yield surface with a tension cut-off and an associative flow rule (refer to Appendix 2.A and Figure 2.15 for details).

To obtain different regimes with different failure modes, the vertical reinforcement ratio ρ_z is varied between 0.1% and 1.5% whereas the horizontal reinforcement ratio ρ_x is kept constant as 1%. A lognormal distribution is assumed for both materials strengths with the mean values and the CoVs as follows: $f_{cm} = 28$ MPa ; $V_{fc} = 0.15$ for concrete and $f_{ym} = 585$ MPa; $V_{fy} = 0.04$ for steel (resulting $f_{cd} = 17.7$ MPa and $f_{yd} = 518.0$ MPa according to Eq. (16) and (17))). The elastic moduli of both materials are accounted for as deterministic values, with $E_c = 30000$ MPa and $E_s = 200000$ MPa. Similar to the previous case study, the actual achieved reliability index β_{MC} and the lognormal distribution approximated reliability index β_{LN} are calculated for the limit state of $R - R_d = 0$ (the same formulation as in Eq.(15)) for each ρ_z - ρ_x combination, where in this case study, R represents the resistance to shear. The results are plotted in Figure 2.10b. Similar to the case of bending, it can be observed that PSFF leads to reliability levels close to or higher than the target one ($\beta_{MC,\min,III} = 2.94$).
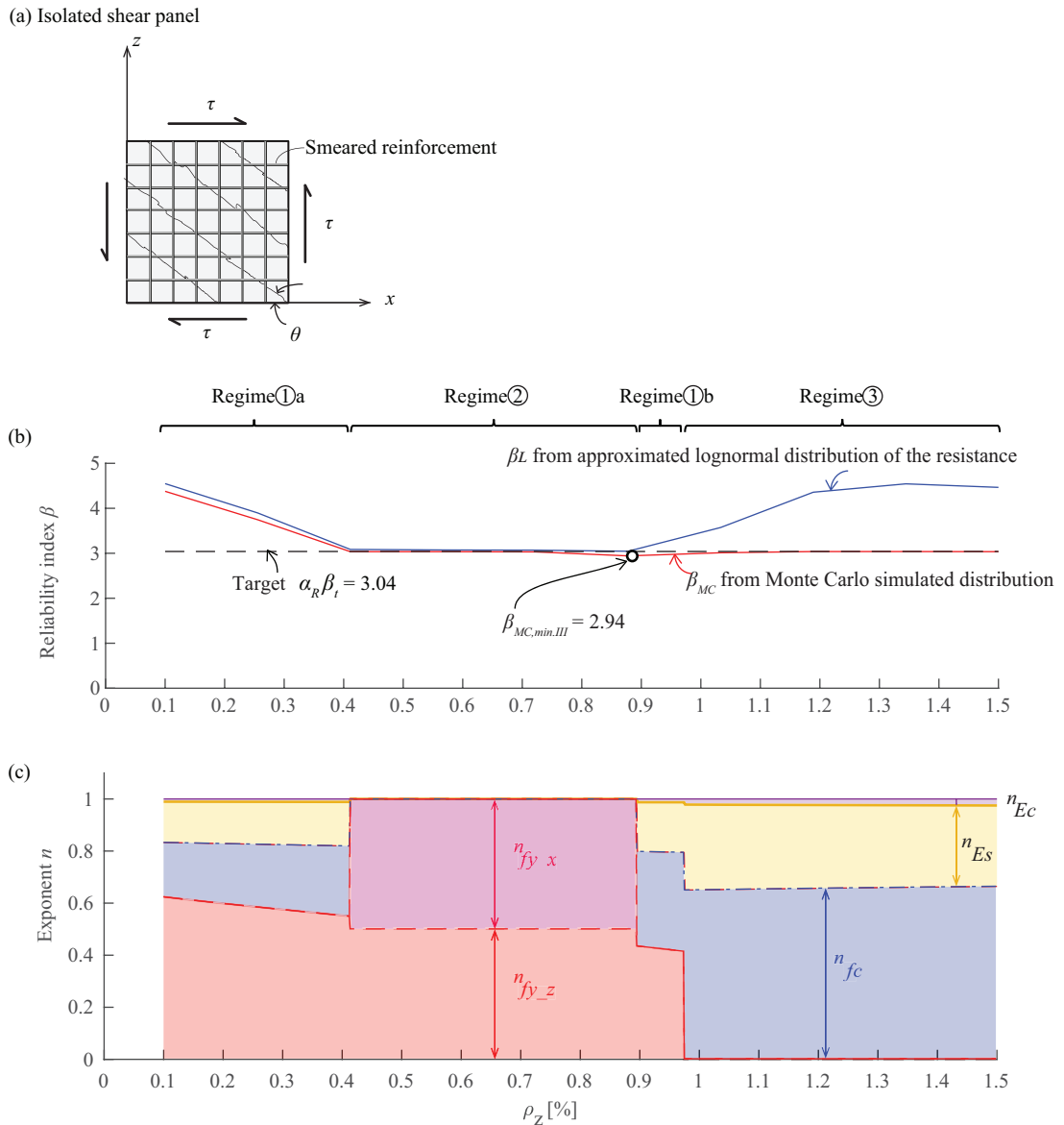
Figure 2.10:   (a) Isolated shear panel; (b) reliability index achieved by PSFF for different vertical reinforcement ratios ρ_z; and (c) exponent sensitivity factors n of concrete compressive strength f_c, steel yield strength of reinforcement f_y (n_{fy_z} and n_{fy_x} are the exponent sensitivity factors for vertical and horizontal reinforcements respectively) , concrete elastic modulus E_c and steel elastic modulus E_s.

2.6.2   Exponent sensitivity analysis and failure regime study

The exponent sensitivity factors are calculated and plotted in Figure 2.10c. It should be noted that, although the strength of vertical and horizontal reinforcements are assumed to be

represented by one random variable f_y, their exponent sensitivity factors are calculated separately (denoted as n_{fy_z} and n_{fy_x} respectively). Several failure regimes are observed to be governing (see Figure 2.10c):

- Regime ① a and b, when the shear resistance is governed by simultaneous yielding of the vertical reinforcement and crushing of the concrete (for Regime ①a: $\rho_z < 0.42\%$ and Regime ① b: $0.9\% < \rho_z < 0.97\%$)

- Regime ②, governed only by yielding of both reinforcements (for $0.42\% < \rho_z < 0.9\%$)

- Regime ③, governed by concrete crushing only (for $0.97\% < \rho_z$)

Accounting for these three regimes, the limit state functions have relatively more complex shapes than the bending case, but the shear resistance is non-decreasing with the material strengths (sufficient transverse reinforcement is assumed for crack control) and consequently, PSFF yields close to the target or conservative reliability levels. The shapes of the limit state function for two representative cases ($\rho_z = 0.4\%$ and $\rho_z = 0.9\%$) are plotted in Figure 2.11.
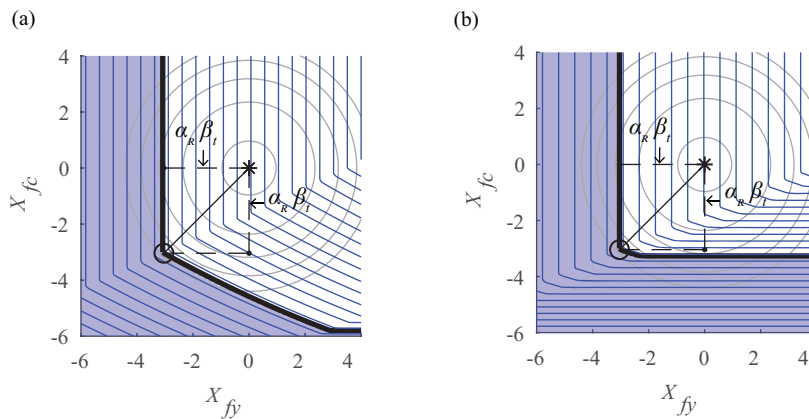
Figure 2.11: Resistance function isolines, limit state function and JPDF plot for (a) ρ_z=0.4% and (b) ρ_z=0.9% case (2D view)

In addition, it can be noted that the influence of the principal tensile strains on the concrete compressive strength introduces a dependency of Regimes ① and ③ on the elastic moduli of the materials (see Figure 2.10). In these cases, the sum of the exponents on material strength parameters are significantly lower than one (an associated consequence of this phenomenon will be discussed more in detail in Section 2.10).

For the purpose of simplicity, the horizontal and vertical reinforcements are modelled as the same type of material and are represented by one random variable f_y in this case. In practice, different types of materials are potentially used for these reinforcements and their material strengths should be modelled as independent random variables. To help understand the influence

34

of increasing number of independent material strength variables, the exponent sensitivity factors on the yielding strength of horizontal reinforcement (n_{fy_x}) and vertical reinforcement (n_{fy_z}) are calculated separately and are plotted separately in Figure 2.10. It can be observed that in the investigated case, in the range where both reinforcement strengths are dominating the resistance (Regime ②), $n_{fy\_x} = n_{fy\_z} = 0.5$. Assuming that the yield strengths of the horizontal and vertical reinforcements are represented by two independent lognormal random variables with the same CoV, then it can be established that the FORM sensitivity factors for both yield strengths are equal to $\dfrac{\sqrt{2}}{2}$. The values are lower than the assumed one in the PSFF ($\alpha_{f_{y,a}} = 1$). This result shows that in these cases, when the number of independent material strength variables increases, PSFF still yields conservative result.

2.7 Case study IV: Girder investigated With Nonlinear finite element analysis

In the previous case study, the effect of presence of different failure modes has been investigated for a small structural component where the acting internal forces are directly imposed or can be determined by equilibrium considerations. In this section, a more complex case is studied, in which Nonlinear Finite Element Analysis (NLFEA) is used to evaluate the load-bearing capacity of a girder which is potentially subjected to both bending and shear failure modes. The applicability of PSFF to such case is further investigated on the basis of reliability analysis. The investigated example shown in Figure 2.12 is inspired by an experiment presented in [Rup13] (test SR38), where the shear and longitudinal reinforcement ratios are adjusted to study the effect of multiple failure modes.

The NLFEA programme JCONC [Fer07] based on the EPSF method developed at the Structural Concrete Laboratory of EPFL is used to perform structural analysis. The applicability of this approach to describe the behaviour of the test series in [Rup13] has been validated in other works [Mut15, Rup13]. In the numerical simulation, all applied loads are assumed to increase monotonically and proportionally with the load factor Q (refer to Figure 2.12). The load factor at the ultimate level $Q = R$ is used to represent the load carrying capacity of the girder.

A lognormal distribution is assumed for both material strengths with the mean values and the CoVs as follows: $f_{cm} = 38$ MPa ; $V_{fc} = 0.15$ for concrete and $f_{ym} = 585$ MPa; $V_{fy} = 0.04$ for steel (resulting $f_{cd} = 24.1$ MPa and $f_{yd} = 518.0$ MPa according to Eq. (16) and(17))). The elastic moduli of both materials are accounted for as deterministic values, with $E_c = 30000$ MPa and $E_s = 200000$ MPa. Similar to the previous case studies, the achieved reliability index for the limit state of $R - R_d = 0$ (the same formulation as in Eq.(15)) is investigated.

(a) Longitudinal view

(b) Cross section view
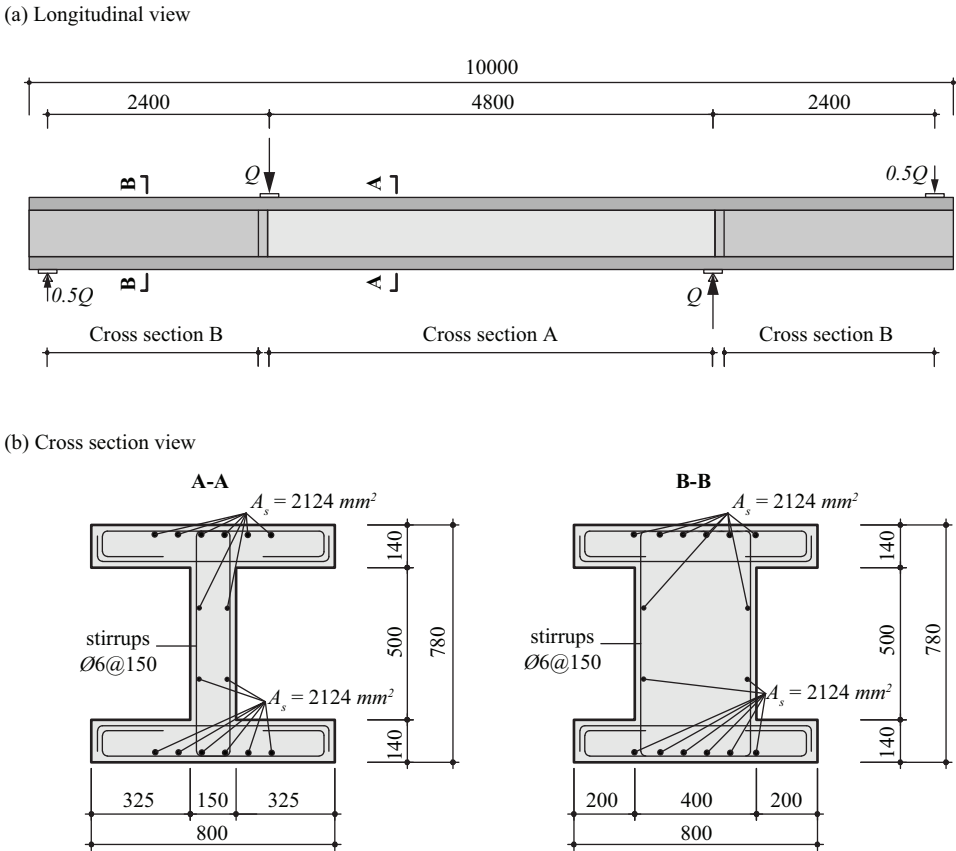
Figure 2.12: Geometry and reinforcement layout of girder (Unit of dimensions: mm)

2.7.1 Reliability analysis

Since the computational cost of NLFEA is significantly higher than that of simple nonlinear analysis methods in the previous cases, it is highly time-consuming to use crude Monte Carlo simulation to perform reliability analysis. In addition, another difficulty in the reliability analysis with NLFEA is that there are usually numerical errors involved, and this can reduce the accuracy of the local sensitivity analysis for the resistance [Eng93, Liu91, Sch11, Soa02]. For this reason, classical reliability methods which rely on the local gradient of the resistance function like FORM are not directly applicable to NLFEA. To overcome these difficulties, the Importance Sampling (IS) method [Mel18] combined with Response Surface Method (RSM) [Raj93] is used to perform reliability analysis (Refer to Appendix 2.B for details).

Table 2.1:   Estimation of exponent sensitivity factors in each sub-region

	Sub-region ①	Sub-region ②	Sub-region ③
Range of (X_{fy}, X_{fc})	[$-\alpha_R\beta_t$,0] x [0 $\alpha_R\beta_t$]	[$-\alpha_R\beta_t$,0] x [$-\alpha_R\beta_t$,0]	[0 $\alpha_R\beta_t$] x [$-\alpha_R\beta_t$,0]
n_{fc}	0.05	0.09	0.17
n_{fy}	0.92	0.84	0.71

Based on the RSM analysis, the exponent sensitivity factors for the material strength variables in different sub-regions in the corresponding standardized normal space are provided in Table 2.1 (Refer to Figure 2.13 for the range of different sub-regions). It can be observed that the sum of n_{fc} and n_{fy} in sub-region ③ is significantly lower than one. This result is consistent with the observation from Case Studies II and III that when the resistance is sensitive to the strain state, the exponent sensitivity factors of the elastic moduli are higher than zero and thus the sum of n_{fc} and n_{fy} are lower than one.

According to the IS reliability analysis, the achieved reliability level is $\beta_{IS} = 3.83$ (corresponding to a failure probability of $P_{f,R} = 6.32 \cdot 10^{-5}$) and the CoV of the evaluated probability of failure is CoV_{Pf}=7.61%. The achieved reliability level is higher than the target level ($\alpha_R\beta_t = 3.04$), which shows that PSFF yields conservative result in this case. The isolines of the resistance function are shown in Figure 2.13b (the isoline plot is based on the response surface fitted using addition sampling points for visualization purpose only). Two main regimes can be observed in the resistance function, suggesting two types of failure modes. This is confirmed by the stress field plot of the sampling point (X_{fy}, X_{fc}) = (0, X_{fcd}) and (X_{fy}, X_{fc}) = (X_{fyd}, 0) plotted in Figure 2.13c and d where it can be observed that different failure modes occurred at these two points:

- At the sampling point (X_{fy}, X_{fc}) = (0, X_{fcd}) (Figure 2.13c), failure occurs with concrete crushing of the web (refer to the black colour of the concrete elements) and yielding of the shear reinforcement (refer to the brown colour of the reinforcement elements).

- At the sampling point (X_{fy}, X_{fc}) = (X_{fyd}, 0) (Figure 2.13d), failure occurs with concrete crushing of the web and yielding of both shear and longitudinal reinforcements.
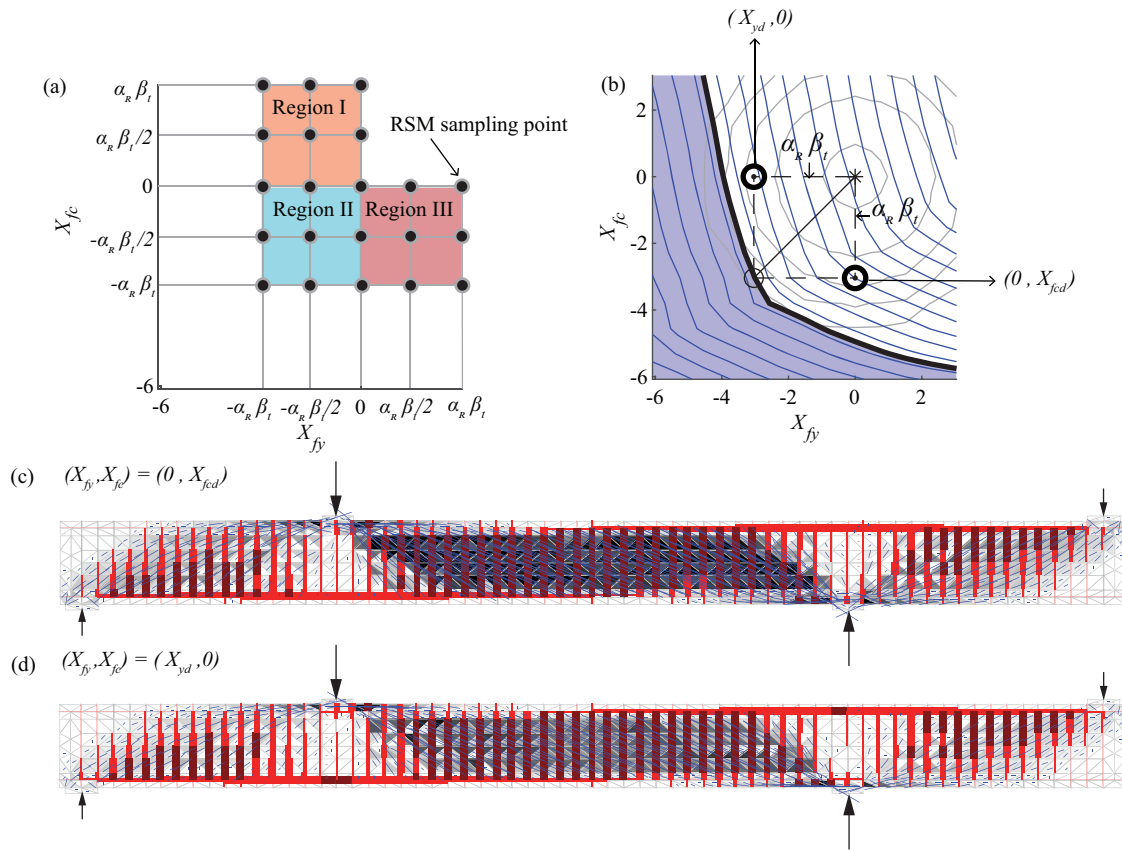
Figure 2.13:   (a) Division of sub-regions and the corresponding sampling points; (b)Resistance function isolines, limit state function and JPDF plot for the girder case (2D view) (c) The stress filed plot of the girder near failure at sampling point $(0 , X_{fcd})$ and (d) sampling point $(X_{fyd} , 0)$.

The reliability analysis result shows that with different failure modes, the PSFF still yields a conservative reliability level. This case confirms that the conclusions of Section 2.2 are also applicable to NLFEA methods.

2.8   Conclusions from case studies

The investigated case studies clearly show that the nature of different failure modes leads to an abrupt change of the sensitivity of the load bearing capacity to the strength variables. This means that in the design of reinforced concrete structures, since steel and concrete strengths have significantly different variabilities, the variability of the resistance variable is strongly influenced by the failure modes. The analytical and numerical studies shown above also show that PSFF provides a satisfactory solution to the multiple failure modes problem. By adopting

conservative FORM sensitivity factors for material strength variables ($\alpha_{f_{c,a}} = \alpha_{f_{y,a}} = 1$), PSFF verifies in an efficient manner the most unfavourable failure modes on the limit state function, provided that the non-decreasing assumption is valid.

2.9   Test of the non-decreasing assumption

Since structural concrete is composed of materials which are not perfectly ductile (limited deformation capacity of concrete and reinforcement steel, potential sliding of cracks without sufficient aggregate interlocking), the non-decreasing assumption of the load-carrying capacity is not always valid for practical structures. To reduce the influence of this phenomenon or even to prevent the decreasing cases, design standards typically define provisions like minimum reinforcement ratios, maximum height of the compression zone due to bending and detailing rules defining maximum reinforcement spacings and appropriate reinforcement anchorages. In design practice, a preliminary check of the non-decreasing assumption can be performed with low computation cost. For the case with two material variables f_c and f_y, the load-carrying capacity can be evaluated at three sampling points; $R(f_{cd}, f_{yd})$, $R(f_{cd}, f_{ym})$ and $R(f_{cm}, f_{yd})$. If the condition of $R(f_{cd}, f_{yd}) \leq R(f_{cd}, f_{ym})$ and $R(f_{cd}, f_{yd}) \leq R(f_{cm}, f_{yd})$ are both fulfilled, then it shows that in the region that is most critical for the reliability analysis, based on the outcomes of the selected sampling points, the non-decreasing assumption is not violated. In this case, the PSFF can still be considered as applicable within the framework of semi-probabilistic method. In essence, this is a simplified sensitivity analysis of the resistance function in the relevant region for reliability analysis. For the cases where the non-decreasing assumption is invalid (for instance such a case can be found in [Cas19]), more refined reliability verification methods [Mel18] than the semi-probabilistic method can be more suitable.

2.10   Discussion on other basic uncertainties

The various case studies in Sections 2.4 – 2.7 show that the sensitivity of resistance (intended as cross-sectional resistance or load-carrying capacity of a structural member) to material strength variables varies significantly amongst different action effects and failure modes. In Section 2.2, it has been shown that in the formulation of PSFF proposed in Eurocode 2 [CEN04], since for reinforced concrete structures, only two partial safety factors are applied on the resistance side, the geometrical uncertainties and the model uncertainties are actually lumped with the material uncertainties. This simplification can be arguable for some cases. Assuming that all the basic uncertainties follow lognormal distributions and their exponent sensitivity factors are known, then the CoV of the resistance variable can be calculated as following:

$$V_R = \sqrt{V_{\text{mod}}^2 + \sum n_{geom,i}^2 V_{geom,i}^2 + \sum n_{f,j}^2 V_{f,j}^2} \qquad (18)$$

Where n_{geom} and n_f refer to the exponent sensitivity factors on geometrical and material uncertainty variables, respectively. The sum over indices i and j indicates that there can be multiple random variables representing each type of basic uncertainty. It should be noted that only one model uncertainty variable is accounted for in Eq.(18), but in some cases there might be more than one model uncertainty variable (for instance in the punching shear resistance model based on Critical Shear Crack Theory [Mut08], potentially there are two model uncertainty variables for the failure criterion model and the load rotation model respectively).

Comparing Eq.(2) with Eq.(18), it can be observed that in the PSFF, the calculation of V_R is actually simplified with the assumption that the exponent sensitivity factors for all the basic uncertainties are equal to one. To help verifying this assumption, using the case study II as an example, the exponent sensitivity factors on the geometrical variables are plotted in Figure 2.14. With respect to the uncertainty of the reinforcement area A_s, it has to be noted that for the regime with reinforcement yielding, it is implicitly considered in the yield strength uncertainty, since according to EN 10080 [EN105], the latter is measured on the basis of the nominal reinforcement area. It can be observed in Figure 2.14 that the exponents on some geometrical variables (e.g. the flexural depth d) are significantly higher than one, so that the assumption used in Eq. (2) can underestimate the influence of geometrical uncertainties on the variability of the resistance. In addition, comparing the exponent sensitivity factors in Figure 2.14 with those in Figure 2.6, it can be observed that the exponent the effective depth d is also significantly higher those on the material variables, especially in the over-reinforced range. In addition, as shown in [Mut23a], the CoV of the model uncertainty is higher than the CoV of the yield strength and for thin members, the same applies also for the CoV of the effective depth. These observations raise the question about whether material uncertainties are still dominating in such cases and if it is still suitable to lump the geometrical and model uncertainties with material uncertainties in a single partial safety factor. Further detailed research needs to be performed to investigate this problem, especially for the safety format calibration of NLFEA method of concrete structures. It is also worth noting that EN 1990:2002 [CEN02] has addressed this problem by requiring that when the geometrical uncertainty is significant for the reliability of the structure, the design value of the geometrical variable (refer to Equation 6.5 of EN 1990:2002 [CEN02]) should be directly used in the limit state verification.
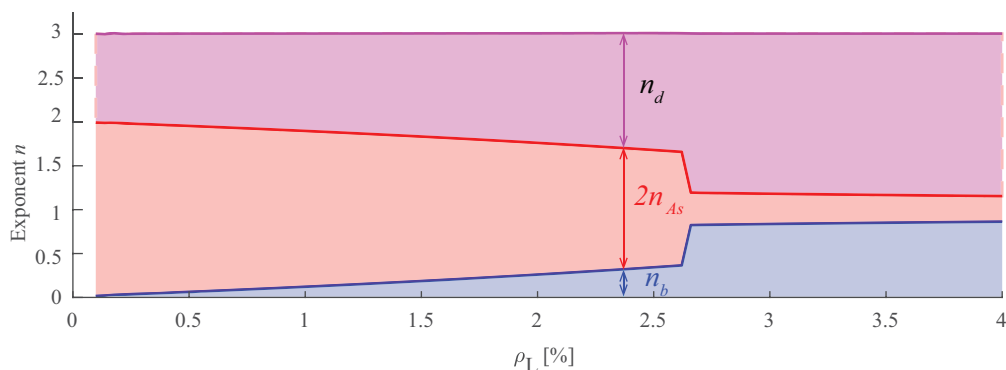
Figure 2.14:   Exponent sensitivity factor n of the cross-sectional flexural depth d, the cross-sectional width b and the steel reinforcement area As for Case Study II

2.11   Conclusions

The basic assumptions, simplifications and applicability conditions of the Partial Safety Factor Format (PSFF) on material strengths for the resistance of concrete structures are investigated in the work with both theoretical considerations and numerical case studies. Some considerations are also provided with respect to effects of the geometrical and model uncertainties. The main conclusions are summarized below:

- It is shown that, for the investigated cases, the PSFF on material strength yields satisfactory reliability levels both for cases subjected to single or to multiple failure modes induced by material uncertainties as long as the non-decreasing assumption of the resistance function is valid (the load-carrying capacity is not reduced by an increase of a material strength).

- The investigation of the sensitivity of the different variables on the load-carrying capacity expressed in terms of exponent sensitivity factors is a powerful tool to detect different failure modes. Exponent sensitivity factor analysis of the full applicable range of a given resistance model reflects the mechanical characteristics of the model. The result can be conveniently combined with different probabilistic modelling of the basic variables for different design situations, allowing to estimate useful indexes (e.g. the First Order Reliability Method (FORM) sensitivity factors and the coefficient of variation of the resistance variable) for calibrating the corresponding safety format.

- Adopting conservative FORM sensitivity factors for material strength variables in the PSFF calibration is necessary because they may vary significantly for different failure modes. This treatment can be conservative for some cases, but has the advantages of being simple to use in design practice and being applicable to a wide range of cases.

- The simplification of integrating the safety elements for geometrical and model uncertainties into the partial safety factors for material strengths can underestimate the influence of geometrical and model uncertainties in some cases. With this respect, further research needs to be performed to study the proper treatment of geometrical and model uncertainties, particularly in the safety format for NLFEA.

- Good tail approximation is instrumental for the effectiveness of safety formats. Approximating the distribution of resistance variable with a single lognormal distribution based on crude Monte Carlo simulation result risks of losing information about the tail distribution and can potentially lead to unsafe results.

Acknowledgements

Appendix 2.A: Principles of the EPSF method

In the Elastic Plastic Stress Field (EPSF) method, the equivalent plastic compressive strength f_{cp} is defined accounting for a concrete brittleness factor η_{cc} and a transverse strain factor η_ε, according to Eq.(19). The brittleness factor η_{cc} follows the relation proposed by Muttoni [Mut90] given by Eq.(20). The damage due to cracking is considered by applying a transverse strain factor η_ε, which is evaluated as a function of the principal tensile strain following the relation proposed by Vecchio and Collins [Vec86], given in Eq. (21). The elastic modulus of concrete E_c is considered independent of its transverse strain state as proposed in Vecchio et al.[Vec94]. It shall be noted that the method considers the principal stress direction to be parallel to the principal strain direction (refer to Figure 15). Based on the EPSF method, the equilibrium conditions and the compatible conditions for the shear panel problem are given in Eq. (22)-(27).

$$f_{cp} = \eta_\varepsilon \eta_{cc} f_c \tag{19}$$

$$\eta_{cc} = \left(\frac{30}{f_c}\right)^{\frac{1}{3}} \leq 1 \tag{20}$$

$$\eta_\varepsilon = \min(1, \frac{1}{0.8+170\varepsilon_{1,c}}) \tag{21}$$

$$\rho_x \sigma_{sx} - \tau \cot \theta = 0 \tag{22}$$

$$\rho_z \sigma_{sz} - \tau \tan \theta = 0 \tag{23}$$

$$\sigma_{c,2} + \tau(\tan \theta + \cot \theta) = 0 \tag{24}$$

$$\tan^2 \theta = \frac{\varepsilon_{c,x} - \varepsilon_{c,2}}{\varepsilon_{c,z} - \varepsilon_{c,2}} \tag{25}$$

$$\varepsilon_{c,1} = \varepsilon_{c,x} + \varepsilon_{c,z} - \varepsilon_{c,2} \tag{26}$$

$$\varepsilon_{s,x} = \varepsilon_{c,x} \quad \text{and} \quad \varepsilon_{s,z} = \varepsilon_{c,z} \tag{27}$$

where $\varepsilon_{c,1}$ and $\varepsilon_{c,2}$ are the principal strains of concrete; τ is the shear stress; ρ_x and ρ_z are the horizontal and the vertical reinforcement ratio; σ_{sx} and σ_{sz} are the stress in the horizontal and the vertical reinforcement; θ is the angle between the second principle strain of concrete and the horizontal direction; $\varepsilon_{c,x}$ and $\varepsilon_{c,z}$ are the horizontal and the vertical strain of concrete and $\varepsilon_{s,x}$ and $\varepsilon_{s,z}$ are the strains of the horizontal and vertical reinforcements.

It should be noted that in this case, due to the form of concrete brittleness factor η_{cc} (which has an exponent of 1/3 on the concrete compressive strength variable), the sum of exponent sensitivity factors for material strength variables are lower than one when concrete strength is higher than 30 MPa. For further details about the influence of this factor on the safety format of concrete structures, please refer to [Moc20].

(a) Isolated shear panel; (b) Steel constitutive law; (c) Mohr's circle and principle strains of concrete; (d) Concrete yield surface and associative flow rule; (e) Concrete constitutive law
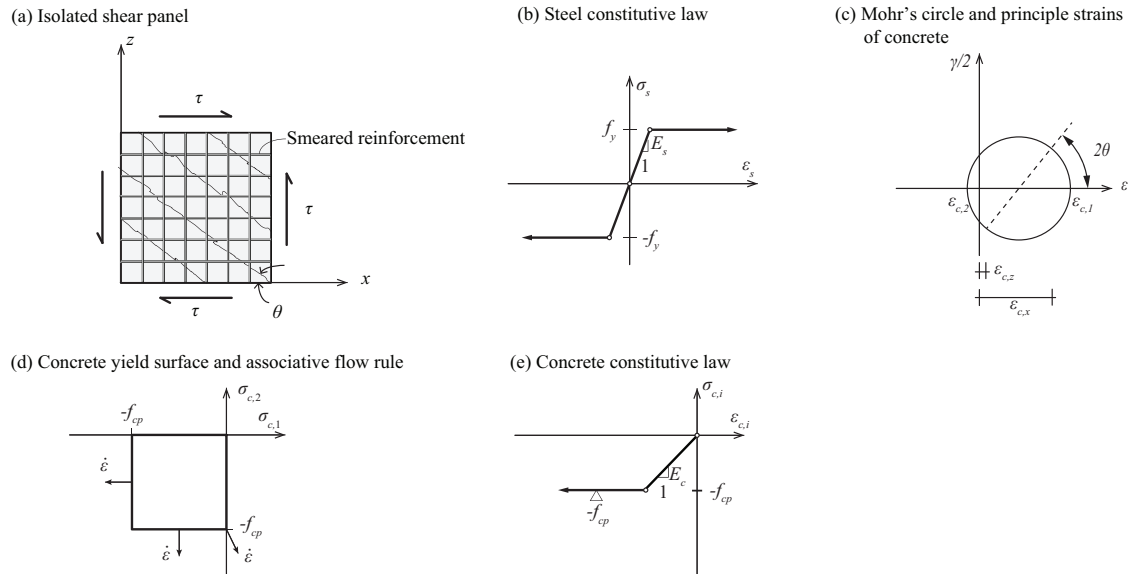
Figure 2.15: (a) Isolated shear panel; (b) Steel constitutive law; (c) Mohr's circle and principle strains; (d) concrete yield surface and associative flow rule and (e) concrete constitutive law.

Appendix 2.B: Reliability analysis with response surface method of case study IV

In this Appendix, the detailed reliability analysis for Case Study IV is presented.

The basic concept of the Importance Sampling (IS) method is to use an Importance Sampling Probability Density Function (ISPDF) instead of the original Joint Probability Density Function (JPSF) of the basic variables to draw sampling points in the Monte Carlo simulation in order to achieve low variance in the estimated probability of failure with a relatively small sample size. The IS method is one type of variance reduction technique in the reliability analysis method with Monte Carlo simulation [Mel18]. The key issue of the IS method is to find suitable ISPDF [Mel18]. An efficient ISPDF is proposed in [Mel18]:

$$h(X) = \varphi(X - X_{d,FORM})$$

(28)

Where X is the vector of the random variables in the standardised normal space and $X = (X_{fy}, X_{fc})$, $h(X)$ is the ISPDF, $\varphi()$ is the original JPDF of X and $X_{d,FORM}$ is the estimated FORM design point.

The ISPDF in Eq.(28) is generated by moving the sampling centre to the estimated most probable failure point (FORM design point) on the limit state function. It can be observed that to implement this method, a rough estimation of the FORM design point is still needed. For this purpose, the Response Surface Method (RSM) is used.

The basic concept of the RSM is to use a small number of sampling points to make a closed-form approximation of the resistance function as a basis for reliability analysis [Raj93]. The Design of Experiment (DOE) technique [Mon17] can be used to select sampling points for effectively constructing the response surface and multivariate linear regression method can be used to fit the response surface [Mon17]. In the RSM, by taking sampling points in a relatively large range in the space of basic variables, the influence of the numerical error in NLFEA can be mitigated. The closed-form response surface function can then be used to estimate the FORM design point with classical HL-RF method [Liu91].

In Case Study IV, a linear polynomial function without interaction in the standardized normal space of the basic variables is used for the response surface, as is given in the following equation:

$$N_R = a_0 + a_1 \bullet X_{f_c} + a_2 \bullet X_{f_y}$$

(29)

Where N_R is the logarithm of the resistance R: $N_R = \ln(R)$; a_0, a_1 and a_2 are the coefficients to be fitted with the data of the sampling points.

From the case studies in this work, it can be observed that different failure modes usually occur with extreme combinations of material strengths. For example, the failure mode of the sampling point with low f_c value and high f_y value tends to be different from that with high f_c value and low f_y value. To account for this phenomenon, the response surface is fitted in sub-regions. The

division of the sub-regions for this case study is shown in Figure 2.13a. This treatment aims at increasing the precision of the response surface fitting with a small computation cost. The resistance function is fitted in each sub-region, which result in three response surface functions. The resistance in the whole space is then defined as the minimum resistance among the three fitted response surface functions:

$$N_R = \min(N_{R,1}, N_{R,2}, N_{R,3}) \tag{30}$$

Where $N_{R,1}$, $N_{R,2}$, and $N_{R,3}$ are the response surface function in sub-region ①, ② and ③.

This treatment aims as mimicking the mechanical behaviour that the dominating failure mode of a structure is the one that results in the lowest loading bearing capacity.

It should be noted that it is also possible to use polynomial functions of higher order or other type of functions for the RSM. In this case, the linear model without interaction is selected because the model coefficients a_1 and a_2 can be directly related to the exponent sensitivity factors n_{fc} and n_{fy} defined in Section 2.3, which directly reflect the differences between failure modes.

The three-level factorial design method [Mon17] is used to select the RSM sampling points in each sub-region, as is shown in Figure 2.13a. In total, 21 sampling points are taken to fit the response surface. Based on the NLFEA results of the sample points, multilinear regression method is applied to estimate the model coefficients. The resulting coefficients and the corresponding p-values in t-test [Mon17] are listed in Table 2.2. The aim of performing t-test [Mon17] is to test if the error level is sufficiently low. If the t-test failure, it suggests either the numerical error of the NLFEA method is too high or the response surface function is not suitable for the given problem. In this case, all the p-values of the t-test are lower than 5%, and the response surface fitting result is considered as acceptable.

Table 2.2:   Estimations of the response surface coefficients and the corresponding p-values of each sub-region of Case study IV

Sub-regions	Sub-region ①			Sub-region ②			Sub-region ③		
(X_{fy}, X_{fc})	$[-\alpha_R\beta_t,0]$ x $[0\ \alpha_R\beta_t]$			$[-\alpha_R\beta_t,0]$ x $[-\alpha_R\beta_t,0]$			$[0\ \alpha_R\beta_t]$ x $[-\alpha_R\beta_t,0]$		
Coefficients	a_0	a_1	a_2	a_0	a_1	a_2	a_0	a_1	a_2
Estimation	-0.24	0.008	0.037	-0.25	0.014	0.034	-0.22	0.025	0.028
p-value	2e-14	9e-8	8e-12	2e-9	2e-4	1e-6	2e-7	3e-4	2e-4

Based on the fitted response surface, the FORM reliability analysis is performed and the FORM design point is estimated. The estimated FORM design point is calculated as $X_{d,FORM} = (-3.45, -1.42)$ in the standardized normal space.

Then, IS reliability analysis is performed using the ISPDF. For the IS analysis, 1000 sampling points are used. It should be noted that in this case, a relatively large number of sampling points with the NLFEA evaluations is taken to reduce the statistical uncertainty. According to the IS reliability analysis, the achieved reliability level is $\beta_{IS} = 3.83$ (corresponding to a failure probability of $P_{f,R} = 6.32 \cdot 10^{-5}$) and the CoV of the evaluated probability of failure is $CoV_{Pf} = 7.61\%$. It should be noted that the CoV of 7.61% corresponds to the CoV of the failure probability for the nonlinear finite element model itself. Considering the magnitude of the probability of failure ($6.32 \cdot 10{-5}$), this level of CoV is considered as acceptable. In this case, since the finite element model is relatively small, it is possible to use a large sample (with 1000 sampling points) to perform the IS analysis. However, when such an approach is not applicable, other methods (e.g. Adaptive Kriging Monte Carlo Simulation method [Ech11]) may be used to perform reliability analysis with reasonable computational time.

NOTATION

Latin upper case letters

A	cross-section area of a structural component
A_C	cross-section area of the concrete column
A_T	cross-section area of the steel tie
$A_{T,\omega}$	normalized cross-section area of the steel tie
$COV_{\hat{P}_f}$	coefficient of variation of the estimator $\hat{P}_{f,R}$
E	elastic modulus of a material
F_i	failure domain of boundary limit state of material i
$G_R(\cdot)$	limit state function for the design resistance
$I[G_R(\cdot)]$	indicator function of $G_R(\cdot)$
N_R	logarithm of the resistance R
$P(\cdot)$	probability function
P_f	probability of failure of the structure
$P_{f,R}$	probability of failure for the design resistance
$P_{f,tag}$	target probability of failure of the structure
$P_{f,tag,R}$	target probability of failure for the design resistance
$\hat{P}_{f,R}$	estimator for probability of failure for the design resistance
Q	load factor
$R(\cdot)$	resistance function
R_0	resistance at a reference point $(f_{1,0}, f_{2,0,...}, f_{p,0})$
R_d	PSFF design value of resistance
R_m	mean value of the Monte Carlo simulated data of resistance
V	a random variable following the importance sampling probability density function
V_R	Coefficient of Variation (CoV) of resistance random variable
V_{mod}	CoV of the model uncertainty variable
V_{geom}	CoV of the geometrical uncertainty variable
V_f	CoV of the material uncertainty variable
V_{fc}	CoV of concrete compressive strength random variable
V_{fy}	CoV of steel yield strength random variable
X	vector of basic random variables in the standardised normal space
X_{fc}	concrete compressive strength random variable transformed to the standard normal space
X_{fcd}	design value of concrete compressive strength in the standard normal space
X_{fy}	steel yield strength random variable transformed to the standard normal space
X_{fyd}	design value of steel yield strength in the standard normal space
$X_{d,FORM}$	estimated FORM design point in the standard normal space

Latin lower case letters

a_0, a_1 and a_2	coefficients of the response surface function
b	width of a cross section
d	flexural depth of a cross section
f_c	concrete compressive strength
f_{cd}	design value of concrete compressive strength
f_{cm}	mean value of concrete compressive strength
f_{cp}	equivalent plastic compressive strength of concrete
f_i	random variable of strength of material i
f_j	parameter j in the resistance function
f_k	characteristic value of material strength variable
f_d	design value of material strength variable
f_y	steel reinforcement yield strength
f_{yd}	design value of steel reinforcement yield strength
f_{ym}	mean value of steel reinforcement yield strength
h	height of a cross section
$h(\cdot)$	the importance sampling probability density function
l	span of a structural component
n_{As}	exponent sensitivity factor for reinforcement area
n_{Ec}	exponent sensitivity factor for concrete elastic modulus
n_{Es}	exponent sensitivity factor for steel elastic modulus
n_d	exponent sensitivity factor for cross-section flexural depth
n_{fc}	exponent sensitivity factor for concrete compressive strength
n_{fj}	exponent sensitivity factor for parameter f_j
n_{fy}, (n_{fy_x}, n_{fy_z})	exponent sensitivity factor for steel yield strength (the indices of x and z refer to the vertical and horizontal directions respectively)
n_{IS}	sample size of IS method
n_{MC}	sample size of Monte Carlo simulation

Greek upper case letters

Δ	a sufficiently small increment of parameter $\ln(f_j)$
$\Phi(\cdot)$	cumulative distribution function of standardized normal distribution

Greek lower case letters

$\alpha_{f_{c,a}}$	FORM sensitivity factor of concrete strength
$\alpha_{f_{y,a}}$	FORM sensitivity factor of steel reinforcement yield strength
α_R	the standardized FORM sensitivity factor for resistance
β_{IS}	achieved reliability index evaluated with Importance Sampling method
β_{LN}	achieved reliability index evaluated with lognormal distribution approximation
β_{MC}	achieved reliability index evaluated with Monte Carlo simulation
β_t	target reliability index
γ_c	partial factor for concrete compressive strength considering material uncertainty only

γ_s	partial factor for steel yield strength considering material uncertainty only
γ_M	partial factors applied to material strength variables (accounting for all basic uncertainties)
γ_m	partial factors applied to material strength variables (accounting for material uncertainties only)
$\varepsilon_{c,1}$	first principal strain of reinforced concrete shear panel
$\varepsilon_{c,2}$	second principal strain of reinforced concrete shear panel
ε_x and ε_z	horizontal and vertical strain of shear panel
η_ε	transverse strain factor of shear panel
η_{cc}	concrete brittleness factor
θ	angle between the second principle strain and the horizontal direction of shear panel
$\mu_{\ln f_c}$	mean value of the logarithmic concrete compressive strength
$\mu_{\ln f_y}$	mean value of the logarithmic steel yield strength
ρ_L	flexural reinforcement ratio of a cross section
ρ_x	horizontal reinforcement ratio of shear panel
ρ_z	vertical reinforcement ratio of shear panel
$\sigma_{c,2}$	second principle stress of concrete in the shear panel
$\sigma_{\ln f_c}$	standard deviation of the logarithmic concrete compressive strength
$\sigma_{\ln f_y}$	standard deviation of the logarithmic steel yield strength
σ_{sx} and σ_{sz}	stress in the horizontal and the vertical reinforcement of shear panel
τ	shear stress of shear panel
$\varphi(\cdot)$	joint probability density function
ω_L	mechanical flexural reinforcement ratio of a cross section

Chapter 3

Model uncertainties and partial safety factors of strain-based approaches for structural concrete: example of punching shear

This chapter is the preprint version of the article mentioned below, submitted to Engineering Structures Journal. The authors of the article are Qianhui Yu (PhD Candidate), João T. Simões and Prof. Aurelio Muttoni (thesis director). The provisional reference is the following:

Yu Q., Simões J. T., Muttoni A., *Model uncertainties and partial safety factors of strain-based approaches for structural concrete: example of punching shear*, Engineering Structures (submitted March 2023)

The work presents in this publication was performed by Qianhui Yu collaborating with João T. Simões and under the supervision of Prof. Aurelio Muttoni, who provided constant and valuable feedbacks, proofreading and revisions of the manuscript.

The main contributions of Qianhui Yu to this article and chapter are the followings:

- Comprehensive literature review regarding the model uncertainty quantification and safety format calibration for nonlinear analysis models of concrete structures.

- Proposition of the model uncertainty quantification framework for strain-based approaches.

- Database collection of punching shear test data.

- Model uncertainty quantification of the Critical Shear Crack Theory (CSCT) punching shear resistance model with Bayesian inference.

- Proposition of the methodology of accounting for the measurement error in the model uncertainty quantification.

- Interpretation of the relationship of the model uncertainties of sub-models and global resistance solutions of the CSCT punching shear resistance models.

- Comparison between the model uncertainties of different Levels-of-Approximation (LoAs) of the CSCT punching shear resistance model of *fib* Model Code 2010.

- Proposition the suitable safety format for different LoAs punching shear resistance model.

- Elaboration of the figures and tables included in the article.

- Writing of the manuscript of the article.

Abstract

The development of mechanical models relating the state of strains and the resistance of reinforced concrete structures has become a trend in the last decades. These types of models are referred to as strain-based approaches. Since strain-based approaches usually involve multiple sub-models and take implicit forms, their model uncertainties tend to be more complex than those of the explicit design equations commonly used in design codes. The characteristics of the model uncertainties of strain-based approaches is investigated using the Critical Shear Crack Theory (CSCT) for the punching shear resistance of structural concrete members as example. Both by performing theoretical parametric analyses and by evaluating relevant experimental data, it is shown that the model uncertainty of global resistance solution of strain-based approach can be viewed as resultant of the model uncertainties of the sub-models. In addition, it is also shown that the model uncertainty of the global resistance solution can be lower than those of the sub-models, depending on their sensitivity relationship. The model uncertainties of different Levels-of-Approximation (LoA) of the CSCT for punching are also compared. The LoA approach intends to provide consistent and progressively refined model for different design tasks in practice. The model uncertainty quantification result confirms that the model uncertainty of higher LoA of CSCT has lower variability and also less conservative bias than lower LoA. Finally, based on the obtained model uncertainties, different types of partial safety formats for strain-based approaches are compared and discussed. Using the CSCT punching shear model as an example, it is shown that the partial safety factors applied to the sub-models are more suitable for higher LoAs since they can effectively account for the change of model uncertainty associated to the change of failure mode. Based on the assumptions described in this work, the relationship between the safety factors of the punching shear provisions in the second generation of Eurocode 2 for the design of new structures and the assessment of existing critical ones is established.

Keywords: model uncertainty, strain-based approaches, structural concrete, punching shear, partial safety factors

3.1   Introduction

In modern design codes for concrete structures (e.g.,[ACI19, CEN02, Fos16, Sta18], the reliability verification is usually performed through calibrated safety formats accounting for the inevitable uncertainties involved in design and construction practice. For the resistance of concrete structures at ultimate limit state, material, geometrical and model uncertainties are normally accounted for in the safety format [Ell80, Eur08, Fos16, JCS01]. The probabilistic modelling of the basic uncertainties is usually performed based on experience, engineering judgement and available objective data for the relevant parameters [Ell80, JCS01]. The

quantification of the uncertainties related to the resistance models is nonetheless becoming increasingly challenging due to models' rising complexity. Their quantification and probabilistic description are however instrumental to ensure a proper reliability verification in design practice.

Resistance models in structural concrete were commonly explicit functions of the basic design variables in the past. Yet, the development of well-established sound mechanical models relating the state of strains and the resistance has been a trend observed in the last decades. These types of structural resistance models are referred to as strain-based resistance models or strain-based approaches in the following. In the area of structural concrete, an example of such models is the Critical Shear Crack Theory (CSCT) [Mut08] (Figure 3.1) for the punching shear, where the resistance of a slab-column connection is not only a function of the geometrical and material parameters of the member, but also of the slab rotation (assumed to be correlated to the opening of the critical shear crack which affects the capacity of the slab to transfer the shear forces to the column). Other examples of strain-based approaches are the Modified Compression Field Theory (MCFT) used to assess the shear resistance of structural concrete [Ben06, Vec86] (Figure 3.2) or, in a more general framework, the Non-Linear Finite Element Analyses (NLFEA) accounting for compatibility and equilibrium conditions together with failure criteria for materials which are strain state dependent (this is for instance the case of the Elastic Plastic Stress Field (EPSF) method [Mut90]).

(a) Slab-column connection
(b) Failure criterion and load-rotation curves of CSCT
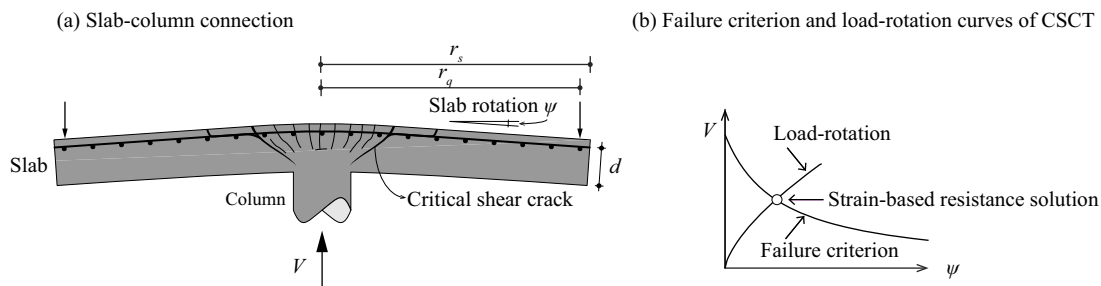
Figure 3.1:   Illustration of (a) a slab-column connection and (b) model of the CSCT for punching shear (refer to Notation section for details)

Since strain-based approaches usually involve multiple sub-models and take implicit forms, the evaluation of the model uncertainties can be conducted at the level of the global resistance solution or of the sub-models considered separately. In this work, using the CSCT for punching shear resistance as an example, the suitable quantification method and the relationship between the model uncertainties of the global resistance solution and those of the sub-models are investigated. The relevance of investigating the CSCT for the punching shear resistance is justified by the fact that it has been adopted for the provisions related to punching shear design in the fib Model Code 2010 [FIB13] and in the second generation of Eurocode for concrete structures [CEN23] (strain-based approach in the annex for the assessment of existing structures).
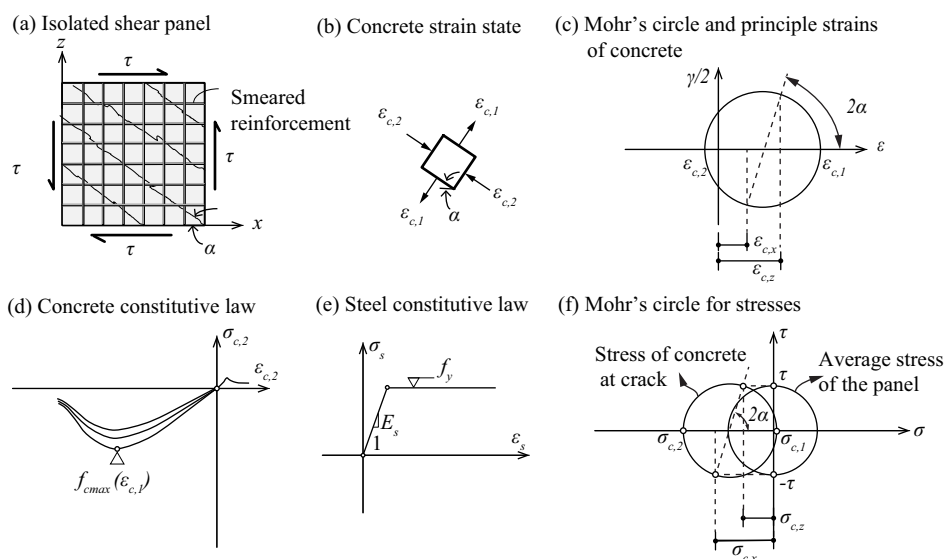
Figure 3.2: Illustration of the analysis of a shear panel with MCFT (a) a reinforced concrete panel subjected to shear force; (b) the strain state of concrete; (c) strain compatibility expressed with Mohr's stress circle (d) concrete constitutive law; (e) steel constitutive law and (f) equilibrium expressed with Mohr's stress circles (refer to Notation section for details)

3.1.1 The Critical Shear Crack Theory for punching shear: main idea

The main idea of the CSCT for punching shear is that the development of a so-called critical shear crack near to the support governs the shear transferring capacity of the slab-column connection (see [Mut08] for further details). The resistance is thus a function of the location, shape and kinematics (function of bending and shear deformations) of this critical shear crack [Gui10, Mut91, Sim18]. A refined model [Sim18] based on the principles of the CSCT [Mut17] has shown that for slender slabs, as proposed by Muttoni in 2008 [Mut08]: (1) a failure criterion can be established as a function of the normalized critical shear crack opening and (2) the critical shear crack opening at failure can be correlated to the rotation of the slab ψ shown in Figure 3.1(a). Therefore, as shown in Figure 3.1(b), the punching shear resistance and the strain state at failure (represented by the slab rotation ψ) can be calculated by intersecting the load-strain relationship (where the strain refers in this specific case to the slab rotation ψ; this relationship representing the response of the slab-column connection) and the failure criterion (this function represents the punching resistance associated to a given crack opening, associated to the rotation ψ). The failure criterion and the load-strain relationship are represented from a mathematical point-of-view by two independent functions respectively. For this reason, it can be seen as the simplest form of strain-based structural resistance models. This type of strain-based structural resistance model is in fact an intermediate step between explicit analytical structural resistance

models (where the resistance is calculated with a closed-form equation on the basis of the geometrical and mechanical material values) and more complex implicit structural resistance models (such as the NLFEA).

Investigating the model uncertainties of simple strain-based resistance models can help understanding the relationship between model uncertainties of simple explicit analytical and complex implicit numerical structural resistance models.

3.1.2 Quantification of model uncertainty for structural concrete resistance analysis

Promoted by the implementation of reliability theory in design codes, the quantification of the model uncertainty of structural resistance models used for concrete structures is a topic that has attracted wide attention of researchers in recent years. Such quantification is usually performed by comparing the calculated resistances to the experimental results included in databases assembling relevant experimental tests performed under controlled conditions [JCS01, Tae93]. Numerous researchers have already performed this work considering the resistance models in the form of analytical design equations included in current design codes [Now03, , Syk13, Syk18, Bel15, Fos15, Fos16, Hal19, Hol16, Ola20, Ste16]. The quantification of the model uncertainty related to Non-Linear Finite Element Analyses (NLFEA) for concrete structures (which are sometimes referred to as global resistance models [Cas19, Eng17, FIB13, Sch12]) has also been extensively investigated [Cas18, Cer18, Eng17, Hau11, Kad15, Sch12]. Engen et al. [Eng17] and Castaldo et al. [Cas18] evaluated the resistance model uncertainty considering different modelling hypotheses to perform NLFEA (influence of the choice of material constitutive laws, finite element type, convergence criterion). Cervenka [Cer18] quantified the model uncertainty related to NLFEA applied to different types of internal forces (bending, shear, and punching shear). Haukaas and Gardoni [Hau11] proposed the Bayesian finite element method, which attempts to account for the model uncertainty as it originates from different sub-models (e.g. constitutive laws, equilibrium and strain compatibility conditions) in a finite element solution.

As observed for instance by Haukaas and Gardoni [Hau11], NLFEA are implicitly composed of different sub-models involving multiple calibrated parameters. This complex nature makes it difficult to quantify the model uncertainties related to NLFEA, which partially justifies the absence of consensus on their treatment. In this context, investigating the model uncertainties of simple strain-based approaches, which represent an intermediate step between explicit analytical closed-form design formulae and complex implicit resistance models, can be a first interesting step.

As with the NLFEA, also in the simple strain-based approaches, the global resistance model is composed of different sub-models (e.g. the failure criterion model and the load-rotation model in the CSCT for punching shear described above). Therefore, it is possible to quantify the model

uncertainty at both the sub-model level and at the global resistance level. For example, in reference [Mut08], for the strain-based punching shear resistance model of the CSCT, the model uncertainty data shows that the variability (represented here by the Coefficient of Variation (CoV)) of the global model uncertainty is lower than that of the failure criterion model. Reasons behind this phenomenon and its implications for the safety format calibration of strain-based approaches will be investigated in this paper.

3.1.3 The model uncertainties of the Levels-of-Approximation (LoA) approach

To allow the application of sophisticated resistance models in daily design practice, an approach by Levels-of-Approximation (LoA) [Mut12, Mut12a] can be explicitly or implicitly adopted. This approach is a codified design strategy that aims at providing consistently and progressively refined design methods that can be flexibly used for different tasks such as preliminary design, detailed design of new structures and assessment of existing ones [Mut12, Mut12a]. The LoA approach has been adopted in the Swiss Code for structural concrete [Mut03, SIA13](since 2003) and in the *fib* Model Code 2010 [FIB13, Mut13]. The LoA approach was intended to be used together with physically sound design models rather than with empirical formulae. When lower LoAs are used, the mechanical parameters in the design model can be assessed in a simple (yet conservative) manner. When more accuracy is required, higher order LoAs can be used with refined calculations of the mechanical parameters [Mut12a]. Four LoAs can be applied for punching shear according to the *fib* Model Code 2010 [FIB13, Mut12a] (provisions based on the CSCT [Mut08] as previously introduced), corresponding to the calculation of the slab rotation based on: simple design equations (LoA I and LoA II); involving linear elastic analysis (LoA III) or eventually nonlinear analysis to calculate the expected strain (LoA IV). With respect to the model uncertainties related to the different LoAs, it is important to say that: (a) a higher LoA is expected to have a lower level of model uncertainty and (b) a lower LoA is likely to have a certain conservative bias in order to yield safe design results despite the higher model uncertainty.

In this work, the model uncertainty of LoA II (normally used for the design of new structures) and LoA IV (often applied in the assessment of critical existing structures) of the CSCT for punching shear will be investigated. The relationship between the model uncertainty of the corresponding sub-models (failure criterion and load-rotation relationship) and that of the global resistance model, as well as the relationship between the model uncertainties related to the different LoAs, are investigated not only from a theoretical point of view, but also by quantifying the corresponding uncertainties based on an evaluation of experimental data applying the Bayesian inference method.

3.1.4 Organisation of the document

In Section 3.2, a theoretical approach based on exponent sensitivity factors [Yu22] (resulting from the assumption that the models can be approximated by a power-multiplicative form) is introduced to investigate the sensitivity of the global resistance solution to governing parameters of the sub-models. With the help of the exponent sensitivity factors [Yu22], and the assumption that the global resistance solution model uncertainty originates from the independent model uncertainties of the sub-models (the assumption will be later validated with experimental data), the theoretical relationship between the model uncertainties of the global resistance model and those of the sub-models is derived in a general format for strain-based approaches. The result is applied in Section 3.3 to the practical case of CSCT for punching shear based on a parametric study of the corresponding exponent sensitivity factors. In Section 3.4, the theoretical derivation and the results obtained with the parametric study are then verified by the quantification of the model uncertainties using a set of experimental data of punching shear tests. The results of the model uncertainties obtained for the database of experimental tests are discussed in Section 3.5. Eventually, Section 3.6 presents a discussion on the different safety formats required for strain-based approaches focusing particularly on the provisions for punching shear design according to the new generation of Eurocode 2 [CEN23].

It is worth mentioning that although applied to the case of punching shear, the methodology followed in this paper to quantify the model uncertainty can also be applied to other strain-based approaches likewise.

3.2 Theoretical analysis on the relationship of models' uncertainties of strain-based approaches

As previously introduced, a strain-based approach is a structural resistance model that is a function of both basic design variables $\mathbf{x}_b = (x_1, x_2, ... x_N)$ (e.g., material and geometrical variables) and, at least, a strain state variable ε. The resistance of a strain-based approach can be expressed in a general form as:

$$\begin{cases} R_{FC} = F_{FC}[(\mathbf{x}_b, \varepsilon), \theta_{FC}] = F_{FC}(\mathbf{x}_{FC}, \theta_{FC}) = \breve{F}_{FC}(\mathbf{x}_{FC}) \cdot \theta_{FC} \\ \varepsilon = F_\varepsilon[(\mathbf{x}_b, R), \theta_\varepsilon] = F_\varepsilon(\mathbf{x}_\varepsilon, \theta_\varepsilon) = \breve{F}_\varepsilon(\mathbf{x}_\varepsilon) \cdot \theta_\varepsilon \\ R_{solu} = R = R_{FC} \end{cases} \tag{1}$$

Where R_{FC} is the resistance according to the failure criterion function $F_{FC}(\cdot)$; $\mathbf{x}_{FC} = (\mathbf{x}_b, \varepsilon)$ is the vector of all input variables of the failure criterion function; θ_{FC} is the model uncertainty random variable of the failure criterion function; $F_\varepsilon(\cdot)$ is the load-strain function; $\mathbf{x}_\varepsilon = (\mathbf{x}_b, R)$ is the vector of all input variables of the load-strain function; R is the load level and θ_ε is the model

uncertainty random variable of the load-strain function. The actual resistance (R_{solu}) according to a strain-based approach is achieved when the load level (R) is equal to the resistance according to the failure criterion (R_{FC}). When the model uncertainty variables are considered to be in multiplication form [JCS01] to the corresponding functions, Eq.(1) can be further simplified, with $\breve{F}_{FC}(\cdot)$ and $\breve{F}_{\varepsilon}(\cdot)$ representing the failure criterion function and the load-strain function excluding the model uncertainty variables.

Alternatively, the solution of a strain-based approach can also be expressed directly as follows (considering the global model uncertainty to be in a multiplicative form):

$$R_{solu} = F_{solu}(\mathbf{x}_b, \theta_{solu}) = \breve{F}_{solu}(\mathbf{x}_b) \cdot \theta_{solu} \tag{2}$$

Where R_{solu} is the resistance solution (calculated by solving the equation set of Eq. (1)), $F_{solu}(\cdot)$ is the resistance solution function, which usually has an implicit form; θ_{solu} is the model uncertainty of the resistance solution as a whole and $\breve{F}_{solu}(\cdot)$ is the function excluding the model uncertainty variable.

It should be noted that Eq. (2), with a global model uncertainty θ_{solu}, represents the solution of the equation set of Eq. (1) where the model uncertainties of the two sub-models are accounted for separately (illustrated in Figure 3.3). It is assumed that the model uncertainty of the resistance solution originates from the uncertainties related to the sub-models. The suitability of this assumption will be further discussed later based on experimental data. In Figure 3.3, the uncertainty of other related failure mode is also illustrated. For example, in the case of punching shear, its load-rotation relationship is related to the flexural behaviour of the structure. When the flexural resistance is reached, the load-rotation relationship will have a plateau due to the formation of a flexural mechanism (assuming a perfectly plastic behaviour) [Mut08]. The influence of other failure modes on the model uncertainty of the strain-based solution (as for instance the flexural failure mode in Figure 3.3) will also be discussed in this paper.
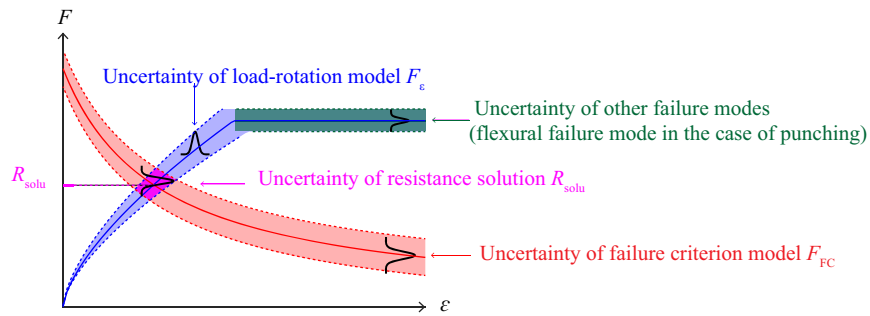
Figure 3.3:   Illustration of the different model uncertainties of a strain-based approach

For the theoretical derivation, the failure criterion and the load-strain functions are approximated by a power-multiplicative form of the variables:

$$\begin{cases} R_{FC} = F_{FC}[(\mathbf{x}_b, \varepsilon), \theta_{FC}] \cong C_{FC} \cdot \prod_{i=1}^{N} x_i^{n_{FC,i}} \cdot \varepsilon^{n_{FC,\varepsilon}} \cdot \theta_{FC} \\ \varepsilon = F_{\varepsilon}[(\mathbf{x}_b, R), \theta_{\varepsilon}] \cong C_{\varepsilon} \cdot \prod_{i=1}^{N} x_i^{n_{\varepsilon,i}} \cdot R^{n_{\varepsilon,R}} \cdot \theta_{\varepsilon} \end{cases} \qquad (3)$$

Where C_{FC}, $n_{FC,i}$ and $n_{FC,\varepsilon}$ are the approximated coefficients of the failure criterion equation, and C_{ε}, $n_{\varepsilon,i}$ and $n_{\varepsilon,R}$ are those of the load-strain equation.

The power-multiplicative form approximation is equivalent of performing a first order Taylor expansion of the two functions after transferring all the variables into the logarithmic space. This transformation is valid assuming that all the variables in Eq. (1) are positive scalar values.

In the following, all the exponent factors ($n_{FC,i}$, $n_{FC,\varepsilon}$, $n_{\varepsilon,i}$ and $n_{\varepsilon,R}$) will be referred to as exponent sensitivity factors, which can be estimated by calculating a numerical derivative of the variable of interest in the logarithmic space [Yu22].

On the basis of the multiplicative form approximation of the sub-models, it is then possible to derive the explicit form of the resistance solution:

$$R_{solu} = \theta_{FC}^{\frac{1}{1-n_{\varepsilon,R}n_{FC,\varepsilon}}} \cdot \theta_{\varepsilon}^{\frac{n_{FC,\varepsilon}}{1-n_{\varepsilon,R}n_{FC,\varepsilon}}} \cdot C_{FC}^{\frac{1}{1-n_{\varepsilon,R}n_{FC,\varepsilon}}} \cdot C_{\varepsilon}^{\frac{n_{FC,\varepsilon}}{1-n_{\varepsilon,R}n_{FC,\varepsilon}}} \cdot \prod_{i=1}^{N} x_i^{\frac{n_{FC,i}+n_{\varepsilon,i}n_{FC,\varepsilon}}{1-n_{\varepsilon,R}n_{FC,\varepsilon}}} \qquad (4)$$

The model uncertainty of the resistance solution can then be derived as:

$$\theta_{solu} = \theta_{FC}^{\frac{1}{1-n_{\varepsilon,R}n_{FC,\varepsilon}}} \cdot \theta_{\varepsilon}^{\frac{n_{FC,\varepsilon}}{1-n_{\varepsilon,R}n_{FC,\varepsilon}}} \qquad (5)$$

From Eq. (5) it can be observed that:

- the sensitivity of the global model uncertainty to the sub-model uncertainties depends on the exponent sensitivity factors, which, as a matter of fact, reflects the shape of the sub-models' functions.

- the global model uncertainty can be lower than the model uncertainty of both sub-models, depending on the values of $n_{\varepsilon,R}$ (the exponent on the load variable in the load-strain relationship) and $n_{FC,\varepsilon}$ (the exponent on the strain variable in the failure criterion). This fact is important for the safety format calibration problem of strain-based solutions.

In the following sections, the relationship between the global model and the sub-models' uncertainties will be further investigated for the example described above.

3.3   Application of the theorical analysis to the case of punching shear according to CSCT

In this section, the resistance model of the CSCT for punching shear of reinforced concrete slabs without shear reinforcement without unbalanced moment (axisymmetric slab-column connection) as proposed by Muttoni [Mut08] will be investigated.

The basic form (without partial safety factors) of the failure criterion of the CSCT [Mut08] is:

$$V_{FC} = F_{FC}(\mathbf{x}_{FC}, \theta_{FC}) = F_{FC}[(\mathbf{x}_b, \psi), \theta_{FC}] = b_{0.5} \cdot d \cdot \sqrt{f_c} \cdot \frac{3/4}{1 + 15 \dfrac{\psi \cdot d}{d_{g0} + d_g}} \cdot \theta_{FC} \tag{6}$$

Where V_{FC} is punching resistance calculated with the failure criterion model $F_{FC}(\cdot)$, $\mathbf{x}_{FC} = (\mathbf{x}_b, \psi)$, ψ is the slab rotation outside the column region and $b_{0.5}$ is the perimeter of the critical section located $d/2$ from the column face.

With respect to the load-rotation relationship, as previously introduced, four different LoA can be used. In the following, only the LoA II (normally used for the design of new structures) and the LoA IV (often used in the assessment of critical existing structures) load-rotation relationships are investigated. The two LoAs share the same failure criterion (Eq. (6)), but differ in the calculation of the rotation ψ.

3.3.1   LoA II load-rotation relationship

The LoA II load-rotation relationship [Mut08] is given by:

$$\psi = F_{LR,II}(\mathbf{x}_\varepsilon, \theta_{LR,II}) = F_{LR,II}[(\mathbf{x}_b, V), \theta_{LR,II}] = \begin{cases} = 1.5 \dfrac{r_s \cdot f_y}{d \cdot E_s} \cdot \left(\dfrac{V}{V_{flex}}\right)^{\frac{3}{2}} \cdot \theta_{LR,II} \text{ when } V < V_{flex} \\ \to \infty \text{ when } V = V_{flex} \end{cases} \tag{7}$$

$$V_{flex} = 2\pi m_R \frac{r_s}{r_q - r_c} = 2\pi d^2 \rho f_y \left(1 - \frac{\rho f_y}{2 f_c}\right) \frac{r_s}{r_q - r_c} \tag{8}$$

Where $F_{LR,II}(\cdot)$ is the LoA II load-rotation function, V is the punching shear load level, V_{flex} is the load associated to the flexural resistance of the slab (yielding to a flexural mechanism [Mut08]) and m_R is the flexural resistance per unit width of the slab.

The punching shear resistance ($V_{solu,II}$) is reached when the punching shear load (V) is equal to the resistance according to the failure criterion (V_{FC}): $V_{solu,II} = V = V_{FC}$. According to the theoretical derivation in Section 3.2, the model uncertainty variables for the LoA II model have the following relationship:

$$\theta_{solu,II} = \theta_{FC}^{\frac{1}{1-n_{\varepsilon,R,II}n_{FC,\varepsilon}}} \cdot \theta_{LR,II}^{\frac{n_{FC,\varepsilon}}{1-n_{\varepsilon,R,II}n_{FC,\varepsilon}}} = \theta_{FC}^{n_{\theta FC,II}} \cdot \theta_{LR,II}^{n_{\theta LR,II}} \tag{9}$$

Where the two exponents $n_{\theta FC,II} = \dfrac{1}{1-n_{\varepsilon,R,II}n_{FC,\varepsilon}}$ and $n_{\theta LR,II} = \dfrac{n_{FC,\varepsilon}}{1-n_{\varepsilon,R,II}n_{FC,\varepsilon}}$ represent the influence

of the model uncertainties of the failure criterion and load-rotation relationship on the resistance solution, respectively.

By comparing Eq. (6) and Eq.(7) to Eq.(3), it can be observed that for the LoA II, in the power multiplicative form approximation of the punching shear resistance model:

- The exponent sensitivity factor associated with the load variable in the load-strain function is equal to $n_{\varepsilon,R,II} = 1.5$ (the subscript II refers to LoA II) when $V < V_{flex}$ and tends to ∞ for $V = V_{flex.}$

- The exponent sensitivity factor associated with the strain variable in the failure criterion $n_{FC,\varepsilon}$ differs from case to case.

In order to get the range of $n_{FC,\varepsilon}$ for representative cases, a parametric study is performed. The ranges of the basic design variables used in it are listed in Table 3.1 (only cases where $V<V_{flex}$ are investigated).

Table 3.1: Design information of geometrical and material variables for parametric study of slab-column connections

Basic variables	Values
f_y	538 MPa
f_c	33.6 MPa
E_s	200 000 MPa
E_c	30 000 MPa
d	varied between 150 and 350 mm
h	$1.2 \cdot d$
c	two cases investigated: $c = 1.5 \cdot d$ and $3 \cdot d$
r_s	$r_s = 25 \cdot 0.22 \cdot h$
ρ	varied between 0.5% and 1.5%
d_g	16 mm

The normalized failure criterion and load-rotation curves for the cases listed in Table 3.1 are plotted in Figure 3.5. The value of the exponent factor of the strain variable in the failure criterion equation ($n_{FC,\varepsilon}$) is calculated for each case at the LoA II resistance solution point. The results are plotted in Figure 3.5(a), where, for clarity of illustration, $-n_{FC,\varepsilon}$ is plotted (as $n_{FC,\varepsilon}$ has a negative value, corresponding to a decrease of the resistance for increasing values of the strain

variable). The resulting exponent factor of the load variable in the load-rotation relationship $n_{\varepsilon,R,II}$ is constant and equal to 1.5 as it can be observed from Eq.(7) (plotted in Figure 3.5 (b)). Consecutively, the values of parameters describing the influence of the failure criterion ($n_{\theta FC,II}$) and of the load-rotation relationship ($-n_{\theta LR,II}$) sub-models' uncertainties on the resistance solution are also calculated and plotted in Figure 3.5(c) and (d) (refer to Eq.(9) for definitions). It can be observed that, for the investigated cases, the value of - $n_{FC,\varepsilon}$ changes within a relatively modest range (from 0.38 to 0.74). Consequently, the values of the exponents $n_{\theta FC,II}$ and $-n_{\theta LR,II}$ are also relatively stable for the investigated cases.
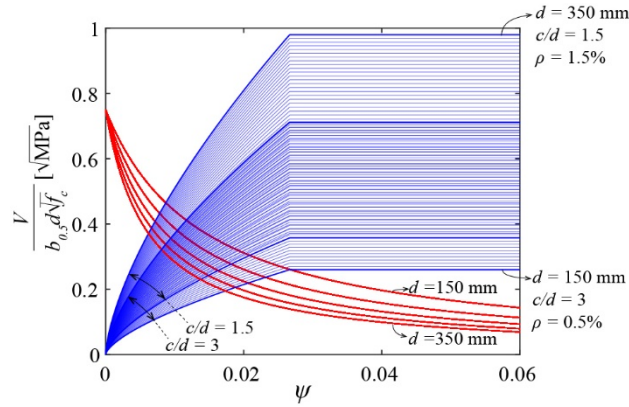
Figure 3.4:   Normalized failure criterion and LoA II load-rotation relationships obtained with the parametric study (refer to Table 3.1 for details)

If both θ_{FC} and $\theta_{LR,II}$ are assumed to be lognormally distributed (to be verified with experimental data), the relationship between the Coefficient of Variation (CoV) of the global model uncertainty and the sub-models' uncertainties can be approximated as follows (based on Eq. (9)):

$$CoV_{solu,II} \cong \sqrt{n_{\theta FC,II}{}^2 \cdot CoV_{FC}^2 + n_{\theta LR,II}{}^2 \cdot CoV_{LR,II}^2} \tag{10}$$

Based on the range of values of $n_{\theta FC,II}$ (0.47 to 0.64) and - $n_{\theta LR,II}$ (0.24 to 0.35), it can be inferred that the CoV of the resistance solution ($CoV_{solu,II}$) is lower than the maximum of the CoV of the sub-models. This result is consistent with the data reported in [Mut08] and already introduced in Section 3.1.2.
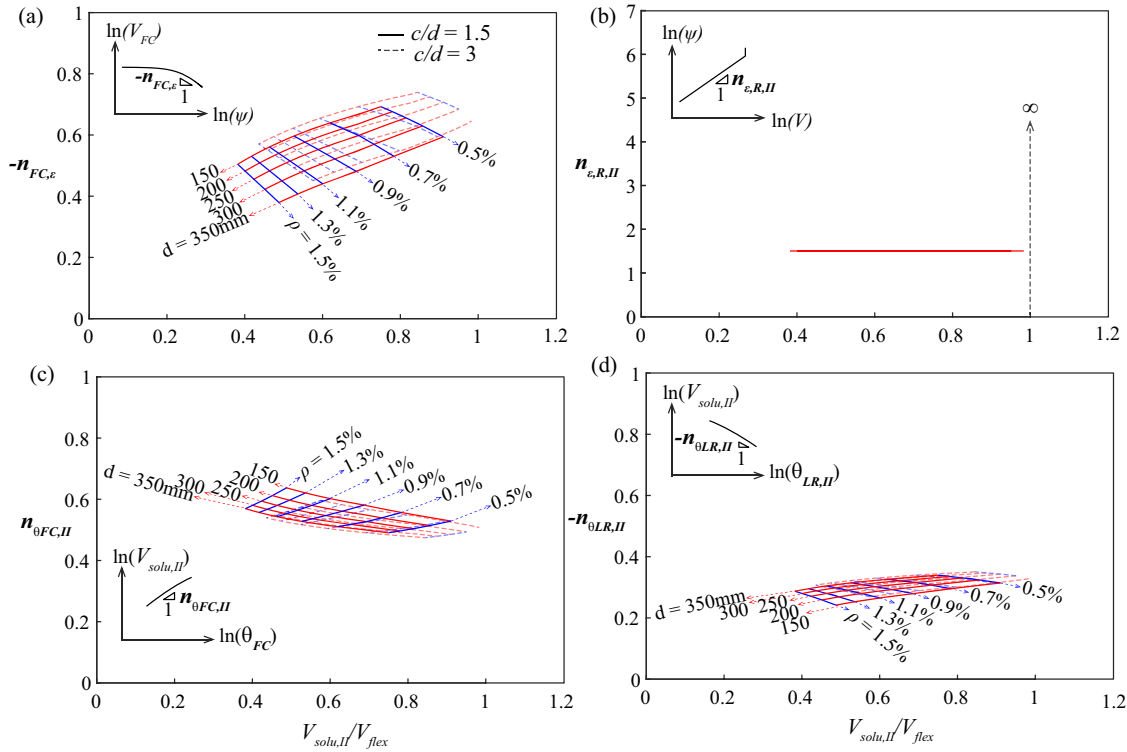
Figure 3.5:   (a) values of $-n_{FC,\varepsilon}$; (c) $n_{\varepsilon,R,II}$; (c) $n_{\theta FC,II}$ and (d) $-n_{\theta LR,II}$ obtained with LoA II plotted as a function of the ratio $V_{solu,II}/V_{flex}$

3.3.2   LoA IV load-rotation relationship

Alternatively, the load-rotation relationship can be evaluated with the LoA IV, which considers explicitly the influence of concrete cracking, steel yielding and tension-stiffening on the flexural behaviour of the structure. The LoA IV load-rotation relationship usually takes an implicit form, which can be represented by the following function:

$$\psi = F_{LR,IV}(\mathbf{x}_\varepsilon, \theta_{LR,IV}) = F_{LR,IV}[(\mathbf{x}_b, V), \theta_{LR,IV}] = \breve{F}_{LR,IV}(\mathbf{x}_b, V) \cdot \theta_{LR,IV} \qquad (11)$$

In this paper, the analytical nonlinear load-rotation relationship presented in [Mut08] considering the quadrilinear moment-curvature relationship for the reinforced concrete cross section is adopted (refer to Appendix 1 of [Mut08] for the full calculation procedure according to LoA IV).

Since the load-rotation relationship takes an implicit form in the LoA IV, the exponent sensitivity factor referring to the influence of the load variable in the load-rotation relationship $n_{\varepsilon,R,IV}$ (the subscript IV refers to the LoA IV) also differs from case to case. Similar to the estimation of the exponents in Section 3.3.1, a parametric study is performed to investigate the ranges of values in which the exponent factors vary (again, only cases where $V<V_{flex}$ are

64

investigated). The normalized failure criterion and load-rotation curves for the parametric study are plotted in Figure 3.6.

<div align="center">
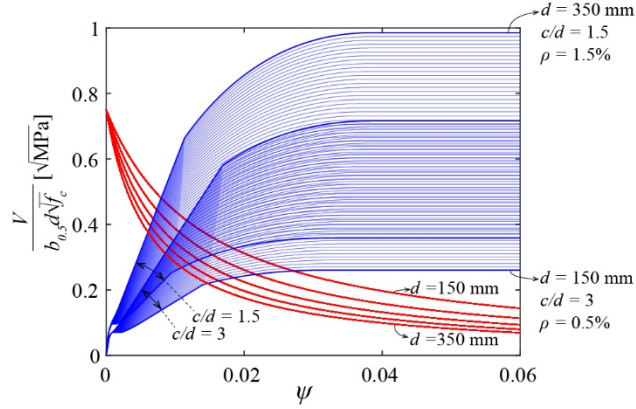
Figure 3.6:   Normalized failure criterion and LoA IV load-rotation relationship obtained for the parametric study

</div>

The values of $-n_{FC,\varepsilon}$ and $n_{\varepsilon,R,IV}$ for each case are calculated at the LoA IV resistance solution point (see results in Figure 3.7(a) and (b)). The values of $n_{\theta FC,IV} = \dfrac{1}{1-n_{\varepsilon,R,IV}n_{FC,\varepsilon}}$ and

$n_{\theta LR,IV} = \dfrac{n_{FC,\varepsilon}}{1-n_{\varepsilon,R,IV}n_{FC,\varepsilon}}$ are also calculated and plotted in Figure 3.7 (c) and (d). The following

phenomena can be observed:

- A regime change can be observed in the values of $n_{\varepsilon,R,IV}$, which is the result of the change of the flexural behaviour of the slab from fully cracked with the reinforcement in the elastic regime to partial yielding of the flexural reinforcement.

- The values of $n_{\varepsilon,R,IV}$ vary within a much larger range (1.1-6.7) than in LoA II. Consequently, $n_{\theta FC,IV}$ and $-n_{\theta LR,IV}$ also vary within significantly larger ranges (0.19-0.71 and 0.12-0.38, respectively). It can also be observed that when the regime change occurs with the increasing punching-to-flexural resistance ratio $V_{solu,IV}/V_{flex}$, the values $n_{\theta FC,IV}$ and $-n_{\theta LR,IV}$ decrease significantly. As a result, it can be anticipated that the model uncertainty of the resistance solution should have decreasing CoV with increasing $V_{solu,IV}/V_{flex,}$. In other words, the model uncertainty of the resistance solution should be heteroscedastic.
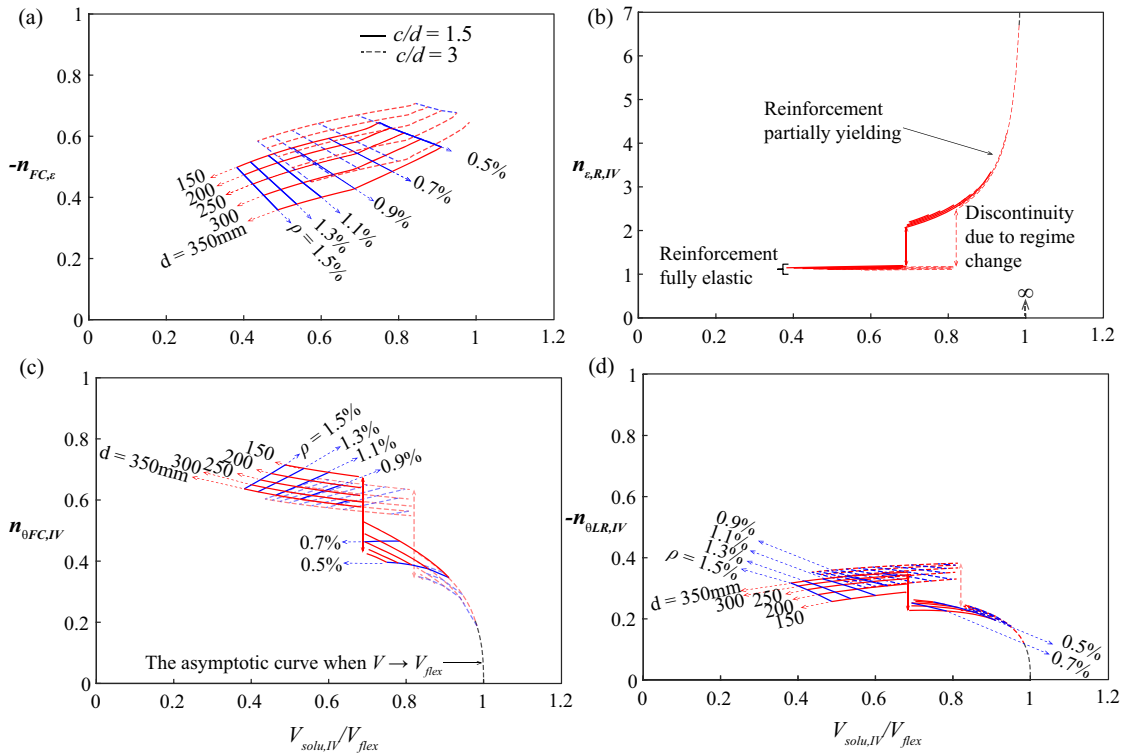
Figure 3.7: (a) values of $-n_{FC,\varepsilon}$, (b) $n_{\varepsilon,R,IV}$, (c) $n_{\theta FC,IV}$ and (d) $-n_{\theta LR,IV}$ obtained for

LoA IV as a function of the ratio $V_{solu,IV}/V_{flex}$

The results of the theoretical derivation above presented are verified in the following sections by quantifying the model uncertainty as a random variable based on a collected database of experimental tests.

3.4 Model uncertainty quantification of CSCT for punching shear

3.4.1 General considerations

The quantification of the model uncertainty of the CSCT for punching shear is performed on the basis of the Bayesian inference framework (refer to Annex 3.A for details). For that purpose, a database [Clé12, Dra16, Ein16, Gua09, Gui10, Hal96, Kin60, Lip12, Fer10, Tas11, Tol88] of 55 tests on the punching shear resistance of slender flat slabs is collected. Only tests of axisymmetric slabs without shear reinforcement, subjected to a centred monotonic loading are selected. Also, in order to investigate the model uncertainty of the load-rotation relationship, only tests with explicitly reported data of the rotation at failure are selected (refer to Annex 3.B

for the details on the test database). It should be noted that the quantification of model uncertainties relies on test data from test reports. With this respect, it has to be considered that the reported test data are inevitably influenced by errors associated with measurement devices and measurement procedures involved in tests [Ell80, Fos16, Gar02]. In this work, the influence of measurement errors in the test data is considered following the method proposed by Gardoni et al. in [Gar02] (refer to Annex 3.A.2 and 3.A.3 for details on the treatment of measurement errors). In the following, the model uncertainties of the sub-models of the CSCT (failure criterion and load-rotation relationship), as well as of the global strain-based resistance model are quantified.

3.4.2   Quantification of model uncertainties following LoA II

In this section, the model uncertainties of the LoA II of the CSCT punching shear resistance model are investigated.

For the failure criterion, the observation of the model uncertainty (denoted as θ_{FC}) for a given result from the collected test database is given by:

$$\theta_{FC} = \frac{V_{FC,test}}{\breve{F}_{FC}(\mathbf{x}_{FC})} = \frac{V_{FC,test}}{\breve{F}_{FC}(\mathbf{x}_b, \psi_{test})} \tag{12}$$

Where $V_{FC,test}$ is the failure load of the test, $\mathbf{x}_{FC}$ are the corresponding input variables and ψ_{test} is the rotation at maximum load of the test (θ_{FC} is illustrated in Figure 3.8(a)).

The Quantile-Quantile plot (Q-Q plot) of the logarithmic θ_{FC} data from the assembled punching shear tests database is shown in Figure 3.8 (b).

Similarly, for the load-rotation relationship, the observation of the model uncertainty variable (denoted as $\theta_{LR,II}$) is given by:

$$\theta_{LR,II} = \frac{\psi_{test}}{\breve{F}_{LR,II}(\mathbf{x}_\varepsilon)} = \frac{\psi_{test}}{\breve{F}_{LR,II}(\mathbf{x}_b, V_{solu,test})} \tag{13}$$

The definition of $\theta_{LR,II}$ is also illustrated in Figure 3.8 (a) and the Q-Q plot of the logarithmic $\theta_{LR,II}$ data from the assembled punching shear test database is plotted in Figure 3.8 (c).

Finally, for the global solution model, the observation of the model uncertainty, denoted as $\theta_{solu,II}$, is calculated as follows:

$$\theta_{solu,II} = \frac{V_{solu,test}}{\breve{F}_{solu,II}(\mathbf{x}_b)} \tag{14}$$

The definition of $\theta_{solu,II}$ is also illustrated in Figure 3.8 (a) and the Q-Q plot of the logarithm of the $\theta_{solu,II}$ data from the assembled punching shear test database is plotted in Figure 3.8 (d).
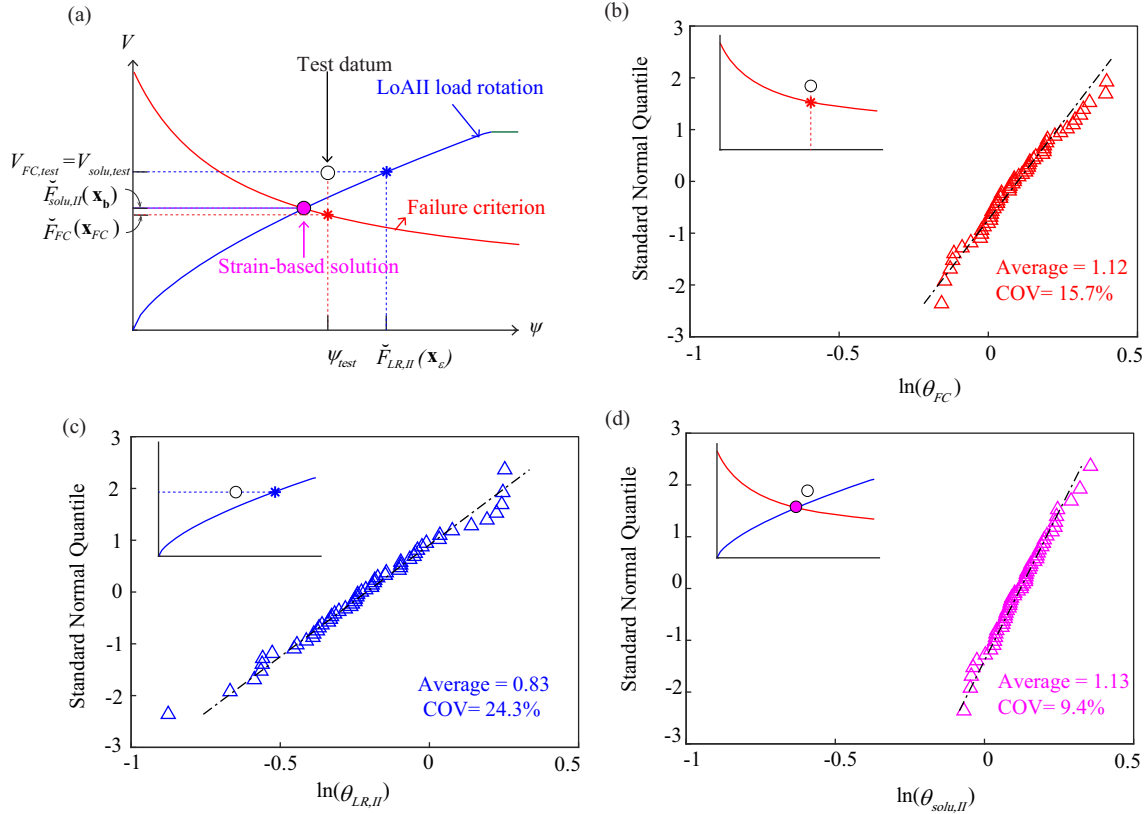
Figure 3.8:   (a) Definition of the model uncertainties of the sub-models (b) Quantile-Quantile plot and statistics (mean value and CoV) of data of the model uncertainty of the failure criterion, (c) LoA II load-rotation model and (d) of resistance solution

The correlation matrix of the model uncertainty data from the failure criterion sub-model, the load-rotation relationship sub-model, and the global resistance model are provided in Table 3.2. It can be observed that the correlation coefficient (calculated as the ratio between their covariance and the product of their standard deviations) between the failure criterion sub-model and the load-rotation sub-model is relatively small (0.25). This result shows that the independency assumption about these two variables is acceptable for these models.

Table 3.2:   Correlation matrix of the model uncertainty data of failure criterion model, load strain model and global resistance solution of CSCT

	θ_{FC}	$\theta_{LR,II}$	$\theta_{solu,II}$
θ_{FC}	1		
$\theta_{LR,II}$	0.25	1	
$\theta_{solu,II}$	0.68	-0.50	1

3.4.3 Bayesian inference of the model uncertainty distributions parameters

Based on the model uncertainty data presented above and applying the Bayesian inference method [Box92] (refer to Annex 3.A.1 for details), posterior distributions and point estimates can be calculated for the model uncertainty distribution parameters. The isolines of the resultant posterior distributions and point estimates of the distribution parameters are plotted in Figure 3.9(a). It should be noted that the Bayesian inference is performed for the mean (μ_θ) and standard deviation (σ_θ) of the logarithm of the model uncertainty variables ($\ln(\theta)$)(refer to Annex 3.A.1 for details), but for clarity of illustration, the approximated mean value ($\tilde{\mu}_\theta$) and the coefficient of variation ($\widetilde{CoV}_\theta$) of the original model uncertainty variable θ are presented. The relationship between the distribution parameters in the original space ($\tilde{\mu}_\theta$ and $\widetilde{CoV}_\theta$) and in the logarithmic space (μ_θ and σ_θ) is approximated as $\tilde{\mu}_\theta \cong \exp(\mu_\theta)$ and $\widetilde{CoV}_\theta \cong \sigma_\theta$. It can also be noticed that the value of $\widetilde{CoV}_\theta$ differs slightly from the reported CoV in Figure 3.8. This is because the value in Figure 3.8 is the sample CoV, but the value $\widetilde{CoV}_\theta$ in Figure 3.9 is based on the posterior estimation of σ_θ.

Furthermore, through probabilistic modelling of the measurement errors (refer to Annex 3.A.2 and 3.A.3 for details), posterior distributions and point estimates of the model uncertainty parameters considering the influence of measurement errors can also be calculated. The resultant posterior distributions and point estimates of the three model uncertainty variables after accounting for the influence of measurement errors are plotted in Figure 3.9(b). It can be observed that measurement errors have a significant influence on the standard deviation of the model uncertainty variables.
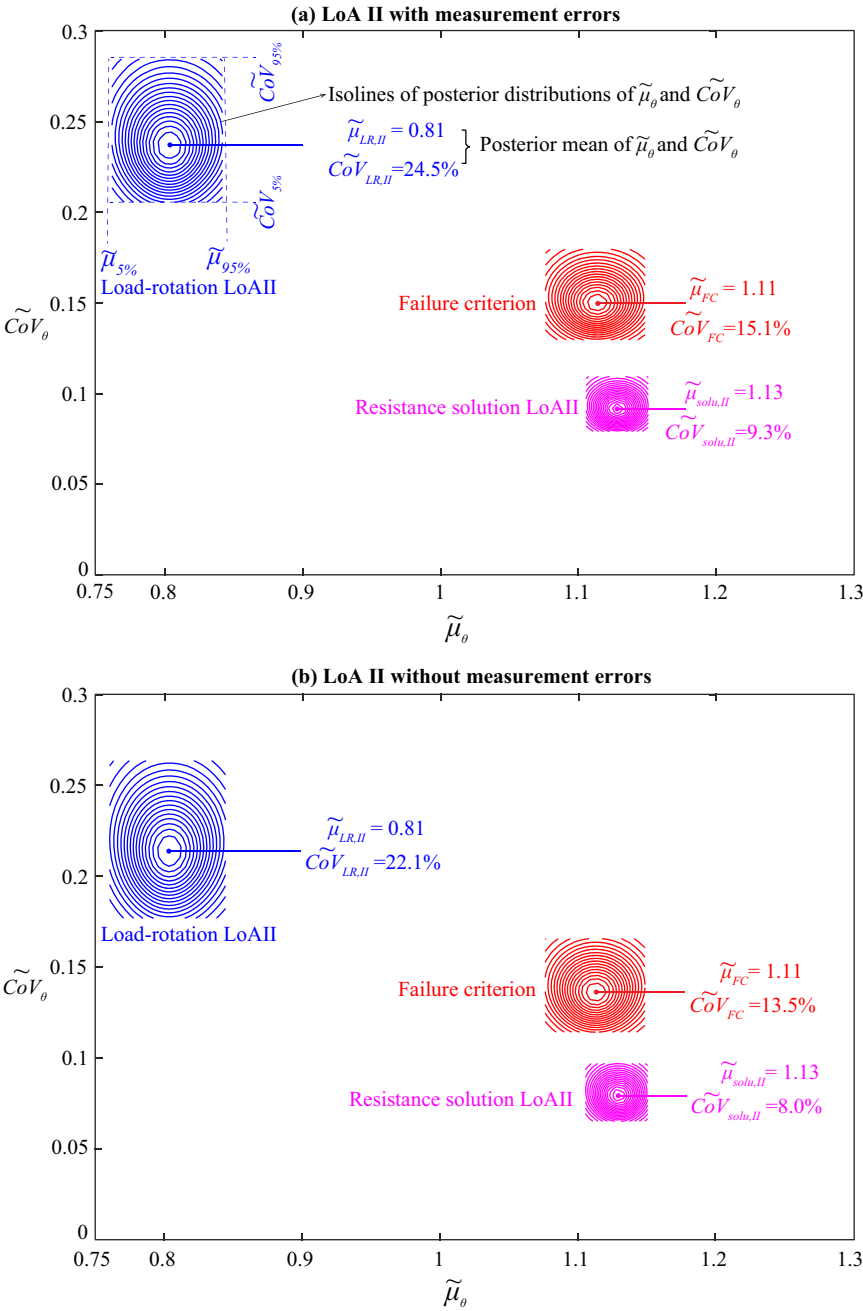
Figure 3.9: Posterior distributions of model uncertainty distribution parameters of LoA II (a)with and (b)without measurement errors

It can be observed from Figure 3.9 that the CoV of the model uncertainty of the global resistance solution (pink) is significantly lower than those of the sub-models (blue and red), which is consistent with the theoretical derivation of Section 3.3. Attention should be paid to this aspect in the calibration of the codified safety format of strain-based approaches.

70

3.4.4 Quantification of model uncertainties following LoA IV

The procedure outlined in the previous section is applied in this section for the LoA IV, notably to calculate the model uncertainty of the load-rotation relationship sub-model and of the global resistance solution. It should be noted that the model uncertainty of the failure criterion sub-model remains the same for LoA II and LoA IV since the same failure criterion is used.

The Q-Q plot of the $\theta_{LR,IV}$ and $\theta_{solu,IV}$ data from the assembled punching shear test database is plotted in Figure 3.10.
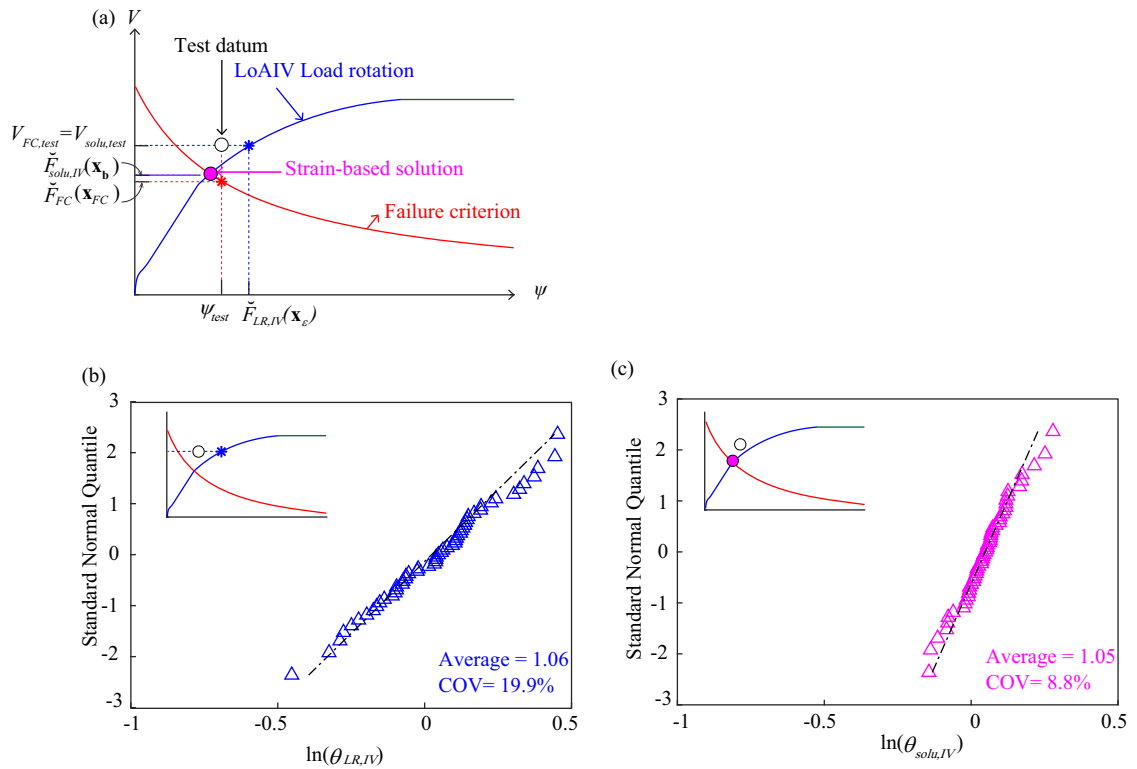
Figure 3.10: (a) Definition of the model uncertainties of sub-model and global solution (b) of LoA IV load-rotation relationship sub-model and (c) of global resistance solution
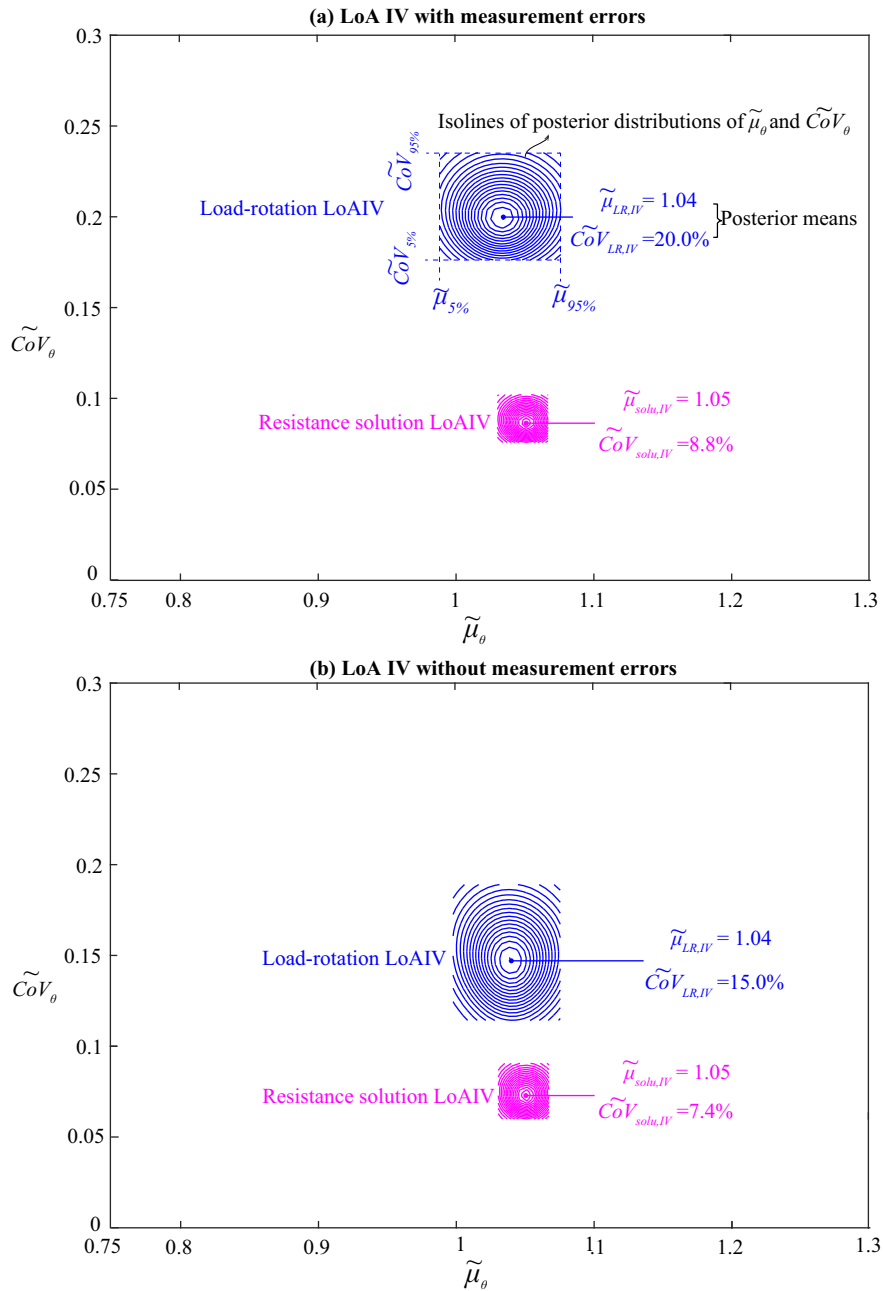
Figure 3.11:   Posterior distributions of model uncertainty distribution parameters of LoA IV (a) with and (b) without measurement errors

Based on the model uncertainty data, following the Bayesian inference method [Box92](refer to Annex 3.A.1 for details), the point estimates of the model uncertainty distribution parameters of the three models can be calculated. Their posterior distributions and point estimates are plotted in Figure 3.11. It can be observed that the measurement errors have a more significant influence on the distribution parameters of the load-rotation relationship model uncertainty of LoA IV than that of LoA II. This result suggests that the influence of other sources of uncertainty (as the

measurement errors) becomes more influential in more refined approaches, which indicates that the application of models with increased complexity and level of detail requires a critical evaluation of additional sources of uncertainties.

3.5 Discussions on the model uncertainties of LoA II and LoA IV

3.5.1 Comparison between the model uncertainties obtained for LoA II and LoA IV

Comparing the Q-Q plots of the model uncertainty data of the LoA II (Figure 3.8) and LoA IV (Figure 3.10) load-rotation sub-models, it can be observed that, as expected, the LoA IV load-rotation model uncertainty data has a smaller CoV (19.9 %) than LoA II (24.3%). Furthermore, it can be observed that the LoA II load-rotation sub-model has a significant conservative bias (mean value equal to 0.83, corresponding to an overestimation of the rotation at the resistance point), while the corresponding LoA IV sub-model has a smaller unconservative bias (mean value 1.06). These results are consistent with the principles of an approach based on LoAs introduced in Section 3.1.3.

From the quantile-quantile plots of LoA II and LoA IV load-rotation model uncertainties (Figure 3.8 and Figure 3.10), it can also be observed that the LoA IV data show a good fit to a lognormal distribution, while LoA II data have relatively larger deviations in the tail region. This is also consistent with the fact that the formula of the LoA II load-rotation relationship has been derived analytically by simplification of the general formula of the mechanically based LoA IV load-rotation relationship [Mut08], but not explicitly accounting for the two regimes described above (elastic and elastic/partial yielding of reinforcement). It is reasonable to assume that the model uncertainty of the LoA II load-rotation sub-model results from both the innate LoA IV load-rotation model uncertainty and the additional epistemic uncertainty introduced by the simplification process. This assumption is further supported by the correlation between the LoA II and LoA IV load-rotation model uncertainty data (with a correlation coefficient of 0.71), as plotted in Figure 3.12, where the cases with the flexural reinforcement remaining fully elastic according to LoA IV are represented by blue dots and those with the flexural reinforcement partially yielding are represented by red dots.
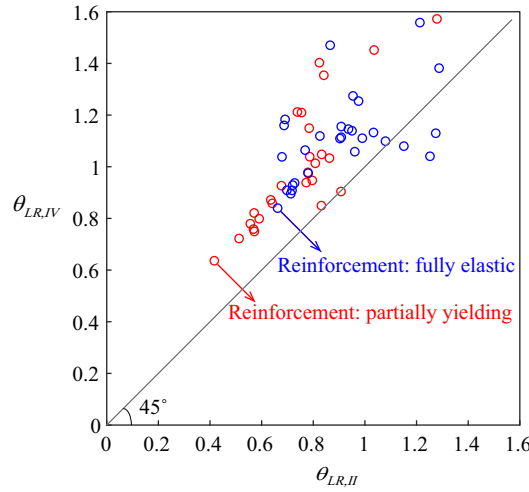
Figure 3.12:   Relationship between the LoA II and LoA IV load-rotation model uncertainty data

3.5.2   Relationship between model uncertainty of sub-models and global resistance solution

The global resistance model uncertainty data is plotted in Figure 3.13 as a function of the punching-to-flexural resistance ratio V_{solu}/V_{flex} for both the LoAII and the LoAIV. Also, the estimated CoVs of the global resistance model uncertainty solution based on the relationship

$$CoV_{solu} \cong \sqrt{n_{\theta FC}^{2} \cdot \tilde{CoV}_{FC}^{2} + n_{\theta LR}^{2} \cdot \tilde{CoV}_{LR}^{2}}$$ (refer to Figure 3.9(a) and 3.11(a) for values of $\tilde{CoV}_{FC}$ and

$\tilde{CoV}_{LR}$) are also calculated and plotted in Figure 3.13. It can be observed that the moving CoV of the model uncertainty data (calculated with 15 neighbour data points) of both LoA II and LoA IV shows a descending trend. It is interesting to note that for LoA IV, the estimated $CoV_{solu,IV}$ has a descending trend following well the test data. This is a resultant of the decreasing values of $n_{\theta FC,IV}$ and $n_{\theta LR,IV}$ with the regime change of the LoA IV load-rotation relationship (see Figure 3.7). From another perspective, the decrease of the moving CoV of the resistance solution model uncertainty originates from the fact that with the increase of the ratio of V_{solu}/V_{flex}, the behaviour is increasingly dominated by the flexural behaviour of the structure (as the amount of flexural reinforcement yielded is increasing, resulting into a softer secant of the load-rotation relationship at the resistance point), which tends to have lower model uncertainty than a punching failure occurring in a regime where most of the flexural reinforcement is responding in the elastic regime.

On the other hand, for LoA II, the estimated $CoV_{solu,II}$ has a relatively constant value since the approximated LoA II load-rotation relationship does not differentiate the different regimes in the flexural response, resulting in a larger deviation of the $CoV_{solu,II}$ from the moving CoV of the test data. This result shows that lower LoAs also tend to have higher statistical uncertainty

resulting from the simplifications and approximations made in the model (additional epistemic uncertainties). It can also be observed that if the model uncertainty is directly approximated by a random variable at the solution level, potentially higher statistic uncertainty will be introduced, since the heteroscedastic nature of the model uncertainty of the resistance solution is ignored. From this perspective, it is more appropriate to quantify the model uncertainties at the sub-model level (especially for higher LoAs), when sufficient data is available.
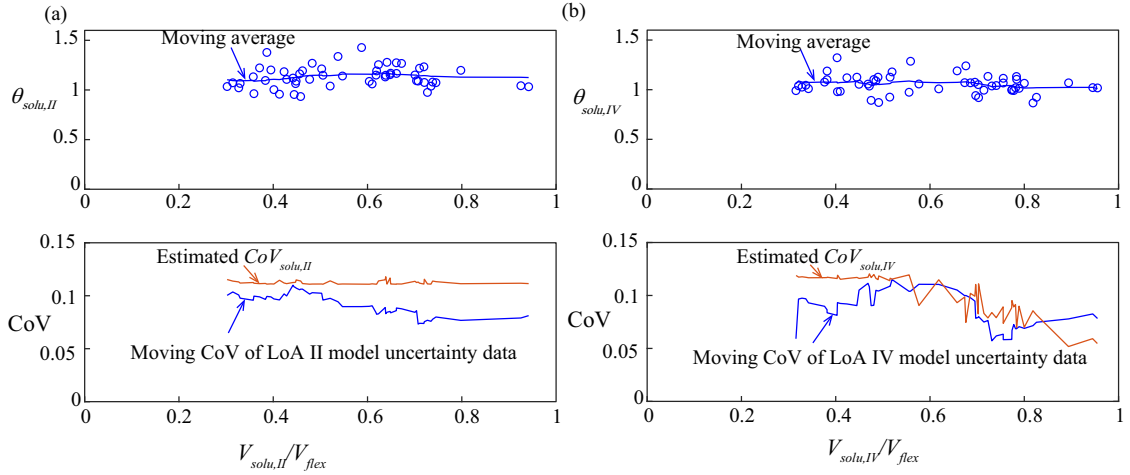
Figure 3.13:   Moving average and moving CoV of (a) LoA II and (b) LoA IV resistance solution model uncertainty data

3.6   Discussion on the partial safety factors for strain-based approaches

The partial safety factor format is widely adopted in the semi-probabilistic approach for codified reliability verification, in which partial safety factors are applied to the governing basic design variables in order to account for different types of basic uncertainties [CEN04, FIB13]. From a theoretical point of view, the partial safety factors required to achieve a target reliability index change from case to case. Nevertheless, in codified design practice, fixed values of partial safety factors are used for practical reasons. These partial safety factors are normally calibrated based on given optimization criteria and various calibration methods are available for that purpose [Fah21, Gay04, Rac00]. The calibration process of the different partial safety factors is however out of the scope of this paper and the following discussion will rather focus on the comparison and the consistency of the partial safety factors to be applied to the same verification (punching shear in the present work) according to the different safety formats. In the following, two types of partial safety factors formats (and notably to the case of CSCT for punching shear) are compared.

On the one hand, Safety Format A uses several partial safety factors (see Figure 3.14(a)): one partial factor γ_{FC} applied to the failure criterion sub-model, another partial factor γ_{def} applied to load-rotation sub-model (assuming that model uncertainties are dominating) and the two partial safety factors to material strength variables used in design codes such as Eurocode [CEN23] and *fib* Model Code 2010 [FIB13] (γ_C for concrete compressive strength and γ_S for steel yielding strength) which apply implicitly to the load-rotation relationship (reducing the flexural resistance V_{flex}). The design values of the failure criterion, the rotation and the punching resistance become:

$$\begin{cases} R_{FC,d} = \dfrac{1}{\gamma_{FC}} \breve{F}_{FC}(\mathbf{x}_{b,d}, \varepsilon_d) \\[2mm] \varepsilon_d = \gamma_{def} \cdot \breve{F}_\varepsilon(\mathbf{x}_{b,d}, R) \\[2mm] R_{solu,d,A} = R_{FC,d} = R \end{cases} \tag{15}$$

On the other hand, safety format B includes the application of a single partial factor γ_V to the resistance solution (in addition to the two partial safety factors γ_S and γ_C which are commonly used for the flexural failure mode):

$$R_{solu,d,B} = \frac{1}{\gamma_V} \breve{F}_{solu}(\mathbf{x}_{b,d}) \tag{16}$$

The effect of applying the partial factors individually to the sub-models (Safety Format A) is illustrated in Figure 3.14 (a) for the LoA IV. It can be observed that when the partial safety factors are applied to the sub-models, they have a nonlinear effect on the resistance solution.

Figure 3.14:　(a) Illustration of the effect of the partial factors of sub-models to the design resistance solution for the cases with f_{yk} = 500 MPa (f_{ym} = 538 MPa), f_{ck} = 30 MPa (f_{cm} = 33.6 MPa), d = 150 mm, h = 200 mm, c =450 mm, r_s = 1100mm and d_g = 16mm and (b) the equivalent partial safety factor $\gamma_{V,IV}$ of Safety format B for constant partial safety factors γ_{FC} and γ_{def} of Safety format A for the LoA IV approach of CSCT

3.6.1 Relationship between partial safety factors of different safety formats

Integrating the multiplicative form approximation of the failure criterion and the load-rotation sub-models of Eq. (3) into Eq. (15) and (16), the following functions can be respectively derived for the design resistance in the two safety formats:

$$R_{solu,d,A} = \gamma_{FC}^{\frac{-1}{1-n_{\varepsilon,R}n_{FC,\varepsilon}}} \cdot \gamma_{def}^{\frac{n_{FC,\varepsilon}}{1-n_{\varepsilon,R}n_{FC,\varepsilon}}} \cdot C_{FC}^{\frac{1}{1-n_{\varepsilon,R}n_{FC,\varepsilon}}} \cdot C_{\varepsilon}^{\frac{n_{FC,\varepsilon}}{1-n_{\varepsilon,R}n_{FC,\varepsilon}}} \cdot \prod_{i=1}^{N} x_{i,d}^{\frac{n_{FC,i}+n_{\varepsilon,i}n_{FC,\varepsilon}}{1-n_{\varepsilon,R}n_{FC,\varepsilon}}} \tag{17}$$

$$R_{solu,d,B} = \gamma_{V}^{-1} \cdot C_{FC}^{\frac{1}{1-n_{\varepsilon,R}n_{FC,\varepsilon}}} \cdot C_{\varepsilon}^{\frac{n_{FC,\varepsilon}}{1-n_{\varepsilon,R}n_{FC,\varepsilon}}} \cdot \prod_{i=1}^{N} x_{i,d}^{\frac{n_{FC,i}+n_{\varepsilon,i}n_{FC,\varepsilon}}{1-n_{\varepsilon,R}n_{FC,\varepsilon}}} \tag{18}$$

By equalling the design resistance obtained with the two safety formats ($R_{solu,d,A} = R_{solu,d,B}$), the following relationship between the partial safety factors associated to the two formats can be analytically established as follows:

$$\gamma_{V} = \gamma_{FC}^{\frac{1}{1-n_{\varepsilon,R}n_{FC,\varepsilon}}} \gamma_{def}^{\frac{-n_{FC,\varepsilon}}{1-n_{\varepsilon,R}n_{FC,\varepsilon}}} \tag{19}$$

On the basis of the values of the exponent sensitivity factors from the parametric analysis (refer to Figure 3.5 and Figure 3.7), it can be inferred that a given pair of partial safety factors γ_{FC} and γ_{def} corresponds to a range of values for γ_{V} due to the variation of the exponents sensitivity factors ($n_{\varepsilon,R}$ and $n_{FC,\varepsilon}$) for the different cases. For the LoA IV, an illustration of the resulting values of $\gamma_{V,IV}$ for fixed values of $\gamma_{FC} = 1.62$ and $\gamma_{def} = 1.33$ is plotted in Figure 3.14(b) (the choices of these values will be explained in Section 3.6.2). The effect of the partial safety factors γ_{C} and γ_{S} (for the flexural failure mode) on the punching shear resistance is also plotted (the factors n_{fc} and n_{fy} represent their corresponding exponent sensitivity factors in the punching resistance solution function). The following observations can be made from Figure 3.14:

-   to achieve the same design resistance, the values of the partial safety factor $\gamma_{V,IV}$ applied to the resistance solution can take a lower value than the partial safety factors individually applied to the sub-models;

-   the partial safety factor $\gamma_{V,IV}$ presents three regimes corresponding to the three regimes at failure considered in the load-rotation relationship (punching with reinforcement remaining elastic, punching with reinforcement partially yielding and flexural failure);

-   the partial safety factors γ_{C} and γ_{S} have a nonnegligible influence on the punching shear resistance in the regime of punching shear failure with the flexural reinforcement partially yielding.

The results in Figure 3.14 show that Safety Format A applied to the LoA IV can effectively account for the change of model uncertainties associated to the different punching shear failure regimes. Due to this reason, Safety Format A is more suitable in higher LoA, where the load-rotation relationship and the failure criterion sub-models are treated as two independent functions and where the different regimes at failure are explicitly accounted for (through the load-rotation relationship).

Following the same procedure, for the LoA II, an illustration of the resulting values of $\gamma_{V,II}$ for fixed values of γ_{FC} and γ_{def} is plotted in Figure 3.15. It can be observed that, unlike the case of the LoA IV, the value $\gamma_{V,II}$ varies in a much smaller range (although a decreasing value of $\gamma_{V,II}$ can be observed for increasing values of the rotation). This results from the fact that the different punching shear failure regimes are not explicitly accounted for and are not differentiated in the load-rotation relationship (due to the simplification made in the load-rotation relationship of LoA II as discussed in Section 3.3.1). This result suggests that for LoA II, both safety formats A and B are suitable. However, it should be noted that since the model uncertainty of the load-rotation relationship is higher for LoA II, the partial safety factors γ_{FC} and γ_{def} should also be higher than those for LoA IV.
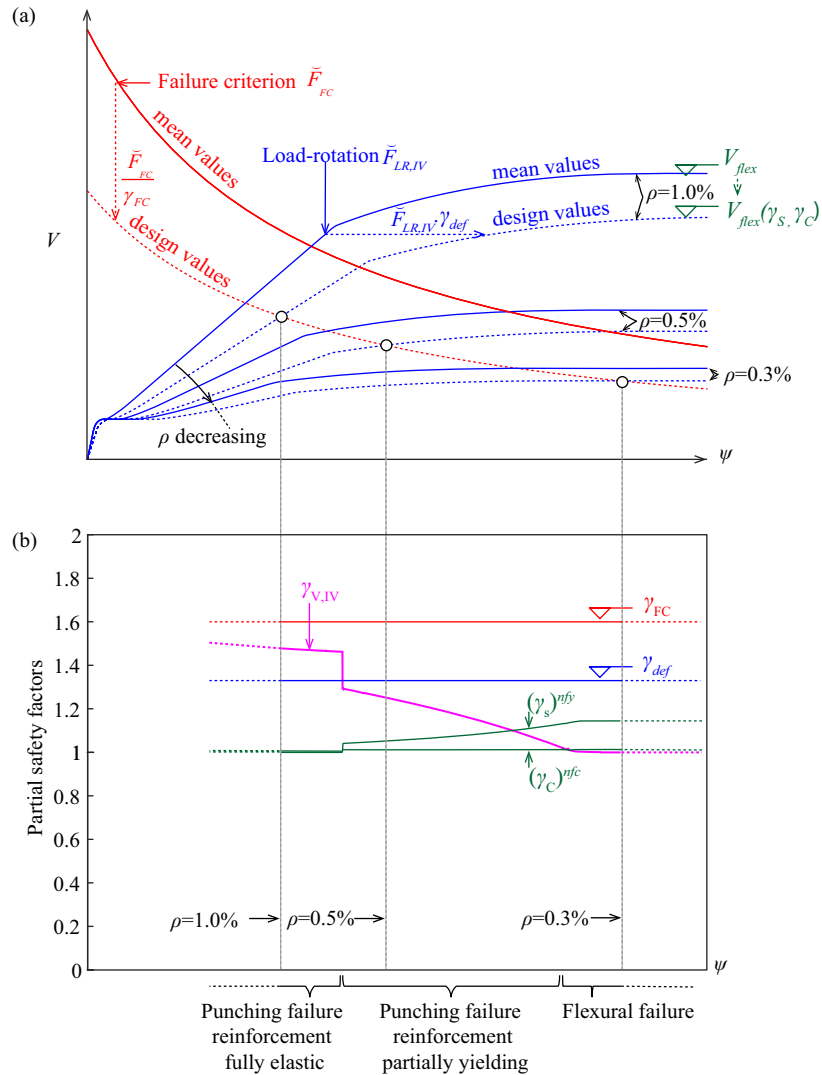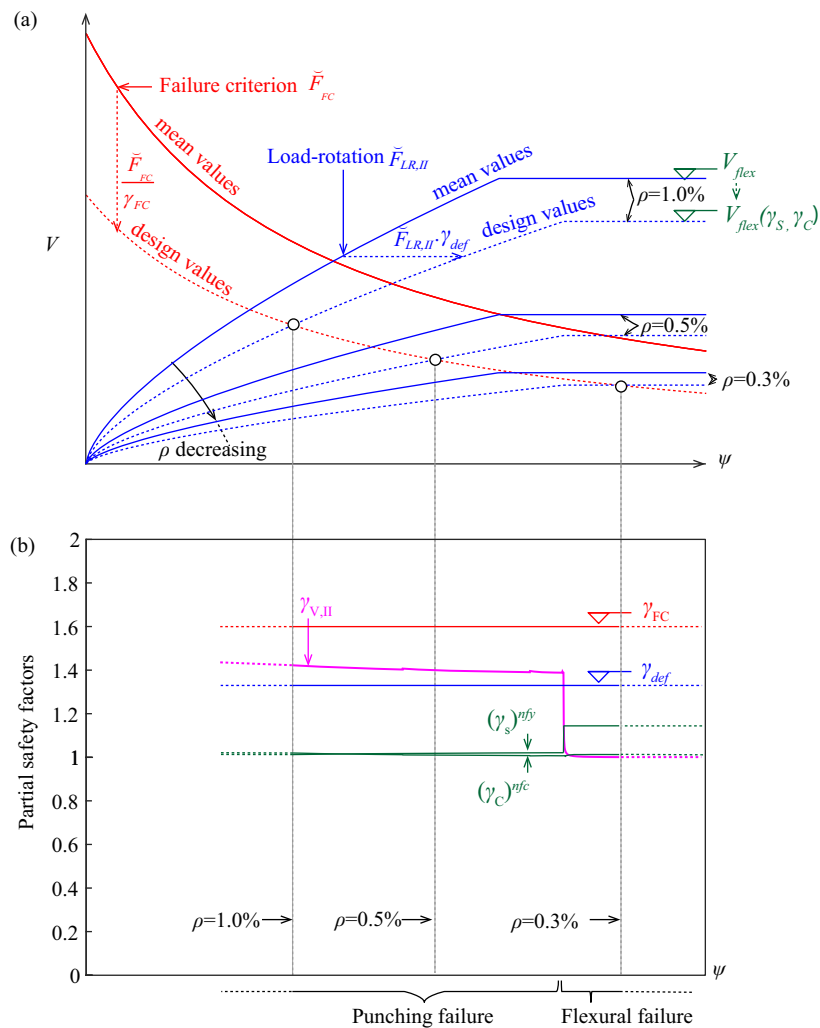

Figure 3.15:   (a)Illustration of the effect of the partial factors on sub-models to the design resistance solution (same geometrical and material parameters as in the LoA IV cases are used) and (b) the equivalent partial safety factor $\gamma_{V,II}$ of

Safety format B for fixed partial safety factors γ_{FC} and γ_{def} of Safety format A for the LoA II approach of CSCT

3.6.2 Relationship between partial safety factors adopted for the punching shear provisions in the second generation of Eurocode 2

In the new generation of the European standard for concrete structures (Eurocode 2 [CEN23]), a closed-form design expression is provided for the punching shear design (Clause 8.4 of prEN1992-1-1:2023 [CEN23], typically to be used for designing new structures). As discussed in reference [Mut23a], this design expression is analytically derived based on a power-multiplicative form approximation of the failure criterion and the LoA II load-rotation relationship (which corresponds to constant values of $n_{FC,\varepsilon}$ and $n_{\varepsilon,R}$). The validity of the approximated closed-form design expression (as well as the values of the exponents $n_{FC,\varepsilon}$ and $n_{\varepsilon,R}$ adopted in it) is confirmed by the relatively low level of model uncertainty associated with it (refer to [Mut23b] for details). For this closed-form design expression, only the safety format B can be adopted (as no distinction can be made between load-rotation and failure criterion sub-models). The calibration of the partial safety factor γ_V required in Safety Format B for such design expression is presented in reference [Mut23]. It accounts not only for the model uncertainty, but also for the material and geometrical uncertainties involved in the design model (refer to [Mut23] for the calibration details), a value of $\gamma_V = 1.40$ is proposed [Mut23b].

Alternative to the closed-form design expression in Clause 8, in Annex I of FprEN1992-1-1:2023 [CEN23] (assessment of critical existing structures), the application of the strain-based punching shear resistance model is also provided. In this case, the Safety Format A is adopted and the following design formula is used:

$$\begin{cases} \dfrac{V_{FC,d}}{b_{0.5}d\sqrt{f_c}} = \dfrac{1}{\gamma_{FC}} \cdot \dfrac{3/4}{1+15\dfrac{\psi_d \cdot d}{d_{g0}+d_g}} \\ \psi_d = \gamma_{def} \cdot \bar{F}_{LR}(\mathbf{x}_{b,d},V) \\ V_{solu,d,A} = V_{FC,d} = V \end{cases} \tag{20}$$

It should be noted that different LoAs of the load-rotation relationship are allowed to be used in Eq.(20). Theoretically, the partial safety factors should be calibrated individually accounting for their respective model uncertainties. However, in order to provide a relatively simple safety format that is convenient in practice, the partial safety factors are not differentiated for the

different LoAs of load-rotation relationships used in Eq.(20) and, to be on the conservative side, the model uncertainties of lower LoA are adopted in the calibration of the partial safety factors.

With the relationship between safety factors presented in Eq. (19), the value of γ_{FC} can be calculated based on the values of γ_V and γ_{def}. Consistent with the functions adopted in the derivation of closed-form design expression of Clause 8.4 of FprEN 1992-1-1:2023 [CEN23, Mut17, Mut23b], $n_{FC,\varepsilon} = -\frac{2}{3}$ and $n_{\varepsilon,R} = \frac{3}{2}$ are adopted (such values also agree with the result of the parametric study of Section 3.3.1) and Eq.(19) relating the different partial safety factor becomes:

$$\gamma_{FC} = \frac{\gamma^2_V}{\gamma^{2/3}_{def}}$$

(21)

Using Eq.(21), the relationship between γ_{FC} and γ_V for different values of γ_{def} is plotted in Figure 3.16. It can also be observed that in most of the cases, the value of γ_{FC} is higher than the value of γ_V.
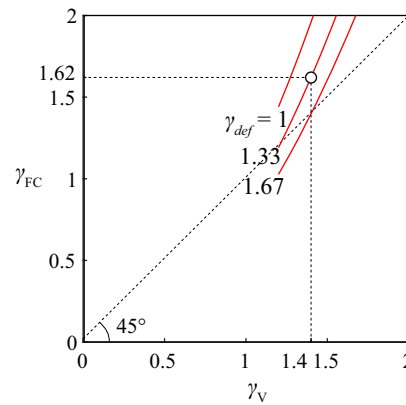
Figure 3.16:   Relationship between the partial safety factor applied to resistance solution γ_V (Safety Format B) and the partial safety factors applied to the sub-models γ_{FC} and γ_{def} (Safety Format A) adopting the exponent factors $n_{FC,\varepsilon} = -\frac{2}{3}$ and $n_{\varepsilon,R} = \frac{3}{2}$

It is further assumed that the global resistance solution of strain-based model in Eq.(20) has the same level of model uncertainty as the closed-form expression. This assumption should be conservative for LoA II and LoA IV since in principle they should have lower level of model uncertainties than the closed-form expression. Following this assumption, the partial safety factor applied to the global resistance solution (Safety Format B) of the strain-based model can be conservatively taken the same as the one for the closed-form design expression as $\gamma_V = 1.40$. Consider in addition that $\gamma_{def} = 1.33$ [Mut08, Fer08], the value of γ_{FC} can be calculated as follows:

$$\gamma_{FC} = \frac{\gamma^2_V}{\gamma^{2/3}_{def}} = 1.62 \tag{22}$$

This set of partial safety factors is adopted in Annex I of FprEN1992-1-1:2023 [CEN23], leading the failure criterion to be written in a general format as:

$$\frac{V_{FC,d}}{b_{0.5}d\sqrt{f_c}} = \frac{1}{\gamma_{FC}} \cdot \frac{3/4}{1+15\dfrac{\psi_d \cdot d}{d_{g0}+d_g}} = \frac{\gamma^{2/3}_{def}}{\gamma^2_V}\frac{3/4}{1+15\dfrac{\gamma_{def} \cdot \psi \cdot d}{d_{g0}+d_g}} \tag{23}$$

It should be emphasized that the relationship of the partial safety factors in Eq.(23) is derived based on the conservative assumption that the model uncertainties of the global resistance solution of higher LoAs are the same as that of the closed-form design expression. Theoretically, more refined calibration of the partial safety factors for higher LoAs can be performed by accounting for their corresponding model uncertainties. The format of Eq.(23) is adopted in Annex I [CEN23] as a conservative and consistent solution for engineering practice and, in addition, it also includes the relationship between the different partial safety factors of different safety formats for the strain-based approaches.

3.7 Conclusions

The model uncertainties of the sub-models and of the global solution of strain based-approaches, their relationship and their impact on the suitable safety format to be adopted in design provisions are investigated in this work.

A general theoretical approach to investigate the above-mentioned issues is first introduced, showing that:

- By approximating the sub-models of a strain-based approach in a power-multiplicative form, it is possible to easily establish the relationship between the model uncertainty of the global solution and those of the sub-models of strain-based approaches.

- The model uncertainty of the global solution can be viewed as a resultant of the model uncertainty of the sub-models. The influence of the sub-models on the uncertainty of global solution depends however on their sensitivity relationship (represented by the exponent sensitivity factors). With this respect, it is shown that the global model uncertainty can be lower than the sub-models' uncertainties, which is a relevant point to be accounted for in the safety format calibration of strain-based approaches.

The theoretical approach introduced in this work is thereafter applied to the strain-based approach of the Critical Shear Crack Theory (CSCT) for punching of reinforced concrete slabs as an example (applying the approach by Levels-of-Approximation, LoA). In addition, the

model uncertainties of the sub-models and of the global solution are also quantified by means of a parametric analysis and experimental data. The main conclusions resulting from this work are:

- The model uncertainty quantification confirms that the global solution uncertainty can be significantly lower than those of the sub-models.

- By analysing two levels of approximation (namely LoA II and LoA IV according to *fib* MC 2010), it is shown that the model uncertainty decreases with the increase of the LoA (consistently with the main principles of such an approach). Furthermore, the model uncertainty of lower LoAs can be considered as a resultant of the uncertainty of higher LoAs and the additional epistemic model uncertainty introduced in the simplification procedure adopted for the derivation of the lower LoA formulae.

- For higher LoAs, an approach based on the application of partial safety factors to the sub-models appears to be more suitable than an approach relying on the application of a single global partial safety factor to the resistance solution, since they can effectively account for the change of model uncertainty associated to the change of the failure mode. Particular attention needs to be paid to the nonlinear relationship between the partial safety factors applied to the sub-models and the resulting design resistance for strain-based approaches.

- It is shown that, if constant partial safety factors are adopted for the sub-models, the resulting global partial safety factor can vary depending on the material and geometrical parameters as well as on the resulting failure modes. For the investigated case, the global partial safety factor for punching according to the LoA IV varies between 1.48 and 1.00.

Based on some assumptions described in this work, the relationship between the safety factors of the punching shear provisions in the second generation of Eurocode 2 for the design of new structures (Clause 8.4) and the assessment of existing critical ones (Annex I) is established, justifying the safety format adopted for the latter.

Annex 3.A Model uncertainty quantification accounting for measurement error

3.A.1   Model uncertainty quantification using Bayesian method

For the purpose of model uncertainty quantification, the Bayesian method for statistical inference of random variables is first briefly summarized.

A general form of the models of interests is considered:

$$F = F(\mathbf{x}, \theta) = F(\mathbf{x}, \Theta) = \breve{F}(\mathbf{x}) \cdot \theta = \breve{F}(\mathbf{x}) \cdot \exp(\nu\sigma_\theta + \mu_\theta) \tag{24}$$

Where F is the output variable of a given model (e.g., the punching strength V_{FC} in the failure criterion model of Eq.(6), the rotation angle ψ in the load-rotation model of Eq. (7) and (11) and the punching resistance V_{solu} in the global solution models), $\mathbf{x}$ is the vector of all input variables of the model, including the basic variables and also the strain or load state variables; θ is the model uncertainty random variable and Θ is the vector of distribution parameters of θ .

Assuming that the model uncertainty variable follows a lognormal distribution (which is consistent with the assumption adopted in literature [JCS01]) and it is in a multiplicative form with the deterministic mechanical model [JCS01], Equation (24) is further extended, where $\Theta = (\mu_\theta, \sigma_\theta)$ are mean value and standard deviation of the logarithmic model uncertainty variable θ , $\breve{F}(\cdot)$ is the deterministic mechanical model, $\exp(\cdot)$ is the natural exponential function, ν is a standard normal distributed variable with zero mean and unit variance. The term $\exp(\nu\sigma_\theta + \mu_\theta)$ in this equation is equivalent to the model uncertainty random variable θ .

To quantify the model uncertainty, the distribution parameters $\Theta = (\mu_\theta, \sigma_\theta)$ need to be estimated based on data observed from relevant experiments. In this paper, Bayesian approach will be used for this purpose.

In Bayesian approach, the updating rule is used to make inference of the parameters Θ :

$$f(\Theta) = \kappa L(\Theta) p(\Theta) \tag{25}$$

Where f(Θ) is the posterior distribution of the parameters accounting for the updated state of knowledge, L(Θ) is the likelihood function representing the objective information contained in a set of observed data related to Θ , p(Θ) is the prior distribution reflecting the a-prior knowledge about Θ and κ is the normalising factor, $\kappa = [\int L(\Theta) p(\Theta) d\Theta]^{-1}$. The likelihood function is proportional to the conditioned probability of the occurrence of the observed data for given value of Θ .

In Bayesian framework, the choice of the prior distribution of the parameters can be based on prior knowledge of the parameters. When there is no prior information available the noninformative prior should be used [Box92].

The likelihood function is the conditional distribution function describing the likelihood of occurrence of observations for given values of Θ . For the model uncertainty variable, the observation values can be collected from a database of relevant test results. For a given test result, the observed model uncertainty value can be calculated as:

$$\theta_j = \frac{F_j}{\breve{F}(\mathbf{x}_j)} \quad j = 1, 2, ..., N_t \tag{26}$$

Where θ_j is observed model uncertainty value of the jth test, F_j is the observed value of F in j^{th} test, $\mathbf{x}_j$ is the vector of input variables of the jth test, $\breve{F}(\mathbf{x}_j)$ is the calculated value based on the model and N_t is the total number of tests in the database.

Since θ is assumed to follow a lognormal distribution with the parameters σ_θ and μ_θ, based on the test database, the likelihood function can then be formulated as:

$$L(\mu_\theta, \sigma_\theta) \propto \prod_{j=1}^{N_T} \left\{ \frac{1}{\sigma_\theta} \varphi(\frac{\ln(\theta_j) - \mu_\theta}{\sigma_\theta}) \right\} \tag{27}$$

Where $\ln(\cdot)$ is the natural based logarithmic function and $\varphi(\cdot)$ is the standard normal probability density function.

Based on the likelihood function in Eq. (27) and the noninformative prior distribution function, theoretically the posterior distribution of Θ is available and point estimates of Θ can be made by calculating the posterior mean values. In addition, the covariance matrix of Θ can also be calculated to evaluate the confidence level in the point estimates. In this paper, to calculate these statistics, the Hamiltonian Monte Carlo simulation method [Nea96] is employed, details of this method can be consulted elsewhere [Nea96, Nea11].

3.A.2 Treatment of measurement error in the Bayesian inference

In Section 3.A.1, the general Bayesian inference procedure for the model uncertainty quantification problem is explained. In this section the quantification method is further advanced by proper treatment of the influence of measurement error in the test data. The method used in the paper is based on the method proposed by Gardoni et al. in [Gar02].

The quantification of model uncertainties relies on test data from test reports. It has to be considered that the reported test results are influenced by the error due to measurement devices and measurement procedures involved in tests [Ell80, Fos16, Gar02].

In order to take the influence of measurement errors into consideration, first they are modelled as random variables. Denote x_i as the true value for the ith input variable and $\hat{x}_i$ as the measured value of the corresponding variable. Assume that the measurement error related to the variable is represented by a random variable e_{xi} and the true value x_i can be represented as the measured value $\hat{x}_i$ multiplied by the measurement error variable e_{xi}:

$$x_i = \hat{x}_i \cdot e_{xi} \tag{28}$$

Accounting for the measurement error terms, Eq.(24) becomes:

$$F = \breve{F}(\mathbf{x}) \cdot \theta = \breve{F}[(\hat{x}_1 \cdot e_{x1}, ..., \hat{x}_N \cdot e_{xN})] \cdot \theta \tag{29}$$

On the basis of Eq. (29), to achieve feasible form of the likelihood function, similar to the approach used in Section 3.2, the multiplicative approximation form of the mechanical model $\breve{F}(\cdot)$ is used. The multiplicative approximation form of $\breve{F}(\cdot)$ is

$$\breve{F}(\mathbf{x}) = \breve{F}[(\hat{x}_1 \cdot e_{x1}, ..., \hat{x}_N \cdot e_{xN})] \cong C \cdot \prod_{i=1}^{N} (\hat{x}_i \cdot e_{xi})^{n_i} \tag{30}$$

Where C and n_i are the approximated first order coefficients of the model. It should be noted that the values of C and n_i vary from test to test.

Then Eq. (29) can be reformulated as:

$$\begin{aligned} F &= \breve{F}(\mathbf{x}) \cdot \theta \cong C \cdot \prod_{i=1}^{N} (\hat{x}_i \cdot e_{xi})^{n_i} \cdot \theta \\ &= \breve{F}(\hat{\mathbf{x}}) \cdot \prod_{i=1}^{N} (e_{xi})^{n_i} \cdot \theta \end{aligned} \tag{31}$$

In the previous derivation, only the measurement errors of the input variables are accounted for. To be consistent, the measurement error of the output variable F is also considered. Similar to the input variables, the measurement error of the output variable is modelled as a random variable e_F and it is considered that the measured value $\hat{F}$ can be represented by the actual value of F multiplied by the measurement error variable: $\hat{F} = F \cdot e_F$. Based on this assumption, the following relationship can be derived:

$$\hat{F} = F \cdot e_F = \breve{F}(\hat{\mathbf{x}}) \cdot \prod_{i=1}^{N} (e_{xi})^{n_i} \cdot \theta \cdot e_F \tag{32}$$

Define $\hat{\theta} = \dfrac{\hat{F}}{\breve{F}(\hat{\mathbf{x}})}$ as the measured model uncertainty variable, based on Eq. (32), it can be derived as:

$$\hat{\theta} = \frac{\hat{F}}{\breve{F}(\hat{\mathbf{x}})} = \theta \cdot \prod_{i=1}^{N} (e_{xi})^{n_i} \cdot e_F \tag{33}$$

Further assume that all the measurement error terms follow independent lognormal distributions (with known distribution parameters), then it can be observed that $\hat{\theta}$ is a lognormally distributed random variable, with the following distribution parameters:

$$\mu_{\hat{\theta}} = \mu_{\theta} + \sum_{i=1}^{N} n_i \mu_{e_{xi}} + \mu_{e_F} \tag{34}$$

$$\sigma_{\hat{\theta}} = \sqrt{\sigma_{\theta}^2 + \sum_{i=1}^{N} (n_i \sigma_{e_{xi}})^2 + \sigma_{e_F}^2} \tag{35}$$

Using the test database, a set of observations values of $\hat{\theta}$ can be calculated. The likelihood function for the model uncertainty variable can be then formulated as:

$$L(\mu_\theta, \sigma_\theta) \propto \prod_{j=1}^{N_T} \left\{ \frac{1}{\sigma_{\hat{\theta}_j}} \varphi(\frac{\ln(\hat{\theta}_j) - \mu_{\hat{\theta}_j}}{\sigma_{\hat{\theta}_j}}) \right\} \tag{36}$$

It should be noted that the values of the exponents n_i vary from test to test. Using the likelihood function of Eq.(36), the posterior distributions of the model uncertainty distribution parameters can be calculated and the corresponding point estimates (posterior means) can be made by Hamiltonian Monte Carlo simulation method [Nea96].

3.A.3. Probabilistic models for measurement errors

The probabilistic modelling of the measurement error terms involved in the CSCT punching shear resistance function is explained in this annex. In this paper, the measurement errors of the geometrical variables, material strength variables, the load and rotation variables are accounted for. In particular, for the measurement error of the effective depth variable d and the slab rotation variable ψ, the database is divided into different groups depending on the quality of measurement in tests. For the effective depth, in most of recent tests, it has been measured on saw-cuts after testing. For this type of test data, a relatively low variability of the measurement error is assumed (Standard deviation= 2 mm) [Mut23]. On the other hand, in the tests without measurement of saw-cuts showing the cross-section after tests, a higher variability is assumed (Standard deviation = 4 mm). For the slab rotation data, in some tests, it is directly measured by inclinometer instrumented on the slabs; in the other tests, it is calculated based on measurement of the displacement of the tested slabs. For the tests with direct measurement of rotation data, a relatively low variability is assumed (CoV=5%), while for the tests with indirect derived rotation data, a higher variability is assumed (CoV = 10%).

All the measurement error variables are assumed to follow lognormal distribution and their assumed CoV values are adapted from [Mut23] and listed in Table 3.3. The mean values correspond to the average of the measured values given in the test reports or to the nominal values

Table 3.3: Measurement error for different experimental variables

Parameter		CoV
Effective depth d	Nominal value or measured before casting	$4/d$ (d in [mm])
	Measured on saw-cuts after testing	$2/d$
Column size c		1%
Maximum aggregate size d_g		10%
Radius of the point of contraflexure r_s		5%
Compressive concrete strength f_c (measured on control specimens)		5.8%
Yield strength of flexural reinforcement f_y (measured on control specimens)		2%
Punching shear resistance (measured in the laboratory)		3%
Rotation ψ at failure	Measured with inclinometers	5%
	Calculated on the basis of deflections	10%

Annex 3.B Tests used in the database

Table 3.4:   Information of the assembled punching shear test database

Reference	Specimen	V_{test} [kN]	ψ_{test} [$\times 10^{-3}$]	$V_{solu,II}$	$\dfrac{V_{test}}{V_{solu,II}}$	$V_{solu,IV}$	$\dfrac{V_{test}}{V_{solu,IV}}$
Kinnunen & Nylander	IA15a-5	254.8	12.0	237.0	1.08	254.6	1.00
[Kin60]	IA15a-6	274.4	15.1	238.6	1.15	257.2	1.07
	IA15c-11	333.2	10.3	288.9	1.15	310.0	1.07
	IA15c-12	331.2	9.2	288.6	1.15	309.9	1.07
	IA30a-24	429.2	14.6	400.0	1.07	423.6	1.01
	IA30a-25	407.7	13.0	377.8	1.08	400.0	1.02
	IA30c-30	490	12.4	433.3	1.13	457.8	1.07
	IA30c-31	539	14.3	429.6	1.25	453.2	1.19
	IA30e-34	331.2	23.0	321.0	1.03	325.6	1.02
	IA30e-35	331.2	20.4	317.8	1.04	324.6	1.02
Guandalini et al.	PG-1	1023	8.9	837.3	1.22	861.4	1.19
[Gua09]	PG-3	2153	8.4	1699.6	1.27	2023.0	1.06
	PG-6	238	11.7	229.1	1.04	244.4	0.97
	PG-7	241	22.3	195.5	1.23	212.8	1.13
	PG-10	540	22.3	451.0	1.20	505.3	1.07
Guidotti	PG11	763	10.3	669.3	1.14	757.0	1.01
[Gui10]	PG19	860	10.5	736.1	1.17	829.3	1.04
	PG20	1094	7.1	977.4	1.12	1036.1	1.06
	PG23	839	10.0	770.1	1.09	846.6	0.99
	PG24	1102	8.6	948.3	1.16	999.8	1.10
	PG25	935	12.4	655.3	1.43	754.3	1.24
	PG26	1175	8.5	853.1	1.38	889.3	1.32
	PG27	900	12.1	704.2	1.28	793.9	1.13
	PG28	1098	7.8	927.8	1.18	975.7	1.13
	PG29	854	10.6	781.7	1.09	858.8	0.99
	PG30	1049	7.5	963.6	1.09	1012.6	1.04
Einpaul et al.	PE10	530	6.5	498.3	1.06	573.1	0.92
[Ein16]	PE11	712	10.1	587.5	1.21	673.7	1.06
	PE9	935	13.8	784.7	1.19	889.9	1.05
	PE12	1206	29.4	989.8	1.22	1092.2	1.10
	PE6	656	4.5	634.3	1.03	662.6	0.99
	PE7	871	6.7	769.4	1.13	809.5	1.08
	PE8	1091	8.7	986.6	1.11	1035.0	1.05
	PE5	1477	12.7	1286.8	1.15	1311.9	1.13
	PE3	961	10.0	800.1	1.20	858.3	1.12
	PE4	985	5.3	1029.4	0.96	1005.7	0.98
Tassinari	PT22	989	15.6	776.7	1.27	887.4	1.11

[Tas11]	PT31	1433	10.6	1129.6	1.27	1215.8	1.18
Clément	PF21	1838	5.2	1540.8	1.19	1632.7	1.13
[Clé12]	PF22	2007	3.8	1965.7	1.02	1931.4	1.04
	PF23	2685	8.3	2008.3	1.34	2088.1	1.29
Lips et al.	PL1	682	6.0	636.2	1.07	665.0	1.03
[Lip12]	PL3	1324	13.2	1196.5	1.11	1216.7	1.09
	PL4	1625	6.5	1483.6	1.10	1476.6	1.10
	PL5	2491	4.7	2588.5	0.96	2466.6	1.01
Tolf	S2.1	603	8.5	646.0	0.93	692.6	0.87
[Tol88]	S2.2	600	10.7	629.1	0.95	672.6	0.89
	S2.3	489	17.8	471.3	1.04	529.8	0.92
	S2.4	444	15.8	455.4	0.97	512.7	0.87
Hallgren	HSC0	965	14.1	888.7	1.09	1025.9	0.94
[Hal96]	HSC1	1021	13.2	888.4	1.15	1026.7	0.99
	HSC2	889	10.9	838.5	1.06	966.7	0.92
Fernández Ruiz et al. [Fer10]	PV1	974	7.6	914.1	1.07	932.8	1.05
Drakatos et al.	PD7	983	20.0	843.0	1.17	944.1	1.04
[Dra16]	PD9	1040	11.3	1036.9	1.00	1058.0	0.98
Average	-	-	-	-	1.13	-	1.05
CoV	-	-	-	-	9.4%	-	8.8%

Notation

Latin upper case letters

C_{FC}	the approximated intercept coefficient of the failure criteria equation
C_{ε}	the approximated intercept coefficient of the load-strain equation
CoV	coefficient of variation of a random variable
$\widetilde{CoV}_{\theta}$	The estimated coefficient of variation of the model uncertainty variable θ
$\widetilde{CoV}_{5\%}$	the estimate of the 5% quantile of the posterior distribution of $\widetilde{CoV}_{\theta}$
$\widetilde{CoV}_{95\%}$	the estimate of the 95% quantile of the posterior distribution of $\widetilde{CoV}_{\theta}$
Es	the elastic modulus of steel reinforcement
$\hat{F}$	the measured value of the output variable F in a model
$\breve{F}(\cdot)$	the deterministic part of a model
$F_{LR,II}(\cdot)$	the LoA II load-rotation function (accounting for model uncertainty variable)
$\breve{F}_{LR,II}(\cdot)$	the deterministic LoA II load-rotation function
$F_{LR,IV}(\cdot)$	the LoA IV load-rotation function (accounting for model uncertainty variable)
$\breve{F}_{LR,IV}(\cdot)$	the deterministic LoA IV load-rotation function
$F_{FC}(\cdot)$	the failure criterion function (accounting for model uncertainty variable)
$\breve{F}_{FC}(\cdot)$	the deterministic failure criterion function
$F_{solu}(\cdot)$	the resistance solution function of strain-based approach
$\breve{F}_{solu,II}(\cdot)$	the deterministic resistance solution function for LoA II
$\breve{F}_{solu,IV}(\cdot)$	the deterministic resistance solution function for LoA IV
$F_{\varepsilon}(\cdot)$	the load-strain function (accounting for model uncertainty variable)
$\breve{F}_{\varepsilon}(\cdot)$	the deterministic load-strain function
$L(\cdot)$	the likelihood function
R	the load level for a structural element
R_{FC}	the strength of a structural element according to the failure criterion model
$R_{FC,d}$	the design failure criterion function
R_{solu}	the resistance solution of a structural element
$R_{solu,d}$	the design resistance of a structural element according to a given safety format
V	the punching shear load level
V_{FC}	the punching strength calculated with failure criterion model
$V_{FC,test}$	the punching shear strength corresponding to a given rotation level observed in an experimental test
V_{flex}	the punching shear load associated with flexural resistance of the slab
$V_{solu,II}$	the punching shear resistance calculated with the LoA II

$V_{solu,IV}$	the punching shear resistance calculated with the LoA IV
$V_{solu,test}$	the punching shear resistance observed in an experimental test

Latin lower case letters

$b_{0.5}$	perimeter of the critical section for punching shear
c	rectangular column size
d	the distance from extreme compression fibre to the centroid of the longitudinal tensile reinforcement (the effective depth)
d_g	the maximum diameter of the aggregate
d_{g0}	the reference aggregate size (d_{g0} = 16 mm)
$\mathbf{e}$	the measurement error vector
e_F	the measurement error of the derived variable F in a model
e_{xi}	the measurement error of the ith variable in a model
$\exp(\cdot)$	the natural exponential function
f_c	the uniaxial compressive strength of concrete (cylinder)
f_{ck}	the characteristic value of the uniaxial compressive strength of concrete
f_{cm}	The mean value of the uniaxial compressive strength of concrete
f_y	the yield strength of steel reinforcement
f_{yk}	The characteristic value of the yield strength of steel reinforcement
f_{ym}	The mean value of the yield strength of steel reinforcement
$f(\cdot)$	the posterior distribution function accounting for the updated state of knowledge
h	the thickness of a concrete slab
$\ln(\cdot)$	the natural based logarithmic function
m_R	the nominal flexural resistance per unit width of the slab
n_{fc}	the exponent sensitivity factor (referred to as exponent below) of concrete compressive strength variable in the resistance solution
n_{fy}	the exponent of the steel yielding strength in the resistance solution
$n_{FC,i}$	the exponent of the ith basic variable in the failure criteria
$n_{FC,\varepsilon}$	the exponent of the strain variable in the failure criteria
$n_{\varepsilon,i}$	the exponent of the ith basic variable in the load-strain function
$n_{\varepsilon,R}$	the exponent of the load variable in the load-strain function
$n_{\varepsilon,R,II}$	the exponent of the shear load for the LoA II load-strain function
$n_{\varepsilon,R,IV}$	the exponent of the shear load for the LoA IV load-strain function
$n_{\theta FC,II}$	the exponent of the failure criterion model uncertainty in the LoA II resistance solution
$n_{\theta FC,IV}$	the exponent of the failure criterion model uncertainty in the LoA IV resistance solution
$n_{\theta LR,II}$	the exponent of the load-rotation model uncertainty in the LoA II resistance solution

$n_{\theta LR,II}$	the exponent of the load-rotation model uncertainty in the LoA IV resistance solution
$p(\cdot)$	the prior distribution function
r_c	the radius of the column
r_q	the radius of the load introduction at the perimeter
r_s	the radius of isolated slab element
$\mathbf{x}$	vector of all input variables of a model
$\hat{\mathbf{x}}$	vector of the measured input variables of a model
$\mathbf{x}_b$	vector of basic variables for a structural element
$\mathbf{x}_{b,d}$	vector of design values of basic variables for a structural element
$\mathbf{x}_{FC}$	vector of all input variables of the failure criterion function
$\mathbf{x}_{\varepsilon}$	the vector of all input variables of the load strain function
v	a standard normal distributed variable (with zero mean and unit variance)

Greek upper case letters

Θ	vector of the mean and standard deviation of the logarithmic model uncertainty variable

Greek lower case letters

α	direction of the crack in a reinforced concrete panel subjected to shear
γ	shear strain
γ_C	the partial safety factor applied to concrete compressive strength
γ_{FC}	the partial safety factor applied to the failure criterion function
γ_{flex}	the partial safety factor for the flexural resistance of a slab
γ_S	the partial safety factor applied to steel yield strength
γ_V	the partial safety factor applied to the resistance solution
γ_{def}	the partial safety factor applied to the load-rotation relationship
ε	strain state variable of a structural element
$\varepsilon_{c,1}$ and $\varepsilon_{c,2}$	principle strains of concrete
ε_d	design value of the load strain relationship
ε_s	strain of steel reinforcement
$\theta_{LR,II}$	the model uncertainty random variable of the LoA II load-rotation model
$\theta_{LR,IV}$	the model uncertainty random variable of the LoA IV load-rotation model
θ_{FC}	the model uncertainty random variable of the failure criterion function
θ_{ε}	the model uncertainty random variable of the load-strain function
$.\theta_{solu}.$	the model uncertainty of the resistance solution as a whole
$\theta_{solu,II}$	the model uncertainty of the resistance solution for LoA II
$\theta_{solu,IV}$	the model uncertainty of the resistance solution for LoA IV

$\hat{\theta}$	the measured model uncertainty random variable (including measurement error)
κ	the normalising factor for the posterior distribution function
μ_{e_F}	the mean value of $\ln(e_F)$
$\mu_{e_{xi}}$	the mean value of $\ln(e_{xi})$
μ_θ	the mean value of the logarithmic model uncertσ_s ainty variable
$\mu_{\hat{\theta}}$	the mean value of the measured logarithmic model uncertainty variable (including measurement error)
$\tilde{\mu}_{5\%}$	the estimate of the 5% quantile of the posterior distribution of $\tilde{\mu}_\theta$
$\tilde{\mu}_{95\%}$	the estimate of the 95% quantile of the posterior distribution of $\tilde{\mu}_\theta$
$\tilde{\mu}_\theta$	the mean value of the original model uncertainty variable $\tilde{\mu}_\theta \approx \exp(\mu_\theta)$
ρ	the reinforcement ratio
$\sigma_{c,1}$ and $\sigma_{c,2}$	the principal stresses of concrete
	stress of steel reinforcement
σ_{e_F}	the standard deviation of $\ln(e_F)$
$\sigma_{e_{xi}}$	the standard deviation of $\ln(e_{xi})$
σ_θ	the standard deviation of the logarithmic model uncertainty variable
$\sigma_{\hat{\theta}}$	the standard deviation of the measured logarithmic model uncertainty variable (including measurement error)
τ	shear stress applied to a shear panel
$\varphi(\cdot)$	the standard normal probability density function
ψ	the rotation angle of a slab outside the column region in a slab column connection
ψ_{test}	the measured rotation angle of the slab in an experimental test

Chapter 4

A consistent safety format and design approach for brittle systems and application to Textile Reinforced Concrete structures

This chapter is the post-print version of the article mentioned below, published in Engineering Structures Journal. The authors of the article are Qianhui Yu (PhD Candidate), Patrick Valeri, Prof. Miguel Fernández Ruiz and Prof. Aurelio Muttoni (thesis director). The reference is the following:

Yu Q., Valeri, P., Fernández Ruiz M., Muttoni A., *A consistent safety format and design approach for brittle systems and application to textile reinforced concrete structures,* Engineering Structures, Vol. 249, 113306, 2021.
(DOI: https://doi.org/10.1016/j.engstruct.2021.113306)

The work presents in this publication was performed by Qianhui Yu collaborating with Patrick Valeri, Prof. Miguel Fernández Ruiz and under the supervision of Prof. Aurelio Muttoni who provided constant and valuable feedbacks, proofreading and revisions of the manuscript.

The main contributions of Qianhui Yu to this article and chapter are the followings:

- Post-process of the data of nine three point bending experimental test of Textile Reinforced Concrete (TRC) beams (measurement after saw-cut of the beam cross sections and Digital Image Correlation data process).

- Modelling of the flexural response of the tested TRC beams and interpretation of the test results.

- Modelling of the assembled cross-beam systems and collection of action effect model uncertainty data on its basis

- Interpretation of the action effect model uncertainty data for different analysis methods.

- Parametric analysis and discussion for the applicability of different action effect analysis models for textile reinforced concrete beams.

- Proposition of suitable action effect analysis methods for textile reinforced concrete beams.

- Calibration of different partial safety formats for the flexural design for textile reinforced concrete structures.

- Elaboration of the figures and tables included in the article.

- Writing of the manuscript of the article.

Abstract

Design and verification of structures in modern codes of practice account for a safety format, ensuring that the probability of failure does not exceed a given threshold. Although specific safety formats are proposed in some cases for special types of structures or analyses, most designs and verifications are currently performed on the basis of the Partial Safety Factor Format (PSFF). This format is applied to cover different materials and structural responses, allowing for a uniform methodology to account for reliability. Such consideration greatly simplifies the design process, but raises concerns on its consistency when different structural responses are observed. In the PSFF as considered in *fib* Model Code and Eurocodes, no explicit distinction is made on the value of the partial safety factors (for actions or materials) depending on whether a structural system has a brittle or a ductile response. This can be potentially inconsistent, as brittle systems have limited or no redistribution capacity of internal forces (which can give rise to premature failures if action effects are poorly estimated), while ductile systems have large potentials to redistribute internal forces and are thus little sensitive to this issue.

In this work, to investigate on the suitability of PSFF for brittle structures, the most suitable manner to determine internal forces for brittle elements failing in bending and the corresponding model uncertainties of action effects are investigated in detail. The concepts are derived from a theoretical perspective and applied to the case of Textile Reinforced Concrete (TRC). This material is a promising development to reduce the carbon footprint of concrete construction and to build lightweight structures, but exhibits a very brittle response in bending (contrary to ordinary reinforced concrete with usual reinforcement ratios). In this work, by means of an experimental and theoretical investigation, it is shown that following a suitable approach to estimate internal forces for brittle systems as TRC leads to a low level of model uncertainty of action effects. This leads to the conclusion that, compared to standard design of ductile systems, no additional correction is required for safety issues. Following this outcome, the partial factors for TRC structures are calibrated. In addition, due to the significance of geometrical uncertainties, a method for designing TRC on the basis of a design value of the effective depth (a reduced value accounting for construction tolerances instead of its nominal dimension) is eventually discussed, showing that it allows for a more uniform level of safety.

Keywords: safety format, brittle response, statically indeterminate system, action effect model uncertainty, Textile Reinforced Concrete, tests

4.1 Introduction

In the last decades, Textile Reinforced Concrete (TRC) has emerged as an interesting alternative to reinforced concrete, allowing to reduce material consumption and the carbon footprint of cementitious-based materials [Gar15, He02, Val20]. This new paradigm relies on the use of a non-metallic fabric as reinforcement (typically made of carbon or glass), which is insensitive to corrosion. As a consequence, cover requirements of the reinforcement can be reduced to minimum static values, allowing to decrease the overall thickness of TRC elements to 10-30 mm. In addition, since no passivation of the reinforcement is required, a low-clinker content cement can also be used allowing to reduce the environmental footprint of the material related to its CO_2 emissions.

Despite the potential of TRC, its practical use remains still limited. This is to a large extent explained by the lack of a consistent design framework. Conventional methods widely accepted for reinforced concrete are potentially not directly applicable to TRC due to its brittle nature. This issue is particularly instrumental in the case of statically indeterminate structures, where redistributions of internal forces are usually required to develop the full structural strength of the system. Other aspects that are critical for the application of TRC in practice are the potential sensitivity of thin elements to construction tolerances and its reduced resistance in case of fire [Col11, Ehl10, Rei08].

Currently, several analytical and numerical models are available to describe the response of TRC members with respect to its sectional behaviour. An extensive review of the state-of-the-art can be consulted elsewhere (see for instance [Bra06, Pel17]). These approaches refer normally to mean material properties and allow determining the average resistance of TRC structural elements (or with a bias factor which should be close to 1.0). However, their application in practice requires accounting for the inevitable uncertainties inherent to structural design. As a consequence, a suitable safety format needs to be implemented, ensuring that the probability of failure does not exceed an acceptable threshold. In the case of the resistance formulae, such format shall account for the variability of the material properties as well as uncertainties related to the calculation model and to construction tolerances.

For the reliability verification of structures, the so-called Partial Safety Factor Format (PSFF) is adopted in many design codes (Eurocodes [CEN02, CEN04] and *fib* Model Code [FIB13] for example). In the PSFF, design values of the basic variables are defined through partial safety factors and limit state verifications are made with the design values of basic variables [CEN02]. Partial factors for different materials and actions need to be calibrated so that the reliability levels for representative structures in design are as close as possible to the target reliability level. With respect to the adoption of a suitable safety format for TRC design, several efforts have been performed in the past [Häu19, Jus15, Kro19, Rem18, Rem20, Wes18] to address the principles of structural reliability and design procedures.

The relationship between individual partial factors in PSFF of Eurocodes is shown in Figure 4.1(adapted from Figure C3 in EN1990:2002 [CEN02] accounting for the new definitions in the draft of the second generation of prEN1990:2020 [CEN20]). It should be noted that in addition to the basic uncertainties listed in Figure 4.1, the partial safety factors should also account for approximations and uncertainties in the safety format calibration. Also, it has to be noted that this figure describes the classical verification method for structures, where the analysis (calculation of internal forces) is conducted separately from the calculation of the associated resistances. Within this frame, the verification is conducted at a given cross section by comparison of sectional internal forces and related resistances. Such procedure will be referred in the following as a local verification. As an alternative, the distribution of internal forces can be calculated considering the response and strength of the materials (following a nonlinear analysis). This allows one to determine directly the load-carrying capacity of the system and will be referred to in the following as a global verification method. In this case, the quantification of the model uncertainties [Eng17] can be quite different and other safety formats [CEN02, FIB13] can be more appropriate.

In Eurocodes [CEN02], the partial factors of actions γ_F and the partial factors of material strength variables γ_M are typically calibrated separately by using constant standardised First Order Reliability Method (FORM) sensitivity factors[CEN02, Has74, Kön81]. Taking advantage of this frame, in order to define a safety format for TRC structures, only the partial factors related to the resistance (materials) need to be recalibrated, while the partial factors for action variables from Eurocodes [CEN02] can theoretically be maintained.

It is interesting to note in Figure 4.1 that the model uncertainty of action effects is accounted for in the partial factor for action variables, γ_F. Such assumption, provided that a constant value of γ_F is adopted, ignores differences related to material response (brittle/ductile response) and analysis method (linear-elastic response/consideration of redistributions). This simplification can lead to unsatisfactory levels of reliability for statically indeterminate brittle structures (as those built with TRC).
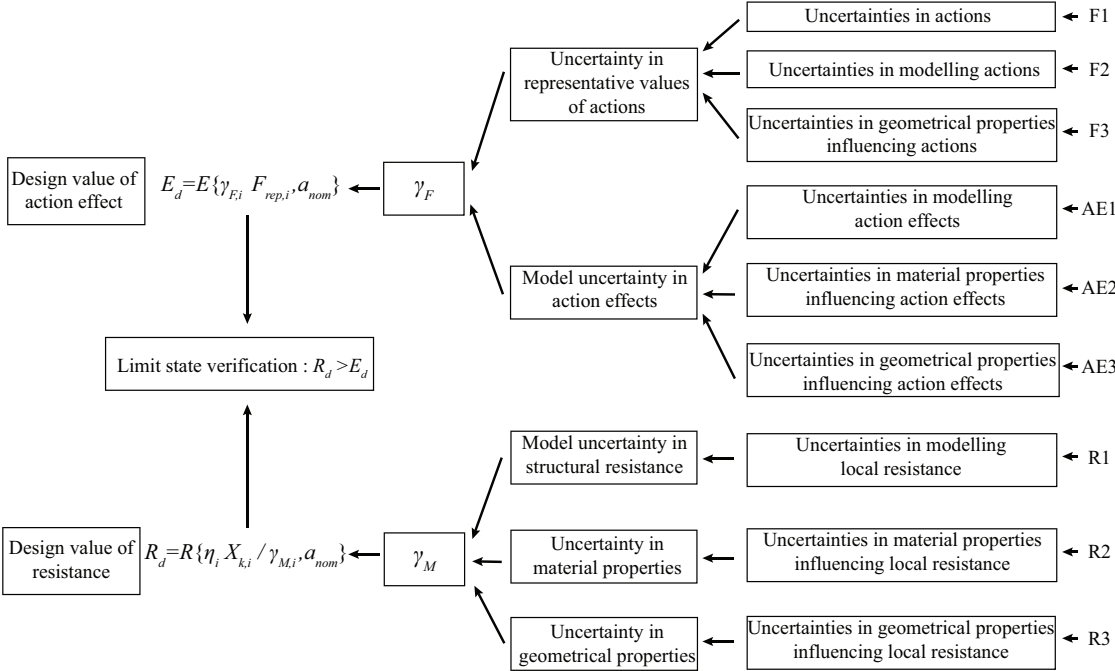
Figure 4.1:   Relation   between   individual   partial   factors   (adapted   from EN1990:2002 [CEN02], refer to Notation section for details)

In this work, the action effect model uncertainty of TRC structures will be investigated on the basis of a statistical evaluation of the results of an experimental programme designed for this purpose. This investigation will focus not only on statically determinate elements, but also on the response of statically indeterminate structures failing in a brittle manner. The safety format and partial factor related to the resistance (γ_M) for TRC structures will then be calibrated based on a proper probabilistic modelling of the basic variables. A suitable model to account for action effects on TRC structures and the corresponding model uncertainty will be presented. On its basis, tailored values of the partial safety factors for TRC will be derived as well as a suitable design approach for calculation of internal forces.

4.2   Action effect model uncertainty in statically indeterminate structures

In this section, the different influences of brittle and ductile responses on statically indeterminate structures are examined with respect to their mechanical consequences and the associated reliability considerations.

4.2.1 Influence of sectional behaviour on the structural response

To illustrate the different model uncertainty of action effects of structures with different sectional response (brittle/ductile), the load-bearing behaviour of statically indeterminate structures with different materials is first investigated. As a representative example, two beams with identical geometry and loading conditions (see Figure 4.2a) but whose material response is different are examined:

- Beam BI refers to the classical response of concrete reinforced with ordinary steel rebars. Its moment-curvature diagram can be approximated by a quadrilinear law showing a plastic plateau with large deformation capacity related to extensive yielding of the longitudinal reinforcement and significant ultimate strain of the reinforcement steel (see Figure 4.2b). This response can be considered as ductile and thus insensitive to imposed deformations (allowing one to calculate the structural capacity according to limit analysis [Nie11]).

- Beam BII refers to a structure reinforced with a brittle reinforcement, as for TRC, whose failure occurs prior to any plastic plateau or to an over-reinforced structure with conventional steel reinforcement where the compression zone crushes before the reinforcement yields. The capacity to redistribute internal forces is limited to the change of stiffness related to the cracked response and the structure can potentially be sensitive to imposed deformations (limit analysis not applicable to calculate its structural capacity).

In a classical design of a reinforced concrete structure, the internal forces are calculated assuming linear uncracked behaviour (not considering cracking nor yielding). This allows neglecting the influence of the reinforcement on the stiffness, so that no iteration is required in designing a new structure. In this case, the sections of the beam described above would be designed so to resist for the external action (q_E) both the maximum sagging moment according to a linear response ($M_{R,sag} = 9/16 \cdot q_E L^2/8$) and the maximum hogging moment ($M_{R,hog} = - q_E L^2/8$), requiring thus different amount of reinforcement at these sections, see Figure 4.2b. In reality, when the load is applied, different phases of response can be observed as shown in Figure 4.2c for the two characteristic sections (hogging and sagging region). Before cracking occurs, the distribution of bending moments follows that of the elastic uncracked behaviour, with proportional increments to the load at both control sections (maximum sagging moment equal to $9/16 \cdot q L^2/8$ and a maximum hogging moment equal to $- q L^2/8$). Cracking occurs first in the hogging region ($q_{cr,hog}$ in Figure 4.2c), leading to a local loss of stiffness. As a consequence, bending moments increase more than proportionally in the sagging region and less than proportionally in the hogging region.

For a higher level of load, cracking at the sagging region also occurs ($q_{cr,sag}$) and the internal forces redistribute thereafter according to the relative stiffness of the hogging and sagging regions. Since the reinforcement in the hogging region is higher due to the design procedure

(Figure 4.2b), its stiffness is also higher and moments increase more than proportionally in the hogging region (Figure 4.2c). Depending on the strength, the hogging or sagging region can first attain their strength. In Figure 4.2c, this case corresponds to the hogging region. Consequently, for beam BII, a brittle failure occurs over the intermediate support, while the sagging region would still have a capacity to increase the acting moment, giving rise to a load carrying capacity lower than the action assumed for design ($q_{R,II} \leq q_E$). On the contrary, for beam BI, the response of the governing section is ductile, and this allows for further redistributions of internal forces, until both regions attain their resistance and the full structural capacity is reached [Mut90] ($q_{R,I} = q_E$), see Figure 4.2c.

It is interesting to note thus that when brittle responses can be expected, evaluations of the internal forces deviating from the actual one can lead to unsafe designs. The consequences of this fact in terms of reliability are however not explicitly accounted for in the current Eurocodes safety format, as the safety element for the model uncertainty of action effects are only accounted for in the partial factors on actions (γ_F), which is independent of the response of the structure and type of action effect analysis model. On the other side, in structures with ductile behaviour, the load carrying capacity corresponds exactly to the load assumed for design, despite the fact that the actual behaviour deviates significantly from the simplified behaviour assumed for the analysis (typically linear elastic behaviour). It can be concluded that for structures with ductile response, the model uncertainty of action effects is relatively small, whereas for brittle response, the model uncertainty of action effects shall be consistently accounted for in accordance with the type of analysis performed. This will be discussed in the following section.

(a) Geometry and actions

(b) Moment-curvature diagrams of representative cross sections

(c) Moment-load diagrams
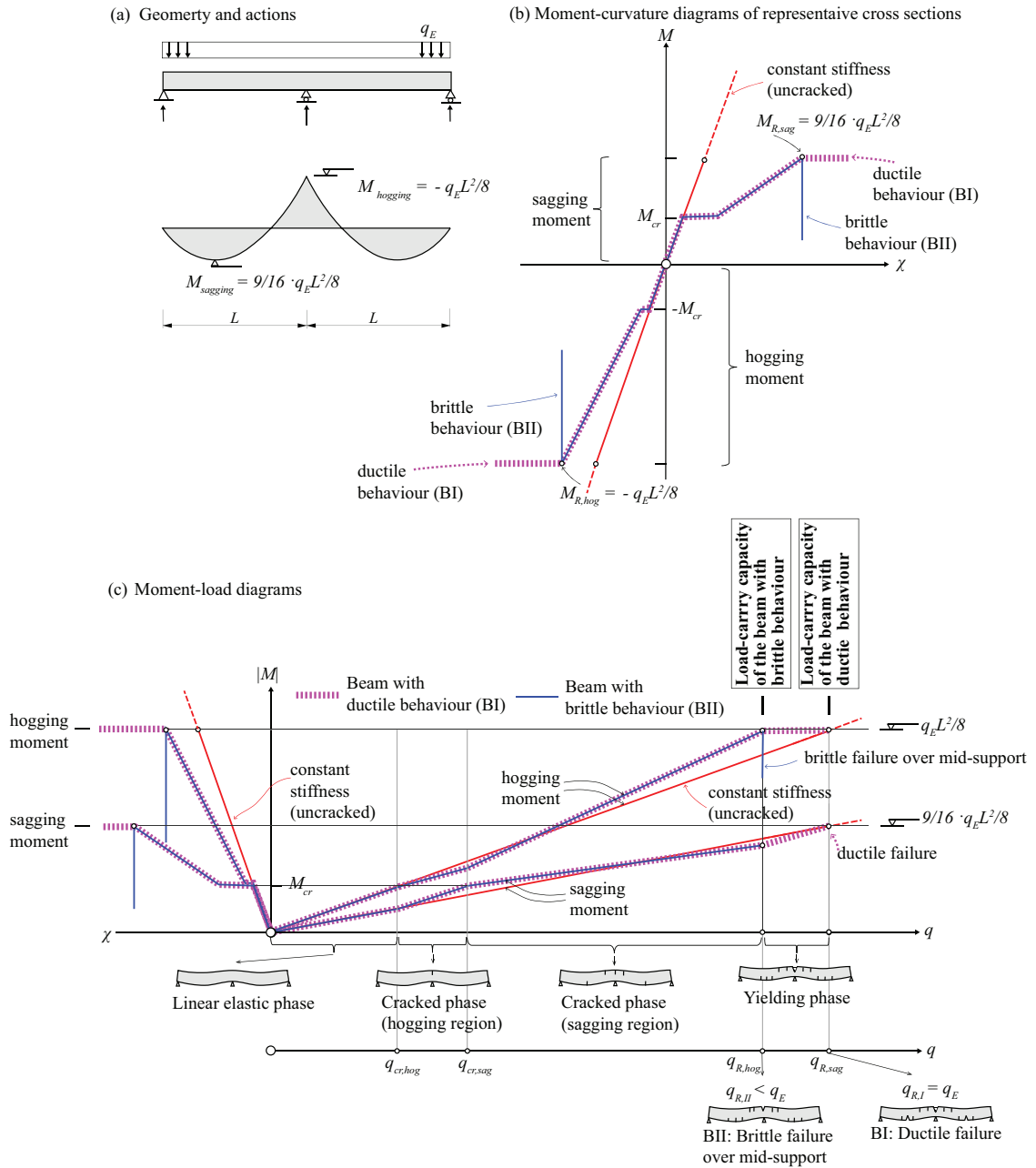
Figure 4.2: Analysis of a statically indeterminate reinforced concrete structure designed according to the internal forces calculated assuming linear uncracked behaviour: (a) geometry and actions; (b) moment – curvature diagrams; and (c) moment – load diagrams

4.2.2 Model uncertainty of action effects in structural concrete

The need for considering the uncertainties in calculating the internal forces in a structure, in addition to the uncertainties related to the actions, has been acknowledged already in the first attempts to quantify the partial safety factors. According to the first discussions within CEB in view of the preparation of the first Model Code [CEB64], the partial safety factor for actions was assumed to account for the uncertainties related to calculation of the internal forces in case of refined analyses. However, for the case of typical structural analysis or in presence of particular uncertainties, an additional partial factor $\gamma_{Sd} = 1.12$ (1.4/1.25) increasing the value of the actions was defined [CEB59]. This additional factor was intended to account for the uncertainties in modelling the structure, for potential errors and for neglected effects [CEB64].

A more detailed description of the uncertainties considered with this additional partial safety factor, including an estimate of the coefficients of variation of the ratio between actual and calculated internal forces E_{exp}/E_{calc} , has been proposed in the CEB Manuals "Structural Safety" [CEB74, CEB74a, CEB80]. The considered uncertainties (coefficients of variation in brackets) were:

(i) effect of differences between the actual structure and the idealized system assumed in the analysis (see uncertainty AE1 in Figure 4.1, 8% for concrete structures and 5% for steel structures);

(ii) approximations in the analysis (5%);

(iii) influence of imperfections during execution on the internal forces (see uncertainty AE3 in Figure 4.1; 5% for concrete structures and 2% for steel structures);

(iv) the effect of neglected actions at ultimate limit state (as for instance imposed deformations, including thermal effects and shrinkage);

(v) the inaccuracy in determining the influence of load combinations with the chosen safety format of partial safety factors (for the uncertainties (iv) and (v), a coefficient of variation of 8% for concrete structures and of 5% for steel structures, respectively).

In addition, also the uncertainty related to the assumed probability functions of the actions has been considered (with a value of the coefficient of variation between 0 and 5% depending on the coefficient of variation of the action). It has to be noted, that in the safety format of Figure 4.1, this effect should be accounted for in the partial safety factor of the actions (see also change in the latest draft of prEN 1990:2020 [CEN20]) so that it is not considered in the following.

The coefficient of variation of the ratio between actual and calculated action effect (E_{exp}/E_{calc}) can be obtained from the square root of the sum of the squares. For concrete structures, the total coefficient of variation becomes $V_{Sd} = 0.125 = (0.08^2 + 0.02^2 + 0.05^2 + 0.08^2)^{0.5}$ whereas for steel structures, $V_{Sd} = 0.076 = (0.05^2 + 0.02^2 + 0.02^2 + 0.05^2)^{0.5}$. In [CEB80], the partial safety factor γ_{Sd} has been calculated based on reliability analysis assuming a probability of failure and a

coefficient of variation for the actions. The obtained values were approximately 1.125 for concrete and 1.075 for steel structures, respectively. Similar values could be obtained following the approach of [CEN02] by assuming lognormal distributions, a target reliability index $\beta_{tgt,50} =$ 3.8 and a sensitivity factor for non-dominating actions (α=0.4) leading to γ_{Sd} =exp(0.4·0.70·3.8·0.125)=1.14.

According to the knowledge of the authors, this is the most detailed description of the uncertainties covered by the partial factor γ_{Sd} still available in the literature and the result has been acknowledged in different codes (current Eurocode "Basis of structural design [CEN02] for instance, defines values of γ_{Sd} between 1.05 and 1.15, see table A1.2(B), note 4). Nevertheless, it has to be noted that the considerations described above reflect the state of knowledge and the engineering practice at that time (1960s and 1970s). They were highly influenced by the concern to calculate the "actual" internal forces as accurate as possible with the tools of that time (typically hand calculations or rudimentary computer programs), but surprisingly, the difference between statically determinate or indeterminate structures hasn't been considered explicitly. In addition, as shown above, for statically indeterminate structures, a significant uncertainty can arise from the difference between the mechanical behaviour assumed for the structural analysis (typically linear elastic uncracked) and the behaviour assumed for calculating the sectional resistance (typically cracked concrete with nonlinear behaviour for concrete and steel).

4.2.3 Definition of the random variables for model uncertainties

From the case study described above, it has been observed that the model uncertainty of action effects (local value of an internal force at a given cross section) will eventually influence the model uncertainty of the load-carrying capacity of a statically indeterminate structure. As shown in the example above, in the classical design approach of structural concrete, the models used to determine action effects and resistance are not necessarily the same. The analysis of action effect is typically determined assuming a linear response and neglecting the influence of cracking (constant uncracked stiffness) whereas, for calculation of the resistance, cracking and the nonlinear response of both concrete and steel reinforcement are considered. As previously discussed, this does not have consequences at ultimate for ductile responses, but can have implications for brittle redundant systems.

With respect to the quantification of the local resistance model uncertainty, a random variable can be defined by comparing the experimentally measured local resistance with the theoretical resistance. It shall be noted that the experimental local resistance data is usually obtained by experimental programmes on statically determinate structures, so that uncertainties related to the calculation of internal forces are not relevant. The local resistance model uncertainty is thus analysed through the following ratio:

$$\theta_{R,local} = \frac{R_{exp}}{R_{calc}} \tag{1}$$

where $\theta_{R,local}$ is the random variable for the local resistance model uncertainty, R_{exp} is the experimental local resistance and R_{calc} is the calculated resistance.

For the action effect model uncertainty, the random variable θ_E is defined in analogy with $\theta_{R,local}$ as:

$$\theta_E = \frac{E_{exp}}{E_{calc}} \tag{2}$$

where θ_E is the random variable for action effect model uncertainty, E_{exp} is the experimental action effect and E_{calc} is the calculated action effect. The definition of θ_E in Eq. (2) has however some inconsistencies because E_{exp} and E_{calc} refer to the local level while the load-carrying capacity of a structural system (potentially redundant) is governed by its global response. Due to this reason, it is not appropriate in general to directly use the variable E_{exp}/E_{calc} for a given cross section to quantify the action effect model uncertainty. Instead, the global resistance model uncertainty variable of a statically indeterminate structure can be defined as:

$$\theta_{global} = \frac{q_{exp}}{q_{calc}} \tag{3}$$

where θ_{global} refers to the random variable for the global model uncertainty, q_{exp} to the experimentally measured load-carrying capacity of a statically indeterminate structure in terms of load factor at ultimate load bearing capacity and q_{calc} to the calculated load-carrying capacity. As shown in the previous case study, the global model uncertainty contains the model uncertainty of action effects and the model uncertainty of local resistance. The model uncertainty of action effects can then be quantified by removing the model uncertainty of local resistance from that of global resistance.

4.3   Experimental programme

To investigate the flexural response of TRC structures and to provide basic test data for investigating the action effect model uncertainty of TRC in statically indeterminate structures, an experimental programme was performed. The test series consisted of nine thin slab strips tested under three-point bending load condition. The tests were performed at the Structural Concrete Laboratory of Ecole Polytechnique Fédérale de Lausanne (Switzerland) and were performed in seven consecutive days at an average age of 301 days (to ensure constant mechanical properties).

4.3.1 Mechanical properties of the materials

The mortar mix described in [Val20b] was used for the experimental programme, composed of nearly 40 % binder and nearly 60 % aggregate (maximum aggregate size 1.6 mm). All specimens were cast on the same day following an identical procedure and preparation of the mix. Compressive tests on the mortar produced in three batches were carried out on 70 ×140 mm cylinders tested at the same period as the beam specimens. The mean value of the strength f_c of 14 compressive tests is given in Table 4.1. As for the elastic modulus and tensile strength of the mortar, values were derived on the basis of f_c value according to the data of [Val20b] (results are provided in Table 4.1).

Table 4.1:   Mechanical properties of the mortar (mean values and coefficients of variation CoV)

		Value	CoV
Elastic Modulus of mortar	E_{cm} [GPa]	31.0	2.58%[1]
Mortar tensile strength	f_{ctm} [MPa]	4.4	9.43% [1]
Mortar compressive strength	f_{cm} [MPa]	128.5	10%

[1] Values according to [Val20b]

The textile fabrics were carbon fibre (CF) meshes. Two types of fabrics were used (named CF01 and CF02 in the following), both coated with epoxy and with a layer of quartz-sand applied to the surface, but with different net cross section area of roving (details on the geometry and main properties can be consulted in [Val20b]). The mechanical properties of the textile fabric are given in Table 4.2. Bare textile (single rovings extracted from the fabric grid) were also tested in tension. Consistent with what has been observed by Valeri et al.[Val20b], a straightening phase of the rovings was first observed, followed by a linear response characterized by the tangent modulus of elasticity of the filament ($E_{tex,m}$) until its tensile strength ($f_{tex,m}$).

Table 4.2:   Mechanical property of textile reinforcement in longitudinal direction (number of tests, CoV in brackets)

Fabric		CF01	CF02(#, CoV)
Net cross section	a_{tex} [mm^2]	0.85	1.70
Nominal perimeter	U_{tex} [mm]	7	11
Grid spacing	e_{tex} [mm]	20.0	17.0
Strength [1]	$f_{tex,m}$ [MPa]	1833	1833 (5, 7.41%)
Elastic modulus [1]	$E_{tex,m}$ [GPa]	228	228 (5, 10.9%)

[1] calculated on the basis of the nominal value of the net cross section

4.3.2 Specimens and experimental results

The specimens had a rectangular cross section (250mm-width and 60mm-height) with varying span L (refer to Figure 4.3 and to Table 4.3). All specimens were cast following the same procedure and dimensions. As the tested span length was different (Table 4.3), variable overhang lengths resulted (L_{o1} and L_{o2} in Figure 4.3). These overhangs varied between 0.3m to 1.2m. Since the self-weight of the beams is relatively small compared to the failure load, the influence of the overhang length in the overall response can be considered as negligible.
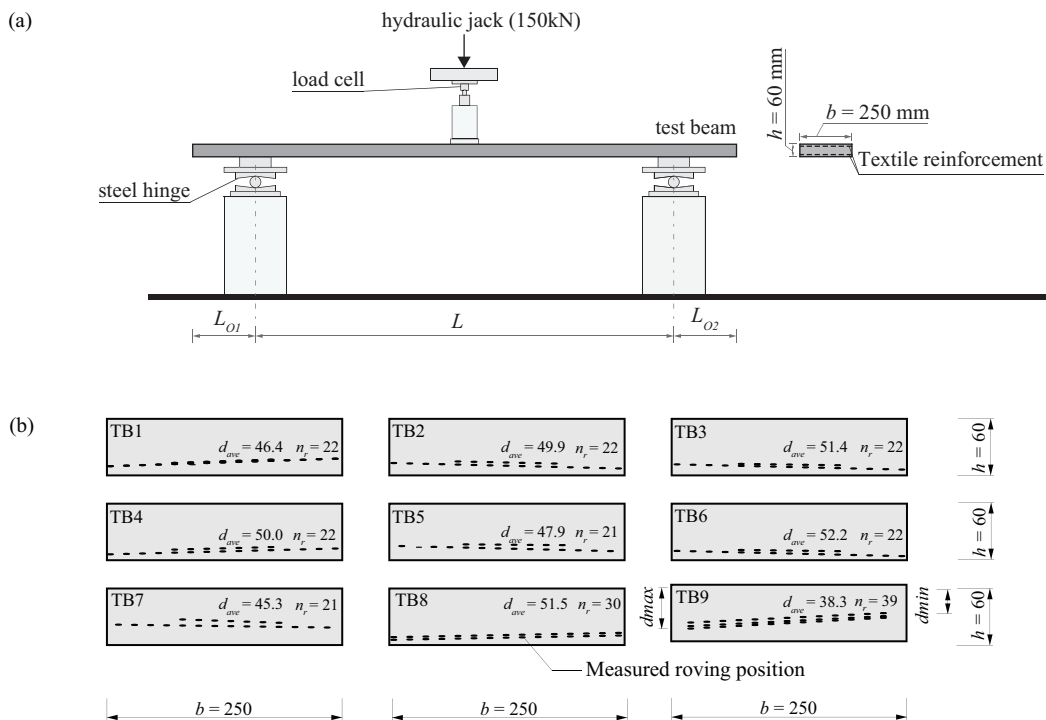
Figure 4.3: Specimens: (a) test setup; and (b) Representative cross section of the tested specimens (units: [mm])

The specimens were reinforced with the textiles CF01 or CF02, that were intentionally not kept with a constant cover, but only attached at their ends. This allowed the textile to vary its position during casting, in order to investigate the influence of construction tolerances and casting procedure in the structural response. After the bending tests were conducted, saw-cuts were performed on the specimens near the cross section failing in bending (representative cross section) and the exact position of the rovings were measured. The illustration of the measured roving positions in each cross-section is given in Figure 4.3b. Since the effective depth was not constant over the beam width, the average flexural depth d_{ave} and the average flexural reinforcement ratios ρ_{ave} are defined as follows:

$$d_{ave} = \frac{\sum_1^{n_r} d_i}{n_r}; \quad \text{and} \quad \rho_{ave} = \frac{n_r a_{tex}}{b d_{ave}} \tag{4}$$

Where n_r refers to the number of rovings in a cross section, d_i to the flexural depth of each roving, a_{tex} to the net cross section of a single roving and b to the cross section width. Details are given in Table 4.3.

Digital Image Correlation (DIC) was performed at the sides of the specimens and used to track their displacement fields following the same methodology as described in [Val20b]. The results of DIC were checked with continuous readings obtained by means of a Linear Variable Displacement Transformers (LVDT) attached to the top side of the mid-span of each specimen. The load-deflection (F-δ) relationships recorded for the tests are shown in Figure 4.4 (δ based on DIC measurements). For low levels of load, a linear response is observed until the cracking moment is reached. Once cracking develops, the response becomes softer, with a stiffness depending on the reinforcement ratio and slenderness. Failure occurred in all specimens in bending in a brittle manner due to rupture of reinforcement.
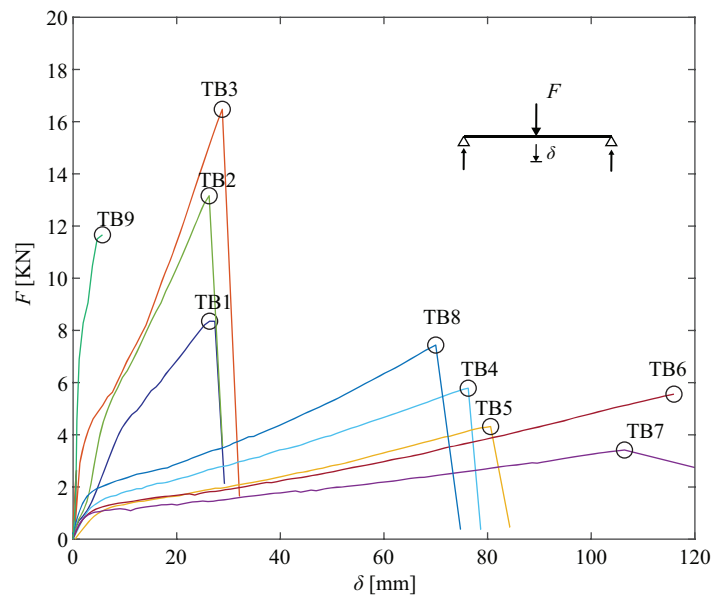
Figure 4.4: Measured load-deflection responses of tested specimens

Table 4.3:   Main parameters of the bending specimen and measured flexural resistance at maximum load

Name	L [m]	Textile type	Number of rovings n_r	a_{tex} [mm^2]	d_{min} [mm]	d_{max} [mm]	d_{ave} [mm]	ρ_{ave} [%]	a/d_{ave}	M_{exp} [kNm]
TB1	1.2	CF02	22	1.7	42.3	50.9	46.4	0.32	12.9	2.36
TB2	1.15	CF02	22	1.7	46.4	53.8	49.9	0.30	11.0	3.33
TB3	1.1	CF02	22	1.7	49.0	55.0	51.4	0.29	11.0	3.64
TB4	2.1	CF02	22	1.7	44.5	54.7	50.0	0.31	21.5	2.77
TB5	2.2	CF02	21	1.7	44.6	52.2	47.9	0.30	23.0	2.23
TB6	2.4	CF02	22	1.7	49.8	54.8	52.2	0.29	22.0	3.04
TB7	2.4	CF02	21	1.7	38.0	49.0	45.3	0.27	25.0	1.99
TB8	2	CF02	30	1.7	48.3	54.9	51.5	0.40	19.4	3.58
TB9	0.63	CF01	39	0.85	29.9	46.3	38.3	0.35	8.2	1.63

4.4   Bending test analysis

The flexural response of TRC can be modelled by considering a linear response of both concrete and textile reinforcement and assuming that plane sections remain plane after deformation (Bernoulli-Navier hypothesis), see Figure 4.5a. This assumption has been extensively investigated and validated in previous investigations [FIB07, Haw18, Heg16, Pre19, Sch12, Tys09, Por16] .
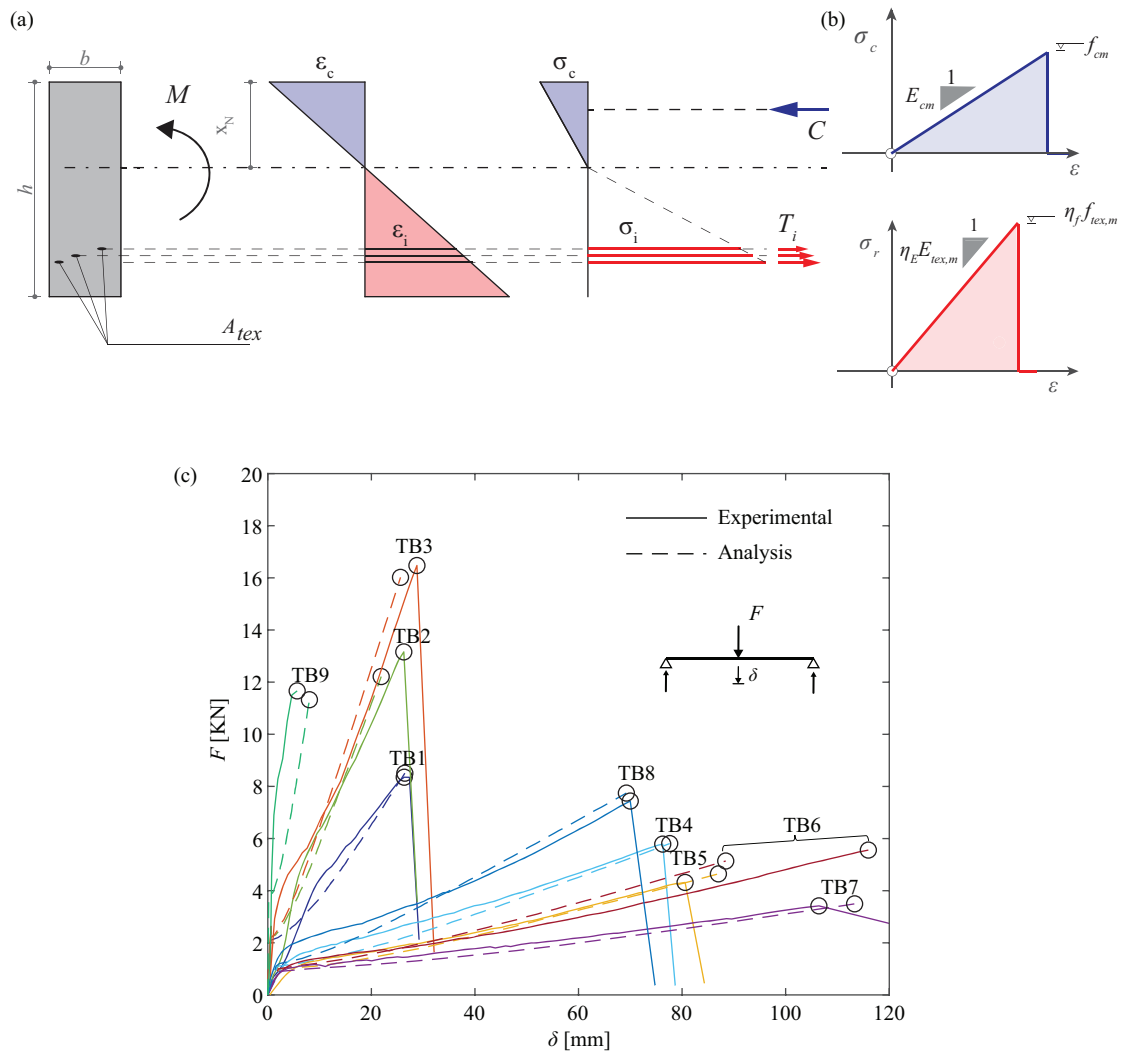
Figure 4.5: (a) Model assumptions for flexural response; (b) material constitutive law of concrete and textile reinforcement and (c) calculated and experimental load-deflection curves

Due to the significant variation of the roving flexural depth in some cross sections, each roving is modelled separately for calculation of the response. Failure occurs in all cases when the outermost roving reaches its tensile strength, as it fails in a brittle manner and the rest of rovings are not capable of withstanding their increase of force. With respect to the properties of the rovings within the concrete section, their strength and stiffness have to be reduced with respect to bare textile properties (in order to account for the delayed activation of stresses and local damage [Chu06, Pho73, Val20b, Vor06]). This will be performed in the following by means of two distinct efficiency factors [Val17, Val20a]. The first, named η_f, reduces the effective textile tensile strength with respect to the bare textile. The second, named η_E, reduces the effective modulus of elasticity of the textile.

The value of the efficiency factors is determined in this work by means of calibration with test results, in order to have an average of measured-to-calculated values equal to 1.0 both in terms of strength and deformation at failure. This yields the value $\eta_f = 0.91$ and $\eta_E = 0.79$. Such an approach is adopted as the aim of this work is the statistical analysis of the TRC response (alternative approaches based on physical models to determine such efficiency factors can be consulted elsewhere [Val20a, Val20b].). It can be noted that the calibrated value of η_E is lower in this case than the value of η_f, which is uncommon in comparison to the results from other researchers [Val20a, Val20b]. This fact can be partly grounded on the fact that the roving position was variable through the length of the specimens and thus the geometry (stiffness and resistance) of the governing cross section in bending is not necessarily constant through the length of the specimen. Also, the influence of the duration of the structural tests, different to that of the material characterization tests, is accounted for in these coefficients which can be relevant for the concrete stiffness.

The calculated load-deflection curves (F-δ) are plotted in Figure 4.5c together with the measured results. The comparison between the tested ultimate resistance R_{exp}, the calculated one R_{calc} and the corresponding maximum deformation of each beam is givens in Table 4.4. The comparison shows that the CoV of the resistance (5.13%) is relatively low (lower than those reported by other authors [Rem18]).

Table 4.4:   Three-point bending test results

Specimen	R_{exp} [kN]	R_{calc} [kN]	R_{exp}/R_{calc}	δ_{exp} [mm]	δ_{calc} [mm]	$\delta_{exp}/\delta_{calc}$
TB1	8.4	8.5	0.99	26.4	26.5	1.00
TB2	13.2	12.2	1.08	26.3	21.9	1.20
TB3	16.5	16.0	1.03	28.8	25.6	1.13
TB4	5.8	5.8	1.00	76.3	77.6	0.98
TB5	4.3	4.6	0.93	80.6	87.0	0.93
TB6	5.6	5.1	1.10	116	88.4	1.31
TB7	3.4	3.5	0.97	106.4	113.3	0.94
TB8	7.4	7.7	0.96	7.4	7.7	0.96
TB9	11.7	11.3	1.04	5.7	8.0	0.71
Average			1.0			1.0
COV			5.13%			17.10%

4.5 Response of statically indeterminate systems of TRC and model uncertainty of action effects

As previously explained, the response of statically indeterminate systems and the corresponding action effect model uncertainties can be significant for the safety format calibration, particularly when a brittle response can be expected. This is for instance the case for TRC, whose response was experimentally examined in the previous Section with reference to statically determinate structures. In order to investigate the response of statically indeterminate TRC structures, a large database will be presented in this section obtained by assembling the test results on determinate members. This database will eventually be used to create a probabilistic model of the action effect model uncertainty.

The main idea to simulate the response of statically indeterminate members based on the response of statically determinate ones is shown in Figure 4.6a (details for a worked example are provided in Appendix 4.B). As it can be seen, a redundant system is generated by assembling two simply supported beams connected at mid span. Such a statically indeterminate system will be referred to in the following as an *assembled cross-beam system*. Due to the symmetry conditions of the system, each component beam has the same load-deflection response as in a three-point bending test and the response of the complete system can be obtained by the superposition of the load-deflection relationship of the two component beams, see Figure 4.6b.
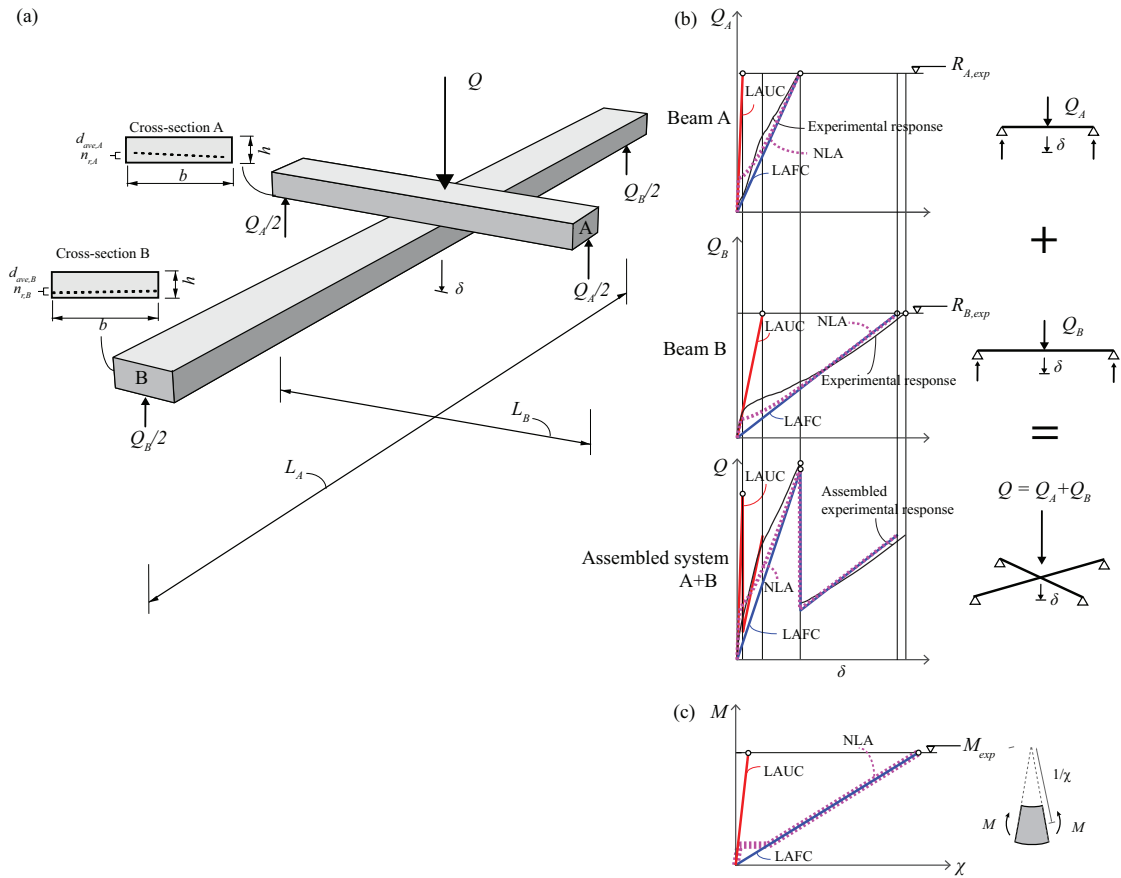
Figure 4.6: (a) Assembled cross-beam system test set-up; (b) load-deflection relationship of the cross-beam system obtained by superposition of both responses of its component beams and (c) considered moment-curvature (M-χ) relationships for different structural analysis models

4.5.1 Action effect model uncertainty for different types of structural analyses

In the following, the experimental results on the assembled cross-beam systems are compared to three types of structural analyses:

- Linear Analysis assuming UnCracked stiffness (LAUC in Figure 4.6b and c).

- Linear Analysis assuming Fully-Cracked stiffness (LAFC in Figure 4.6b and c).

- NonLinear Analysis assuming uncracked and cracked behaviour. This analysis is conducted assuming a trilinear moment-curvature relationship and the actual extent of cracked and uncracked regions (NLA in Figure 4.6b and c).

In order to quantify the model uncertainty of action effects, the local resistance model uncertainty will be removed from the global model uncertainty. To do so, tailored values of the efficiency factor η_f are calibrated for each individual beam, in order to match the experimental

resistance, see Table 4.5. The action effect model uncertainty for each analysis method can then be defined as:

$$\theta_{E,LAUC} = \frac{Q_{exp}}{Q_{LAUC}} \tag{5}$$

$$\theta_{E,LAFC} = \frac{Q_{exp}}{Q_{LAFC}} \tag{6}$$

$$\theta_{E,NLA} = \frac{Q_{exp}}{Q_{NLA}} \tag{7}$$

where Q_{exp} refers to the experimental resistance of an assembled cross-beam system by superimposing the experimental response of its two component beams. The terms Q_{LAUC}, Q_{LAFC} and Q_{NLA} refer to the global resistances (load-carrying capacities) of the assembled cross-beam system calculated with LAUC, LAFC and NLA methods respectively and $\theta_{E,LAUC}$, $\theta_{E,LAFC}$ and $\theta_{E,NLA}$ refer to the corresponding action effect model uncertainty variables for the three types of analysis.

Table 4.5:   Tailored efficiency factor η_f for the basic beams

Specimen	TB1	TB2	TB3	TB4	TB5	TB6	TB7	TB8	TB9
η_f	0.90	0.98	0.94	0.91	0.85	1.00	0.88	0.87	0.95

4.5.2   Data of action effect model uncertainty for different types of structural analyses

By combining the nine bending tests of basic beams presented in Section 4.3, a total of 36 assembled cross-beam systems can be generated. The resulting action effect model uncertainty data is plotted in Figure 4.8a. The assembled experimental load-deflection curves of six representative cases and the corresponding load-deformation curves with LAUC, LAFC and NLA are shown in Figure 4.7. A summary of the results of all the assembled cross-beam tests is also provided in Table 4.6 and plotted in Figure 4.8a. As it can be noted, both NLA and LAFC give very close prediction to the actual resistance, while LAUC has a relatively larger scatter, suggesting that the simplifications made about the uncracked stiffness of the structure components result in a higher model uncertainty for statically indeterminate structures. In addition, NLA allows reproducing the different stages of response (uncracked or partially cracked) in a realistic manner.

To further increase the size of sample for action effect model uncertainty data, the number of components of a cross-beam system can still be increased in order to generate more combinations. Following the same methodology, assembled cross-beam system composed of

three to five components are further investigated. In total, 372 different cross-beam systems are generated and the resulting action effect model uncertainty data is plotted in Figure 4.8b. A summary of the statistics of the assemble cross-beam tests is provided in Table 4.6. It can be observed that, with the enlarged database, the difference between the model uncertainty data of the NLA, LAUC and the LAFC method is more pronounced, which confirms that the NLA and LAFC result in a lower level of action effect model uncertainty than the LAUC.
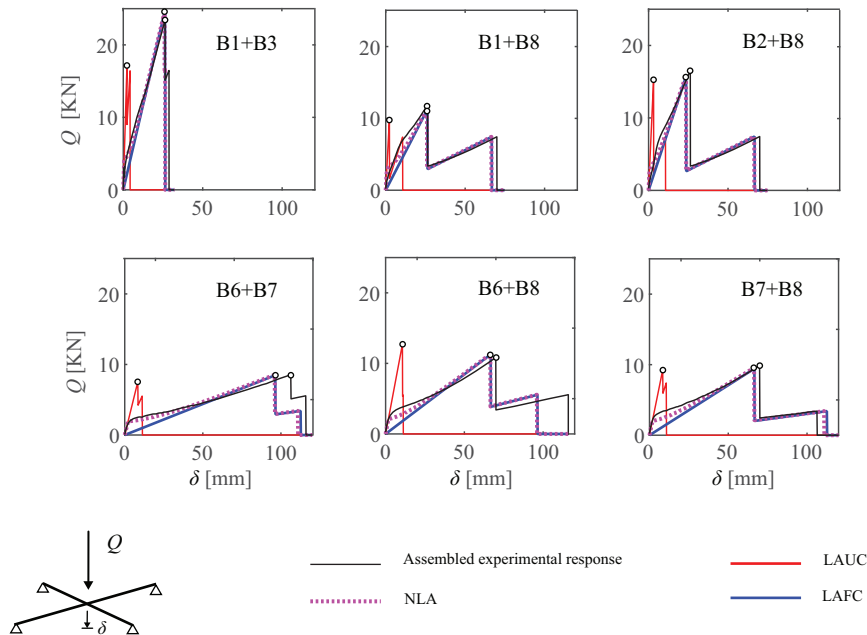
Figure 4.7:   Representative assembled cross-beam system cases

Table 4.6:   Statistics of the cross-beam system tests with two components and two to five components

Number of components	Number of assembled tests	Load effect analysis	Variable	Average value	CoV
Two	36	LAUC	$\theta_{E,LAUC}$	1.05	8.51%
	36	LAFC	$\theta_{E,LAFC}$	1.02	4.01%
	36	NLA	θ_{NLA}	1.01	3.35%
Two to five	372	LAUC	$\theta_{E,LAUC}$	1.14	11.01%
	372	LAFC	$\theta_{E,LAFC}$	1.06	4.47%
	372	NLA	θ_{NLA}	1.03	3.39%

As shown in Figure 4.1, the action effect model uncertainty of statically indeterminate system results from multiple sources as: the uncertainties related to the structural modelling of action

effects; the uncertainties in material properties influencing action effects; and the uncertainties in geometrical properties influencing action effects. The result shows that NLA yields lowest CoV level, which signifies that NLA can significantly reduce the uncertainties related to the structural modelling of action effect. Comparing the tail region of NLA, LAUC and LAFC from the Quantile-Quantile plot [Sch17] (vertical axis referring to quantiles in a standard normal distribution) of $\theta_{E,NLA}$, $\theta_{E,LAFC}$ and $\theta_{E,LAUC}$ data (see Figure 4.8a) it seems however that in the tail region there is no significant difference between these three distributions. This is explained by the fact that the tail region is composed only of results concerning two beams (specimens 6 and 9) influencing the response of all methods to evaluate the internal forces, see 4.8c.
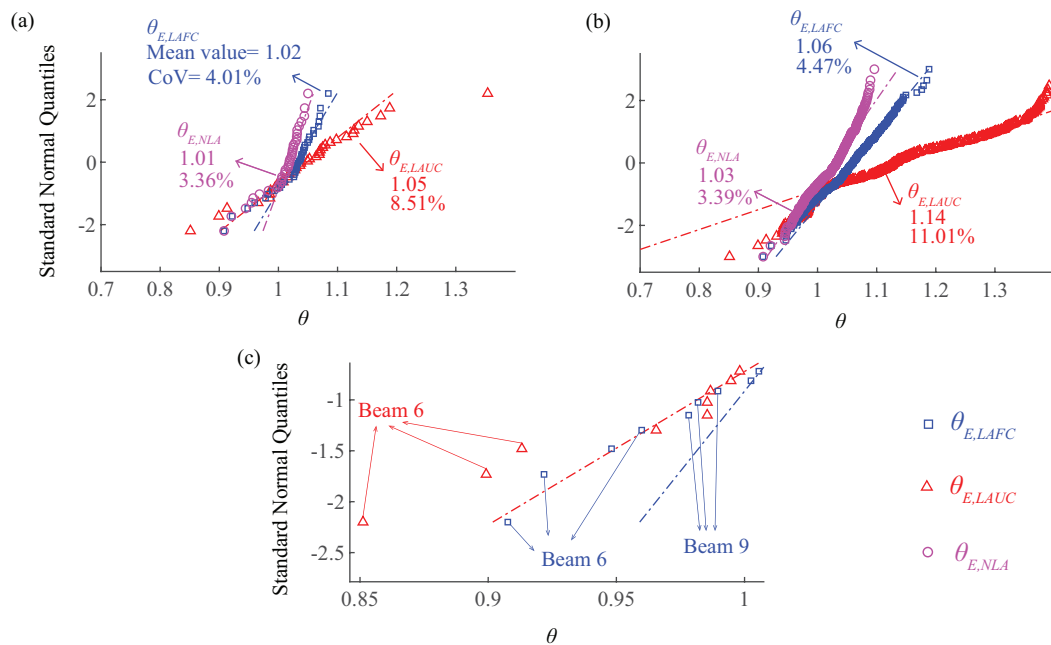
Figure 4.8:   Quantile-Quantile plot for action effect model uncertainty sample data of (a) cross-beam of two components; (b) cross-beam of two to five components; and (c) detail of tail region for cross-beam of two components

4.6   Limits of applicability of linear analyses assuming uncracked and fully-cracked behaviour

The analyses on statically indeterminate structures based on the assembled cross-beams are based on the three-point bending tests data tested within this research program. This implies that only a limited range of the basic design variables has been explored. In this Section, the applicability of LAUC and LAFC will be investigated for a wider range of design cases.

To that aim, the same methodology of the assembled cross-beam system is used in this section. The basic data for the three-point bending test is in this case estimated on the basis of a non-linear analysis (tri-linear moment-curvature relationship). This approach was previously observed to lead to the most realistic results, and to reproduce the various regimes of response (see Figure 4.7). A series of numerical assembled cross-beam system case studies are generated by varying the span L, the cross-section height h, and the textile reinforcement cross-section area A_{tex} of the component beams. By comparing the structural analysis result (global resistance of the structures) from the LAUC and the LAFC with that of NLA, the limit of applicability of LAUC and LAFC is further examined.

4.6.1   Range of design parameters of numerical case study

In the numerical cases, assembled cross-beam systems with two component beams with rectangular cross-sections (refer to Figure 4.6) are studied. In order to investigate the influence of the variation of relative stiffness between the component beams, the dimensions of the first component beam in the assemble cross-beam system is kept constant and the dimensions of the second beam are varied in the selected range.

For all the component beams of the assembled cross-beam systems, the cross-sectional width is kept constant ($b = 250$ mm). The material parameters are also kept constant, adopting the same material properties as for Section 4.3. To simplify the simulation, all textile reinforcements in a given beam are considered to be aligned at the same depth. Three independent parameters are used to characterize the beams in the numerical cases: the span L, the cross-section height h, and the textile reinforcement cross section area A_{tex}. The vector composed of the three design parameters form the design vector X_{num} for a given component beam:

$$X_{num} = [L, h, A_{tex}] \tag{8}$$

For a given component beam, the other parameters are dependent on the values of its design vector X_{num}: the cross-sectional effective depth of a given component beam (d) is assumed to be proportional to the height h with a constant ratio $d = 0.85h$ and the reinforcement ratio ρ is defined as $\rho = \frac{A_{tex}}{bd}$.

In each numerical case, two beams are assembled. The design vector of component beam A is always kept constant as $X_{num,A} = [L_A, h_A, A_{tex,A}]$, with L_A=1.7 m, $h_A = 60$ mm and A_{tex}= 66.3 mm^2 (resulting in $\rho_A = 0.52\%$). The design vector of component beam B (denoted by $X_{num,B,ijk}$ with i,j,k =1-10) is varied. The design parameters of beam B are varied within the following range: $L_{B,i} = (1.0\text{-}4.0)$ m; $h_{B,j} = (30\text{-}120)$ mm and $A_{tex,B,k} = (23.8\text{-}142.8)$ mm^2 , resulting in $\rho_{B,ijk} =$ (0.09-2.24)% (i,j,k =1-10). For each parameter, ten equally spaced values in the ranges specified are considered, leading to a total of 1000 cases. For example, for the case of $[i,j,k]$=[1,1,10],

$X_{num,B,ijk} = [L_{B,1}, h_{B,1}, A_{tex,B,10}]$, with $L_{B,1} = 1.0$ m, $h_{B,1} = 30$ mm and $A_{tex,B,10} = 142.8$ mm^2 (resulting in $\rho_B = 2.24\%$).

For each case, the resistance of the assembled cross-beam system analysed with LAUC and LAFC (refer to Appendix 4.B for the detailed analysis method) are compared with that analysed with NLA in order to get the corresponding action effect model uncertainty data:

$$\theta_{E,LAUC,num} = \frac{Q_{NLA}}{Q_{LAUC}} \tag{9}$$

$$\theta_{E,LAFC,num} = \frac{Q_{NLA}}{Q_{LAFC}} \tag{10}$$

It should be noted that $\theta_{E,LAUC,num}$ and $\theta_{E,LAFC,num}$ only contains uncertainties related to the structural modelling of action effects and are thus different than the definition of $\theta_{E,LAUC}$ and $\theta_{E,LAFC}$ in the previous section (Section 4.5.1 Eq. (5)-(6)).

4.6.2 Results of the case study

The histograms of the resulting $\theta_{E,LAUC,num}$ and $\theta_{E,LAFC,num}$ data for all cases are plotted in Figure 4.9 and the statistical values are given in Table 4.7. It can be observed that, in general, the LAFC results in smaller scatter in the action effect model uncertainty.
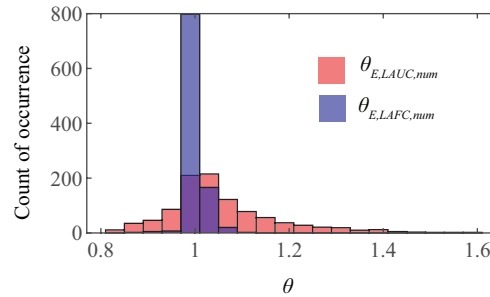
Figure 4.9:   Histogram of the $\theta_{E,LAUC,num}$ and $\theta_{E,LAFC,num}$ data from the numerical assembled cross-beam system case study

Table 4.7:   Statistics of the numerical cross-beam system tests with two components

Number of fictitious tests	Load effect analysis	Variable	Average value	COV
1000	LAUC	$\theta_{E,LAUC,num}$	1.06	11.21%
1000	LAFC	$\theta_{E,LAFC,num}$	1.00	1.66%

To have a better understanding of the limit of applicability of the two methods, the resulting $\theta_{E,LAUC,num}$ and $\theta_{E,LAFC,num}$ for the cases with $h_B = 80$ mm are plotted in Figure 4.10. As it can be seen in this figure, $\theta_{E,LAUC,num}$ has significantly higher variation than $\theta_{E,LAFC,num}$. For the cases

when the reinforcement ratio of both beams is similar, the LAUC method yields a $\theta_{E,LAUC,num}$ value close to 1, but in a wide range of cases the value of $\theta_{E,LAUC,num}$ deviates significantly from 1. On the other hand, the LAFC yields in most cases $\theta_{E,LAFC,num}$ values close to 1. This confirms the applicability of the LAFC method in general. The result of the LAFC only deviates significantly from the expected value when the reinforcement ratio of Beam B is close to the minimum reinforcement ratio for bending. This means that a significant portion of the beam remains uncracked at failure and thus, the fully cracked assumption deviates from the actual response. For practical purposes, this situation can be avoided by requiring a reinforcement ratio higher than the minimum. It is also interesting to notice that in the cases where the two component beams have the same reinforcement ratio ($\rho_B = \rho_A = 0.52\%$), despite the variation of other parameters, the result $\theta_{E,LAUC,num}$ and $\theta_{E,LAFC,num}$ values remain close to 1. This is because the ratio between the uncracked stiffness of the two beams are the same as the ratio between their fully cracked stiffness in these cases.

As a conclusion from the previous considerations, it can be observed that, unlike for ordinary reinforced concrete structures, it is not advised to use the LAUC method to perform action effect analysis for TRC structures. A LAFC can, on the other hand, be applied provided that sufficient amount of flexural reinforcement is provided. It should also be noted that the previous comments focus on the cases with bending failure governed by rupture of the textile reinforcement (covering also cases with low levels of axial compression forces). Other failure modes (such as failures for very high levels of compression forces or shear) remain outside of the scope of this work (covered by other partial safety factors).
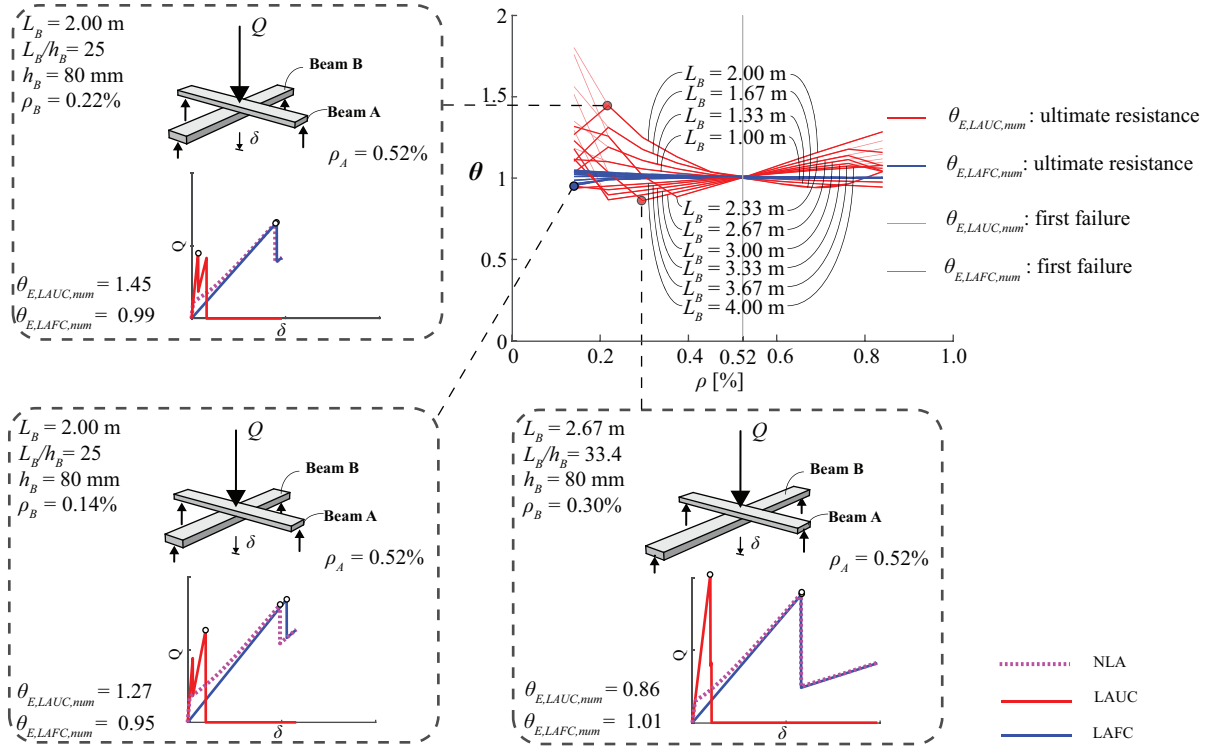
Figure 4.10:   Results of $\theta_{E,LAUC,num}$ and $\theta_{E,LAFC,num}$ for cases with h_B = 80 mm

4.7   Safety format of TRC structures

In this section, the reliability verification framework of Eurocodes [CEN02] is used to calibrate the safety format for TRC structures on the basis of probabilistic reliability theory. Similar to the case of reinforced concrete structures, a number of uncertainties (associated to material, geometry and modelling) shall be accounted for in the partial factor for TRC. In addition, due to the brittle behaviour of TRC structures, it is necessary to discuss if additional safety considerations are needed for the model uncertainty of action effects (a common situation with respect to design of other reinforced concrete elements failing in a brittle manner by punching or second-order effects). In the following, the probabilistic modelling of the basic uncertainties is discussed and two types of safety formats are proposed for TRC structures. The efficiency of the proposed safety formats for TRC structures is discussed based on the reliability analysis of representative cases.

4.7.1 Basic uncertainties in the design of TRC structures

4.7.1.1 Material uncertainties

Two material strength basic variables are involved in the reliability analysis problem of TRC structures: the tensile strength of textile reinforcement and the concrete compressive strength. The material strength variables are assumed to follow lognormal distribution according to the recommendations in [JCS01]. For the concrete compressive strength, the distribution parameters provided in the second generation of Eurocode prEN1992-1-1:2020 [CEN02] are used, where the coefficient of variation (CoV) is taken as 15.6%, which accounts for both the uncertainty in concrete cylinder strength and the uncertainty in the in-situ strength efficient factor η_{is} [CEN02]. For the distribution parameters of the textile reinforcement tensile strength, the statistics of the data from [Val20b] are used, where the CoV of the tensile strength of textile reinforcement is taken as 15% (which accounts for the uncertainty in the single roving tensile strength based on test results). These distribution parameters are consistent with data from other researchers [Rem18]. The uncertainty in the efficiency factor η_f of textile reinforcement is not accounted for in the material uncertainty, but in the uncertainty of the resistance model (calibration factor). It should be emphasized that with respect to the statistical properties for the textile reinforcement tensile strength, they should be based on the data provided by the manufacturer or derived from specific tests (products can have highly variable properties). The probabilistic modelling of the material strength variables used in the safety format calibration in this work is summarized in Table 4.8.

Table 4.8: Probabilistic modelling of basic random variables for safety format calibration of TRC

Uncertainty	Variable	Distribution	Mean	CoV	Standard deviation
Material	Textile reinforcement tensile strength f_{tex}	Lognormal [JCS01]	$f_{tex,m}$	15% [Val20b]	-
	Concrete compressive strength f_c	Lognormal [JCS01]	$\eta_{is}f_{cm}$	15.6% [CEN02]	-
Geometrical	Flexural depth d	Normal [JCS01]	d_{nom}	-	3 [mm] [Rem18]
Model	Resistance model uncertainty $\theta_{R,local}$	Lognormal [JCS01]	1.0	10% [Rem18]	0.1

4.7.1.2 Geometric uncertainties

Since the case of bending is considered and the material strength of textile reinforcement is calculated on the basis of the nominal value of the roving area, the governing geometrical value is the effective geometrical depth (d). Its uncertainties are mainly related to how the reinforcement is fixed during casting, to the type of the member (with flanged or full cross section), to the casting and control procedure and to the type of reinforcement (stiff or soft). Statistical data of the flexural depth variable can be found in literature. According to [Rem18], a mean value of -0.2 mm and a standard deviation of 2.0 mm of the measured data is observed for the deviation (error) of the flexural depth from nominal values ($d-d_{nom}$). This shows that it is possible to have relatively good quality control of the position of the textile reinforcement in TRC structures. For practical applications of TRC structures, the distribution parameters of the flexural depth random variable will be considered related to their quality control and allowable execution tolerance. Since the total thickness of TRC structures is in general much smaller than in ordinary concrete structures, the assumptions of execution tolerances of concrete structures are not considered applicable to TRC structures. Referring to the data from [Rem18] and also taking the efficiency of the textile reinforcement into account, a tolerance of +/- 5 mm for the error of effective depth ($d-d_{nom}$) will be assumed in the following. The error of effective depth ($d-d_{nom}$) is assumed to follow a normal distribution, with a mean value of 0, and -5 mm corresponds to the 5% fractile. Based on the normal distribution assumption, the standard deviation of $d-d_{nom}$ can then be calculated as 5/1.645 = 3.0 mm. Since d_{nom} is a deterministic value, the flexural depth variable d has the same standard deviation (3 mm) as $d-d_{nom}$, see Table 4.8. It should be noted that, with a constant value of execution tolerance for the flexural depth, the CoV of the flexural depth variable decreases with the increasing thickness of the structure. The same phenomenon has also been noticed in reinforced concrete structures in the second generation of Eurocode prEN1992-1-1:2020 [CEN20].

4.7.1.3 Model uncertainties

Two types of model uncertainties are considered for the partial factor calibration of TRC structures: (i) the resistance model uncertainty and (ii) the action effect model uncertainty. For the resistance model uncertainty variable, $\theta_{R,local}$, the model used to analyse the tests presented in this work showed a fairly low CoV (equal to 5.13%). Such low value results partly from the fact that a calibrated value of the efficiency factor η_f was adopted. When designing TRC structures, a general value of this efficiency factor shall be adopted (not calibrated based on tests), potentially leading to a higher value of CoV of the model uncertainty variable. Based on the work of other researchers[Häu19, Rem18, Rem20], a reasonable value for the CoV can be considered as 10%, that will also be used in the following, see Table 4.8.

For the action effect model uncertainty, as previously explained in Figure 4.1, it is theoretically accounted for in the partial factors for the actions provided in Eurocodes. It shall yet be noted that the model uncertainty of action effects accounted for by these partial factors depend neither

on the material response (brittle or ductile) nor on the structural analysis methods (LAUC, LAFC, NLA or others). For TRC structures, it has been shown in this work that when using NLA or LAFC for a redundant structure, the model uncertainty of action effects is relatively low compared to the values reported in Section 4.2.2 and to other uncertainties reported in Table 4.8 (maximum CoV=4.47% for the investigated cases). This is however not the case for LAUC (maximum CoV=11.01%). Based on this consideration, it is proposed that both NLA and LAFC methods can be used to calculate the action effect (internal forces) of TRC structures without the need to adjust the action effect model uncertainty level. LAUC cannot however be used, unless additional specific considerations were made on the safety factors.

4.7.2 Safety format proposals

Based on the characteristic of basic uncertainties involved in the resistance of TRC structures, two types of safety formats are proposed.

4.7.2.1 Safety format I: partial factor $\gamma_{tex,I}$ for the tensile strength of textile reinforcement and consideration of nominal dimensions

The first proposal for the safety format is based on the use of a partial factor for the strength of the textile and the use of nominal values for the geometric dimensions. This approach corresponds thus to current design practice for conventional reinforced concrete structures, but providing a tailored partial safety factor for the strength of the reinforcement.

The calculation of the value of the partial safety factor can be performed assuming that the resistance function R can be approximated by a lognormal distribution (detailed information about such an estimation is provided in Appendix 4.A). Thus, the partial safety factor $\gamma_{tex,I}$ for calculation of the design value of the tensile strength of textile reinforcement ($f_{tex,d} = f_{tex,ck}/\gamma_{tex,I}$) can be calculated based on the approximated value of the CoV of the resistance, V_R:

$$\gamma_{tex,I} = \frac{f_{tex,ck}}{f_{tex,d}} = \exp(\alpha_R \beta_{tgt} V_R - 1.645 V_{ftex}) \tag{11}$$

Where $f_{tex,d}$ refers to the design value of the textile tensile strength, $f_{tex,ck}$ to its characteristic (5% fractile) value, α_R to the FORM sensitivity factor for the resistance (adopted equal to 0.8 [CEN02]), β_{tgt} to the target reliability index and $\beta_{tgt} = 3.8$ for structures with medium consequence class and a reference period of 50 years at the ultimate limit state [CEN02], V_R to the CoV of the resistance variable and V_{flex} the CoV of the material (15% according to Table 4.8). With respect to V_R, its value can be approximately estimated (detailed information about such an estimation is provided in Appendix 4.A) by considering the CoVs for the material, geometrical and model uncertainties (refer to Table 4.8) as:

$$V_R \approx \sqrt{V_{\theta_R}^2 + V_{f_{tex}}^2 + V_d^2} \qquad (12)$$

The general format to calculate the design value of the resistance (R_d) can thus be established as:

$$R_d = R\{\frac{f_{tex,ck}}{\gamma_{tex.I}}, \frac{f_{ck}}{\gamma_C}, d_{nom}\} \qquad (13)$$

Where f_{ck} refers to the characteristic compressive strength of concrete, γ_C to its partial safety factor (1.5 according to Eurocode prEN1992-1-1:2020 [CEN20]) and d_{nom} to the nominal value of the geometrical dimensions.

Detailed information about the safety format calibration method is provided in Appendix 4.A. As it can be noted, the estimated value of V_R varies with the change of the nominal effective depth of the structure (see Table 4.8). For the investigated range of the nominal effective depth (15-60 mm), the estimated value of V_R ranges between 0.19 and 0.27 (see detailed results in Appendix 4.A). It should be noted that according to prEN1990:2020 [CEN20], when V_R is higher than 0.20, the approximated Eq.(11) is not applicable for the partial factor calibration anymore. In this section, however, Eq.(11) is still used to make a first approximated calculation of the partial safety factor. Its effectiveness will be verified by the reliability case study in Section 4.7.3. Considering the wide applicable range of the safety format, referring to the approximated estimation values of V_R, a relatively conservative value of $V_R = 0.225$ is selected in the following and the value of the partial factor $\gamma_{tex,I}$ is then calculated as:

$$\gamma_{tex,I} \approx 1.55 \qquad (14)$$

It should be noted that the partial factor for concrete compressive strength $\gamma_C = 1.5$ from Eurocode prEN1992-1-1:2020 [CEN20] is also adopted in this research. The effectiveness of this proposal will be verified in Section 4.7.3 by calculating the actual achieved reliability level of representative cases.

4.7.2.2 Safety format II: partial factor $\gamma_{tex,II}$ for the tensile strength of textile reinforcement and consideration of design values for the dimensions

As shown in previous paragraph, for thin members, the geometrical uncertainties (related to the effective depth) can become governing. For this reason, it makes sense to separate the geometrical uncertainties from material and model uncertainties as previously discussed by [Rem18, Rem20]. Considering the general form of the limit state function and the probabilistic models of the basic uncertainties (see details in Appendix 4.A), the material and model uncertainties will be lumped into one partial factor $\gamma_{tex,II}$ applied to the tensile strength of textile reinforcement. With respect to the geometrical uncertainties, they will however be considered apart, by means of a design value of the effective depth (this alternative possibility using design values of geometrical dimensions is already given by prEN1992-1-1:2020

[CEN20]). The partial safety factor can thus be estimated with the help of FORM sensitivity factors as:

$$\gamma_{tex,II} = \frac{f_{tex,ck}}{f_{tex,d}} = \exp\left(\sqrt{\alpha_{ftex}^2 + \alpha_\theta^2}\sqrt{V_{ftex}^2 + V_\theta^2}\alpha_R\beta_{tgt} - 1.645V_{ftex}\right) \tag{15}$$

Details on this derivation and the values for the various parameters are given in Appendix 4.A of this chapter. With respect to the design value of the effective depth, it is calculated by reducing the nominal value by a distance of Δ_d:

$$d_{design} = d_{nom} - \Delta_d \tag{16}$$

whose value results (see Appendix 4.A for details):

$$\Delta_d = \alpha_d\alpha_R\beta_{tgt}\sigma_d \tag{17}$$

Based on the safety elements defined above, the general format to calculate the design value of resistance can be defined:

$$R_d = R\{\frac{f_{tex,ck}}{\gamma_{tex,II}}, \frac{f_{c,ck}}{\gamma_C}, d_{design}\} \tag{18}$$

By applying this methodology, the value of the partial factor $\gamma_{tex,II}$ and Δ_d can be derived for the given range of d_{nom}, as shown in Figure 4.11 for representative cases.
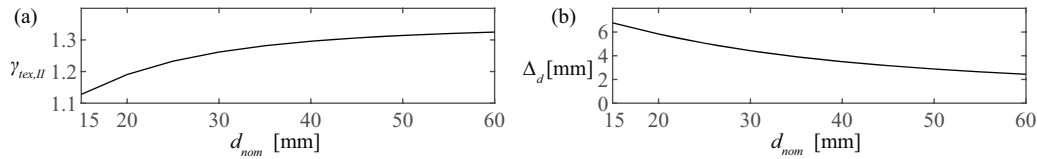
Figure 4.11: Estimated values as a function of nominal effective depth: (a) $\gamma_{tex,II}$; and (b) Δ_d

It can be observed that the estimated value of $\gamma_{tex,II}$ ranges between 1.13 and 1.33 and the value of Δ_d between 6.8 mm to 2.4 mm. As a reasonable and safe estimate, the following values are suggested:

$$\gamma_{tex,II} \approx 1.25 \tag{19}$$

$$\Delta_d \approx 6\ mm \tag{20}$$

The effectiveness of this proposal will be verified and compared with Proposal I in Section 4.7.3 by calculating the actual achieved reliability level of representative cases.

4.7.3 Comparison and verification of the two safety format proposals

A series of representative cases are investigated in the following to compare the previous proposals. To that aim, the classical design method of verifying at sectional level is considered, implying that the influence of statically indeterminate structures is taken into account by the partial factor on actions. The geometry of the studied cross section is shown in Figure 4.12a. The range of the key design parameters used in this case study series is listed in Table 4.9. The value of cross-section height h and reinforcement ratio ρ are varied in a deterministic manner to generate a series of different cases.
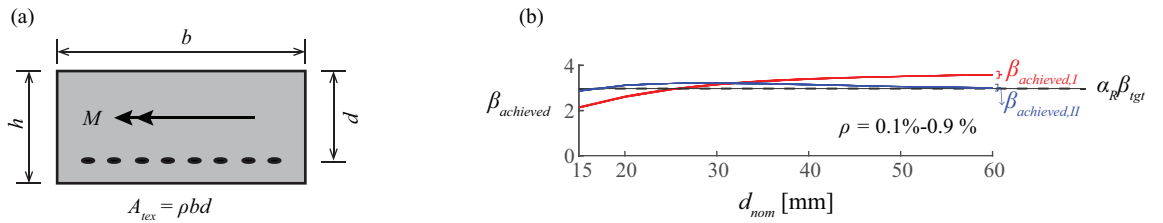
Figure 4.12: (a) Geometry of the investigated cross section and (b) achieved reliability index of the invesitigated bending case with the two safety format proposals

Table 4.9: Key design parameters for the representative cases

Variable	$f_{tex,m}$ [MPa]	f_{cm} [MPa]	b [mm]	h [mm]	d_{nom} [mm]	ρ
Value	1800	150	250	18.75 – 75	0.8h	0.1% - 0.9%
Variable type	Random variable	Random variable	Deterministic	Deterministic	Random variable	Deterministic

For the reliability analysis, the basic uncertainties introduced in Section 4.7.1 (listed in Table 4.8) are accounted for. The general form of the performance function g is defined as:

$$g = \theta_{R,local} R(f_{tex}, f_c, d) - R_d \qquad (21)$$

Based on the safety format proposals, the design value of the resistance for the two safety formats can be calculated using Eq.(13) and Eq.(18) and the reliability analysis is performed using FORM to calculate the actual achieved reliability $\beta_{achieved}$ for the two types of safety formats as:

$$Prob(g < 0) = \Phi(-\beta_{achieved}) \qquad (22)$$

Where *Prob* () refers to the probability function, g to the performance function, Φ to the cumulative probability function of standardized normal distribution and $\beta_{achieved}$ refers to the actual achieved reliability index for a given case. The reliability analysis is performed with

FORM method and the achieved reliability index from the two safety proposals are plotted in Figure 4.12b.

As it can be observed, the value of the achieved reliability level for Proposal I, $\beta_{achieved,I}$, ranges between 2.12 to 3.66 and the value of the value of the achieved reliability level for Proposal II, $\beta_{achieved,II}$, ranges between 2.87 to 3.22. Comparing the achieved reliability index for the two proposals with the target of $\alpha_R \beta_{tgt}$ = 3.04, it can be observed that in most of the range of the investigated cases, both safety formats result in acceptable levels of reliability. However, for Proposal I, when the effective depth is very low (smaller than 20 mm), the achieved reliability level is lower than the acceptable level (±0.5 target level) [Kön81]. It can also be observed that the maximum achieved reliability level for Proposal I is even high for large thicknesses, suggesting potentially uneconomic design. Proposal II yields a more uniform level of reliability.

4.8   Conclusions

This work investigates on a suitable safety format and analysis method for Textile Reinforced Concrete (TRC) structures. The results of an experimental programme on nine TRC slabs are presented and the implications of a brittle response on the reliability of a structure are discussed. Its main conclusions are listed below

- Structures presenting brittle responses (implying limited or none redistribution capacity of internal forces) can fail for load levels below those considered for design if the calculation of internal forces deviates from the actual response (typically, elastic-uncracked behaviour assumed in the calculation of internal forces). This situation does not occur for a ductile response and raises questions on the consideration of model uncertainty of action effects within the Partial Safety Factor Format (PSFF) as considered in Eurocodes.

- The analysis of statically indeterminate TRC structures shows that performing a linear elastic calculation of internal forces considering fully cracked stiffness properties for all sections is a suitable manner to estimate the internal forces and response of TRC. This holds true provided that more than minimum amount of reinforcement are provided in the structure.

- Alternatively, using a nonlinear analysis (considering the development and extent of cracking) is also a suitable manner to estimate the internal forces. It is even more accurate than the previous, but requiring a significant effort for analysis.

- Estimating internal forces on the basis of the uncracked stiffness of the sections (as usually performed for ordinary reinforced concrete) can lead to relatively large deviations on the response and internal forces of a brittle structure as TRC. Such method

shall not be used for design unless specific considerations were implemented to cover this increased uncertainty.

- Since for thin members, the variability of the effective depth can be significant compared to the mean value, the geometrical uncertainties can play a major role in calibrating the partial safety factors for designing structures at ultimate limit state. On the basis of reliable internal forces (determined by a linear-elastic fully cracked analysis or a nonlinear analysis), a safety format can be considered for TRC following the PSFF. Two ways for so doing are detailed in the manuscript:

  o Consideration of a partial safety factor for the tensile strength of the textile ($\gamma_{tex} = 1.55$) and nominal dimensions. All uncertainties (material, geometrical and model) are lumped into the partial safety factor of the textile.

  o Consideration of a reduced partial safety factor for the tensile strength of the textile ($\gamma_{tex} = 1.25$) and design dimensions (reduction of 6 mm in effective depth). In this case, material and model uncertainties are accounted for in the partial safety factor of the textile while geometrical uncertainties are considered in the design dimensions.

  o In general, the second safety format is preferable, leading to a more uniform level of safety.

It shall be noted that the aim of this investigation is to propose a safety format for designing TRC and a methodology for calibrating the associated safety factors and parameters. For practical applications, the values proposed in this investigation (γ_{tex} and Δ_d) should be tailored on the basis of actual values of material and geometrical uncertainties, which can depend on the material used, production method and quality control procedure.

Acknowledgements

Appendix 4.A: Derivation of the safety format proposals for TRC structures

In this annex, the methodology used for the safety format calibration of TRC structures is presented. The annex is based on the semi-probabilistic reliability verification approach of the Eurocodes [CEN02]. To that aim, the target reliability index β_{tgt} provided in EN1990:2002 [CEN02] for structures with medium consequence class and a reference period of 50 years at the ultimate limit state is used (β_{tgt} = 3.8).

The partial factors used in the semi-probabilistic reliability verification approach of the Eurocodes [CEN02] are calibrated based on the First Order Reliability Method (FORM) [Has74, Mad86]. Based on the FORM, to achieve the target reliability level, the partial factor for each basic random variable can be defined with the aid of the FORM sensitivity factors, which are the directional cosines of the vector between the mean value point and the FORM design point in standardised normal space.

In principle, independently of the type of safety format selected, the required partial factors to achieve the exact target reliability level are different for each individual case due to the difference in the shape of the limit state function. The shape of the limit state function depends on the mechanical model of the corresponding limit state as well as the probabilistic modelling of the basic uncertainties involved in the limit states. However, to simplify the design procedure, in the semi-probabilistic approach, the values of the partial factors are fixed and selected with the criterion that the achieved reliability level for representative design cases are as close as possible to the target value. Another important simplification in the safety format calibration in Eurocodes is to adopt standardised FORM sensitivity factors for the resistance variable and the action effect variable. The FORM sensitivity factor for the resistance α_R is assumed to take the value of 0.8 and that for the action effect α_E is assumed to take the value of -0.7 provided that the ratio between the standard deviation of the action effect variable and the resistance variable is within the range of 0.16 to 7.6 [CEN02]. Using these standardised values makes it possible to separate the task of calibrating the partial safety factors on the resistance side and on the action effect side, which largely simplified the safety format calibration procedure. On the basis of such simplification, the target for the calibration of the partial factors for the resistance of TRC structures becomes:

$$Prob(R - R_d < 0) = \Phi(-\alpha_R \beta_{tgt}) \tag{23}$$

When using the FORM or other reliability methods to calibrate the partial factors, iterative procedures are usually needed. However, under some conditions, simple analytical solutions can be derived for the partial factors. This can be done by making reasonable assumptions about the form of the limit state function. The resulting partial factors can eventually then be verified with the FORM or full-probabilistic reliability methods for the representative design cases. This strategy will be followed in this work when calibrating the safety format for TRC structures.

Considering the basic random variables involved in the resistance of TRC structures, the general form of the resistance function can be assumed as:

$$R = \theta_{R,local}R(f_{tex}, f_c, d) \tag{24}$$

The specific form of the resistance function depends on mechanical model of the resistance and also the values of the basic variables.

For calculation of the bending resistance of TRC structures, the methodology presented in Section 4.3 is considered, based on the Bernoulli-Navier assumption. The resistance of a cross section can be controlled either by the tensile strength of the textile reinforcement or by the compressive strength of concrete (but not by the two material strengths at the same time). The cases where the resistance is controlled by concrete strengths are not within the scope of this work, as they are similar to conventional over-reinforced concrete structures, and the safety elements for this type of cases are actually applied through the partial factor on concrete compressive strength. For the cases where the resistance is controlled by the textile reinforcement, Eq. (24) can be further simplified to the following form:

$$R = \theta_{R,local}R(f_{tex}, d) \tag{25}$$

It is then reasonable to make an additional assumption considering that the resistance can be approximated by a multiplicative form of the basic random variables:

$$R = \theta_{R,local}R(f_{tex}, d) \approx A_R\theta_{R,local}f_{tex}d \tag{26}$$

Where A_R represents a coefficient that depends on the other deterministic parameters related to the resistance. Based on the assumption in Eq.(26), the CoV of the resistance V_R can be calculated approximately as:

$$V_R \approx \sqrt{V_{\theta_R}^2 + V_{f_{tex}}^2 + V_d^2} \tag{27}$$

It should be noted that Eq.(27) would be a close approximation if all the basic variables follow lognormal distributions, but in this case the flexural depth d is modelled as a normally distributed variable. In any case, Eq.(27) can still be a reasonable approximation for the purpose of estimating the partial factors. The validity of the above assumptions will eventually be verified by reliability analysis of representative cases with the selected partial factors.

With respect to the value of V_d, it depends on the nominal flexural depth, and this results in different values of V_R for cases with different flexural depths. For instance, for the range of d_{nom} = 15-60 mm, the approximated value of V_R is plotted in Figure 4.13a.
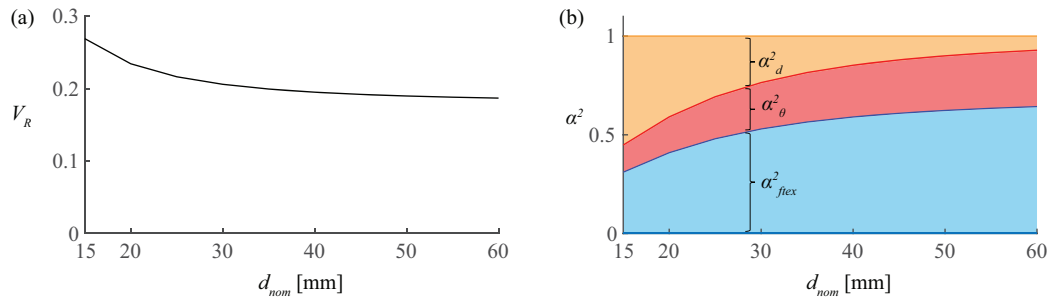
Figure 4.13: Analysis of the influence of d_{nom}: (a) V_R; and (b) FORM sensitivity factors

Following the same strategy, the FORM sensitivity factors for the basic variables can also be estimated as follows:

$$\alpha_{ftex} \approx \sqrt{\frac{V_{ftex}^2}{V_{\theta_R}^2 + V_{ftex}^2 + V_d^2}} \tag{28}$$

$$\alpha_{\theta_R} \approx \sqrt{\frac{V_{f_{\theta_R}}^2}{V_{\theta_R}^2 + V_{ftex}^2 + V_d^2}} \tag{29}$$

$$\alpha_d \approx \sqrt{\frac{V_{f_d}^2}{V_{\theta_R}^2 + V_{ftex}^2 + V_d^2}} \tag{30}$$

The change of the FORM sensitivity factors with the flexural depth is plotted Figure 4.13b. It should be stressed that the above analysis is based on two approximations: the assumption that the resistance can be approximated as a multiplicative form of the basic variables and the assumption that the resistance can be approximated by a lognormal distribution. From this analysis, it can be observed that the FORM sensitivity factor for the flexural depth decreases with increasing depth. It can further be observed that for the cases where the mean value of the flexural depth is relatively small, its uncertainty becomes dominant. Since the flexural depth follows a normal distribution (see Table 4.8), in the cases when the uncertainty of the flexural depth is dominating, the assumption that the resistance follows lognormal can be not valid anymore. This means the estimated FORM sensitivity factors of the range where the flexural depth is small can deviate from the actual value. Nevertheless, the estimated values can still provide important information for the safety format calibration problem and can be used as a useful reference. The estimated values of the CoV of the resistance variable and the FORM sensitivity factors of basic variables are used in the safety format calibration in Section 4.7 and their effectiveness is eventually verified by reliability analysis of representative cases.

Appendix 4.B: Analysis of an assembled cross-beam system

The aim of this annex is to provide a detailed example of the assembled cross-beam system, following the procedure explained in Section 4.5. The assembled cross-beam composed of beam TB1 and TB8 is used for this purpose. For beam TB1 (refer to Section 4.3 for the values of the parameters of beam TB1), the uncracked cross-sectional flexural stiffness EI_{UC} is:

$$EI_{UC} = E_{cm} \frac{bh^3}{12} = 1.40 \cdot 10^8 \ [\text{kN} \cdot \text{mm}^2] \tag{31}$$

Thus, the uncracked stiffness of the beam TB1 results:

$$\left(\frac{dQ}{d\delta}\right)_{LAUC} = \frac{48EI_{UC}}{L^3} = 3.88 \ [\text{kN/mm}] \tag{32}$$

And the cracked cross-sectional flexural stiffness EI_{FC} of beam TB1 is:

$$EI_{FC} = \frac{bx_N^3}{3} E_{cm} + \sum_{i=1}^{n_r} (d_i - x_N)^2 a_{tex} E_{tex,m} = 1.13 \cdot 10^7 \ [\text{kN} \cdot \text{mm}^2] \tag{33}$$

Where x_N refers to the position of the neutral axis (see Figure 4.5) and the fully-cracked stiffness of beam TB1 is:

$$\left(\frac{dQ}{d\delta}\right)_{LAFC} = \frac{48EI_{FC}}{L^3} = 0.31 [\text{kN/mm}] \tag{34}$$

The uncracked and fully-cracked stiffness of beam TB8 can be calculated with the same method. Based on this information, the load-deflection curves of the assembled system using LAUC and LAFC methods are calculated and plotted in Figure 4.14. For the NLA, a trilinear moment-curvature relationship is assumed for each beam and the actual extent of cracked and uncracked regions are accounted for. The resultant response of the assembled system using NLA method and the assembled experimental response are plotted in Figure 4.14. for the selected case.
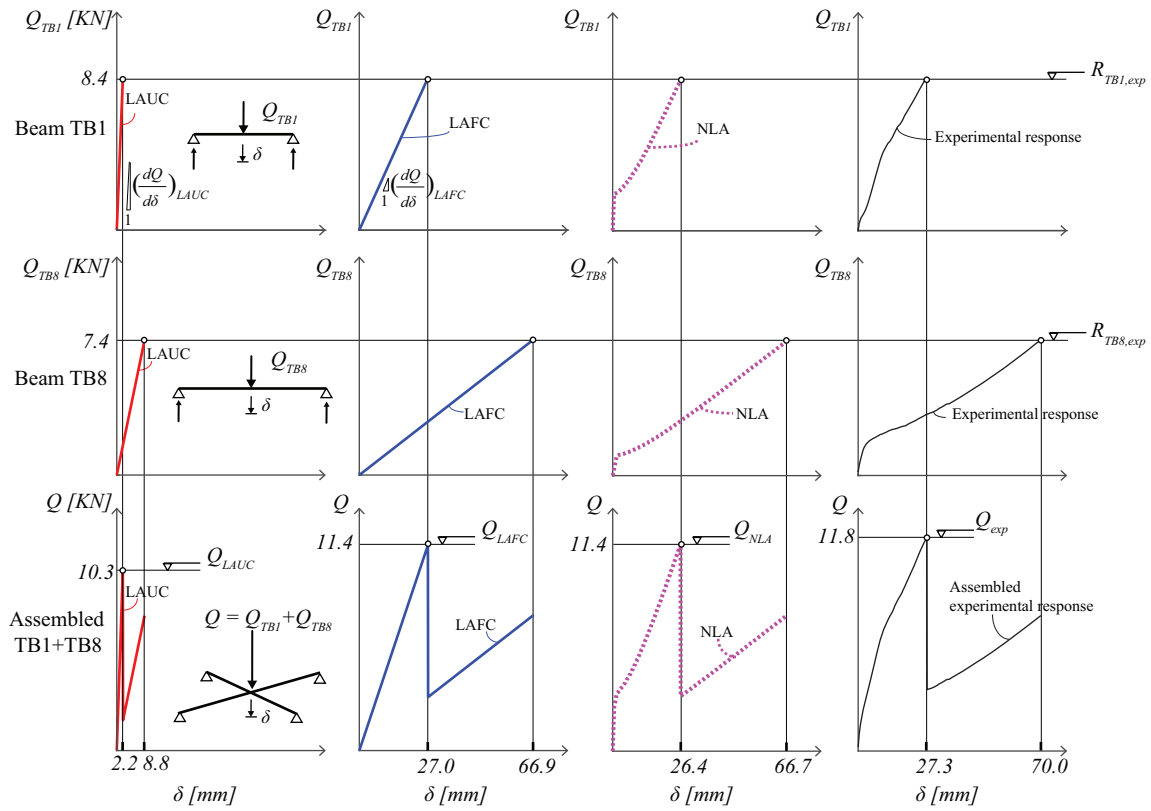
Figure 4.14:   Response of the assemble cross-beam system composed of beam TB1 and TB8

Notation

Latin upper case letters

A_{tex}	total area of textile reinforcement in a beam cross section
A_R	coefficient in the multiplicative form approximation of the resistance function
E_{calc}	calculated action effect at a given cross section of a structure
E_{cm}	mean value of the elastic modulus of concrete (motar)
E_{exp}	experimental action effect at a given cross section of a structure
E_d	design value of action effect
$E_{tex,m}$	mean value of the elastic modulus of textile reinforcement
EI_{FC}, EI_{UC}	fully cracked and uncracked flexural rigidity of a cross section
F	load applied to a tested beam
F_{rep}	representative value of action variables
L	span of a beam
L_{o1}, L_{o2}	overhang of a beam in three point bending test
M	bending moment of a cross section
M_I, M_{II}	bending moment of a cross section of beam BI and BII
M_{cr}	cracking moment of a cross section
M_{exp}	ultimate bending resistance of a tested beam
$M_{hogging}$	maximum hogging moment of a beam according to a linear response
$M_{sagging}$	maximum sagging moment of a beam according to a linear response
$M_{R,hog}$	resistance of a beam cross section to the hogging moment
$M_{R,sag}$	resistance of a beam cross section to the sagging moment
Prob ()	probability function
Q	load applied to an assembled cross-beam system
Q_A, Q_B	load transferred to a component beam of an assembled cross-beam system
Q_{exp}	experimental resistance of an assembled cross-beam system
Q_{LAFC}	resistance calculated with Linear Analysis assuming Fully-Cracked stiffness (LAFC)
Q_{LAUC}	resistance calculated with Linear Analysis assuming UnCracked stiffness (LAUC)
Q_{NLA}	resistance calculated with NonLinear Analysis (NLA)
R_{calc}	calculated local resistance of a structure
R_{exp}	experimental local resistance of a structure
R_d	design value of resistance
U_{tex}	nominal perimeter of the roving of textile reinforcement
V_d	Coefficient of Variant (CoV) of the flexural depth random variable
V_{ftex}	CoV of the textile reinforcement tensile strength random variable
V_R	CoV of the resistance random variable
V_{Sd}	CoV of the action effect model uncertainty
$V_{\theta R}$	CoV of the model uncertainty of local resistance
X_k	the characteristic value for a material strength variable
X_{num}	the design vector for a component beam in the numerical cross-beam system study

Latin lower case letters

a_{nom}	nominal value of geometrical variables

a_{tex}	net cross section of the roving of textile reinforcement
b	width of a beam cross section
d	flexural depth of a roving in a cross section
d_{ave}	average flexural depth of all the rovings in a cross section
d_{max}	maximum value of the flexural depth of all the rovings in a cross section
d_{min}	minimum value of the flexural depth of all the rovings in a cross section
d_{design}	design value for the flexural depth
d_{nom}	nominal value for the flexural depth
e_{tex}	grid spacing of the textile reinforcement
f_c	the compressive strength of concrete (motar)
$f_{c,ck}$	characteristic value for concrete (motar) compressive strength
f_{cm}	mean value of the compressive strength of concrete (motar)
f_{ctm}	mean value of the tensile strength of the concrete (motar)
f_{tex}	the textile reinforcement tensile strength
$f_{tex,ck}$	characteristic value of the textile reinforcement tensile strength
$f_{tex,d}$	design value of the textile reinforcement tensile strength
$f_{tex,m}$	mean value of the textile reinforcement tensile strength
$g()$	performance function
h	height of a beam cross section
n_r	number of textile rovings in a cross section
q_{calc}	the calculated global resistance of a statically indeterminate structure in terms of load factor
$q_{cr,hog}$	external load level when the hogging region of a beam cracks
$q_{cr,sag}$	external load level when the sagging region of a beam cracks
q_E	external action
q_{exp}	experimental global resistance of a statically indeterminate structure in terms of load factor
$q_{R,hog}$	external load level when the hogging region of a beam reaches the ultimate resistance
$q_{R,sag}$	external load level when the sagging region of a beam reaches the ultimate resistance
$q_{R,I}$	external load level when beam BI reaches its load carrying capacity
$q_{R,II}$	external load level when beam BII reaches its load carrying capacity
x_N	position of the neutral axis of a cross section

Greek upper case letters

Δ_d	reduction factor for the flexural depth
$\Phi()$	cumulative distribution function of standardized Normal distribution

Greek lower case letters

α_d	FORM sensitivity factor of the flexural depth random variable
α_E	FORM sensitivity factor for action effects
α_{ftex}	FORM sensitivity factor of the textile reinforcement strength random variable
α_θ	FORM sensitivity factor of the model uncertainty of local resistance random variable
α_R	FORM sensitivity factor for the resistance
$\beta_{achieved}$	achieved reliability index
$\beta_{achieved,I}$	achieved reliability index for safety format proposal I
$\beta_{achieved,II}$	achieved reliability index for safety format proposal II

β_{tgt}	the target reliability index
$\beta_{tgt,50}$	the target reliability index for a reference period of 50 years
γ_C	partial factor for concrete compressive strength
γ_F	partial factors applied to action variables
γ_M	partial factors applied to material strength variables
γ_{Sd}	partial factors for action effect model uncertainty
$\gamma_{tex,I}$	partial factor for textile reinforcement strength in safety format Proposal I
$\gamma_{tex,II}$	partial factor for textile reinforcement strength in safety format Proposal II
δ	mid-span deflection of a structure
δ_{cal}	calculated mid-span deflection of a structure
δ_{exp}	experimental mid-span deflection of a structure
ε_c	strain of concrete
ε_i	strain of a single textile reinforcement roving
η	mean value of the conversion factors for material strength variables
η_E	efficiency factor for the textile modulus of elasticity
η_f	efficiency factor for the textile tensile strength
η_{is}	the in-situ strength efficient factor of concrete
θ_E	random variable for action effect model uncertainty
$\theta_{E,LAFC}$	action effect model uncertainty variable for LAFC
$\theta_{E,LAFC,num}$	action effect model uncertainty variable for LAFC evaluated with numerical method
$\theta_{E,LAUC}$	action effect model uncertainty variable for LAUC
$\theta_{E,LAUC,num}$	action effect model uncertainty variable for LAUC evaluated with numerical method
$\theta_{E,NLA}$	action effect model uncertainty variable for NLA
θ_{global}	random variable for the global resistance model uncertainty
$\theta_{R,local}$	random variable for the local resistance model uncertainty
ρ	flexural reinforcement ratio of a cross section
ρ_{ave}	average flexural reinforcement ratio of a cross section
σ_c	stress of concrete
σ_i	stress of a single textile reinforcement roving
χ	curvature of a cross section

Chapter 5

Conclusions and Outlook

5.1   Conclusions

This chapter summarises the conclusions of this thesis. In addition, an outlook on the research which could be addressed in future works to advance the state-of-the-art is included.

This work explores the different aspects of the partial safety format calibration problem involved in the resistances of reinforced concrete structures. In general, it is concluded that a suitable probabilistic modelling of the basic uncertainties is fundamental for an effective partial safety format calibration, which should be based on a good understanding of the mechanical behaviour of the relevant load bearing mechanisms. On its basis, a detailed safety format composed of calibrated partial safety factors for the dominating uncertainties is an effective reliability verification approach for both classical analytical design equations and advanced nonlinear analysis methods like strain-based approaches and NonLinear Finite Element Analysis.

In the following, the main conclusions of this work are listed by chapter.

Chapter 2: *Considerations on the partial safety factor format for reinforced concrete structures accounting for multiple failure modes*

Focusing on material uncertainties, the basic assumptions, simplifications and applicability conditions of the Partial Safety Factor Format (PSFF) for the design resistance of concrete structures are investigated. By a detailed analysis of the shapes of the limit state functions of different resistance models, the similarities between the simple analytical models and more advanced nonlinear analysis models are demonstrated. The main conclusions of this chapters are the followings:

- ▪ Exponent sensitivity factor analysis of some typical structural resistance models for reinforced concrete structures shows that it is an efficient tool to detect different failure modes. In addition, performing exponent sensitivity analysis of basic uncertainty variables of the full applicable range of a resistance model and estimating the reliability index using approximated First Order Reliability Method (FORM) on its basis can

provide valuable information for the safety format calibration of the corresponding model.

- On the basis of the investigation of the basic assumptions, simplifications and applicability conditions of the PSFF on material strength variables, it is concluded that the PSFF yields satisfactory reliability levels both for cases subjected to single or multiple failure modes as long as the non-decreasing assumption of the resistance function is valid.

- Adopting conservative FORM sensitivity factors for material strength variables in the PSFF calibration is necessary because they may vary significantly with the change of failure modes. This treatment can be conservative but has the advantage of being simple to use in design practice and being applicable to a wide range of cases.

- The simplification of integrating the safety elements for geometrical and model uncertainties into the partial safety factors for material strengths can underestimate the influence of geometrical and model uncertainties in some cases.

- Good tail approximation is instrumental for the effectiveness of safety formats. Approximating the distribution of resistance variable with a single lognormal distribution based on crude Monte Carlo simulation result risks of losing information about the tail distribution and can potentially lead to unsafe results.

Chapter 3: *Model uncertainties and partial safety factors of strain-based approaches for structural concrete: example of punching shear*

The characteristics of the model uncertainties of the implicit strain-based approaches (composing of multiple sub-models) are investigated. A general theoretical analysis based on the power-multiplicative form approximation of the sub-models shows that the model uncertainty of the global solution can be viewed as a resultant of the model uncertainty of the sub-models. The influence of the sub-models on the uncertainty of global solution depends however on their sensitivity relationship (represented by the exponent sensitivity factors). With this respect, it is shown that the global model uncertainty can be lower than the sub-models' uncertainties, which is a relevant point to be accounted for in the safety format calibration of strain-based approaches.

The theoretical approach is then applied to the strain-based approach of the Critical Shear Crack Theory (CSCT) for punching of reinforced concrete slabs. The resulting major conclusions are:

- Analysis of the model uncertainty data of the sub-models the CSCT punching shear models confirms that they can be approximated by independent lognormal distributions.

- Comparison between the model uncertainty data of the sub-models and the global resistance solutions confirms the theoretically derived relationship based on the exponent analysis.

- By analysing two levels of approximation of the punching shear resistance model (namely LoA II and LoA IV according to *fib* MC 2010), it is shown that the model uncertainty decreases with the increase of the LoA (consistently with the main principles of such approach). Furthermore, the model uncertainty of lower LoAs can be considered as a resultant of the uncertainty of higher LoAs and the additional epistemic model uncertainty introduced in the simplification procedure adopted for the derivation of the lower LoA formulae.

On the basis of model uncertainty analysis result, the suitable safety format for the CSCT punching shear resistance models is discussed. The conclusions are:

- For higher LoAs, an approach based on the application of partial safety factors to the sub-models appears to be more suitable than an approach relying on the application of a single global partial safety factor to the resistance solution, since they can effectively account for the change of model uncertainty associated to the change of the failure mode. Particular attention needs to be paid to the nonlinear relationship between the partial safety factors applied to the sub-models and the resulting design resistance for strain-based approaches.

- If partial safety factors are adopted for the sub-models, the resulting global partial safety factor can vary depending on the material and geometrical parameters as well as on the resulting failure modes. For the investigated case, the global partial safety factor for punching according to the LoA IV varies between 1.48 and 1.00.

- The relationship between the safety factors of the punching shear provisions in the second generation of Eurocode 2 for the design of new structures (Clause 8.4) and the assessment of existing critical ones (Annex I) is established, justifying the safety format adopted for the latter.

Chapter 4: *A consistent safety format and design approach for brittle systems and application to textile reinforced concrete structures*

The suitable safety format and analysis method for Textile Reinforced Concrete (TRC) is investigated accounting for the influence of brittle behaviour on the reliability of such structures. The main conclusions are:

- Structures presenting brittle responses (implying limited or none redistribution capacity of internal forces) can fail for load levels below those considered for design if the calculation of internal forces deviates from the actual response (typically, elastic-uncracked behaviour assumed in the calculation of internal forces). This situation does not occur for a ductile response.

- The analysis of statically indeterminate TRC structures shows that performing a linear elastic calculation of internal forces considering fully cracked stiffness properties for all sections is a suitable manner to estimate the internal forces and response of TRC. This

holds true provided that more than minimum amount of reinforcement are provided in the structure.

- Alternatively, using a nonlinear analysis (considering the development and extent of cracking) is also a suitable manner to estimate the internal forces. It is even more accurate than the previous, but requiring a significant effort for analysis.

- Estimating internal forces on the basis of the uncracked stiffness of the sections (as usually performed for ordinary reinforced concrete) can lead to relatively large deviations on the response and internal forces of a brittle structure as TRC. Such method shall not be used for design unless specific considerations were implemented to cover this increased uncertainty.

- Since for thin members, the variability of the effective depth can be significant compared to the mean value, the geometrical uncertainties can play a major role in calibrating the partial safety factors for designing structures at ultimate limit state. On the basis of reliable internal forces (determined by a linear-elastic fully cracked analysis or a nonlinear analysis), two types of PSFF are calibrated for the flexural resistance of TRC:

  o Consideration of a partial safety factor for the tensile strength of the textile ($\gamma_{tex} = 1.55$) and nominal dimensions. All uncertainties (material, geometrical and model) are lumped into the partial safety factor of the textile.

  o Consideration of a reduced partial safety factor for the tensile strength of the textile ($\gamma_{tex} = 1.25$) and design dimensions (reduction of 6 mm in effective depth). In this case, material and model uncertainties are accounted for in the partial safety factor of the textile while geometrical uncertainties are considered in the design dimensions.

  o In general, the second safety format is preferable, leading to a more uniform level of safety.

5.2   Outlook and future works

Some questions related to the topics studied in this research remain open. In the following, some of these future research lines are outlined:

- The model uncertainty quantification of the NonLinear Finite Element Analysis (NLFEA) approaches still pose many challenges to be dealt with in future works. A major challenge is the scarcity of test data on the global response of structures. Taking the case of the punching shear resistance of slab-column connections as an example, in this work, the model uncertainty quantification is performed based on data from

laboratory tests of isolated slab-column connections. The corresponding investigations on the partial safety format is also performed at the isolated slab-column connection elment level. By contrast, in practice, the majority of the flat slabs are continuous structures with multiple spans supported by several columns and walls, which can have significantly different behaviour from isolated slab-column connection potion due to the influence of Compressive Membrane Action (CMA), the redistribution of internal bending moments that can occur in continuous flat slabs and the non-uniform distribution of shear stress along the control perimeter. Calibrating the partial safety format at the isolated structural potion level is suitable when the verification of the punching shear resistance of a flat slab is performed adopting conservative assumptions regarding the global behaviour (neglecting the beneficial influences of CMA and internal force redistribution) and adopting conservative assumptions for the non-uniform distribution of the shear force along the control perimeter. However, when a more refined analysis of the punching shear resistance is required (e.g. in the assessment of critical existing structures) and the global behaviour of continuous flat slab structure including the beneficial effects of CMA and internal forces redistribution are accounted for by NLFEA, theoretically, the corresponding safety format needs to be re-calibrated with the model uncertainties of the continuous flat slab structures, which can be different from those of isolated specimens. However, due to the complexity of full-scale tests on continuous flat slabs, as well as the resources needed for that purpose, very little test data is available at this scale. The difference between the scale of the available benchmark test data and the scale of the NLFEA model used in the calculation of structural load bearing capacity is a problem that needs to be investigated in future works.

▪ Another important question is related to the categorization of the model uncertainties of the NLFEA approaches. It has been shown in Chapter 3 that the model uncertainty of global resistance solution of strain-based punching shear resistance model tends to be heteroscedastic as a resultant of the different influences of the sub-models for different cases. For the punching shear resistance model, it is applicable to perform the model uncertainty quantification at the sub-model level since it has a relatively simple form with clearly defined and mechanical-based sub-models. However, it can be anticipated that such an approach is not necessarily applicable for more complex NLFEA with multiple calibrated parameters in multiple sub-models. For this type of model, the only feasible approach is to represent the model uncertainty at the global resistance level. It is reasonable to anticipate that the global resistance model uncertainty of such models can also be heteroscedastic due to similar reasons as for the case of the strain-based punching shear resistance model. Researchers have tried to categorize the global uncertainty of the NLFEA by differentiating ductility level [Eng17] or governing failure modes [Cer18]. In this work, it is shown that the exponent sensitivity analysis is an effective tool to identify the influence of different failure modes in the structural resistance model (also in the cases with multiple failure modes coupling). In future

researches, to categorize the model uncertainties of the global resistance solution of NLFEA on the basis of the exponent analysis of the relevant variables can be a promising direction to achieve a better representation of model uncertainties of such models.

- Regarding the treatment of material uncertainties, the influence of their spatial variation and correlation needs to be further investigated in future research. For example, the tension stiffening effect of concrete after cracking can have a significant influence on the punching shear resistance of slab-column connections in continuous slabs. The tension stiffening effect depends on the crack pattern of the structure, which is influenced by the spatial variation of the property of concrete. How to properly account for the influence of this type of effect on the reliability of reinforced concrete structures still needs to be investigated.

Appendix A

Safety format calibration example: the anchorage strength model of shear reinforcement in beams and slabs

This Appendix is a part (Section 6.8 and Appendix D) of the post-print version of the article mentioned below, published in Engineering Structures Journal. The authors of the article are Frédéric Monney, Qianhui Yu (PhD Candidate), Prof. Miguel Fernández Ruiz (thesis co-director) and Prof. Aurelio Muttoni (thesis director). The reference is the following:

Monney F., Yu Q., Fernández Ruiz M., Muttoni A., *Anchorage of shear reinforcement in beams and slabs*, Engineering Structures, Vol.265, 114340, 2022.
(DOI: https://doi.org/10.1016/j.engstruct.2022.114340)

The main contributions of Qianhui Yu to this article and this annex are the following:

- Probabilistic modelling of the basic uncertainties of the anchorage strength model

- Proposition of the reliability analysis and the safety format calibration methodology for the anchorage strength model

- Interpretation, analysis and discussion of the reliability analysis and safety format calibration result.

- Writing of the manuscript of section 6.8 and Appendix D of the article.

Appendix A.1: Safety format calibration for the anchorage strength model

This appendix presents the process of the safety format calibration procedure for the anchorage strength model for shear reinforcement in beams and slabs developed by Monney et al. in [Mon22].

Based on the average behaviour observed in tests, the anchorage strength model is developed and takes the following form (refer to [Mon22] for details of the development of the mechanical model and refer to Notation section for definition of the symbols):

$$\sigma_{sR} = 4 \cdot \frac{l_{tail}}{\varnothing} \min(\tau_b; \tau_{tail,spall})\left(1 + 2 \cdot k_3 \cdot k_4\right) + 4 \cdot \frac{\varnothing_{mand}}{\varnothing} \tau_b \cdot k_4\left(1 + k_3 \cdot \frac{\alpha}{2}\right) +$$

$$4 \cdot f_y \left(k_1\left(2 + \sin\alpha \cdot k_2\right)\left(1 + 2 \cdot k_3 \cdot k_4\right) + 0.0168 \cdot k_2\right)$$

where

$$\tau_b = \eta_{cp} \frac{0.6 \cdot f_c^{2/3}}{1 + \dfrac{0.75 \cdot \eta_l}{f_R} \dfrac{w}{\varnothing}}$$

$$\tau_{tail,spall} \approx \left(\eta_{is} \cdot \eta_{ct} \cdot 0.3 \cdot f_c^{2/3} \cdot \left(\frac{c}{\varnothing} + \frac{1}{2}\right) - \frac{f_y}{50} \frac{\varnothing}{l_{tail}}\right)\left(\frac{d_{dg}}{1.6\varnothing}\right)^{1/3} + \eta_{is} \cdot 2.4 \text{ MPa}$$

$$(1)$$

$$k_1 = 0.00672$$

$$k_2 = \frac{6}{\left(1 - \cos\alpha\right) \cdot \left(\dfrac{\varnothing_{mand}}{\varnothing} + 1\right)}$$

$$k_3 = \frac{1}{2.5 - \dfrac{\alpha}{2}}$$

$$k_4 = \sin\alpha - \frac{\alpha}{2}\cos\alpha$$

To use this model in codified design practice, the unavoidable uncertainties involved in design need to be accounted for and the design equation (including partial factors) for the developed model needs to be calibrated to fulfil the corresponding reliability requirements.

The target reliability requirement of Eurocode for the ultimate limit state design for structures with medium consequence class and a reference period of 50 years (with a target reliability index of $\beta_{tgt} = 3.8$) is considered and the design equation for the proposed anchorage strength model (Eq.(1)) is calibrated accordingly. The material, geometrical and model uncertainties involved in the model need to be accounted for in the safety format calibration. The probabilistic modelling of the uncertainties involved in the independent input variables of the model are shown in Table A.1. The distribution of the model uncertainty (considered as an independent random variable multiplied to the model) is also provided in Table A.1. It should be noted that

the distribution parameters for the concrete cover c are derived based on its allowance value for deviation according to Eurocode 2 [CEN04, ISO13]. In Eurocode 2 (Clause 4.4.1.1 and 4.4.1.3), the acceptable deviation for concrete cover for buildings is recommended as 10 mm. Taking this into account, the minimum allowed concrete cover c_{min} ($c_{min} = c_{nom} - 10$ [mm]) is assumed to be the 5 % fractile of its distribution. It should also be noted that the bar diameter $\emptyset$ is not considered as an independent random variable because the uncertainty in the area of cross section of the bar is already included in f_y and f_R. Also, the crack width w is not accounted as an independent random variable because it is a derived variable based on the independent input variable.

Table A.1:   Distribution parameters of the basic uncertainties of the achorage strength model

Basic variable f_i	Distribution type	Coefficient of Variation V_i	Bias factor μ_i [1]	Reference
Model uncertainty	lognormal	0.129	1.05	[Mon22]
$f_{c,ais}$ [2]	lognormal	0.156	$e^{1.645 \cdot V}$	[Mut23]
f_y	lognormal	0.045	$e^{1.645 \cdot V}$	[Mut23]
α	lognormal	0.05	1	assumed
$\emptyset_{mand}$	lognormal	$(0.2 \cdot \emptyset/1.645)/\emptyset_{mand}$	1	assumed
l_{tail}	lognormal	$(\emptyset/1.645)/l_{tail}$	1	assumed
c	lognormal	$\ln(c_{nom}/(c_{nom}-10))/1.645$	1	[CEN04]
d_g	lognormal	0.1	1	[Mut23]
f_R	lognormal	0.005	1	[Dar98]

[1] The value in this columns refer to the ratio between the mean value and the value used in the design formulae (characteristic for material strength variables and nominal for other variables) [Mut23]

[2] $f_{c,ais}$ actual in-situ compressive concrete strength

The semi-probabilistic approach and the simplification of using standardised FORM (First Order Reliability Method) sensitivity factors [CEN02] for the resistance ($\alpha_R = 0.8$) is adopted in the following safety format calibration procedure. Accounting for the standardized FORM sensitivity factor, the reliability requirement for design equation of the anchorage strength can be expressed as:

$$P\left(\sigma_{sR} - \sigma_{sRd} < 0\right) = \Phi\left(-\alpha_R \cdot \beta_{tgt}\right) \tag{2}$$

Where P() is the probabilistic function, σ_{sR} is the anchorage strength variable, σ_{sRd} is the design anchorage strength (calculated with partial safety factors) and Φ is the cumulative probability function of the standardised normal distribution.

To facilitate the partial factor calibration, the CoV of the anchorage strength model (V_R) is first estimated approximately based on exponent sensitivity analysis [Yu20] of the basic input variables:

$$V_R = \sqrt{\sum n_i^2 \cdot V_i^2} \qquad (3)$$

Where n_i are the exponent sensitivity factor for basic variable f_i (defined as the partial derivative of the logarithm of the anchorage strength σ_{sR} to the logarithm of the variable f_i at the mean value point of the basic variables). Details of the assumptions and approximations in the exponent sensitivity analysis and the estimation of V_R can found in references [Yu20, Yu21].

The resulting CoVs for cases with different combinations of design parameters are plotted in Figure A.1 From the CoV plots, it can be observed that as a result of the two different failure modes (spalling failure and pull-out failure) involved in the anchorage strength model, the V_R plots show two regimes and the dominating variable for the variability of the model change with the dominating failure mode. When the concrete cover value is relatively low, the spalling failure mode is dominating and the variability of concrete cover variable is dominating. On the other hand, with relatively high concrete cover value, the pull-out failure mode is dominating and the model uncertainty becomes dominant.
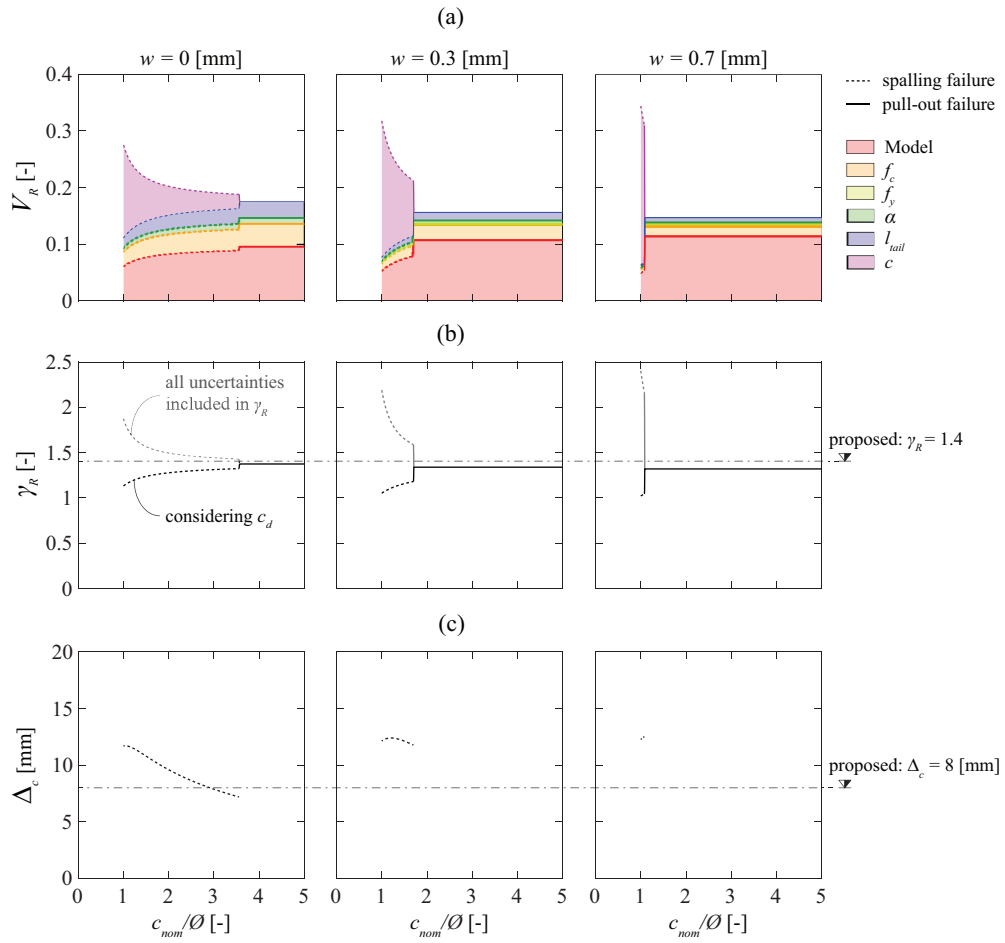
Figure A.1:   (a) CoV of the resistance variable; (b) partial safety factor; and (c) design
value of the concrete cover. (Parameters used: poor bond conditions; $\varnothing 14$;
$d_g = 16$ [mm]; $\eta_l = 4$; $l_{tail} = 5\varnothing$; $\varnothing_{mand} = 4\varnothing$; $\alpha = 90$ [°]; $f_c = 38$ [MPa];
$f_y = 500$ [MPa]; $f_R = 0.056$).

Based on the previous observations, the following format of the design equation for the
anchorage strength model is proposed:

$$\sigma_{sRd} = \sigma_{sR}\left\{ f_{ck}, f_{yk}, ..., c_d \right\} \frac{1}{\gamma_R} = \sigma_{sR}\left\{ f_{ck}, f_{yk}, ..., c_{nom} - \Delta_c \right\} \frac{1}{\gamma_R}$$

$$= \frac{1}{\gamma_R}\left[\begin{array}{c} 4 \cdot \dfrac{l_{tail}}{\O} \min(\tau_b; \tau_{tail,spall})\left(1 + 2 \cdot k_3 \cdot k_4\right) + 4 \cdot \dfrac{\O_{mand}}{\O} \tau_b \cdot k_4 \left(1 + k_3 \cdot \dfrac{\alpha}{2}\right) + \\[2mm] 4 \cdot f_{yk}\left(0.00672 \cdot \left(2 + \sin\alpha \cdot k_2\right)\left(1 + 2 \cdot k_3 \cdot k_4\right) + 0.0168 \cdot k_2\right) \end{array} \right]$$

where   (4)

$$\tau_b = \eta_{cp} \frac{0.6 \cdot f_{ck}^{2/3}}{1 + \dfrac{0.75 \cdot \eta_l}{f_R} \dfrac{w}{\O}}$$

$$\tau_{tail,spall} \approx \left(\eta_{is} \cdot \eta_{ct} \cdot 0.3 \cdot f_{ck}^{2/3} \cdot \left(\frac{c_d}{\O} + \frac{1}{2}\right) - \frac{f_{yk}}{50} \frac{\O}{l_{tail}} \right)\left(\frac{d_{dg}}{1.6\O}\right)^{1/3} + \eta_{is} \cdot 2.4 \text{ MPa}$$

In the proposed format in Eq. (4) (which is based on Eq.(1) incorporating the partial safety factors), the design values are obtained with the partial safety factor γ_R and with a reduction Δ_c of the concrete cover ($c_d = c_{nom} - \Delta_c$, where c_{nom} is the nominal concrete cover). The motivation of using a design value of the concrete cover c_d is to achieve a uniform reliability level for cases dominated by different failure modes. It should be noted that the approach of applying design value of dominating geometrical variables in the design equation is also adopted in Eurocode [CEN23, CEN02].

The required values for the partial safety factor γ_R and Δ_c to achieve the target reliability level ($\alpha_R \cdot \beta_{tgt}$) are estimated based on FORM theory considering that concrete cover is an independent variable and that the rest of the uncertainties are lumped into another independent random variable (in a similar approach as the one presented in [Yu21] but considering a lognormal distribution for the concrete cover). The resulting equations are given below, with representative cases plotted in Figure A.2.

$$\gamma_R = \frac{\exp\left(\sqrt{1 - \alpha_{FORM,c}^2} \cdot \alpha_R \cdot \beta_{tgt} \cdot \sqrt{V_R^2 - \alpha_{FORM,c}^2 V_R^2}\right)}{\prod (\mu_i)^{n_i}}$$

$$\Delta_c = c_{nom} - \frac{c_{nom}}{\exp\left(\alpha_{FORM,c} \cdot \alpha_R \cdot \beta_{tgt} \cdot V_c\right)}$$

(5)

Where $\alpha_{FORM,c}$ are the approximated FORM sensitivity factor for variable c (estimated as $\alpha_{FORM,c} = n_c \cdot V_c/V_R$). The following values for the two safety factors are proposed based on the analysis results:

$$\gamma_R \approx 1.4$$
$$\Delta_c \approx 8 \text{ [mm]}$$

(6)

To verify the effectiveness of the selected combination of safety factors, reliability analysis of representative cases is performed with Monte Carlo simulation method. Accounting for the probabilistic models of the basic variables, the achieved reliability for the design strength is calculated with the following equation:

$$\gamma_R = \frac{\exp\left(\sqrt{1 - \alpha_{FORM,c}^2} \cdot \alpha_R \cdot \beta_{tgt} \cdot \sqrt{V_R^2 - \alpha_{FORM,c}^2 V_R^2}\right)}{\prod (\mu_i)^{n_i}}$$

$$\Delta_c = c_{nom} - \frac{c_{nom}}{\exp\left(\alpha_{FORM,c} \cdot \alpha_R \cdot \beta_{tgt} \cdot V_c\right)}$$

(7)

For each case, one million sample points are used in the Monte Carlo simulation to ensure proper tail approximation of the anchorage strength variable (refer to [Yu20] for details about the necessity of tail approximation in the cases of multiple failure modes). The achieved reliability indexes of the investigated cases are plotted in Figure A.2. The result shows that with the proposed combination of safety factors, a satisfactory range of the achieved reliability level (ranging between 2.5 and 3.5) is achieved, which confirms the applicability of the proposed safety format.

It should also be noted that the value Δ_c for calculating the design value c_d can potentially be reduced when the concrete cover is updated on the basis of measurements (e.g. in the assessment of existing structures). Under this circumstance, the value of Δ_c can be calculated based upon updated information about the probabilistic model of the concrete cover with the procedure outlined in this section.
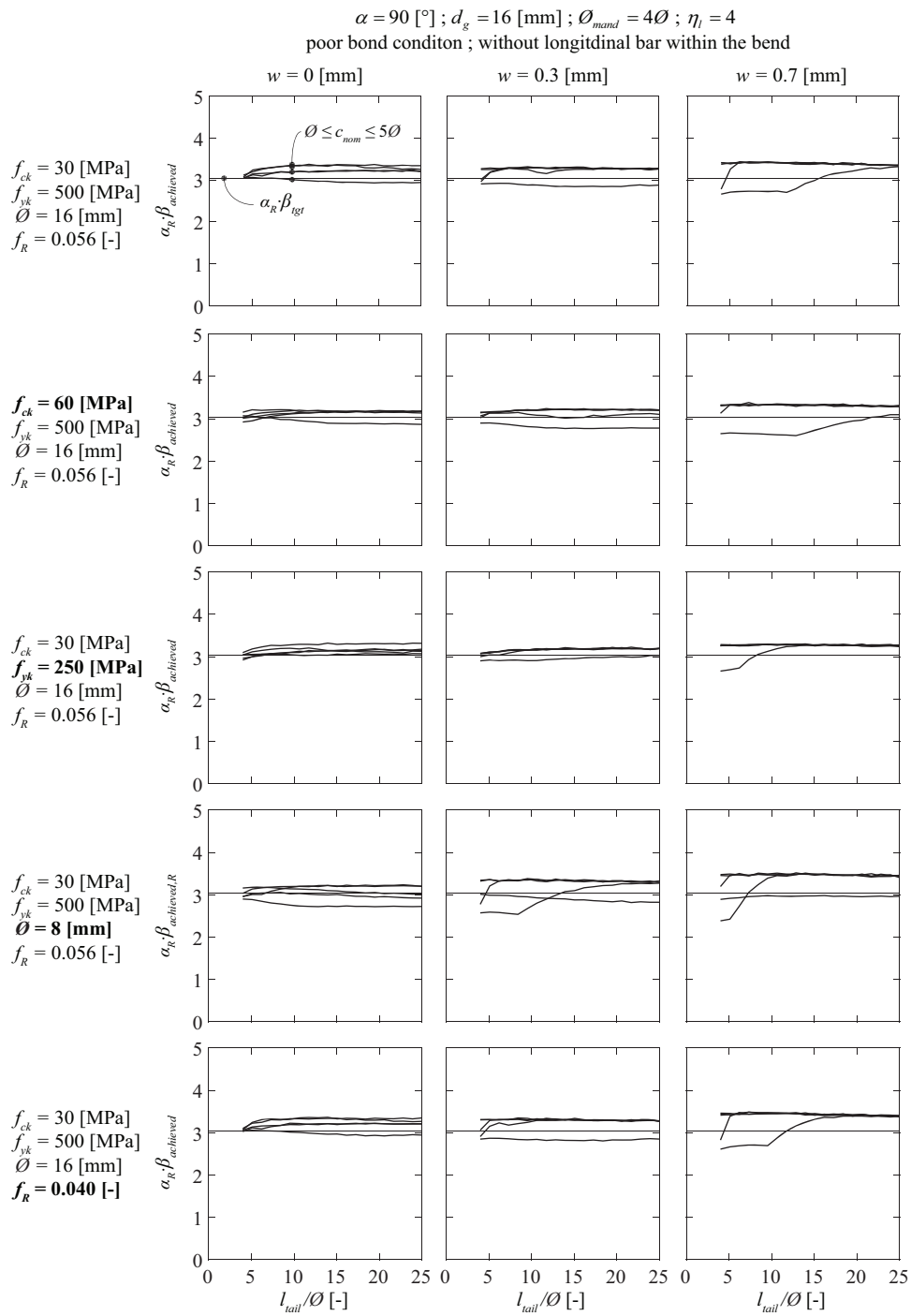
Figure A.2:   Achieved reliability index for different cases.

Notation

Latin lower case letters

c	concrete cover
c_{min}	minimum value of concrete cover
c_{nom}	nominal value of concrete cover
c_d	design value of the concrete cover
d_{dg}	maximum aggregate size parameter
d_g	maximum aggregate size
f_c	concrete cylinder compressive strength
$f_{c,ais}$	actual in-situ concrete compressive strength
f_{ck}	characteristic value of the concrete compressive strength
f_i	basic variable
f_R	bond index
f_y	yield strength of reinforcement
f_{yk}	characteristic value of the yield strength of the reinforcement
k_1 to k_4	factors of the model
l_{tail}	tail length
n_i	exponent sensitivity factor of basic variable f_i
w	in-plane crack opening

Latin upper case letters

V_i	Coefficient of Variation of basic variable f_i
V_R	Coefficient of Variation of the resistance function

Greek lower case letters

α	bending angle
$\alpha_{FORM,c}$	approximated FORM sensitivity factor for concrete cover
α_R	First Order Reliability Method sensitivity factor for resistance
$\beta_{achieved}$	achieved reliability index
β_{tgt}	target reliability index
γ_R	partial safety factor for the anchorage strength model
η_{cp}	coefficient accounting for casting effects on bond conditions
η_{ct}	brittleness factor of concrete in tension
η_{is}	strength reduction factor to account for casting position effect
η_l	number of lugs per rib
σ_{sR}	anchorage strength calculated with the model
σ_{sRd}	design anchorage strength
τ_b	bond stress

| $\tau_{tail,spall}$ | average bond stress for failures induced by spalling in the tail region |

Greek upper case letters

| Δ_c | reduction of concrete cover for design |

Others

$\O$	bar diameter
$\O_l$	longitudinal bar diameter within the bend
$\O_{mand}$	mandrel diameter (= inner diameter after bending of the bar)
Φ	cumulative probability function of the standardised normal distribution
P()	probabilistic function

Bibliography

[AAS20]   **AASHTO**, *AASHTO LRFD Bridge Design Specifications, 9th Edition*, Washington D.C., USA, 2020.

[ACI19]   **ACI Committee 318**, *Building Code Requirements for Structural Concrete (ACI 318-19) and Commentary*, American Concrete Institute, 624 p., Farmington Hills, USA, 2019.

[All13]   **Allaix Diego L., Carbone V. I., Mancini G.**, *Global safety format for non-linear analysis of reinforced concrete structures*, Structural Concrete, 14, 29-42, 2013.

[Bel15]   **Belletti B., Pimentel M., Scolari M., Walraven J. C.**, *Safety assessment of punching shear failure according to the level of approximation approach*, Structural concrete, 16, 366-380, Berlin, 2015.

[Ben12]   **Ben Ftima M., Massicotte B.**, *Development of a Reliability Framework for the Use of Advanced Nonlinear Finite Elements in the Design of Concrete Structures*, Journal of structural engineering, American Society of Civil Engineers, 138, 1054-1064, New York, N.Y., 2012.

[Ben06]   **Bentz E. C., Vecchio F. J., Collins M. P.**, *Simplified Modified Compression Field Theory for Calculating Shear Strength of Reinforced Concrete Elements*, ACI Structural Journal, Vol.103, No 4, pp. 614-624, 2006.

[Box92]   **Box G. E. P.**, *Bayesian inference in statistical analysis 1st ed.*, J. Wiley, New York, 1992.

[Bra06]   **Brameshuber W.**, *Textile reinforced concrete-state-of-the-art report of RILEM TC 201-TRC*, Reunion Internationale des Laboratoires et Experts des Materiaux, Systemes de Construction et Ouvrages (RILEM), 2006.

[Cas18]   **Castaldo Paolo, Gino Diego, Bertagnoli G., Mancini G.**, *Partial safety factor for resistance model uncertainties in 2D non-linear finite element analysis of reinforced concrete structures*, Engineering structures, 176, 746-762, OXFORD, 2018.

[Cas19]   **Castaldo Paolo, Gino Diego, Mancini G.**, *Safety formats for non-linear finite element analysis of reinforced concrete structures: discussion, comparison and proposals*, Engineering Structures, 193, 136-153, 2019.

[CEB59]   **CEB**, *Bulletin 19: Technical conclusions of the 5th CEB meeting in Vienna*, Comité Européen du Béton Bulletin: Section on Structural Safety, 94, Paris, France, 1959.

[CEB64]   **CEB**, *Practical unified recommendations for the design and execution of structures in reinforced concrete (in French: Recomemndations pratiques unifiées pour le calcul et l'éxécution des ouvrages en béton armé*, 257, Paris, 1964.

[CEB74]   **CEB**, *Manuel de calcul "flambement - instabilité"*, Paris, 1974.

[CEB74a]   **CEB**, *Manuel "sécurite des structures" concepts généraux, charges et actions*, Paris, 1974.

[CEB80]   **CEB**, *Manuel "sécurité des structures" : concepts généraux, actions, combinaisons et sollicitations agissantes résistances et sollicitations résistantes, états-limites divers et situations diverses, règles générales d'application 2 ème éd.*, Paris, 1980.

[CEB80a]   **CEB**, *Bulletin 127: Manuel sécurité des structures : 1ère partie*, 1-316, Paris, 1980.

[CEB80b]   **CEB**, *Bulletin 128: Manuel sécurité des structures : 2ème partie*, 317-658, Paris, 1980.

[CEB88]   **CEB**, *Bulletin 191: General principles on reliability for structures : a commentary on ISO 2394*, 51, Lausanne, 1988.

[CEB93]   **CEB**, *CEB-FIP Model Code 1990*, Comité Euro-International du Béton (CEB), 460 p., London, UK, 1993.

[CEN02]   **CEN**, *EN 1990:2002: Eurocode: Basis of Structural Design*, European Committee for Standardization (CEN), Brussels, Anglais, 2002.

[CEN04]   **CEN**, *EN 1992-1-1:2004: Eurocode 2: Design of concrete structures – Part 1-1: General rules and rules for buildings*, European Committee for Standardization (CEN), Brussels, 2004.

[CEN20]   **CEN**, *prEN 1990:2020: Eurocode: Basis of structural and geotechnical design*, 2020.

[CEN23]   **CEN**, *Final draft FprEN 1992-1-1: Design of concrete structures - Part 1-1: General rules and rules for buildings, bridges and civil engineering structures*, European Committee for Standardization (CEN), 405, Brussels, Belgium, 2023.

[Cer08]   **Cervenka V.**, *Global Safety Format for Nonlinear Calculation of Reinforced Concrete*, Beton- und Stahlbetonbau, 103, 37-42, 2008.

[Cer18]   **Cervenka V., Cervenka J., Kadlec L.**, *Model uncertainties in numerical simulations of reinforced concrete structures*, Structural concrete, 6, 19, 2004-2016, 2018.

[Chu06]   **Chudoba R., Vorechovsky M.**, *Stochastic modeling of multi-filament yarns. I. Random properties within the cross-section and size effect*, International journal of solids and structures, 3, 43, 413-434, OXFORD, 2006.

[Clé12]   **Clément T.**, *Influence de la précontrainte sur la résistance au poinçonnement des dalles en béton armé*, Thèse EPFL, n°5516, 224 p., Lausanne, Switzerland, 2012.

[Col11]   **Colombo I. , Colombo M., Magri A., Zani G., di Prisco M.**, *Textile Reinforced Mortar at High Temperatures*, Applied Mechanics and Materials, 82, 202-207, 2011.

[Cor69]   **Cornell C. A.**, *A Probability-Based Structural Code*, ACI Journal, 12, 66, 974-985, 1969.

[CSA14]   **CSA** , *CSA Standard A23.3-14: Design of concrete structures*, Canadian Standard Association, Ottawa, Canada, 2014.

[Dar98]   **Darwin D., Idun E. K., Zuo J., Tholen M. L.**, *Reliability-Based Strength Reduction Factor for Bond*, Structural Journal, Vol. 95, No. 4, pp. 434-443, 1998

[Der09]   **Der Kiureghian Armen, Ditlevsen O.**, *Aleatory or epistemic? Does it matter?*, Structural Safety, 31, 105-112, 2009.

[Dit94]   **Ditlevsen O.**, *Distribution arbitrariness in structural reliability*, Structural Safety and Reliability, Schuëller, Shinozuka and Yao (eds), 1241-1247, Rotterdam, 1994.

[Dit96]   **Ditlevsen O., Madsen H. O.**, *Structural reliability methods*, Chichester, 1996.

[Dra16]   **Drakatos I.-S., Muttoni A., Beyer K.**, *Internal slab-column connections under monotonic and cyclic imposed rotations*, Engineering Structures, 123, pp. 501-516, 2016.

[Ech11]   **Echard B., Gayton N., Lemaire M.**, *AK-MCS: An active learning reliability method combining Kriging and Monte Carlo Simulation*, Structural safety, 33, 145-154, Amsterdam, 2011.

[Ehl10]   **Ehlig D., Jesse F., Curbach M.**, *High temperature tests on textile reinforced concrete (TRC) strain specimens*, 2nd ICTRC. Textile Reinforced Concrete. Proceedings of the International RILEM Conference on Material Science (MatSci), 1, 141-151, 2010.

[Ein16]   **Einpaul J.**, *Punching Strength of Continuous Flat Slabs*, EPFL PhD Thesis, n°6928, 209 p., Lausanne, Switzerland, 2016.

[Ein16]   **Einpaul J., Bujnak J., Fernández Ruiz M., Muttoni A.**, *Study on Influence of Column Size and Slab Slenderness on Punching Strength*, ACI Structural Journal, V. 113, pp. 135-145, Farmington Hills, USA, 2016.

[Ell78]   **Ellingwood B.**, *Reliability basis of load and resistance factors for reinforced concrete design*, NATIONAL BUREAU OF STANDARDS, 110, 95, Washington, 1978.

[Ell94]   **Ellingwood B.**, *Probability-based codified design: past accomplishments and future challenges*, Structural Safety, 3, 13, 159-176, 1994.

[Ell80]   **Ellingwood B.**, *Development of a probability based load criterion for American national standard A58 : building code requirements for minimum design loads in buildings and other structures*, NBS SPECIAL PUBLICATION 577, 222, Washington, 1980.

[EN105]   **EN10080:2005**, *Steel for the reinforcement of concrete. Weldable reinforcing steel - General*, European Committee for Standardization (CEN), Brussels, Belgium, 2005.

[Eng93]   **Engelund S., Rackwitz R.**, *A benchmark study on importance sampling techniques in structural reliability*, Structural safety, 12, 255-276, Oxford, 1993.

[Eng17]   **Engen M., Hendriks M.A.N., Köhler J., Øverli J. A., Åldstedt E.**, *A quantification of the modelling uncertainty of non-linear finite element analyses of large concrete structures*, Structural safety, 64, 1-8, 2017.

[Eur08]   **European Concrete Platform**, *Eurocode 2 Commentary*, European Committee for Standardization (CEN)), Brussels, 2008.

[Fah21]   **Fahrni R., De Sanctis G., Frangi T.**, *Comparison of reliability- and design-based code calibrations*, Structural Safety, 88, 102005, 2021.

[Fer08] **Fernández Ruiz M., Fürst A., Guandalini S., Hunkeler F., Moser K., Muttoni A., Seiler H.**, *Sécurité structurale des parkings couverts*, Société Suisse des Ingénieurs et des Architectes, 106 p., Zürich, Switzerland, 2008.

[Fer07] **Fernández Ruiz M., Muttoni A.**, *On Development of Suitable Stress Fields for Structural Concrete*, ACI Structural Journal, Vol. 104, No 4, pp. 495-502, Farmington Hills, USA, 2007.

[Fer10] **Fernández Ruiz M., Muttoni A., Kunz J.**, *Strengthening of flat slabs against punching shear using post-installed shear reinforcement*, ACI Structural Journal, V. 107 N° 4, pp. 434-442, USA, 2010.

[FIB07] **FIB**, *FRP reinforcement in RC structures*, Fédération Internationale du Béton (FIB), 160, 2007.

[FIB13] **FIB**, *fib Model Code for Concrete Structures 2010*, fib, First Edition, UK, 2013.

[Fos15] **Foster S. J., Stewart M. G., Sirivivatnonon V., Loo K. Y., Ahammed M. , Ng T. S., Valipour H.**, *A Re-evaluation of the Safety and Reliability Indices for Reinforced Concrete Structures Designed to AS3600, UNICIV Report R-464*, School of Civil and Environmental Engineering, UNSW, 201, 2015.

[Fos16] **Foster S. J., Stewart M. G., Loo M. , Ahammed M. , Sirivivatnonon V.**, *Calibration of Australian Standard AS3600 Concrete Structures: part I statistical analysis of material properties and model error*, Australian journal of structural engineering, Taylor & Francis, 17, 242-253, 2016.

[Fre56] **Freudenthal A. M.**, *Safety and the Probability of Structural Failure*, Transactions of the American Society of Civil Engineers, American Society of Civil Engineers, 121, 1337-1375, 1956.

[Gar15] **Garcia-Lodeiro I., Fernández-Jimenez A., Palomo A.**, *Cements with a low clinker content: versatile use of raw materials*, Journal of Sustainable Cement-Based Materials, 4, 140-151, 2015.

[Gar02] **Gardoni P., Der Kiureghian Armen, Mosalam K. M.**, *Probabilistic Capacity Models and Fragility Estimates for Reinforced Concrete Columns based on Experimental Observations*, Journal of engineering mechanics, American Society of Civil Engineers, 10, 128, 1024-1038, 2002.

[Gay04] **Gayton N., Mohamed A., Sorensen J. D., Pendola M., Lemaire M.**, *Calibration methods for reliability-based design codes*, Structural Safety, 1, 26, 91-121, 2004.

[GB10]   **GB 50010-2010**, *GB 50010-2010: Code for Design of Concrete Structures*, Ministry of Housing and Urban-Rural Development of the People's Republic of China, 427, Beijing, Chinese, 2010.

[Gua09]   **Guandalini S., Burdet O., Muttoni A.**, *Punching tests of slabs with low reinforcement ratios*, ACI Structural Journal, V. 106, N°1, pp. 87-95, USA, 2009.

[Gui10]   **Guidotti R.**, *Poinçonnement des planchers-dalles avec colonnes superposées fortement sollicitées*, Thèse EPFL, n°4812, 230 p., Lausanne, Switzerland, 2010.

[Hal96]   **Hallgren M.**, *Punching Shear Capacity of Reinforced High Strength Concrete Slabs*, Doctoral thesis KTH Stockholm, Stockholm, Sweden, 1996.

[Hal19]   **Halvoník J., Kalická J., Majtánová L., Minárová M.**, *Reliability of models aimed at evaluating the punching resistance of flat slabs without transverse reinforcement*, Engineering Structures, 188, 627-636, 2019.

[Has74]   **Hasofer A. M., Lind N. C.**, *Exact and invariant second-moment code format*, Journal of the Engineering Mechanics Division, 111-121, 1974.

[Hau11]   **Haukaas T., Gardoni P.**, *Model Uncertainty in Finite-Element Analysis: Bayesian Finite Elements*, Journal of engineering mechanics, American Society of Civil Engineers, 137, 519-526, 2011.

[Häu19]   **Häussler-Combe U., Weselek J., Jesse F.**, *A Safety Concept for Non-Metallic Reinforcement for Concrete under Bending*, ACI structural journal, 116, 2019.

[Haw18]   **Hawkins W., Orr J., Ibell T., Shepherd P.**, *An Analytical Failure Envelope for the Design of Textile Reinforced Concrete Shells*, Structures, 15, 56-65, 2018.

[He02]   **He Z., Liang W. Q., Li B. X., Li X. G.**, *Preparation of super composite cement with a lower clinker content and a larger amount of industrial wastes*, Journal Wuhan University of Technology, Materials Science Edition, Wuhan University of Technology, 17, 78-81, 2002.

[Heg16]   **Hegger J., Will N.** , *Textile-reinforced concrete: Design models*, Textile Fibre Composites in Civil Engineering, Woodhead Publishing, 8, 189-207, 2016.

[Hol16]   **Holický M., Retief J. V., Sýkora M.**, *Assessment of model uncertainties for structural resistance*, Probabilistic engineering mechanics, 45, 188-197, 2016.

[Ioo15]   **Iooss B., Lemaître P.**, *A review on global sensitivity analysis methods*, Operations Research/ Computer Science Interfaces Series, 59, 101-122, 2015.

[ISO86]   **ISO**, *ISO 2394:1986 General principles on reliability for structures*, ISO/TC 98/SC 2 Reliability of structures, 1986.

[ISO13]   **ISO**, *EN 13670 Execution of concrete structures*, International Organization for Standardization, 72 p., 2013.

[JCS01]   **JCSS**, *Probalistic Model Code*, Part III, 2001.

[Jus15]   **Just M.**, *Sicherheitskonzept für Textilbeton*, Beton- und Stahlbetonbau, S1, 110, 42-46, Berlin, German, 2015.

[Kad15]   **Kadlec L., Cervenka V.**, *Uncertainty of numerical models for punching resistance of RC slabs*, FIB Symposium , Copenhagen, Denmark, 2015.

[Kin60]   **Kinnunen S., Nylander H.**, *Punching of Concrete Slabs Without Shear Reinforcement*, Transactions of the Royal Institute of Technology, N° 158, 112 p., Stockholm, Sweden, 1960.

[Kön81]   **König G., Hosser D.**, *The simplified level II method and its application on the derivation of safety elements for level I*, Comité Euro-International du Béton (CEB), Bulletin No. 147, pp. 147-224, Lausanne, Switzerland, 1981.

[Kro19]   **Kromoser B., Preinstorfer P., Kollegger J.**, *Building lightweight structures with carbon-fiber-reinforced polymer-reinforced ultra-high-performance concrete: Research approach, construction materials, and conceptual design of three building components*, Structural concrete, 20, 730-744, 2019.

[Lip12]   **Lips S., Fernández Ruiz M., Muttoni A.**, *Experimental Investigation on Punching Strength and Deformation Capacity of Shear-Reinforced Slabs*, ACI Structural Journal, Vol. 109, pp. 889-900, USA, 2012.

[Liu91]   **Liu P. L., Der Kiureghian Armen**, *Optimization algorithms for structural reliability*, Structural safety, 9, 161-177, 1991.

[Mad86]   **Madsen H. O., Krenk S., Lind N. C.**, *Methods of structural safety*, Englewood Cliffs, 1986.

[Mar21]   **Marelli S., Lamas C. , Konakli K. , Mylonas C. , Wiederkehr P., Sudret B.**, *UQLab user manual -- Sensitivity analysis UQLab-V1.4*, Chair of Risk, Safety and Uncertainty Quantification, ETH Zurich, Zürich, Switzerland, 2021.

[May26]   **Mayer M.**, *Die Sicherheit der Bauwerke und ihre Berechnung nach Grenzkräften anstatt nach zulässigen Spannungen*, Julius Springer, Berlin, German, 1926.

[Mck00]   **Mckay M. D., Beckman R. J., Conover W. J.**, *A Comparison of Three Methods for Selecting Values of Input Variables in the Analysis of Output From a Computer Code*, Technometrics, 42, 55-61, 2000.

[Mel18]   **Melchers R. E.**, *Structural reliability analysis and prediction 3rd ed.*, Wiley, Hoboken, N.J, 2018.

[Moc20]   **Moccia F., Yu Q., Fernández Ruiz M., Muttoni A.**, *Concrete compressive strength: From material characterization to a structural value*, Structural Concrete, 21 p., 2020.

[Mon17]   **Montgomery D. C.**, *Design and analysis of experiments 9ed.*, Wiley, Hoboken, NJ, 2017.

[Mut90]   **Muttoni A.**, *Die Anwendbarkeit der Plastizitätstheorie in der Bemessung von Stahlbeton*, Birkhäuser Verlag, Institut für Baustatik und Konstruktion ETH Zürich, No 176, 164 p., Basel, Switzerland, German, 1990.

[Mut91]   **Muttoni A., Schwartz J.**, *Behavior of Beams and Punching in Slabs without Shear Reinforcement*, IABSE Colloquium, Vol. 62, pp. 703-708, Stuttgart, Germany, 1991.

[Mut03]   **Muttoni A.**, *Introduction à la norme SIA 262*, Documentation SIA, D 0182 Introduction à la norme SIA 262, pp. 5-9, Zürich, Switzerland, 2003.

[Mut08]   **Muttoni A.**, *Punching shear strength of reinforced concrete slabs without transverse reinforcement*, ACI Structural Journal, pp. 440-450, USA, 2008.

[Mut10]   **Muttoni A., Fernández Ruiz M.**, *Design through an incremental approach: the Swiss experience*, Joint IABSE-fib Conference, 8 p., Dubrovnik, Croatia, 2010.

[Mut12]   **Muttoni A., Fernández Ruiz M.**, *The levels-of-approximation approach in MC 2010: application to punching shear provisions*, Structural Concrete, Vol. 13, No 1, pp. 32-41, 2012.

[Mut12a]   **Muttoni A., Fernández Ruiz M.**, *Levels-of-approximation approach in codes of practice*, Structural Engineering International: Journal of the International Association for Bridge and Structural Engineering (IABSE), 2, 22, 190-194, 2012.

[Mut13]   **Muttoni A., Fernández Ruiz M., Bentz E. C., Foster S. J., Sigrist V.**, *Background to the Model Code 2010 Shear Provisions - Part II Punching Shear*, Structural Concrete, Ernst & Sohn, Vol.14, No. 3, pp. 195-203, Berlin, Germany, 2013.

[Mut15]   **Muttoni A., Fernández Ruiz M., Niketic F.**, *Design versus Assessment of Concrete Structures Using Stress Fields and Strut-and-Tie Models*, ACI Structural Journal, Vol.112, No 5, pp. 605-616, Farmington Hills, USA, 2015.

[Mut17]   **Muttoni A., Fernández Ruiz M., Simões J. T.**, *The theoretical principles of the critical shear crack theory for punching shear failures and derivation of consistent closed-form design expressions*, Structural concrete, pp. 1-17, 2017.

[Mut19]   **Muttoni A., Fernández Ruiz M.**, *From experimental evidence to mechanical modeling and design expressions: The Critical Shear Crack Theory for shear design* , Structural Concrete, Vol. 20, Issue 4, pp. 1464-1480, 2019.

[Mut23]   **Muttoni A.**, *Background document to 4.3.3 and Annex A in FprEN 1992-1-1:2023: Partial safety factors for materials*, Report EPFL-IBETON 16-06-R11, 21, 2023.

[Mut23a]   **Muttoni A., Fernández Ruiz M., Simões J. T., Hernández Fraile D., Hegger J., Siburg C., Kueres D.**, *Background document to section 8.4 – Punching (FprEN 1992-1- 1:2023) Report EPFL 17-01-R5*, 2023.

[Mut23b]   **Muttoni A., Simões J. T., Faria D. M. V., Fernández Ruiz M.**, *A mechanical approach for the punching shear provisions in the second generation of Eurocode 2*, Hormigón y acero, Spanish, 2023.

[Nea11]   **Neal R. M.**, *MCMC using Hamiltonian dynamics*, Handbook of markov chain monte carlo, Chapman and Hall/CRC, 113-160, New York, 2011.

[Nea96]   **Neal R. M.**, *Bayesian Learning for Neural Networks 1st ed.*, Springer New York, New York, NY, 1996.

[Nie11]   **Nielsen M. P., Hoang L. C.**, *Limit Analysis and Concrete Plasticity*, CRC Press, 3rd edition, 788 p., Boca Raton, USA, 2011.

[Now03]   **Nowak A. S., Szerszen M. M.**, *Calibration of design code for buildings (ACI 318): Part 1 - Statistical models for resistance*, ACI structural journal, 3, 100, 377-382, 2003.

[Ola20]   **Olalusi O. B., Spyridis P.**, *Uncertainty modelling and analysis of the concrete edge breakout resistance of single anchors in shear*, Engineering structures, 22, 111112, 2020.

[Ols03]   **Olsson A., Sandberg G., Dahlblom O.**, *On Latin hypercube sampling for structural reliability analysis*, Structural Safety, 25, 47-68, 2003.

[Pac21]   **Pacheco J., Sá M. F., Correia J. R., Silvestre N., Sorensen J. D.**, *Structural safety of pultruded FRP profiles for global buckling. Part 2: Reliability-based*

evaluation of safety formats and partial factor calibration, Composite structures, 257, 113147, 2021.

[Pel17]   **Peled A.**, *Textile reinforced concrete*, CRC Press, Boca Raton, Florida, 2017.

[Pho73]   **Phoenix S. L., Taylor H. M.**, *The asymptotic strength distribution of a general fiber bundle*, Advances in applied probability, 2, 5, 200-216, Cambridge, UK, 1973.

[Pim14]   **Pimentel M., Brühwiler E., Figueiras J.**, *Safety examination of existing concrete structures using the global resistance safety factor concept*, Engineering Structures, Vol. 70, pp. 130-143, 2014.

[Por16]   **Portal N. M., Thrane L. N., Lundgren K.**, *Flexural behaviour of textile reinforced concrete composites: experimental and numerical evaluation*, Materials and Structures, 50, 2016.

[Pra51]   **Prager W., Hodge P. G.**, *Theory of perfectly plastic solids*, J. Wiley, New York, 1951.

[Pre19]   **Preinstorfer P., Kromoser B., Kollegger J.**, *Flexural behaviour of filigree slab elements made of carbon reinforced UHPC*, Construction and Building Materials, 199, 416-423, 2019.

[Rac00]   **Rackwitz R.**, *Optimization - The basis of code-making and reliability verification*, Structural Safety, 22, 27-60, 2000.

[Rac77]   **Rackwitz R.**, *First order reliability theories and stochastic models*, Proceedings of the 2nd International Conference on Structural Safety and Reliability, 1977.

[Raj93]   **Rajashekhar M. R., Ellingwood B.**, *A new look at the response surface approach for reliability analysis*, Structural safety, 12, 205-220, Oxford, 1993.

[Rei08]   **Reinhardt H. W., Krüger M. , Raupach M., Orlowsky J.**, *Behavior of Textile-Reinforced Concrete in Fire*, ACI Symposium Publication, 250, 99-110, 2008.

[Rei08]   **Reinhardt H. W., Krüger M. , Raupach M., Orlowsky J.**, *Behavior of Textile-Reinforced Concrete in Fire*, ACI Symposium Publication, 250, 99-110, 2008.

[Rem18]   **Rempel S.**, *Zur Zuverlässigkeit der Bemessung von biegebeanspruchten Betonbauteilen mit textiler Bewehrung*, RWTH Aachen University, Aachen, Germany, German, 2018.

[Rem20]   **Rempel S., Ricker M., Hegger J.**, *Safety Concept for Textile-Reinforced Concrete Structures with Bending Load*, Applied Sciences, Multidisciplinary Digital Publishing Institute, 10, 7328, 2020.

[Ros72]   **Rosenblueth E., Esteva L.**, *Reliability Basis for Some Mexican Codes*, ACI Symposium Publication SP-31-1, American Concrete Institute, 31, 1-42, Detroit, Michigan, 1972.

[Rup13]   **Rupf M., Fernández Ruiz M., Muttoni A.**, *Post-tensioned girders with low amounts of shear reinforcement: Shear strength and influence of flanges*, Engineering structures, Vol. 56, pp. 357-371, 2013.

[Sal00]   **Saltelli A., Chan K., Scott E. M.**, *Sensitivity analysis*, Wiley, 475, 2000.

[Sch12]   **Schladitz F., Frenzel M., Ehlig D., Curbach M.**, *Bending load capacity of reinforced concrete slabs strengthened with textile reinforced concrete*, Engineering structures, 40, 317-326, Kidlington, 2012.

[Sch11]   **Schlune H., Plos M., Gylltoft K.**, *Safety formats for nonlinear analysis tested on concrete beams subjected to shear forces and bending moments*, Engineering structures, 33, 2350-2356, Kidlington, 2011.

[Sch12]   **Schlune H., Plos M., Gylltoft K.**, *Safety formats for non-linear analysis of concrete structures*, Magazine of Concrete Research, 64, 563-574, 2012.

[Sch17]   **Schneider J., Vrouwenvelder T.**, *Introduction to Safety and Reliability of Structures*, IABSE Structural Engineering Documents, 5, 164 p., Zürich, Switzerland, 2017.

[Sho68]   **Shooman M. L.**, *Probabilistic reliability : an engineering approach*, New York (N.Y.) : McGraw-Hill, 524, 1968.

[SIA13]   **SIA 262**, *Construction en béton*, 102, 2013.

[Sig13]   **Sigrist V., Bentz E. C., Fernández Ruiz M., Foster S. J., Muttoni A.**, *Background to the Model Code 2010 Shear Provisions - Part I: Beams and Slabs*, Structural Concrete, Vol. 14, No 3, pp. 204-214, Berlin, Germany, 2013.

[Sim18]   **Simões J. T., Fernández Ruiz M., Muttoni A.**, *Validation of the Critical Shear Crack Theory for punching of slabs without transverse reinforcement by means of a refined mechanical model*, Structural Concrete, pp. 191-216, 2018.

[Soa02]   **Soares R. C., Mohamed A., Venturini W. S., Lemaire M.**, *Reliability analysis of non-linear reinforced concrete frames using the response surface method*, Reliability Engineering & System Safety, 75, 1-16, 2002.

[Sob90]   **Sobol I. M.**, *On sensitivity estimation for nonlinear mathematical models*, Matematicheskoe modelirovanie, Vol.2(1), 112-118, Russian, 1990.

[Sta18]   **Standards Australia**, *AS 3600:2018 : Concrete Structures*, 264, Sydney, 2018.

[Ste16]   **Stewart M. G., Foster S. J., Ahammed M. , Sirivivatnonon V.**, *Calibration of Australian Standard AS3600 concrete structures part II: reliability indices and changes to capacity reduction factors*, Australian journal of structural engineering, 4, 17, 254-266, 2016.

[Syk13]   **Sykora M., Holický M., Krejsa J.**, *Model uncertainty for shear resistance of reinforced concrete beams with shear reinforcement according to EN 1992-1-1*, Transactions of the VŠB--Technical University of Ostrava, Civil Engineering Series, 2, 13, 150, 2013.

[Syk18]   **Sykora M., Krejsa J., Mlcoch J., Prieto M., Tanner P.**, *Uncertainty in shear resistance models of reinforced concrete beams according to fib MC2010*, Structural concrete, 19, 284-295, 2018.

[Tae93]   **Taerwe L.**, *Towards a consistent treatment of model uncertainties in reliability formats for concrete structures*, CEB Bulletin d'Information 219 Safety and Performance Concepts, 5-61, 1993.

[Tas11]   **Tassinari L.**, *Poinçonnement non symétrique des dalles en béton armé*, Thèse EPFL, n°5030, 163, Lausanne, Switzerland, 2011.

[TÉC14]   **TÉCNICAS ASSOCIAÇÃO BRASILEIRA DE NORMAS**, *NBR 6118: Projeto de estruturas de concreto - Procedimento*, Rio de Janeiro, Portuguese, 2014.

[Tol88]   **Tolf P.**, *Influence of the slab thickness on the strength of concrete slabs at punching. Tests with circular slabs. (In Swedish: Plattjocklekens inverkan pa betongplattors hallfasthet vid genomstansning. Försök med cikulära plattor.)*, Royal Institute of Technology, Dep. of Structural Mechanics and Engineering, Bulletin 146, 64 p., Stockholm, Sweden, Swedish, 1988.

[Tys09]   **Tysmans T., Adriaenssens S., Cuypers H., Wastiels J.**, *Structural analysis of small span textile reinforced concrete shells with double curvature*, Composites Science and Technology, 69, 1790-1796, 2009.

[Val20b]   **Valeri P, Fernández Ruiz M., Muttoni A.**, *Tensile response of textile reinforced concrete* , Construction and Building Materials, Vol. 258, 22 p., 2020.

[Val20a]   **Valeri P, Fernández Ruiz M., Muttoni A.**, *Modelling of Textile Reinforced Concrete in bending and shear with Elastic-Cracked Stress Fields* , Engineering Structures, 215, 14 p., 2020.

[Val17]   **Valeri P, Fernández Ruiz M., Muttoni A.**, *cemsuisse report 201407: Building in a lighter and more sustainable manner : textile reinforced concrete for thin structural elements*, IBETON, Ecole Polytechnique Fédérale de Lausanne, Lausanne, 2017.

[Val20]   **Valeri P, Guaita P., Baur R., Fernández Ruiz M., Fernández-Ordóñez D., Muttoni A.**, *Textile reinforced concrete for sustainable structures: Future perspectives and application to a prototype pavilion*, Structural Concrete, pp. 1-17, 2020.

[Vec86]   **Vecchio F. J., Collins M. P.**, *The modified compression-field theory for reinforced concrete elements subjected to shear*, ACI Structural Journal, Vol. 83, No. 2, pp. 219-231, USA, 1986.

[Vec94]   **Vecchio F. J., Collins M. P., Aspiotis J.**, *High-Strength Concrete Elements Subjected to Shear*, ACI Structural Journal, Vol.91, No 4, pp. 423-433, Farmington Hills, USA, 1994.

[Vor06]   **Vorechovsky M., Chudoba R.**, *Stochastic modeling of multi-filament yarns: II. Random properties over the length and size effect*, International journal of solids and structures, 3, 43, 435-458, OXFORD, 2006.

[Wes18]   **Weselek J., Häussler-Combe U.**, *Calibrating safety factors for Carbon Concrete*, Beton- und Stahlbetonbau, 14-21, S2,113, German, 2018.

[Yu20]   **Yu Q., Muttoni A., Fernández Ruiz M.**, *Partial Safety Factor Format for the Resistance of Structural Concrete Considering Multiple Failure Modes*, Proceedings of the fib Symposium 2020, 2003-2010, Shanghai, China, 2020.

[Yu21]   **Yu Q., Valeri P, Fernández Ruiz M., Muttoni A.**, *A consistent safety format and design approach for brittle systems and application to textile reinforced concrete structures*, Engineering Structures, 249, 2021.

[Yu22]   **Yu Q., Fernández Ruiz M., Muttoni A.**, *Considerations on the partial safety factor format for reinforced concrete structures accounting for multiple failure modes*, Engineering Structures, 264, 114442, 2022.

[Yu23]   **Yu Q., Simões J. T., Muttoni A.**, *Model uncertainties and partial safety factors of strain-based approaches for structural concrete: example of punching shear*, Engineering Structures, (submitted for peer review in March, 2023).

Qianhui Yu

Civil Engineer

+41 78 637 54 98
qianhui.yu@epfl.ch
Rue de Genève 77bis, 1004 Lausanne
12.02.1990

Education

2018 - 2023	**PhD Candidate** *Structural Concrete Laboratory (IBETON), Swiss Federal Institute of Technology (EPFL), Lausanne, Switzerland*
2016 - 2018	**Visiting student** *Structural Concrete Laboratory (IBETON), Swiss Federal Institute of Technology (EPFL), Lausanne, Switzerland*
2012 - 2015	**M.Cs. in Civil Engineering** *Tongji University, Shanghai, China*
2012 - 2015	**B.S. in Civil Engineering** *Tongji University, Shanghai, China*

Professional Experience

2022-present	**Member of *fib* COM3, Task Group 3.1 Reliability and safety evaluation: full-probabilistic and semi-probabilistic methods for existing structures** *The International Federation for Structural Concrete(fib)*
2018 - 2023	**PhD assistant** Research on the reliability analysis and safety format calibration of reinforced concrete structures *IBETON, EPFL, Lausanne, Switzerland*
2018 - 2021	**Teaching assistant** For courses "Concrete structures", "Conceptual design of Bridges", "Concrete Bridges", "Concrete structures, selected topics", "Advanced design of concrete structures", "Stress field". *IBETON, EPFL, Lausanne, Switzerland*

Publications

2023	Yu Q., Simões J. T., Muttoni A., *Model uncertainties and partial safety factors of strain-based approaches for structural concrete: example of punching shear*, Engineering Structures, submitted March 2023
2022	Yu Q., Fernández Ruiz M., Muttoni A., *Considerations on the partial safety factor format for reinforced concrete structures accounting for multiple failure modes*, Engineering Structures, Vol. 264, 2022

2021	Yu Q., Valeri P., Fernández Ruiz M., Muttoni A., *A consistent safety format and design approach for brittle systems and application to textile reinforced concrete structures*, Engineering Structures, Vol. 249, 2021
2022	Monney F., Yu Q., Fernández Ruiz M., Muttoni A., *Anchorage of shear reinforcement in beams and slabs*, Engineering Structures, Vol.265, 2022
2021	Moccia, F, Yu Q., Fernández Ruiz M., Muttoni A., *Concrete compressive strength: From material characterization to a structural value*, Structural Concrete, Vol.22, 2021
2018	Yu Q., Fernández Ruiz M., Muttoni A., *Design of concrete structures using structural optimization based on the stress field Method*, Proceedings of the 12th fib International PhD Symposium in Civil Engineering, Prague, Czech Republic, 2018

Awards

2016	**Visiting student scholarship** *China Scholarship Council (CSC), Beijing, China*
2012	**Excellent Graduate Student Award** *Tongji University, Shanghai, China*
2011	**Leadership Enrichment and Regional Networking Program Scholarship** *Temasek Foundation and National University of Singapore (NUS), Singapore*

Languages

Chinese	Native
English	Fluent
French	Basic